Republic of Iraq
Ministry of Higher Education and Scientific Research
University of Babylon
College of Science
Department of Biology

Biosynthesis of Selenium Nanoparticles from *Bacillus clausii* and Evalution of Antibacterial , Antibiofilm and Cytotoxicity Assay

A Dissertation

Submitted to the Council of the College of Science University of Babylon, in Partial Fulfillment of the Requirements for the Degree Doctor of Philosophy In Sciences / Biology

By

Hawraa Jawad Kadhim omran

B.Sc. Microbiology /University of Babylon (2007)

M.Sc. Microbiology/University of Babylon (2014)

Supervised By

Prof. Dr.Wejdan Ridha Taj- Aldeen

2022 A.D 1444 A.H

بِسْمِ اللَّـهِ الرَّحْمَـٰنِ الرَّحِيمِ

قَـالُـوا سُبْـحَـانَـكَ لَا
عِلْـمَ لَـنَـا إِلَّا
مَـا عَـلَّـمْـتَـنَـا
إِنَّـكَ
أَنْـتَ الْـعَـلِـيـمُ الْـحَـ
كِـيـمُ ﴿٣٢﴾

صدق الله العلي العظيم

سورة البقرة

الآية " ٣٢ "

The Supervisor's Certification

I certify that this thesis entitled " **Biosynthesis of Selenium Nanoparticles from *Bacillus clausii* and Evalution of Antibacterial , Antibiofilm and Cytotoxicity Assay** " was prepared by " ***Hawraa Jawad Kadhim omran*** " under our supervision in the University of Babylon /College of Science /Department of Biology as a partial fulfillment of the requirements for the Degree of Doctor of Philosophy in Biology .

Signature :

Prof. Dr. Wejdan Ridha Taj-Aldeen

Department of Biology / College of Science

University of Babylon

Data : / / 2022

In view of the available recommendation, I put forward this thesis for debate by the examining committee .

Signature:

Assist. Prof. Dr. Adi Jassim Abd AL-Razzaq

Head of Biology Department

Data : / / 2022

Examination Committee

We, the examiner committee , certify that we have read the thesis entitled **" Biosynthesis of Selenium Nanoparticles from *Bacillus clausii* and Evalution of Antibacterial , Antibiofilm and Cytotoxicity Assay "** and have examined the student **" *Hawraa Jawad Kadhim omran* "** in its contents, and that in our opinion it is accepted as a thesis for the degree of Doctor in Philosophy of Biology - Microbiology with **" Excellent "** estimation .

Signature:
Prof. Dr. Abeer Fauzi Murad AL-Rubaye
College of Science for women
University of Babylon
Chairman

Signature:
Prof. Dr. Shaimaa Jassim AL-Sultany
College of Science
University of Babylon
Member

Signature:
Assist. Prof. Dr. Yazi Abdullah Jassim
College of Science
University of Babylon
Member

Signature:
Assist. Prof. Dr. Mais Emad Ahmad
College of Science
University of Baghdad
Member

Signature:
Assist. Prof. Dr. Iman Fadhel Abdul-Hussin
College of Biotechnology
Al-Qasim Green University
Member

Signature:
Prof. Dr. Wejdan Ridha Taj-Aldeen
College of Science
University of Babylon
Member & Supervisor

Approved for the College Committee of graduate studies

Signature:
Prof. Dr. Mohammed Mansour Kadhum AL Kafaji
Dean of College of Science
University of Babylon

Dedication

If the Dedication expresses even part of the fulfillment, then the Dedication is due …

To the soul of (grandmother's)

To the source of tender, love and advice..

(Mother & Father)

To whom I hold my dearest in life , my brothers and my dear sister **(Rawaa)**

To my dear children (Qaswar , Hawraa , Asal) and my husband (Dhiya)

To every knowledge student
I dedicate this study

Hawraa

Acknowledgements

***Initially** , I thank Almighty God for giving me the strength and the will to complete this work for the required degree*

My deepest thanks to University of Babylon and I would like to thank the staff of College of Science / Department of Biology , for their kind assistance

It is my pleasure to express my deep thanks and gratitude to my supervisor Professor Dr. Wejdan Ridha Taj- Aldeen who has provided me with valuable scientific guidance and continuous support throughout the period of preparation, and has devoted a large part of her time for the purpose of writing this dissertation.

Sincere thanks are due to the Dr. Nawfal Al-Dujaily, Dr. Hassan Hachim , Mrs. Zahraa , Mrs. Helen . Thanks to every teacher who contributed to my education in my life.

I would like to thank my family for their support in all times .

***Finally** , thanks and appreciation are to my colleagues and to all those who helped me in completing this work*

Hawraa

Summary

The biological method for the synthesis of nanoparticles occupies an important area due to economic and ecofriendly benefits when compared with physical and chemical synthesis methods. Hence ,this study aims to prepare selenium nanoparticles through the biological method from *Bacillus clausii* strain (4G219) that was diagnosed by VITEK2 system and 16srRNA gene sequencing .

The morphological and structural properties of selenium naanoparticles were determined by UV – visible spectroscopy and the absorption peak was observed at 260 nm wavelength , Field Emission Scanning Electron Microscope (FESEM) (diameters of SeNPs ranging from 37.58 – 75.16 nm) showing that the synthesized nanoparticles were crystalline, moderately stable and have rod shape , energy dispersive X-ray spectroscopy (EDX) revealed that the most principal sharp signal observed was belong to selenium nanoparticles . In XRD , the size of selenium nanoparticle was found to be similar with data obtained from (AFM) with size (18.215 nm , 19. 28 nm) respectively . Fourier Transform Infrared Spectroscopy(FTIR) spectra of SeNPs showed the present of some functional groups .

One hundred – sixty five sample of urine were collected from patients with clinical symptoms and suspected to Urinary Tract Infection (UTI) admitted in Al-Hilla teaching hospital and Public health laboratory in Babylon province during a period from (March - October) 2021 . 115(69.6%) isolates were positive culture , four type of pathogenic bacteria were diagnosed (*Escherichia coli , Enterococcus faecalis , Klebsiella pneumoniae , Staphyllococcus saprophyticus)* , most of them were resistant to antibiotics especially *Enterococcus faecalis* .

The antibacterial activity of selenium nanoparticles examined against these four pathogenic bacteria . Ten different concentrations of SeNPs (2, 4,

8, 16, 32,64,128, 256,512 and 1024 µg/ml) were used . Minimum inhibitory concentration (MIC) 32 µg/ml , Minimum bactericidal concentration (MBC) 64 µg/ml for both *Enterococcus faecalis* and *Staphylococcus Saprophyticus* , while MIC and MBC for *Klebsiella pneumoniae* and *Escherichia coli* were 64 µg/ml and 128 µg/ml , respectivily .

The synergistic effect of SeNPs was investigated with six antibiotics (Azithromycin , Ciprofloxacin , Trimethoprime / sulphamethoxazole Doxycycline , nitrofurantoin and Ampicillin) against pathogenic bacteria. The synergistic effect of Doxycycline with SeNPs in all tested bacteria that sensitive to Doxycycline were decreased , and the isolates that were sensitive to antibiotic became intermediate and intermediate became resistant to antibiotic .

Antioxidant activity of SeNPs was determined using (2,2-Diphenyl-1-picryl- hydrazyl)(DPPH) . The selenium nanoparticles had the highest antioxidant activity 39.6 % , 63.1% and 74.2 % at concentration 50, 100 and 150 µg/ml , respectivily . Selenium nanoparticles with all concentration did not show any hemolysis for the tested whole blood .

In biofilm formation assay out of all positive culture (115) isolates , 60 (52.1%) isolates gave a positive ability to form biofilm . The antibiofilm activity of selenium nanoparticles on some pathogenic bacteria formation biofilm was quantified in plate 96 well assay , The MIC of SeNPs on biofilm formation in (*Escherichia coli* and *Klebsiella pneumoniae*) was 128 µg/ml , and 64 µg/ml for *Staphylococcus Saprophyticus* and *Enterococcus faecalis* . The MICs of SeNPs against biofilm were found to be twice the MIC of planktonic state .

The cytotoxic response of prostate cancer PC3 cell line and normal hepatic WRL68 cells showed that no significant cytotoxic effect of Se NPs against PC3 cells at concentrations 25 and 50 µg/ ml . Nevertheless, Se NPs

at 100, 200 and 400 µg/mL exhibited a dose dependent decrease in PC3 cell viability with maximum inhibition rate of 51.27±2.77% of PC3 cells at 400 µg/ml. Regarding WRL68 cells, the sensitivity of the cells to SeNPs treatments was less than that of PC3.

Gene expression of virulence factor of (*Hly* , *FimH* , *Luxs* , *qsec*) genes of *E.coli* and (*ESP* , *HLY* , *gelE* , *fsrA*) genes of *E.faecalis* were evaluated by Real- time quantitive polymerase chain reaction (RT- qPCR) before and after treatment with SeNPs The results revealed that SeNPs effective on genes expression by down regulation .

The conclusion of this study found the ability of *Bacillus clausii* to synthesis of selenium nanoparticle . These SeNPs were proved to be antibacterial, antibiofilm, antioxidant, anticancer activity of PC3 and WRL 68 , and down regulation for virulence factor .

List of Contents

List of Appendices

List of Figures

List of Tables

List of Abbreviations

Abbreviation	Meaning
16S rRNA	16S Ribosomal Ribonucleic acid
AFM	Atomic Force Microscope
Akr1B10	Aldo-ketoreductase1B10
AMR	antimicrobial resistance
AST	Antibiotic Susceptibility Test
ATP	Adenosine Triphosphate
BHIB	Brian Heart Infusion Broth
CDC	Centers for Disease Control
cDNA	complementary- DNA
CLSI	Clinical and Laboratory Standards Institute
CT	cycle threshold
DMSO	Dimethyl sulfoxide
DPPH	1,1-Diphenyl-2-picrylhydrazyl
EDTA	Ethylene diamine tetraacetic acid
EDXS	Energy Dispersive X-Ray Spectroscopy
EPS	extracellular polymeric substances
EUCAST	European Committee on Antimicrobial Susceptibility Testing
FDA	Food and Drug Administration
FT IR	Fourier transform infrared spectrophotometer
GSH-Px	Glutathione Peroxidase
IDD	Iodothyronine Deiodinases
MB	Methylene Blue
MBC	Minimum bactericidal concentration
MHA	Mueller Hinton Agar
MIC	Minimum inhibitory concentration
NCBI	National center for biotechnology Information
NCCLS	national committee for clinical laboratory standards
NNI	National Nanotechnology Initiative
NP	Nanoparticle

OD	Optical density
PBS	Phosphate buffer saline
PCR	Polymerase chain reaction
RNA	Ribonucleic Acid
ROS	Reactive Oxygen Species
RPMI	Roswell Park Memorial Institute Medium
RT-PCR	Real-Time Polymerase chain reaction
Se	selenium
SeC	selenocysteine
SEM	Scanning Electron Microscopes
SeNPs	Selenium nanoparticles
SPR	Surface Plasmon resonance
TCP	Tissue Culture Plate
TNF-α	Tumor nicrosis factor - α
TR	Thioredoxin Reductase
UTI	Urinary tract infection
WHO	World Health Organization
XRD	X ray diffraction

Chapter One

Introduction

1. Introduction

Urinary tract infections (UTIs) are the most common infection in a clinical setting and the second most prevalent infection after respiratory tract infections (Bizuayehu *et al*., 2022) . Worldwide , UTIs affect about 150 million people every year (Öztürk and Murt , 2020) . In most cases the infectious agents are *Enterobacteriaceae* ,including *Escherichia coli* , *Klebsiella* sp. , *Enterobacter* sp. and *Proteus* sp., and Gram-positive bacteria such as *Enterococcus faecalis* , *Streptococcus agalactiae* and *Staphylococcus* spp . *Staphylococcus saprophyticus* is a member of the coagulase-negative staphylococci , which are commonly responsible for 5%–10% of UTIs (Gajdács *et al*., 2019) .

Bacterial resistance is the capability of bacterial cells to prevent antibiotic bacteriostatic or bactericidal effects (Munita and Arias , 2016) . Resistance of antibiotic is one of the most serious global public health issues; it has the capacity to kill 700,000 people and might rise to ten million in 2050 (Mancuso *et al*., 2021). In 2019, due to its impact on human health , the World Health Organization included antimicrobial resistance (AMR) as one of the top ten threats to global health (WHO , 2019) . According to the evidence , The rising threat of multidrug-resistant bacteria and biofilm-associated illnesses necessitates the development of new bactericidal methods . As a result, new and emerging nanoparticle-based materials in the field of antimicrobial chemotherapy have received a lot of attention (Makabenta *et al*., 2021) .

The formation of microbial biofilms enables single planktonic cells to assume a multicellular mode of growth. During dispersion, the final step of the biofilm life cycle, single cells egress from the biofilm to resume a planktonic lifestyle. As the planktonic state is considered to be more vulnerable to antimicrobial agents and immune responses, dispersion

is being considered a promising avenue for biofilm control (Rumbaugh and Sauer , 2020) . Biofilm form through a complex cascade of events that encapsulate bacteria within self-assembled (EPS) . Viscous layer that prevents the entry of chemo-therapeutic agents , leading to the recalcitrance of bacteria . Bacteria inside the biofilm are resistant to external stress and evade the host immune system Biofilm- associated tissue infections are the sole cause of nosocomial infections(Oliveira *et al*., 2022) .

Nanotechnology is a new field of study that combines nanotechnology and biotechnology to give nano science . The diameter of the nanoparticles ranges between (1-100) nm , their chemical activity , large surface area , charge density and ability to interact with the bacterial-cell enabled them to enhance the antimicrobial activity by generating reactive oxygen species or free toxic metal ions (Fardsadegh and Jafarizadeh-Malmiri , 2019 ; Alam *et al*., 2020).

Nanoparticles are manufactured by physical , chemical and biological methods. In biological methods plants , fungi and bacteria were used to prepare nanomaterials . One of the benefits of this method is that it is environmentally friendly, economical , and less toxic when compared to other methods . As for the physical and chemical methods which that used in manufacturing , they produce high radiation and toxic reducing materials , which have the ability to affect human and other living organisms (Jeevanandam *et al*., 2022 ; Parvej *et al*., 2022) .

In biological systems , Selenium nanoparticles have many nanomedicine applications due to their anti-cancer , anti-microbial and anti-oxidant properties , and the cytotoxicity of selenium nanoparticles was lower than that of silver nanoparticles (Hosnedlova *et al*., 2018) . Polymers , dendrimers , liposomes , silicon and metal NPs (Zn , Fe , Au ,

Ti , Se and others) have all been employed as effective therapeutic agents and drug delivery carriers (Anjum *et al*., 2021 ; Ikram *et al*., 2021 ; Mojarad-Jabali *et al*., 2021; Nikzamir *et al*., 2021 ; Rahimi *et al*., 2021; Motiei Pour *et al*., 2022 ; Sattar *et al*., 2022) . Because of their high stability and low toxicity , SeNPs are now widely accepted and recommended for use in a variety of scientific branches (Gunti *et al*., 2019) .

Bacillus have the obvious benefit over other prospective probiotics in that they can be generated easily and economically effectively by drying and last well through shelf life. They will also survive gastric acidity and make it into the intestine, the rumored location of action (Upadrasta *et al*., 2016) . *Bacillus clausii*, a spore-forming probiotic, is able to colonize the gut. It is a rod-shaped, nonpathogenic, aerobic, Gram-positive bacterium, able to survive transit through the acidic environment of the stomach and colonize the intestine even in the presence of antibiotics (Bordea , 2020) .

The present work aims to biosynthesis of selenium nanoparticles by non-pathogenic bacteria , and then study the antibacterial , antioxidant , haemolysis , anticancer activity of SeNPs and finally study the action mode of selenium nanoparticles on pathogenic bacteria by the following :

- Biosynthesis of selenium Nanoparticles by *Bacillus clausii* and purification partially .
- Characterization of biosynthesized selenium Nanoparticles by UV-visible spectrophotometer, FESEM, EDS , XRD, AFM and FTIR .
- Antibacterial activities of selenium Nanoparticles against bacteria that caused UTI infections.

- Detection the antibiotics susceptibility test and the synergetic effect of SeNPs with antibiotic against gram negative and gram positive bacteria .
- Anticancer activity of SeNPs aganist PC3 cell line and cytotoxicity against WRL 68 cell line .
- Biological assay of selenium nanoparticle such as antibiofilm , antioxidant and hemolysis
- Measurement the gene expression of gene encoding to hemolysin, attachment, biofilm production and biofilm regulation with and without selenium nanoparticles .

Chapter Two

Literature Review

2. Literature review

2.1 Urinary tract infection

Urinary tract infection (UTI), the second-ranked infectious diseases, are recognized as a big concern relating to global healthcare systems (Behzadi and Behzadi , 2017) . UTIs are known as multi-microbial infectious diseases, which can be happened by bacteria (Gram-positive and/or Gram-negative strains) and fungi. Among Gram-negative bacteria, the member of Enterobacteriaceae , in particular, *Escherichia coli* and *Klebsiella pneumoniae* are the most common uropathogenic bacterial agents, which may cause different types of UTIs (Behzadi , 2018) .

Furthermore G $^{-ve}$ bacteria , including Streptococci , Staphylococci and Enterococci, are involved in UTIs in humans . On the other hand, fungi and particularly *Candida albicans* strains may act as opportunistic pathogenic fungi for causing UTIs. However, the non - *C. albicans* such as *C. glabrata* and *C. tropicalis* are reported from some countries as the predominant species of the causative agents of UTIs (Okojie and Omorokpe , 2018) .

There are different types of UTIs including acute and/or chronic, asymptomatic and/or symptomatic (mild/moderate and/or severe), complicated and/or uncomplicated, and community and/or nosocomial acquired infections . If the UTIs occur ≥ three times in a year or ≥ two times continuously after disappearance (treatment) of the first infection in a half year, they are recognized as recurrent UTIs (rUTIs) (Johansen *et al*., 2016) .

In addition to this diversity, as the human's urinary tract is divided into two parts of lower and upper sections, the UTIs may occur in the lower part of the UT (known as cystitis) and/or upper part of the UT (known as nephritis) . These characteristics are in association with microbial pathogenomics, duration of infection , and the abilities of human host (Foxman, 2010) .The threshold of microbial population for UTIs is reported as ≥100,000 living cells or colony-forming unit (CFU) per urine milliliter (ml); however, it varies from 100 to 1000 to 100,000 CFU/ml. Of course, the UTIs without syndromes and with syndromes are recognized as asymptomatic and symptomatic UTIs, respectively (Jepson *et al*., 2012) .

2.2 Nanomaterials

The term nanometer was first used in 1914 by Richard Adolf Zsigmondy . The American physicist and Nobel Prize laureate Richard Feynman introduced the specific concept of nanotechnology in 1959 in his speech during the American Physical Society's annual meeting . This is considered to be the first academic talk about nanotechnology (Zafar , 2022) . Due to the nanoscale dimension , nanomaterials exhibit exceptional properties that differ from those of their bulk counter parts (Baig *et al*., 2021) .

Medical nanotechnology uses materials with nano range size, which is generally1–100 nm . These materials are applied in the design , fabrication , regulation , and application of therapeutic drugs or devices (Ali *et al*., 2021) . Typical nanomaterials possess several common characteristics : high surface-to-volume ratio , enhanced electrical conductivity , superparamagnetic behavior , spectral shift of optical absorption , and unique fluorescence properties . In the medical field , nanomaterials can be applied in drug transportation , increased

permeability enabling crossing through biological barriers and improved biocompatibility are also noticeable features (Nayak *et al*., 2021) . The high surface-to-volume ratio of some nanomaterials can assemble with biomolecules or residues , which can enhance the specificity of chemical drug complex in targeted therapy , thereby enhancing the efficacy of nanomaterial-based treatment while reducing its toxicity to normal cells (Cheng *et al*., 2021) .

Many researchers have used the term nanomaterial if the size is a few nanometers or smaller than a few tens of nanometers , whereas others have even used the term nanomaterial for anything less than a micrometer (Baig *et al*., 2021) .

The physical and chemical properties of nanomaterials depend upon their precise composition , shape , and size . The effects of nanomaterial on health and the environment also depend upon their size, shape, etc. A single internationally accepted definition of nanomaterials is challenging to find , and a rigorous definition of nanomaterials is still under discussion in the scientific community (Patel *et al*., 2021).

2.3 Nanoparticle synthesis approaches

The nanomaterials prepared through two basic methods :first **(Top-down)** systems: where tiny manipulations of little number of atoms or molecules fashion elegant patterns, through mechanical- physical methods like grinding, milling and crushing for producing nanoparticles, this method was used for producing Nano composites and Nano-grained bulk materials like metallic and ceramic nanomaterials in extensive size distribution (10 - 1000 nm) , while second method was **(Bottom-up)** system , numerous molecules were self-assembled in parallel steps, as a function of their molecular recognition characters, this processing produced more complex structures from atoms or molecules, also, this

method produce a uniform controlling sizes, shapes and size ranges of nano materials , figure (2.1) (Abobatta , 2018) .

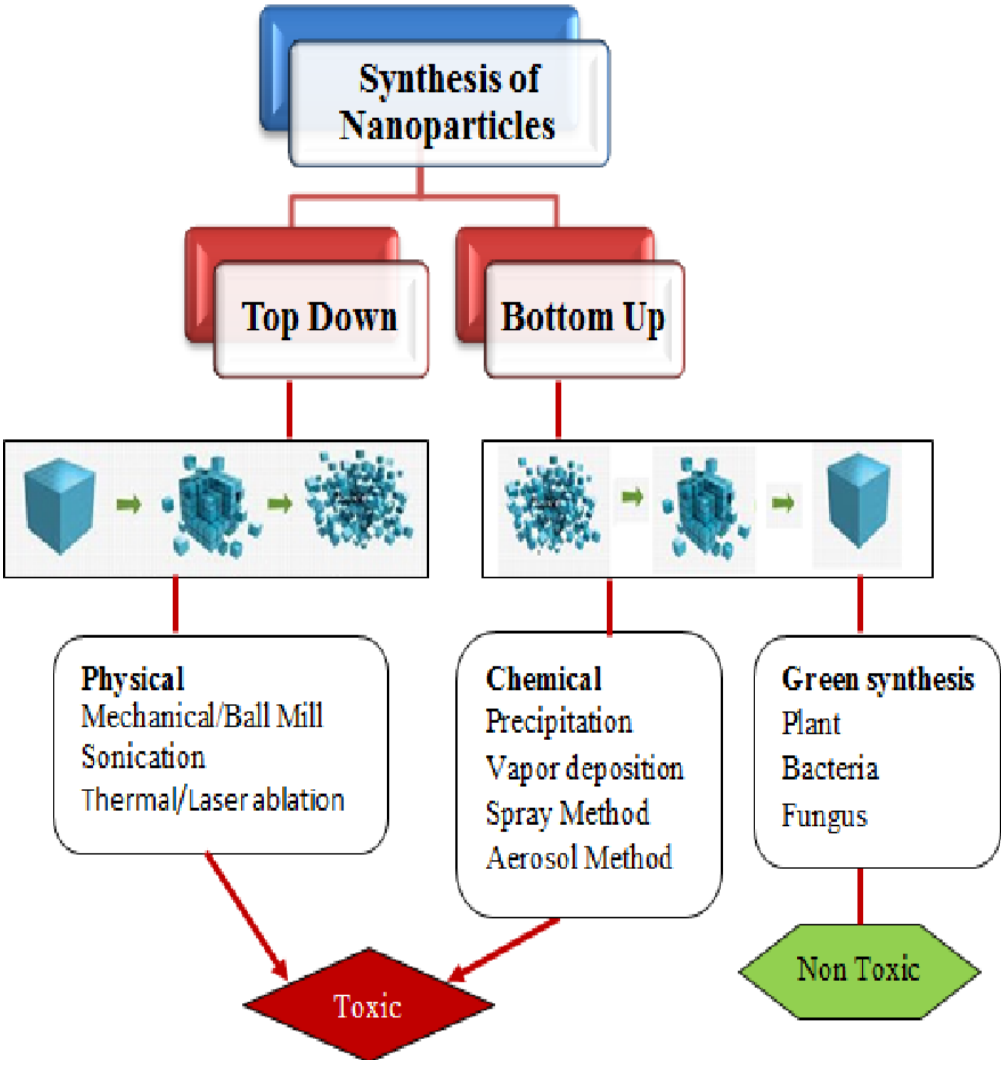

Figure (2.1): Schematic diagram for top-down and bottom – up synthesis of nanoparticle (Chaudhari and Nikam, 2018) .

Nanoparticles can be synthesized by several methods such as physical ,chemical and biological method. The nanoparticles can be synthesized using the top-down in physical approach and bottom-up in chemical and biological approach (Saleh , 2021). Different types of physical and chemical methods are employed for the synthesis of nanoparticles but the use of these methods requires both strong and weak chemical reducing agents and protective agents which are mostly toxic,

flammable, cannot be easily disposed due to environmental issues and , a low production rate and elevated temperatures for synthesis process in addition these are capital intensive and are inefficient in materials and energy use (Rahimi and Doostmohammadi, 2019).

Although the chemical and physical methods are able to produce small quantities of nanoparticles with a defined size and shape in a relatively long time, they are complicated, outdated, costly, inefficient and produce hazardous toxic wastes that are harmful not only to the environment but also to human health (Murugesan *et al*., 2019 ; Kumar and Prasad , 2021) .

The biological method for the synthesis of nanoparticles employs biological agents such , fungi (Zhang *et al*., 2019) , bacteria (Alam *et al*., 2020) , actinomycetes (Ranjitha and Ravishankar , 2018) , and plant extracts (Pyrzynska and Sentkowska , 2021) . The biological agents secrete a large amount of enzymes, which are capable of hydrolyzing metals and thus bring about enzymatic reduction of metals ions (Das *et al*., 2017) . Moreover, leaf extracts , seed extracts , root extracts , bulbs , and latex of plants were used to synthesize gold , silver, and palladium nanoparticles (Azizi *et al*., 2014) Biological materials such as honey, starch, and ascorbic acid were used to synthesize gold , silver , palladium, carbon, and platinum nanoparticles (Reddy *et al*., 2012) .

The purpose of highlighting the biological synthesis of nanoparticles was because of its easiness of rapid synthesis, controlled toxicity, controlling size characteristics, reasonable, and ecofriendly approach (Ingale and Chaudhari , 2013) . Biological method of nanoparticles synthesis would help to remove harsh processing conditions by enabling the synthesis at physiological, temperature, pressure, and at the same time at lower cost. One of the options to achieve this goal is to use microorganisms to synthesize nanoparticles (Ndwandwe *et al*., 2021).

2.4 Characterization of nanoparticles

2.4.1 UV-visible Spectroscopy

The technique of spectrophotometry is generally used for the qualitative and quantitative estimation of biomolecules such as proteins, sugar, carbohydrates, amino acids, nucleic acids and vitamins. UV–visible spectroscopy has proven to be extremely useful for analyzing various nanoparticles like : selenium , gold , silver , etc (Anderson *et al*., 2019 ; Hashem and Salem , 2022). The observation of high large surface plasmon peaks at visible regions (400–600 nm) for different metal nanoparticles with sizes varying from 2 to 100 nm has been well reported. A UV–visible spectrophotometer is made up of two parts: a spectrometer for producing light of various wavelengths and a photometer for measuring light intensity(Zayed *et al*., 2019).

2.4.2 Scanning electron microscopy (SEM)

Scanning electron microscopy (SEM) offers the topographical and elemental knowledge of NPs with an almost infinite field depth for useful amplifications. In the evaluation of elementary structure, grain size, roughness of the surface , porosity, distribution of dimensions, homogeneity, inter-metal distribution and diffusion of NP, scanning electron microscopy can also be used (Van Malderen , 2017).

The mechanism of action is based on the passage of finely focused scanned electron beam across the surface of the sample; this generates backscattered electrons, secondary electrons, and characteristic X-rays. When collected by detectors, These signals form images of the scanned sample displayed on a cathode ray tube screen(Goldstein *et al*., 2017).

2.4.3 Energy-Dispersive X-ray Spectroscopy (EDX)

Energy dispersive spectroscopy investigates surface analysis and elemental characterization of the sample. Basic principle involves the

study of the emitted X-rays of different energies coming from the sample when a beam of electron strikes its elements. The amount and composition of metal nanoparticles can be easily identified from the surface of the given sample (Shirley and Jarochowska , 2022).

The rays issued have been observed and their energy analysed. Since the energy of x-rays is distinctive for any aspect, it could be used to analyze the sample components(Shahbaz *et al*., 2022).

2.4.4 Atomic force microscope(AFM)

Atomic force microscopy (AFM) is a tool of exceptionally high resolution that can be used to study the morphology of a sample as well as quantify its mechanical properties at atomic resolution (Wang *et al*., 2021). AFM employs a microscopic physical probe to "grope" the microcosm and analyze the morphology of the sample under study in three-dimensional space, extracting information from the very slight interaction between the probe and the sample surface. AFM images can be collected in an aqueous medium, making it an important method of studying the action of nanoparticles in a biological context (Deng *et al*., 2018) .

The functionalized probe can be used to classify individual molecules or interactions powers like ligand-receptor interactions. As a result, AFM has a good future in biomedicine and clinical medicine, especially in cancer diagnosis and treatment. Cell dynamics is an important biomarker for identifying cell states(Wang *et al*., 2016).

2.4.5 X-ray diffraction (XRD)

The X Ray Crystallography is a strong technique for the analysis of the three-dimensional structure of macromolecules like protein or nucleic acids in the crystal phase. The technology is also known as a method of radiation diffraction (Spiliopoulou *et al*., 2020). There are many methods

for the three-dimensional structure analysis , the most effective methods was x-ray crystallography. Along with amorphous compounds such as polymers, X-ray diffraction is used to determine the atomic arrangements and thickness of thin films (Maveyraud and Mourey, 2020).

Two steps are involved in the use of the microscope. At the beginning , light is incident on the target and is diffracted in a variety of directions , then the lens captures and reassembles the diffracted rays to create an image . X-rays was used to detect diffraction from molecules , and a screen to reassemble the picture (Oake *et al*., 2019).

2.4.6 Fourier Transform Infrared Spectroscopy (FTIR)

FTIR technique is a vibrational spectroscopic technique that has various uses in the study of excavated textiles. For organic compounds, molecular vibrations result in the formation of distinct absorption bands in the spectra, which may aid in their detection (Hospodarova *et al*., 2018) **.**

FTIR is used to assess the heterogeneous structure and surface behavior of materials by gathering data on the maximum values at particular lambda values in absorption and reflection spectra. A Fourier transform (mathematical operation) is used to convert the data collected from all wavelengths traveling through the sample to the real spectrum. The FTIR technique is used to study the vibrational structures of solids(Chen *et al*., 2015).

2.5 Selenium

Selenium (Se) is an essential dietary trace element which presents in human beings (Fang *et al.*, 2018). Selenium which is a building block of the selenocysteine, that mainly involved in the synthesis and catalytic function of selenoproteins such as peroxidases and reductases (Hadrup *et al*., 2016) .

Many selenoproteins believed to be having oxidoreductase activity which plays an important role in regulation of the physiological redox balance. Due to the narrow therapeutic window and toxicity margins , selenium is widely replaced by the selenium nanoparticle which is believed to be having a wide therapeutic window and reduced toxicity which is also having the optimized body distribution (Khurana *et al*., 2019).

Selenium is a metalloid having different oxidation states : selenium (0) , selenide (-2), selenite (+4), and selenate (+6) , inorganic selenium mainly founds in the soil , while organic selenium mostly founds in soil, air and plants . Presently there are 25 selenium proteins which are known to play a role as antioxidants, with selenite, selenomethionine, methylselenocysteine and selenocysteine are the compounds which are mostly studied , because of their application in disease prevention and therapy. Many Studies revealed that the elemental selenium is less toxic and preferential biological activity compared with its other forms (Maiyo and Singh , 2017) .

The elemental selenium mainly involved in the antioxidant defines system that play a vital role in protecting against oxidative stress. In several studies they showed that the Selenium can upregulates the level of enzymes such as Glutathione peroxidase (GPx) , with the supply of Selenium and reducing the cellular damage by preventing the accumulation of free radical species . Se^0 is believed to be having more attention due to its low toxicity and more bioavailability when compared with Se (4) and Se (6), meanwhile they both have free radicals capturing ability (Kondaparthi *et al*., 2019) .

It is difficult to apply of selenium in food and medicine fields because of its poor water solubility and their ability to convert into a grey analogue . The water solubility of the selenium nanoparticle can be

enhanced by reducing their size and increasing their surface area with application of the nanotechnology (Zhai *et al*., 2017) .

The selenium can improve the cell mediated immune responses when it is supplied in the form of sodium selenite to head and neck cancer patients during radiation and surgery. The selenoproteins are required for the normal function of the activated T cells and the T cells are sensitive to Reactive Oxygen Species (ROS) when the deficiency of selenoproteins occurs, it leads to ROS elevation, so selenoproteins, cannot proliferate in response to the T cell receptor stimulation. Selenium depletion leads to irreversible brain injury. The Selenium can deliver to brain by specific selenoprotein called selenoprotein P , which is believed to be improving the neuronal survival and also prevent cell death caused by beta-amyloid accumulation (Solovyev *et al*., 2018) .

2.6 Nano-selenium

Nano-Se could be defined as nano-elemental selenium or nano-Se manufactured for use in nutritional supplements and developed for applications in medical therapy (Hu *et al*., 2012) . It is bright red, highly stable, and of nano-size in the redox state of zero (Se^0). Nano-Se has a higher efficiency in upregulating selenoenzymes and exhibits less toxicity than selenite (Hosnedlova *et al*., 2018).

From three allotropes of Se^0 , the gray and the black ones are biologically inert, which is due to their insolubility (El-Ramady *et al*., 2014) . A variety of bacteria , fungi and plant extracts have been used to synthesize Se nanoparticles of different size and morphology (Kimura *et al*., 2014 ; Sharma *et al*., 2014 ; Srivastava and Mukhopadhyay, 2015) .

Biogenic Se nanoparticles could be synthesized from Se salts especially selenite and selenates in the presence of reducing agents (biomolecules) such as phenols, alcohols, proteins, and amines. These previous biomolecules can be used to reduce Se salts in vitro, but the by-

products released in the environment may be hazardous to flora and fauna (Husen and Siddiqi , 2014).

2.7 Therapeutic applications of SeNPs

Based on the improved properties of SeNPs over Se, they have been explored in various disease conditions. SeNPs offer improved bioavailability with the added advantage of decreased toxicity. The pro-oxidant, as well as the antioxidant effects provide different avenues for exploration in a variety of pathological conditions. Some studies focused on the role of SeNPs as antimicrobial , antioxidant , anticancer agent , in drug delivery , in reducing inflammation (Jolly *et al*., 2020) .

2.7.1 Role of SeNPS as antimicrobial

SeNPs possess the antimicrobial activity thus inhibiting the growth of microbes such as bacteria, fungi, and viruses. Biologically synthesized SeNPs (from bacterium *Ralstonia eutropha*) has been showed to possess antimicrobial activity at a concentration of 100, 100, 250, and 100 µg/mL by inhibiting 99% growth of *Pseudomonas aeruginosa, Staphylococcus aureus, Escherichia coli*, and *Streptococcus pyogenes* respectively. Furthermore, it has been observed that SeNPs at a concentration of 500µg/mL inhibits the growth of pathogenic fungi *Aspergillus clavatus* (Srivastava and Mukhopadhyay, 2015) .

Lactobacillus plantarum and *Lactobacillus johnsonii* reduced selenium dioxide to cell-associated elemental selenium nanoparticles. The cell-free spent culture media, from both *Lactobacillus* species that had been grown with selenium dioxide for 48 h, showed enhanced antifungal activity against *Candida albicans* (Kheradmand *et al*., 2014) . The antiviral activity of SeNPs has been investigated on H1N1 influenza virus and was found that the combined use of oseltamivir and amantadine-

loaded SeNPs strongly inhibits the generation of ROS and activation of p53 phosphorylation and AKT (Li *et al*., 2017 ; Li *et al*., 2018) .

2.7.2 Role of SeNPS as antioxidant

Selenium was playing an important role in forming selenoproteins that help synthesize glutathione peroxidase enzymes . More specifically, Selenium nanoparticles are noted to upregulate the expression of peroxidase (GPx) by forming selenophosphate (Kondaparthi *et al*., 2019). ROS such as superoxide anion (O_2^-), 1,1-diphenyl-2-picrylhydrazyl, singlet oxygen ($^1O_2$) , and carbon-centered free radicals were scavenged by Selenium NPs (Kumar and Prasad , 2021) . According to some studies, the activity of glutathione peroxidase (GSH - Px) in the liver of weanling pigs increases significantly when the animals are fed a Nano-Selenium diet (concentration range of 0.50 and 1.0 mg/kg) instead of an inorganic form of selenium (Zhang *et al*., 2007) .

Another study found that Nano-Selenium protects against acetaminophen (APAP) which induced hepatotoxicity by improving liver function and oxidative stress mediated by catalase, SOD, and GSH, as well as decreasing hepatic DNA fragmentation and hepatic biomarker of cell death (Amin *et al*., 2017). Similarly, Selenium NPs protect against K2Cr2O7-induced thyroid damage by correcting free T3 and T4 levels as well as GSH, catalase, SOD, and MDA levels (Khurana *et al*., 2019) .

2.7.3 Role of SeNPS as an anticancer agent

The anticancer property of SeNPs is due to that selenium inducing glutathione S-transferase (GST) (Wang *et al*., 2007) . SeNPs mitigates the problems of drug resistance and toxicities connected with chemotherapeutic agents. SeNPs have the potential to suppress the growth of cancer cells via the induction of cell cycle arrest at S phase (Luo *et al*., 2012) .

Cancer cells selectively incorporate SeNPs via endocytosis, and then these SeNPs induces the apoptosis of cancer cell by triggering apoptotic signal transduction pathways (Hosnedlova *et al*., 2018) . SeNPs have been observed to inhibit the growth of prostate LNCaP cancer cells moderately via caspases mediated apoptosis *in vitro* (Kong *et al*., 2011) . Furthermore, it has been observed that SeNPs, along with *Lactobacillus Brevis*, stimulates the immune response via enhancing the production of interferon and delayed-type hypersensitivity response in a metastatic breast cancer mice model (Yazdi *et al*., 2012) .

Introduction of biologically synthesized SeNPs (concentration as low as 2 μg Se·mL-1) were competent enough to suppress the proliferation and induce caspase-independent necrosis in human prostate adenocarcinoma cells (PC3) (Sonkusre *et al*., 2014) . In addition to their anticancer potential alone, SeNPs when used in combination with 5-Flourouracil (5-FU) has been shown to enhance the anticancer potential of the drug in A375 human melanoma cells . Figure (2.2) demonstrates the mode of SeNPs action as an potential anticancer agent and carrying out the apoptosis (Jolly *et al*., 2020) .

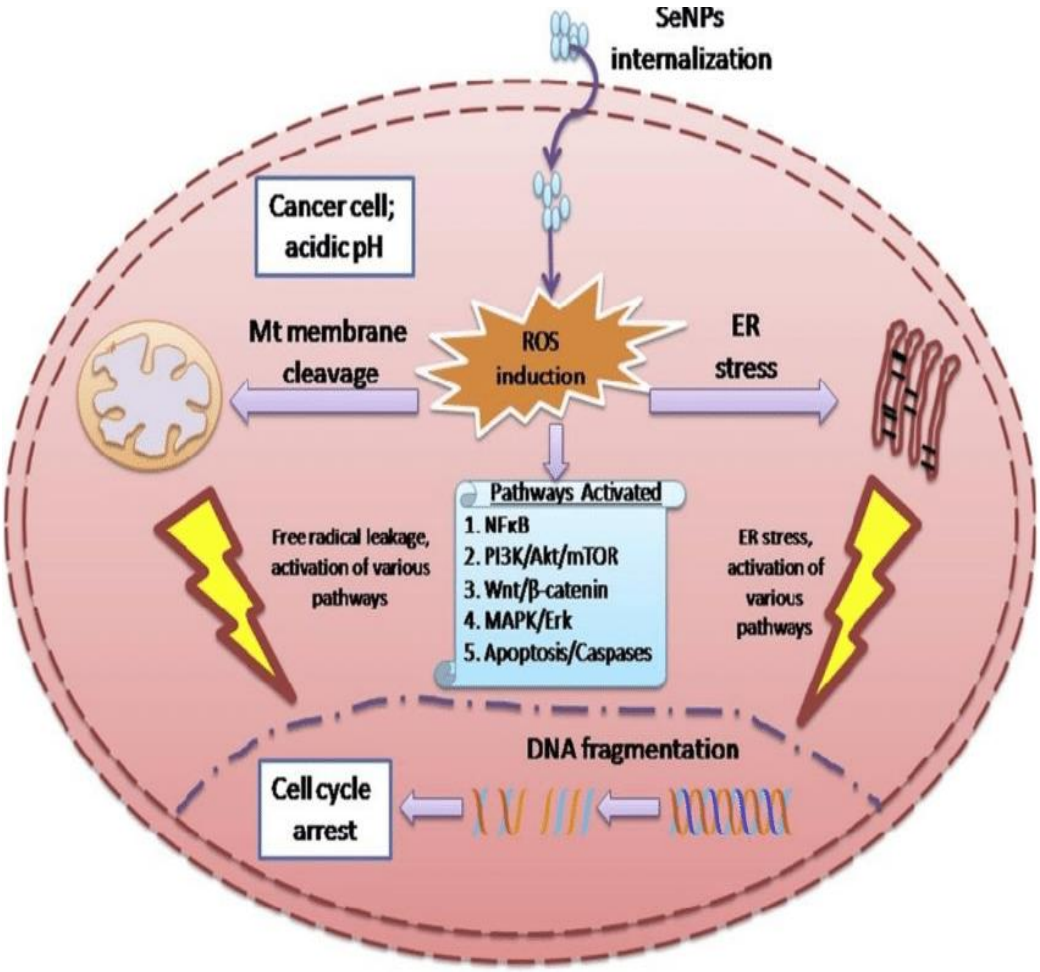

Figure (2.2) : The mechanism of SeNPs as an anticancer agent (Nayak *et al.*, 2021) .

2.7.4 Role of SeNPs in drug delivery

SeNPs have been used as a drug delivery system for anticancer drugs/agents, for active immunization via carrying antigens and also for genes to the appropriate site , figure (2.3) (Khurana *et al.*, 2019) . The selective/effective uptake and drug accumulation at the target site are possible because of the nanosize of these particles. SeNPs have been found to deliver siRNA against specific oncogenic gene (Sonkusre *et al.*, 2014) .

The usage of several surface decorators increases the cellular uptake and anticancer potential of nanoparticles (Yang *et al.*, 2012). SeNPs were functionalized with *Spirulina* polysaccharides (SPS) , SPS

surface decoration markedly increased the cellular uptake and cytotoxicity of SeNPs against various cancer cell lines. The SPS-SeNPs was observed to suppress the growth of cancer cell via apoptosis, as manifested by an increment of the sub-G1 cell population, fragmentation of DNA, condensation of chromatin, and translocation of phosphatidyl-serine (Li *et al.*, 2016) .

Many research reported that polyamidoamine dendrimer-modified SeNPs efficiently deliver the siRNA and cisplatin to A549/DDP cells for reversal multidrug resistance. This combination induces apoptosis of cells via PI3K/Akt/mTOR and MAPK/ERK pathways in A549/DDP cells . Furthermore, SeNPs has proved to be as a carrier for the delivery of doxorubicin for targeting breast cancer with lesser toxicity and improved anticancer potential (Yang *et al* ., 2012 ; Zheng *et al*., 2015) .

The delivery of siRNA using RGDfC-conjugated functionalized SeNPs is successful against liver carcinoma (Xia *et al*., 2017) . It activates Wnt/β-catenin signaling and sparks Bcl-2 mediated apoptosis (Zhao *et al*., 2017) .

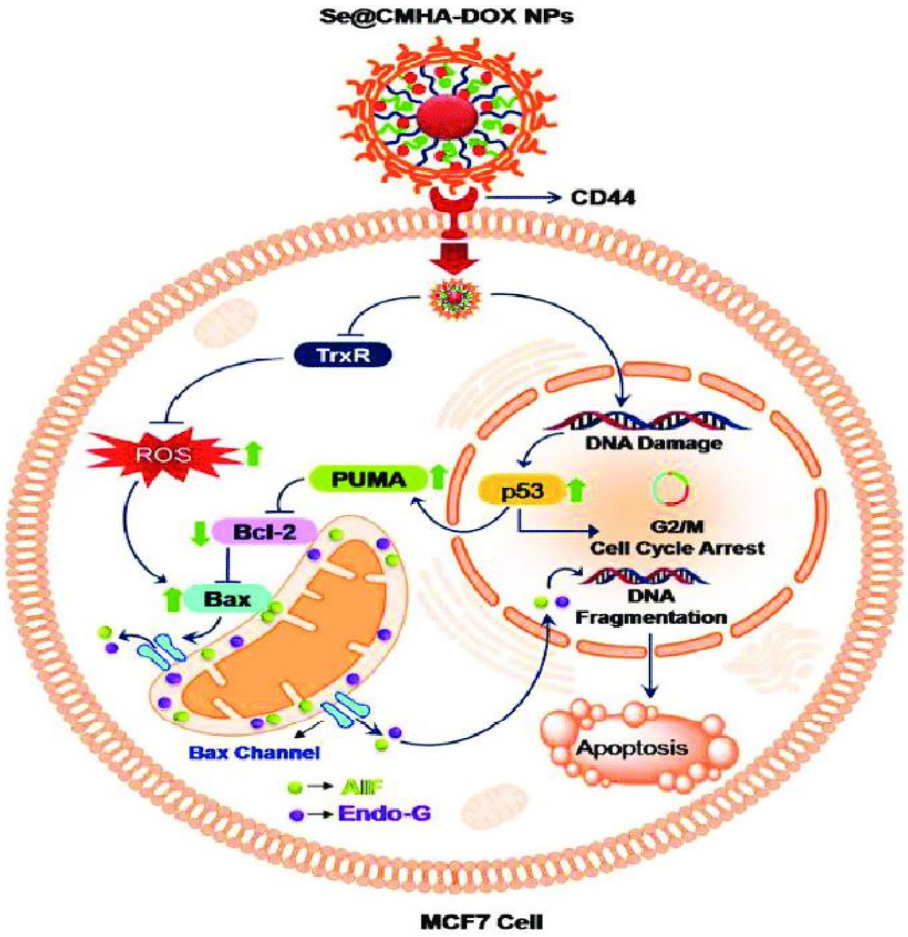

Figure (2.3) : Role of SeNPs in drug delivery (purohit *et al.*, 2017)

2.7.5 Role of SeNPS in reducing inflammation

Inflammation is the earliest step in the onset of a disease/injury leading to accretion of body fluids, white blood cells and release of prostaglandins and several inflammatory mediators (Ricciotti and FitzGerald , 2011). The nuclear factor kappa-B (NF-κB) signaling pathway has been associated with enhanced inflammatory response and its activation has been significantly correlated with interleukin-6 and TNF-α production. Selenium may inhibit the activation of NF-κB by modulating selenoprotein genes expression , figure (2.4) (Duntas , 2009) .

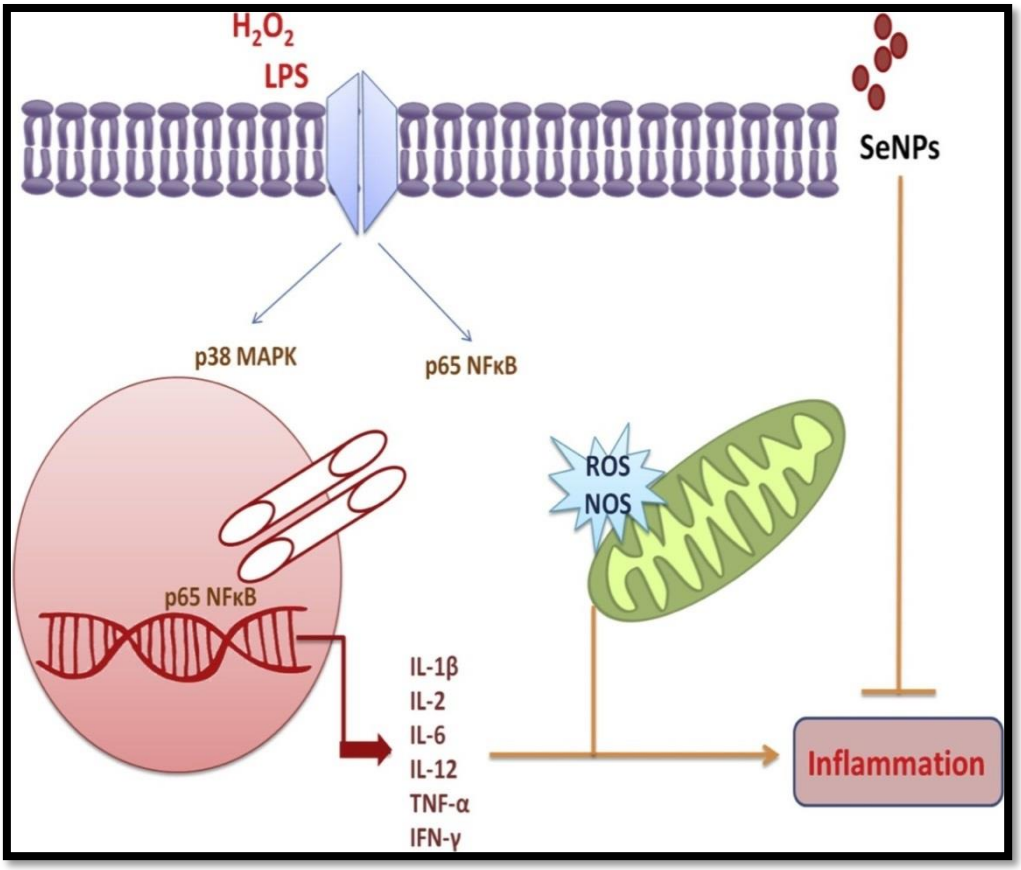

Figure (2.4) : Anti-inflammatory effects of SeNPs (Khurana *et al.*, 2019) .

It has been observed that SeNPs decorated with Ulva lactuca polysaccharide (ULP) (ULP-SeNPs) significantly inhibited the proinflammatory cytokines (IL-6 and TNF-α) and the nuclear factor kappa-B(NFκB) signalling in dextran sodium sulphate induced colitis (Zhu *et al.*, 2017) . Similarly, it has been recently found that SeNPs decreases the expression of genes of pro inflammatory mediators like tumor necrosis factor-α (TNF-α), prostaglandin E_2 ($PGE_{2)}$ and thiobarbituric acid reactive substances (TBAR) in inflammation induced irradiated rats (El-Ghazaly *et al.*, 2017) .

Administered of melatonin-SeNPs (MT-se) at doses of 5, 10, or 20 mg/kg to Bacillus Calmette–Guérin (BCG)/lipopolysaccharide (LPS) (BCG/LPS) treated mice for 10 days, significantly reduced the increase in plasma aminotransferase, reduced the severe extent of hepatic cell

damage and the immigration of inflammatory cells. The MT-Se particles also attenuated the increase in the content of thiobarbituric acid-reactive substances and enhanced the decrease in reduced activities of superoxide dismutase and glutathione peroxidase (GPx). However, treatment with MT-Se suppressed the increase in nitric oxide levels both in plasma and liver tissue. Furthermore, supplementation with MT-Se at the dose of 10 mg/kg (composed of 9.9 mg/kg melatonin and 0.1 mg/kg selenium) had great capability to protect against hepatocellular damage than a similar dose of melatonin (10 mg/kg) or selenium (0.1 mg/kg) alone. This effect may relate to its higher antioxidant efficacy in decreasing lipid peroxidation and increasing GPx activity (Wang *et al*., 2005) .

2.8 Nutritional sources of selenium

Dietary selenium comes from meat, nuts, cereals and mushrooms. Brazil nuts are the richest dietary source (though this is soil-dependent, since the Brazil nut does not require high levels of the element for its own needs) (Junior *et al*., 2017) .The US Recommended Dietary allowance of selenium for teenagers and adults is 55 μg/day (Ghimire *et al*., 2019) . Selenium as a dietary supplement is available in many forms, including multi-vitamins/mineral supplements, which typically contain 55 or 70 μg/serving . Selenium-specific supplements typically contain either 100 or 200 μg/serving (Constantinescu-Aruxandei *et al*., 2018 ; Trüeb , 2020).

In June 2015, the US Food and Drug Administration (FDA) published its final rule establishing there quirement of minimum and maximum levels of selenium in infant formula (FDA , 2015) .The selenium content in the human body is believed to be in the 13–20 mg range (Aliasgharpour and Rahnamaye Farzami , 2013) .

2.9 High and Low level of Selenium

Although selenium is an essential trace element, it is toxic if taken in excess. Exceeding the tolerable upper intake level of 400 micrograms per day was considered harmless and lead to selenosis (Krohn *et al*., 2016). This 400 μg tolerable upper intake level is based primarily on a 1986 study of five Chinese patients who exhibited overt signs of selenosis and a follow up study on the same five people in 1992(Krinsky *et al*., 2000).

Se concentration in edible parts of main crops ranged from 0.005 mg kg^{-1} to 4.17 mg kg^{-1}, and cereal plants had a higher Se-enrichment ability than tuber plants. The probable dietary intake of Se in high-Se areas was decreased to 959.3 μg d^{-1} in recent years, which might be attributed to tap water as drinking water in recent year rather than well water-dependent and changes in dietary structure, but still far above the permissible value of 400 μg d^{-1} (Lyu *et al*., 2022) .

Serum selenium showed limited association with consumption of locally produced foods, while pulses and vegetables, along with cereals and pulses, were associated with higher hair and nail selenium contents, respectively. Association of a number of adverse health endpoints with serum and hair selenium was stronger than for nail selenium contents. Such endpoints included higher prevalence of nausea and vomiting, bad breath, worm infestation, breathlessness exert and bad breath, chest pain, hair and nail abnormalities and loss, garlic odor, edema, spontaneous abortion, and overall selenosis. In contrast, we gathered no evidence of dermatitis or loss of appetite in residents most exposed to selenium (Chawla *et al*., 2020) .

Elemental selenium and most metallic selenides have relatively low toxicities because of low bioavailability (Garousi, 2015) . Arsenic (As) and cadmium (Cd) are elements arousing major public health

concerns associated with environmental pollution, high toxicity potential, and carcinogenic nature. However, selenium (Se) at low doses and incorporated into enzymes and proteins has antioxidant properties and protects animals and humans from the risk of various diseases . In general, recent reports show that Se, regardless of its form (as selenite, selenomethionine, nanoSe, or Se from lentils), can reduce As- or Cd-mediated toxicity in the liver, kidney, spleen, brain, or heart in animal models and in cell culture studies. Se antagonizes the toxicity of As and Cd mainly through sequestration of these elements into biologically inert complexes and/or through the action of Se-dependent antioxidant enzymes (Zwolak , 2020) .

Hydrogen selenide is an extremely toxic, corrosive gas. Selenium also occurs in organic compounds, such as dimethyl selenide, seleno-methionine, seleno-cysteine and methylseleno-cysteine, all of which have high bioavailability and are toxic in large doses (Fan and Vinceti , 2015). Biomarkers of Se status decline strongly in pregnancy, severe illness, or COVID-19, reaching critically low concentrations. Notably, these conditions are associated with an increased risk for autoimmune disease (AID). Positive effects on the immune system are observed with Se supplementation in pregnancy, autoimmune thyroid disease, and recovery from severe illness (Schomburg , 2021) .

Selenium deficiency, defined by low (<60% of normal) selenoenzyme activity levels in brain and endocrine tissues, occurs only when a low selenium level is linked with an additional stress, such as high exposures to mercury or increased oxidant stress from vitamin E deficiency (Ralston and Raymond , 2010) .

Selenium interacts with other nutrients, such as iodine and vitamin E , and other minerals, such as zinc and copper (Mann and Truswell , 2017) . High doses of Se supplements in pregnant animals might disturb

the Zn:Cu ratio and lead to Zn reduction; in such treatment cases, Zn levels should be monitored. Further studies are needed to confirm these interactions (Kachuee *et al*., 2013) .

2.10 *Bacillus clausii*

Classification

Kingdom ; (Eubacteria)

Domain ; (Bacteria)

Phylum ; (Firmicutes)

Class ; (Bacilli)

Order ; (Bacillales)

Family ; (Bacillaceae)

Genus ; (*Bacillus*)

Species ; (*clausii*)

Bacillus clausii is a gram-positive, the cell wall is made up of the peptidoglycan murien , spore forming rod , *B. clausii* cells tend to line up into chain-like formation ,observable as a long rod cell. *B. clausii* is an endospore producing microbe that creates ellipsoidal spored located sub-terminally or para-centrally in the sporangium , widely used as probiotic (Paparo *et al*., 2020) .

Probiotics have been used for hundreds of years to treat different diseases. They have been used since the 1960s to treat viral diarrhea in children and the side effects of antibiotic administration (Jayanthi and Sudha , 2015) . Antibiotic-associated side effects with Clostridioides difficile diarrhea are well known scenarios , therefor probiotics were proven to be efficient in treatment (Guarino *et al*., 2015) .

Recent research on safety of *Bacillus clausii* administration has concluded that it has intrinsic resistance mechanisms to some antibiotics (e.g. macrolides) , but it does not have toxin producing genes or transferrable antimicrobial resistance, making it very safe (Upadrasta *et*

al., 2016 ; Lakshmi *et al*., 2017). Since then, several studies have been carried out demonstrating no related side effects linked to its use (Sudha *et al*., 2013).

Side effects have been inconsistently reported and have not been adequately assessed. In spite of this, according to the World Health Organization, probiotics might be responsible for systemic infections and deleterious metabolic activities (Doron and Snydman , 2015) .

B. clausii was found to be resistant to broad-spectrum antibiotic chloramphenicol, anti-mycobacterial rifampicin, beta-lactamase inhibitor amoxiclav, first-generation antibiotic cefaloridine, penicillin ampicillin, and tetracycline. *B. clausii* was resistant to both the aminoglycoside antibiotics (streptomycin and kanamycin) . Off first-generation fluoroquinolones studied, *B. clausii* was resistant to ciprofloxacin but partially sensitive to norfloxacin, ofloxacin and to macrolide azithromycin (Srinivas , 2020) .

Spores of *Bacillus* are heat stable, capable of surviving the low pH of the gastric barrier, additionally products made on them can be stored at room temperature without any deleterious effect on viability (Abbrescia *et al*., 2014) .

2.11 Mechanism of resistance to antibiotics

The treatment of infections is increasingly complicated by the ability of bacteria to develop resistance to antibiotics. Bacteria may be intrinsically resistant to one or more classes of antibiotics, or may acquire resistance by de novo mutation or by the acquisition of resistance genes from other organisms. Better understanding of mechanisms of antibiotic resistance would allow the development of control strategies to reduce the spread of resistant bacteria and their evolution. Bacteria may be intrinsically resistant to a class of antibiotics or may acquire resistance

(Sartelli *et al*., 2016) . Main mechanisms of resistance to antibiotics that illustrated in figure (2.5) can be caused by :

- inactivation of the antibiotic through hydrolysis or modification
- an alteration or the protection of the target site of the antibiotic that reduces its binding capacity
- the modification of metabolic pathways to circumvent the antibiotic effect
- the reduced intracellular antibiotic accumulation by decreasing permeability and/or increasing active efflux of the antibiotic from the cell by a series of membrane-associated pumping proteins .

Bacteria can develop resistance to antibiotics by mutating existing genes (vertical evolution) or by acquiring new genes from other strains or species (horizontal gene transfer) (Kapil *et al*., 2020) . Many of the antibiotic resistance genes are carried on genetic elements (plasmids, transposons or phages) that act as vectors that transfer these genes to other members of the same bacterial species, as well as to bacteria in another genus or species (Bag *et al*., 2019) .

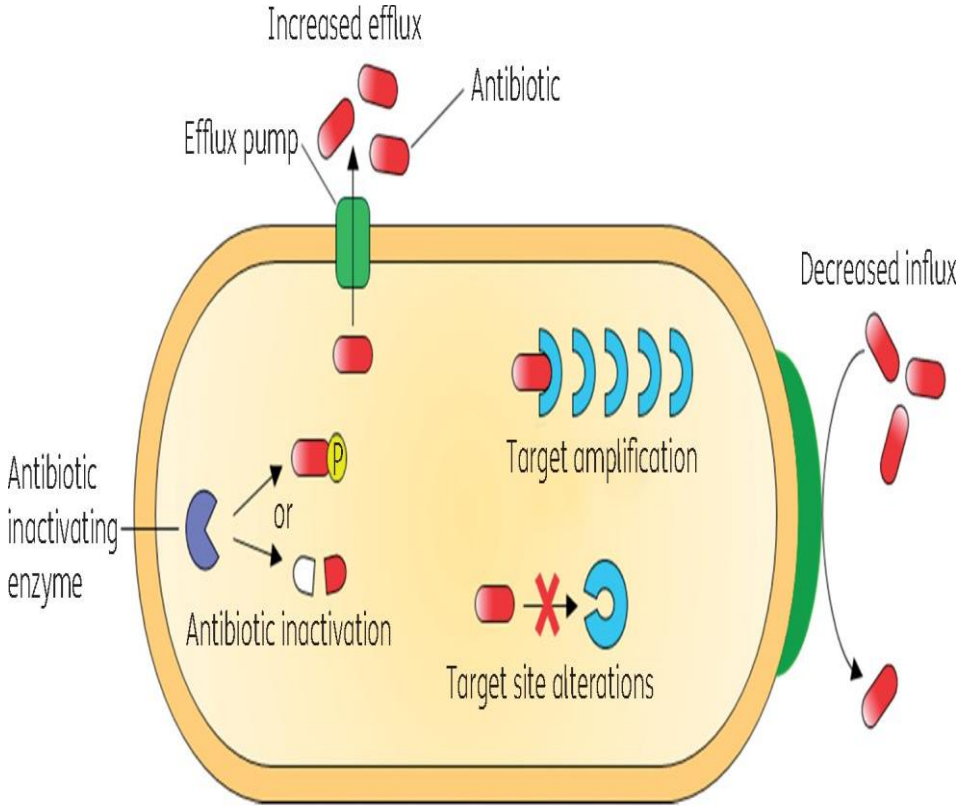

Figure (2.5) : Antibiotic resistance mechanisms of bacteria (Alav *et al*., 2018).

2.12 Antimicrobial Action Mechanisms of SeNPs

Antimicrobial activity of SeNPs, alone or in combination with standard antibiotics , has been tested against a wide range of microorganisms, including Gram-negative , Gram-positive bacteria, and fungi (El-Deeb *et al*., 2018 ; Medina Cruz *et al*., 2018) . However, studies are rare about the mechanisms of antimicrobial action of these nanoparticles. In general, it has been proposed that some nanoparticles can follow three mechanisms: (i) cell wall and membrane damage, (ii) intracellular penetration, and (iii) oxidative stress(Sánchez-López *et al*., 2020 ; Zhang *et al*., 2021) .

2.12.1 cell wall and membrane damage

Cell wall and membrane components could be involved in different adhesion pathways for nanoparticles. One of the functions of the cell wall and membrane is to protect the microorganism against environmental

threats while maintaining its homeostasis, allowing nutrients transport within the cell . The cell wall of Gram-negative bacteria has a thin layer of peptidoglycan with an additional outer membrane consisting of lipopolysaccharide. On the other hand, the cell wall of Gram-positive bacteria is typically thicker and is mainly composed of peptidoglycans (Slavin *et al*., 2017) . These structures are changed by the physical interaction between cell wall and nanoparticles and more affecting against gram-negative bacteria (Calvo and Martinez-Martinez , 2009).

Cell wall confers a negative charge on both Gram-positive and negative bacteria at neutral pH (Chung *et al*., 2004) . However, Gram-negative bacteria represent the set of microorganisms with the highest negative charge. In addition, Gram-negative bacteria have an outer membrane composed of phospholipids with partially phosphorylated lipopolysaccharides that increase the negative charge of their cell envelope (Gopinath *et al*., 2017) .

This negative charge is supposed to influence the interactions between the bacterium cell wall and the NPs or ions released from them. When SeNPs are interacted with bio-organic compounds positively charged, such as proteins or amino acids, they are attracted to the cell negative wall binding by electrostatic interactions. These nanoparticles lead to the formation of a strong bond with membranes, causing cell wall rupture and permeability (Galić *et al*., 2020 ; Filipović *et al*., 2021).

Thus, the interaction between SeNPs and microorganisms begins with their adhesion to the microbial wall and cell membrane. This binding is based on the electrostatic attraction between the negatively charged microbial cell membrane and the positive or less negatively charged SeNPs (Zhang *et al*., 2021) . After the attraction and interaction of SeNPs with the microorganism, structural and morphological changes are caused by the SeNPs, leading to the interruption of both membrane permeability

and respiratory functions. This effect takes place through membrane depolarization, disruption of cell integrity, and finally, cell death (Huang *et al*., 2016 ; Chandramohan *et al*., 2019) .

As a result of increased membrane permeability and cell wall disruption, cell contents, including proteins, enzymes, DNA, ions, metabolites and energy reserves, seep into the environment (Zhang *et al*., 2021 ; Nguyen *et al*., 2017) . SEM and TEM analyses showed that when bacteria are treated with SeNPs, they have a cellular contraction and take an irregular shape compared to a control group of bacteria (Huang *et al* ., 2016 ; Nguyen *et al*., 2017 ; Chandramohan *et al*., 2019 ; Huang *et al*., 2019) .

For example, after incubation of *E. coli* and *S. aureus* with coated SeNPs, cell lysis and intracellular leakage were observed in *E. coli*, while in *S. aureus*, there were sunken cell walls and cytoplasmic release, including cell wall disorganization (Huang *et al*., 2016) .

In addition, the mechanism by which SeNPs damage bacteria cytoplasmic membrane is by producing a rapid depolarization of the membrane (Calvo and Martinez- Martinez , 2009) . On the other hand SeNPs have a related mechanism to metabolic interference through the alteration of intracellular concentrations of adenosine triphosphate (ATP) (Huang *et al*., 2019) .

2.12.2 Intracellular penetration and damage

Metabolic functions of the cell are affected since NPs penetrate through the membrane , especially when it presents a certain level of damage interacting with DNA and proteins (Fu *et al*., 2015) . This action represents one of the proposed mechanisms for the antimicrobial activity of NPs, which is based on the release of ions (Skalickova *et al*., 2017) .

In this sense, several researchers have reported that Se^0 is soluble in trace concentrations in aqueous environments . Therefore, the amount

of Se ions released from SeNPs is likely to be very small. In other words, the antimicrobial effects of Se ions may be too weak, representing a non significant mechanism of SeNPs (Huang *et al*., 2019 ; Galić *et al*., 2020).

Although the studies are very recent, they mark a trend in research proposals to encompass the entire set of antimicrobial mechanisms associated with the penetration of compounds through the cell membrane of bacteria and their subsequent interaction within their metabolism.

2.12.3 Oxidative Stress

Reactive oxygen species (ROS) are oxygen-containing molecules that have a strong redox potential. Under normal conditions, the production of ROS and the antioxidant capacity of the cell are balanced. However, if there is an imbalance between the antioxidant mechanism and the excessive production of ROS, the redox balance of the cell favours oxidation, and this causes oxidative stress. Furthermore, oxidative stress is a cellular process involved in many aspects of cell signalling, although when it occurs excessively, it causes irreversible damage to cell metabolism, affecting viability (Abdal Dayem *et al*., 2017; Johnson and Hug , 2019 ; Sánchez-López *et al*., 2020) .

Many researcher reports that after the addition of SeNPs, these are absorbed on the surface of bacteria and trigger cellular oxidative stress (Abdal Dayem *et al*., 2017 ; Wang *et al*., 2017 ; Zhang *et al*., 2021) . To overcome this stress, cells exhibit protective responses that include enzymatic or non-enzymatic defence mechanisms (Fu *et al*., 2015) .

When oxidative stress overcomes defence mechanisms, the cell wall and biomolecules such as proteins, lipids and DNA are subjected to damage caused by ROS and free radicals such as hypochlorous acid (HOCl), hydrogen peroxide (H_2O_2), hydroxyl radical (OH), superoxide anion (O_2^-) and singlet oxygen ($^1O_2$) (Abdal Dayem *et al*., 2017 ; Wang *et al*., 2017).

ROS generation is responsible for antibacterial activity when Bio-SeNPs were tested against Gram-positive and Gram-negative bacteria (Zhang *et al*., 2021) .

2.13 The selective toxicity of nanomaterials on in vitro cancer cell models

Several mechanisms are involved in NP-mediated in vitro toxicity in normal (i.e. noncancerous) and cancerous cells. Cellular responses to NP exposure might include those at cell , organelle and gene level or a combination of them (Patil *et al*., 2016). Direct cytotoxic effects might be apoptosis or necrosis (or both) mediated , with a number of mechanisms leading to cell death, changes in proliferation patterns and effects on cell differentiation. High levels of reactive oxygen species (ROS) production , downregulation of antioxidant enzyme coding genes , lipid peroxidation and genotoxic effects, may be involved in the integrated cellular response to NPs (Choi *et al*., 2016 ; Abdal Dayem *et al*., 2017) .

Apoptosis is a common response of cells to NP treatment . Azizi and colleagues found that albumin-coated silver NPs (AgNPs) LD50 were several times lower for breast cancer cells than for normal white blood cells. Apoptosis assays such as Annexin V and microscopy counts of apoptotic bodies demonstrated that albumin-coated AgNPs exert pro-apoptotic selective effects on breast cancer cells while normal blood cells remained viable at the tested concentrations and times of exposure (Azizi *et al*., 2017) .

Chapter Three

Materials
and
Methods

3. Materials and Methods

3.1 Materials

3.1.1 Equipments and instruments

Equipments and instruments used in this study are listed in (table 3.1).

Table (3.1): Equipments and instruments used in this study.

Equipment and Instruments	Manufacture company	Origin
Atomic Force Microscope (AFM) , X ray diffraction (XRD)	Broker	Germany
Autoclave	Labtech	Korea
Balance (electrical)	Denver	Canada
Centrifuge	Hitachi	Japan
Deep freezer , VITEK 2- Compact system1	Biomerieux	France
Digital camera	Sony	Japan
Distillator	GFL	Germany
ELISA system	Beekman	Austria
Fourier Transform Infrared (FT-IR)	Perkin-Elmer 1725x	Japan
Hood	Bio Lab	Korea
Incubator , Oven	Memmert	Germany
Light Microscope	Olympus	Japan
Micro and cooling centrifuge	Hermle Labortechnik	Germany
Micropipette	Eppendrof	Germany
pH meter	Orient	USA
Refrigerator	Beko	Korea
Scanning electron microscope	FEI	Netherland
Shaking incubater	Gallenkamp	England
Thermocycler	Bio- Rad	USA
UV-visible spectrophotometer	Shimadzu	Japan
Vortex mixer	Thermolyne	USA

3.1.2 Chemical and biological materials

The Chemical and biological materials used in present study are listed in (table 3.2)

Table (3.2): Chemical and biological materials used in this study .

Materials	Manufacture company	Origin
2,2-diphenyl-1-picrylhydrazyl	Sigma-Aldrich	USA
Ethanol (96%)	BDH	England
Glycerol	Sigma	USA
Hydrochloric acid (HCl)	EMC	Germany
Methanol	BDH	England
Phosphate buffer saline (PBS)	Bioworld	USA
Sodium selenite (Na_2SeO_3)	Sigma	USA
Sodium hydroxide (NaOH)	EMC	Germany
Gram stain	Himedia	India
Ethidium Bromide Solution	Bio Basic	Canada
DNA Ladder 100 bp	Promega	USA
DNA loading dye	Promega	USA
Agarose	Conda	USA
Crystal violet powder	BDH	England
Sucrose	Himedia	India
Tris-EDTA (TE) buffer	Bio Basic	Canada

3.1.3 Culture Media

The culture media which used in the present study and the purpose from used it listed in table (3.3).

Table (3.3) : Culture media that used in this study with their purpose .

Culture Media	Company/origin	Purpose
Nutrient agar	Himedia /India	used for the growth and isolate bacterial types
Brain heart infusion broth	Himedia /India	Used for preservation of bacteria
Brain heart infusion agar	Himedia /India	Used for growth ,activation and maintenance of bacteria
Chromogenic Agar	Orientation/ France	used for the growth and differentiate between bacterial types in urine
Luria Bertani broth	Lab /USA	Used for maintenance and propagation of UPEC
Muller Hinton agar	Lab /USA	Determine the sensitivity test of bacteria to antibiotic
MacConky agar	Lab /USA	Growth of G-ve bacteria and determination their ability to lactose fermentation
Mannitol salt agar	Himedia/ India	Growth and isolate of staphylococci and determination the bacterial ability to mannitol fermentation
RPMI-1640 Medium	Gibco/ U.K	Used for cell growth and viability
Serum-medium	Gibco/ U.K	Used for growth cell and inactivate Trypsin EDTA

3.1.4 Antibiotic discs

The antibiotics used in this study are listed in table (3.4).

Table (3.4): Antibiotic Disc , Symbol and Potency

Antibiotic class	Antimicrobial agent	Symbol	Disk content (µg) (potency)	Mode of action
Penicillins	Ampicillin	AM	10	Cell wall synthesis inhibitors
B-LACTAM COMBINATION AGENT	Amoxicillin/calvulanic	AMC	30	Cell wall synthesis inhibitors
Carbapenems	Imipenem	IPM	10	Cell wall synthesis inhibitors
Aminoglycosides	Amikacin	AK	30	Protein synthesis inhibitor
Macrolides	Azithromycin	AZM	15	Protein synthesis inhibitor
Tetracyclin	Doxycycline	DO	30	Protein synthesis inhibitor
Fluoroquinolones	Ciprofloxacin	CIP	5	DNA synthesis inhibitor
Quinolones	Nalidixic acid	NA	30	DNA synthesis inhibitor
Nitrofurans	Nitrofurantoin	F	300	DNA synthesis inhibitor
Folate pathway Antagonistic	Trimethoprim / Sulfamethoxazole	SXT	25	Folic acid Synthesis inhibitor

3.1.5 Kits :

The commercial kits used in the present study are shown in table (3.5)

Table (3.5): kits for identification of bacteria and extraction of RNA

No.	Kit	Company	Country
1	**VITEK-2 compact system kit**	Biomerieux,	France
2	**Total RNA Extraction Kit**	iNtRON	Korea
	Trizol reagent 100ml		
3	**RealMOD™ Green SF 2X qPCR mix**	iNtRON	Korea
	RealMODTM Green SF 2X qPCR mix (1ml)		
4	**Go Taq® G2 Green Master Mix Kit**	iNtRON	Korea
5	**DNase I enzyme kit**	Promega	USA
	DNase I enzyme		
	10x buffer		
	Free nuclease water		
	Stop reaction		
6	**AccuPower® RocketScript™ RT PreMix**	Bioneer	Korea
	RocketScript Reverse Transcriptase (200U)		
	5X reaction buffer		
	dNTP 250µM		
	DTT 0.25mM		
	RNase Inhibitor (1U)		
7	**Wizard® SV Gel and PCR Clean-Up System**	Promega	USA
	Membrane Binding Solution		
	Membrane Wash Solution (concentrated)		
	Nuclease-Free Water		
	Wizard® SV Minicolumns		
	Collection Tubes (2ml)		

8	**MTT kit**	Intron	Korea
	MTT solution 3-(4,5-dimethylthiazol-2yl) 2,5diphenyl -2H- tetrazolium bromide		
	Solubilization solution		

3.1.6 Primers

Real Time PCR primers for quantification gene expression detection in Enterococcus faecalis and Escherichia coli were designed in this study by using NCBI Genbank database and Primer3 plus primer design software. These primers were provided by Macrogen company from Korea as following table (3.6) , (3.7) :

Table (3.6): *Enterococcus faecalis* qPCR detection gene primers with their nucleotide sequence .

Primer	Sequence (5'-3')		Product Size	Genbank code
Esp gene	F	TAAAGAAGAGAGCGGAGACACG	135 bp	KF550185.1
	R	ACAAGTTGCGCTTTGTGACC		
hly gene	F	GCATCAGCAGGAAATGAGTCG	90 bp	KF020739.1
	R	AGCTCCGACGGTAATTACAGAC		
gelE gene	F	AGGCGGTTACGTTTTAGCTG	143 bp	DQ845100.1
	R	TTTTGAATCCGTCCCAGTCG		
fsrA gene	F	TTGAACAACTGCATCCAGATTTG	128 bp	HE574483.1
	R	TGAGACTGGTACTTCCGTTCC		
16rRNA gene	F	GCAGCAAACGCATTAAGCAC	125 bp	LT844634.1
	R	AAGGTTCTTCGCGTTGCTTC		

Table (3.7): *Escherichia coli* qPCR detection gene primers with their nucleotide sequence .

Primer	Sequence (5'-3')		Product Size	Genbank code
hly gene	F	CTGGATGTTGTCTCCGGAATTC	78bp	MN708341.1
	R	TGTTCCTGTATGTGCGTCAC		
fimH gene	F	ATGCGGGCAACTCGATTTTC	94bp	JX847135.1
	R	GCTGGAATAATCGTACCGTTGC		
luxS gene	F	AAGACGTGCTGAAAGTGCAG	148bp	NC_000913.3
	R	TCTTCGTTGCTGTTGATGCG		
qseC gene	F	TCGCCTGGAAACAAACAACG	75bp	NC_000913.3
	R	TTAACCGCTTGGCAAACAGC		
16rRNA gene	F	TTCGATGCAACGCGAAGAAC	122 bp	AJ567540.1
	R	TTTCACAACACGAGCTGACG		

3.2 Methods

3.2.1 Study Design

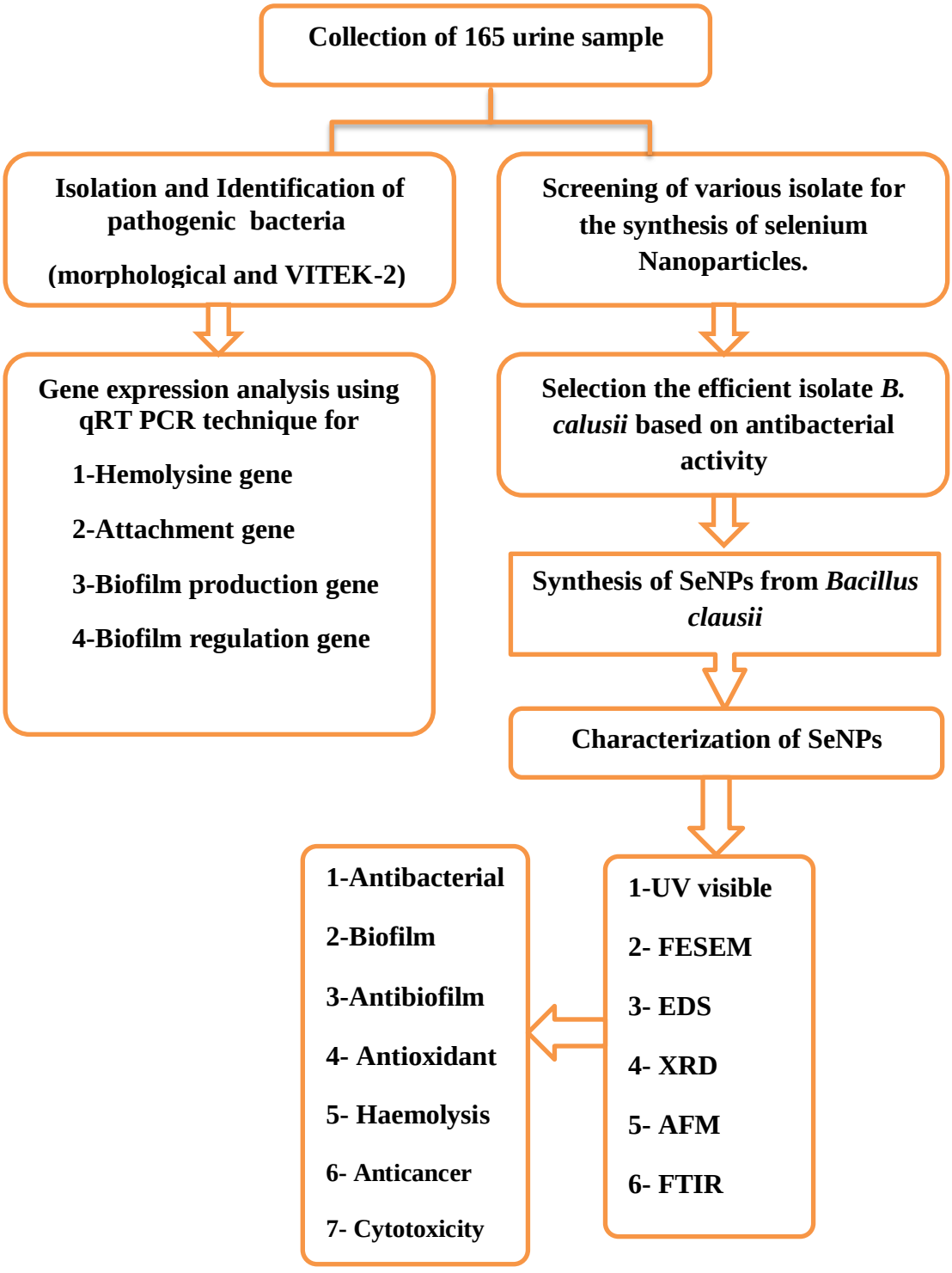

3.2.2 Collection of sample

A 165 samples of urine were collected from patients with clinical symptoms and suspected to UTI admitted in Al-Hilla Teaching Hospital and Public Health Laboratory in Babylon province during a period from (March - October 2021) . About 10 ml of Clean-Catch midstream urine of the patients that were diagnosed by a physician depending on clinical manifestation as patient with UTI was collected in the morning in sterile containers , ensure that the patient has not taken any drug for three days before collection of urine samples . Samples were transported to the laboratory in the college of science .

3.2.3 Media preparation and sterilization technique

All culture media presented in table (3.3) were prepared according to the manufacturing company instructions .The constituents were dissolved in distilled water completely , sterilized by autoclaving at 121Cº for 15min at 15 pound/inch^2. After cooling to 45-50 C° each medium was dispensed into sterile petri dishes in case of agar media and in sterilized screw tubes in the case of broth media . The work performed in laminar flow cabinets . Then , poured media were incubated for 24hr at 37 C° to ensure sterility. (MacFaddin , 2000).

3.2.4 Preparation of Reagents & Solution

3.2.4.1 Phosphate Buffer Saline (PBS)

Phosphate buffer saline was prepared by dissolving 1 tablet of (PBS), PH 7.2 in 100 ml deionized distilled water (DDW) . It was used in biofilm and antibiofilm experiments (Collee *et al*., 1996).

3.2.4.2 Hydrochloric acid (0.25 M)

It was prepared by adding 20.444 ml of 37.5% hydrochloric acid , and slowly dilute to 1 liters D.W. in a volumetric flask. Then allowed the

solution to cool to ambient temperature and properly mix it (Chen *et al*., 2020).

3.2.4.3 Sodium Hydroxide (NaOH) Solution (1M)

Sodium hydroxide (1M) was prepared by dissolving 4g of NaOH up to 50 ml of distilled water; this solution was used to adjust the pH during pH optimization step (Baker and Silverton, 2014).

3.2.4.4 DPPH Solution (0.1mM)

2,2-Diphenyl-1-picrylhydrazyl solution prepared by dissolving 0.00394 g. of 2,2-Diphenyl-1-picrylhydrazyl in 100ml ethanol (99.8%). The solution was used for detection of antioxidant activity of SeNPs (Sentkowska and Pyrzyńska , 2022).

3.2.4.5 TBE Solution

TBE buffer was prepared as 10x by Promega company. Tris-borate-EDTA buffer used at concentration of 1 X (1: 10 dilution of the concentration stock). The stock solution was diluted by D.W. and stored at room temperature.

3.2.4.6 Crystal Violet Solution(1%)

Crystal violet solution was prepared by dissolving 1gm of crystal violet in 100 ml Distilled water (Vandepitte *et al*., 2003).

3.2.4.7 Trypsin-(EDTA) solution

It was prepared by dissolving 15gm of trypsin-EDTA in 125 ml of D.W and constantly added by stirring the volume completed to 1 liter, and then filtration by using 0.22 μm Millipore filters and stored at (- 80˚C). These solution was used to detach and disaggregate the adherent monolayer cells from the bottom of the culture vessel in cytotoxicity assay .

3.2.5 Preservation and maintenance of bacterial isolate

The preservation and maintenance of isolates were done according to (Silhavy *et al*., 2010) as follows:

3.2.5.1 Short term preservation

The positive cultures were stored on nutrient agar at 4C° until further testing.

3.2.5.2 Long term preservation

Fresh 24 hr nutrient agar cultured isolates frozen in 20% glycerol brain –heart infusion broth and stored at -20 C° until required.

3.2.6 Morphological Identification of Isolates

The collected specimens were inoculated on nutrient agar and incubated for 24 hr at 37 C°. Dishes that did not appear grow within 24 hr were incubated for another 24 hr before counting negative result . After that, the isolated colonies were further subjected to subculture and purification on MacConkey agar, mannitol salt agar and Chromogenic agar , all positive culture subjected to VITEK-2 compact system to confirm the result (Munoz-Dávila *et al*., 2013).

3.2.7 Identification of bacteria by VITEK-2 Compact System

Suspension of bacteria was prepared according to the manufacturer's instructions. An adequate number of colonies was obtained by transferring an overnight pure culture and suspending it in 3.0 ml of sterile saline in (polystyrene) test tube. Adjustment of turbidity to 0.5 McFarland was made. Employing a Densi-Chek turbidity meter. Finally, the vitek-2 chamber with the specimen suspension tubes was loaded with the Gram negative -ID, and Gram positive -ID cassette (Karagöz *et al*., 2015).

3.2.8 Selection the efficient isolate that producing SeNPs

Eight isolates of bacteria (*Lactobacillus plantarium , Lactobacillus casei , Lactobacillus lactis , Lactobacillus bulgaricus , Bacillus cereus ,*

Bacillus subtilis , Bacillus clausii , Bacillus licheniformis) obtained from the laboratories of the Faculty of Science were screened for biosynthesis of selenium nanoparticles. These isolates were grown in brain heart infusion broth for 24 hr at 37 ° C. After incubation , the colloidal suspension was centrifuged at 10,000 rpm for 15 min , 4° C . The precipitate was discarded , and the supernatant was applied to the Na_2SeO_3 . An efficient isolate (*Bacillus clausii*) was selected based on colour change , antibacterial activity and absorption spectrum .

3.2.9 Molecular Identification of *Bacillus clausii*

Sequencing the 16sRNA gene has been used in this study for the identification of *Bacillus clausii* (Patrone *et al*., 2016).

3.2.9.1 Extraction of Bacterial Genomic DNA

Total DNA was extracted from culture broth, 1.5 ml of culture broth pipetted into Eppendorf tubes then centrifuged at 4,300 rpm for 5 min and the supernatant discarded , 200 µl of TE buffer was added , vortexes well , boiled for 15 min in water-bath , and then put on ice immediately for 1 min , this was centrifuged again at 6,700 rpm for 10 min and the supernatant was collected, which contains DNA for use as DNA template (Suwanjinda *et al*., 2007). DNA concentration and purity was estimated by nanodrop at absorbance (260 /280 nm) , DNA integrity was detected in Agarose gel electrophoresis (Bunu *et al*., 2020) .

3.2.9.2 The mixture of PCR reaction.

The polymerase chain reaction (PCR) was used to amplify fragments of DNA using Go Taq® G2 Green Master Mix Kit (promega/ USA). The reaction mixture of the specific interaction used for gene diagnosis is listed in table (3.8) and Primers that used in this study listed in table (3.9) .

Table (3.8): Contents of the Reaction Mixture of PCR

Contents of reaction mixture	Volume
Master Mix (2X)	12.5 µl
Template DNA	5 µl
Forward primer (10pmol/microliter)	2 µl
Reverse primer (10pmol/microliter)	2 µl
Nuclease free water	3.5 µl
Total	25 µl

Table (3.9): 16S rRNA primer pair

Primer name	Sequence(5-3)	Product Size (bp)	Reference
CF	5-AGAGTTTGATCCTGGCTCAG-3	1470	Loy *et al*., 2002
CR	5-GGTTACCTTGTTACGACTT-3		

PCR assay was carried out upon molecular identification using universal primers that was shown in table (3.9) . These primers synthesized by (Macrogen/Korea).Primers were dissolved using sterile DNAase free ddH_2O (PCR grade water). The stock solution (100 pmol/microliter) was prepared by adding ddH_2O to the vial containing lyophilized primer while working solution of 10 pmol/microliter was made by mixing 10 microliter of the stock primer and 90 microliter of free ddH_2O to reach a final volume 100 microliter ,the stock and working solution were stored in (-20) C° . .

3.2.9.3 PCR Program

The following parameters were used for PCR cycle independently of different researches .The optimum conditions applied in the thermo cycler are clarified in table (3.10) .

Table (3.10) : PCR conditions for amplification of 16S rRNA gene

Step	Phase	Temperature (°C)	Time	No. of cycles
1	**Initial Denaturation**	95	5 min	1
2	**Denaturation**	95	30 sec	35
3	**Annealing**	53	45 sec	
4	**Extension**	72	100 sec	
5	**Final extension**	72	5 min	1
6	**Storage**	4	Hold	1

3.2.9.4 Detection of Amplified Products by Agarose Gel Electrophoresis

Gel electrophoresis was used for detection of DNA , 1.5 gm of Agarose was weighted and applied to 100 ml of TBE (1X) buffer and microwaved until the solution became clear. After cooling the agarose to 50 C°, 5 microliter of ethidium bromide dye was added to 100 ml of melted agarose gel , and poured on preparing tray. Comb was removed after the hardening of agarose leaving wells , 5-10 microliter of DNA was mixed with 1-2 microliter of loading dye , TBE (1X) buffer was added to the electrophoresis tank. A tray with agarose was immersed in electrophoresis tank. Each well was loaded with 6microliter of DNA sample and standard molecular weight of DNA ladder (100-1500 bp) were loaded in a first well. Electrophoreses ran at 75 volt for 40 min . Gel was visualized with UV transilluminator at 280 nm and photographed by using digital Camera (Mishra *et al*., 2009).

3.2.9.5 Clean – up the gel slice to sending for sequencing

DNA purification was done by using (Wizard® SV Gel and PCR Clean-Up System) (Promega /USA) . To prepare membrane washing solution ,75 milliliters of ethanol (95%) was mixed with 15 milliliters of membrane wash solution (concentrated) . After each usage , the bottle top was carefully closed to avoid evaporation.

Agarose gel slice containing relevant DNA fragments was excised and the extra agarose removed to minimize the size of the gel slice , these steps were done by using a clean scalpel . Membrane binding solution was added at ratio of 10 µl per 10 mg of agarose gel slice . The mixture was vortexed and heated at 65 C° until the gel slice has been completely dissolved .The tube was vortexed every few minute to speed up the melting of gel slice . The tube was centrifuged quickly at room temperature , to guarantee that the content are at the bottom of the tube . The DNA fragment purification steps as following :

- In the collecting tube , SV Minicolumn was placed . After that the dissolved gel mixture was transferred to the SV Minicolumn assembly and incubated for 1 min at room temperature .
- The SV Minicolumn assembly was centrifuged at 13500 rpm for 1 min , discard flowthrough and reinsert Minicolumn into collection tube .
- The SV Minicolumn was washed by adding 700 µl of membrane wash solution (previously diluted with ethanol 95%) , centrifuged for 1 min at 13500 rpm , discard flowthrough and reinsert Minicolumn into collection tube , then repeated washing again by centrifuging for 5 min at 13500 rpm with 500 µl of membrane wash solution .
- The collecting tube was emptied , and the SV Minicolumn assembly was centrifuged for 1 min to evaporate any leftover ethanol.
- Carefully transfer SV Minicolumn to a clean 1.5 ml microcentrifuge tube , 50µl of nuclease free water was pipetted directly into the center of column without contacting the membrane . Then , incubated for 1 min at room temperature and centrifuged for 1 min at 13500 rpm .

- The SV Minicolumn has been removed and the eluted DNA was kept in a micro-centrifuge tube at -20 C° and then sent to gene sequence

3.2.9.6 Similarity Search by BLASTN

DNA sequence was analyzed for the sequence similarity to the existing DNA sequences available in the database at National Center for Biotechnology Information (NCBl), website (www.ncbi.nlm.nih.gov/blast). National Library of Medicine (NLM), and National institute of Health (NIH) .

3.2.10 Biosynthesis of Selenium nanoparticles by using *Bacillus clausii*

The pure culture of *Bacillus clausii* 5 ml were inoculated in flask containing 500 ml of brian heart infusion broth and incubated at 37 C° for 24hr . After incubation , the colloidal suspension was centrifuged at 10,000 rpm for 15 min at 4C° , the precipitate was removed and the supernatant was then passed through millipore filter (0.2 µm) to get rid of impurities . 3 mM of Na_2SeO_3 were prepared and added to 250 ml of supernatant , pH of supernatant was adjusted to (8) and then incubated for 48 hr at 37C^o in a shaking incubator (150 rpm) in aerobic condition (Singh *et al*., 2014) .

After that the reaction mixture was centrifuged at (10000 rpm , 4 C° for 10 min) , the supernatant was discarded and the sediment was taken . In order to purify selenium nanoparticles , these sediment was washed with DDW , these step were repeated three times. The final suspension was dried in oven at 40 C° for 18-24 hr . The dried powder was collected carefully and stored in sample vials for further analysis (Dhanjal and Cameotra , 2010) .

3.2.11 Characterization of Biosynthesized selenium nanoparticles

The physical characteristics of selenium nanoparticles were characterized by UV-Visible absorption spectroscopy, SEM coupled with EDXS , XRD , AFM and FTIR .

3.2.11.1 UV-Visible Spectra analysis

UV-vis spectroscopy was used for the determination of selenium nanoparticles in solution . Two ml of a aliquot selenium nanoparticles was measured in a 1 cm path-length quartz cuvette and scanned at a medium scan rate 2 nm / second , in the range of (200 – 800) nm, The absorbance at which the peak was formed was noted (Gangadoo *et al*., 2017) .

3.2.11.2 Analysis by Field Emission scanning electron microscopy (FESEM)

Field Emission Scanning electron microscope (FESEM) was used for characterization the morphological and size of selenium nanoparticles in electron microscope unit , / University of Kashan . The SEM was carried by smearing the sample on a small piece of adhesive carbon tape that was fixed on a brass stub. The sample was then subjected to gold coating using a sputtering unit for 10 sec at 10 mA of current. The gold coated sample placed in the SEM chamber and secondary electron/back scattered electron images were recorded. The microscope operated with different magnification ranging from 15000 x to 35000 x and voltage 20-30 KV (Ramamurthy *et al*., 2013) .

3.2.11.3 Analysis by energy dispersive X-ray spectroscopy (EDX)

Energy dispersive spectroscopy (EDS) was performed to confirm the conversion of selenium ions into elemental selenium (Se) using a FEI Tecnai

F20 TEM/STEM operated at 200 kV. A small aliquot of the sample was pipetted onto a carbon coated 200 mesh copper grid (Gangadoo *et al*., 2017).

3.2.11.4 X-ray diffraction (XRD)

The X-ray diffraction was used for characterization of selenium nanoparticle at University of kashan , the powder of selenium nanoparticle was used for test. The nanoparticle sample was dispersed on a low background noise sample holder and analyzed in a Bruker D8 Advance X-Ray diffractometer equipped with a LynxEYE detector. X ray diffraction analysis was operated at a voltage of 40 kV, with current of 40 mA, with copper radiation of 1.54060 Å. The scanning was performed in the 2θ range of 10° to 40° at 0.02°/min with time constant of 1.2 s. (Gangadoo *et al*., 2017) .

3.2.11.5 Atomic force microscope(AFM)

Atomic force microscope(AFM) was used for characterization the selenium nanoparticle in University of Kashan , A drop of (SeNPs) was placed on a slide and a thin smear was made. The smear was air-dried and the slide was scanned and observed under Atomic Force Microscope (Model- Nanosurf easyscan 2 AFM , Switzerland) (Singh *et al*., 2014).

3.2.11.6 Fourier Transform Infrared Spectroscopy (FTIR)

The transmittance of the prepared formulations was accomplished by FT-IR spectrophotometer , in a spectral range of 400-4000 cm^{-1} at 2 cm^{-1} resolution. The data sets were averaged over 64 scans (Tugarova *et al*., 2018) .

3.2.12 Influence of Selenium Nanoparticle Against pathogenic bacteria

3.2.12.1 Antibacterial activity of selenium nanoparticles

This method was done on Muller Hinton agar as described in (Boroumand *et al*., 2019) **:**

- Turbidity of each bacterial isolates compared to McFarland 0.5 standard to get the right concentration for each of them .
- A 0.1 ml of each bacterial isolates were added to petri dish containing Muller Hinton agar and spread by spreader and left the dishes for an 1 hr.
- Wells were made by using cork borer (5 mm diameter) as it was equal distance between the well and the other.
- The SeNPs were dissolved with deionized water to get various concentrations (100 , 300 , 500) µg/ ml.
- A 40 microliter of each concentration of Se NPs were added to each well and incubated in the incubator at 37 ° C for 24 hr .
- Nanoparticles inhibition zones were measured by a ruler .

3.2.12.2 Detection of Minimum inhibitory concentration (MIC) of nanoparticle

The MIC is a lowest selenium nanoparticles concentration that inhibited completely the bacterial growth can be detected by using micro-titerplate method , The turbidity of bacterial suspension was compared and matched with the turbidity of 0.5 McFarland units . The McFarland 0.5 standard corresponds approximately to a homogeneous suspension of 1.5×10^8 cells/ml , An amount of 100 µl of BHI media was transferred to each well , 100 µl of SeNPs (2048 µg/ml) was added in each well of Column 2 . Serial dilutions were performed from Column 2 to Column 11, to obtain the final NPs concentrations, which varied from 1024µg/ml in (2^{nd} well) to 2 µg /ml in (11th well).

A 10 microliter of bacterial inoculum were added to each well , except all wells of (column 1). NPs free well (Column 12) containing medium and inoculum and (column 1) contained media only . The microtiter plate incubated at 37°C for 24 hr . OD at 570 nm was recorded

spectrophotometrically . MIC was determined as the lowest NP concentration showing absence of growth as compared with the growth in the SeNPs -free well (Kumar *et al*., 2015) .

3.2.13 Antibiotic Susceptibility Test (AST)

The antibiotic resistance of bacterial isolates was assessed using disc diffusion method , according to the national committee for clinical laboratory standards (NCCLS) guidelines(Kiehlbauch *et al*., 2000). The bacterial suspension 0.5 McFarland standard was inoculated by swabbing the MHA surface 3 times by rotating to ensure an even distribution , after 10 min antibiotic discs of Azithromycin (15 μg), Nitrofurantion (300 μg), Imipenem (10 μg), Amikacin (30 μg) , Nalidixic acid (30 μg) , Ciprofloxacin(5 μg) , Doxycycline (30 μg) , Amoxicillin/calvulanic acid (30 μg) , Trimethoprime / sulphamethoxazole (25 μg) , Ampicillin (10 μg) were placed on Mueller Hinton agar (MHA) surface and kept at 37 C° for 24 h (Sharma and Chauhan, 2014).

3.2.14 Synergistic effect of nanoparticle and antibiotic

The antagonistic activity of antibiotic and selenium nanoparticles combination were determined by the modified disc diffusion method according to the NCCLS guidelines . The MHA plates were seeded with the above antibiotic disc impregnated with selenium nanoparticle (32 μg /ml) for (*E. faecalis* and *S. saprophyticus*) and (64 μg /ml) for (*K. pneumoniae and E.coli*) along with plain antibiotic disc taking as positive control , the MHA plates were kept at 4C° for 1 hr to allow the proper diffusion , after that kept at 37 C° for 24 hr . The zones of inhibition were measured by using a caliper micrometer against the back of the petri plates (Varak and Priya, 2019).

3.2.15Antioxidant assay of SeNPs

Antioxidant activities of SeNPs synthesized from *Bacillus clausii* were detected by using DPPH (2,2-Diphenyl-1-picryl- hydrazyl) radical

scavenging assay according to the procedure described by (Sentkowska and Pyrzyńska, 2022) as the following :

100 µl of SeNPs with different concentration (50 , 100 , 150 µg/ml) was mixed with 100 µl of DPPH (final DPPH concentration : 0.1 mmol/L) in a 96 well microplate . The reaction mixture was incubated in dark at room temperature for 30 min . The absorbance of the mixture was recorded at 517 nm spectrophotometrically using ELISA reader. The negative control consisted of methanol-DMSO mixture and DPPH solution, while ascorbic acid was used as a reference .The inhibition of the DPPH radical by selenium was calculated according to the following special formula:

$$inhibition\ (\%) = \frac{(Abs\ of\ control - Abs\ of\ test)}{(\text{Abs of control})}\ X\ 100$$

3.2.16 Haemolysis Effect of SeNPs

Haemolysis assays were performed on the human red blood cells of one healthy donor and collected in anticoagulant EDTA tube : 2 ml of blood was applied to each tube and incubated for 30 m with SeNPs (50, 100 , 150 µg/ml) which suspended in tyrode .Triton X- 100 1% was used as positive control , Tyrode as negative control. The suspension was incubated at room temperature on a shaking plate during 1 hr , 4 hr and 24 hr . After the incubation time, the suspension was centrifuged at 10 000 xg over 5 min and then read OD in spectrophotometer at 550 nm. Positive and negative controls induced 100% and 0% of lysis, respectively (Mesdaghinia *et al*., 2019) .

3.2.17 Biofilm formation assay

3.2.17.1 Congo red method

Congo red method is used for qualitative assessment of biofilm formation. The result was recorded as changing the color of a colony from

red to black on the Congo red agar . Congo red agar is a specially formulated medium consisting of brain heart infusion broth (37 gm/L), sucrose (5 gm/L), agar (10 gm/L), and Congo red (8 gm/L) . To obtain Congo red agar we prepared a Congo red stain as stock solution, autoclaved at 121 C° for 20 min then applied to autoclaved BHI agar supplemented with sucrose at a temperature of 55 Cº. The bacterial strains were inoculated and incubated at 37 C° for (24 – 48) hr , then read the result as following: if the bacteria formed black colonies with a dry crystalline consistency that was mean it biofilm producer isolates while if it formed red colonies that was mean the non-biofilm producer isolates (Ruchi *et al*., 2015).

3.2.17.2 Microtiter Plate Method (MTP)

Microtiter plate (MTP) is a quantitative method to determine biofilm production by microtiter plate reader as described by (Jaffar *et al.,* 2016) in following steps:

- Cultured isolates and incubated overnight at 37 Cº.
- Bacterial suspension was prepared in Mueller-Hinton Broth (MHB) supplemented with 1% glucose and adjusted to 0.5 McFarland.
- Then , 180µl of Mueller-Hinton Broth (MHB) that supplemented with 1% glucose and 20µl of bacterial suspensions are inoculated into 96-well flat-bottomed sterile polystyrene micro titer plate (3 wells for each strain) .
- Microtiter plate was incubated in 24 hr at 37C° .
- The sessile isolates of which biofilms formed on the walls of micro titer plate are stained with only 150 µl of 0.1% crystal violet for 10 min , after planktonic cells in wells of micro titer plate are discharged by washing twice with phosphate-buffered saline (PBS) (pH 7.2) and wells are dried at 60°C for 1hr .

- After drying wells of microplate , dye of biofilms that lined the walls of the microplate was resolubilized by 150µl of 95% ethanol.
- Then, microtiter plate was measured at 620 nm by a microtiter plate reader.

Each assay was performed in triplicate and the average optical density was considered . According to their optical densities, the adherence capability of each bacterial cell was classified into three categories: above the mean optical density of the negative control (containing broth only) were considered the cut-off optical density (ODc) (Mathur *et al.,* 2006) . Isolates were classified as follows :

(ODc < OD < 2×ODc)…….... Weakly-adherent.
(2×ODc < OD < 4×OD)……. Moderately-adherent.
(4×OD < OD)……. Strongly-adherent.

3.2.18 Antibiofilm activity of SeNPs

The antibiofilm effect of SeNPs against various pathogens was determined in vitro by using 96 wells polystyrene microtiter-plates method (Khiralla and El-deeb, 2015 ; Miglani and Tani-Ishii , 2021) , Antibiofilm procedure include :

- Bacterial cell suspension (0.1ml) have been inoculated in 1.9 ml BHI broth and adjusted to 0.5 McFarland .
- One hundred microliter of the cultured BHI broth which supplemented with 1% glucose transferred into each well of 96- well microtiter-plate .
- One hundred microliter of SeNPs (2048 µg/ml) was added in each well of column 2 . Serial dilutions were performed from column 2 to column 11, to obtain the final NPs concentrations, which varied from 1024µg/ml in (2^{nd} well) to 2 µg /ml in (11th well).

- Ten microliter of bacterial cell suspension that prepared in step 1 was added from column 2 to column 12 . column 1 contain (BHIB+1% glucose) serve as negative control , column 12 contain (BHIB+1% glucose) and stimulated culture act as positive control . Plates were incubated at 37 C° for 24 hr .
- After the incubation period, contents of the microtiter-plates were emptied and the wells were washed three times with 200 microliter of phosphate buffered saline (PBS, pH 7.2).
- The remaining adhered bacteria were fixed with 200 microliter of methanol (99 %) per well . After 15 min , the microtiter-plates were stained with 200 microliter per well of 0.1 % crystal violet for 5 min .
- The surplus of stain was rinsed off by placing the microtiter-plates under slow running tap water. After drying , 200 microliter of 33% acetic acid was added to the wells.
- The biofilm growth was read at 620 nm using micro plate reader . Therefore , varying amount of biofilm formation by various isolates could be quantitated by comparing OD values of stained adherent

cells . Isolates which gave an OD <0.120 were classified as non-adherent and weak biofilm producers ; OD values of 0.120 to 0.240 were classified as moderately adherent and moderate biofilm producers ; OD value of > 0.240 was classified as strongly adherent and high biofilm producers (Magesh *et al.*, 2013) .

3.2.19 Determination the Toxicity of SeNPs on (PC3) Cancer Cell Line and (WRL 68) normal cell line.

This method was performed in vitro to investigate the possible cytotoxic effect of different SeNPs concentration on Prostat cancer cell line (PC3) and normal hepatic cell line (WRL 68).

3.2.19.1Cell Line Maintenance:

When the cells in the vessel formed confluent monolayer, the following protocol was performed (Geraghty *et al*., 2014) :

- The growth medium was aspirated and the cell sheet washed with PBS.
- Two to three ml trypsin/EDTA solution was added to the cell. The vessel was turned over to cover the monolayer completely with gentle, rocking. The vessel allowed incubation at 37 C° for (1 – 2) min until the cells were detached from the vessel.
- Fresh complete RPMI medium (15-20 ml) was added and cells were dispersed from the wedding surface into growth medium by pipetting.
- Cells were redistributed at required concentration into culture vessels, flasks or plates whatever needed and incubated at 37 C° in 5% CO_2 Incubator.

Cell concentration was achieved by counting the cells using the haemocytometer and applying the formula:

$$Total\ cell\ \frac{count}{ml} = cell\ count \times dilution\ factor(sample\ volume) \times 10^4$$

3.2.19.2 MTT Cytotoxicity Assay

The cytotoxic effect of SeNPs in different concentration (25 ,50 ,100, 200 and 400 µg/ml) was performed by using MTT kit (Intron Biotech) as following :

- Cancer cells ($1x10^{4}$ – $1x10^{6}$ cells/ml) were grown in 96 flat well micro- titer plates, in a final volume of 200µl complete culture medium per each well. The microplate was covered by sterilized

parafilm and shacked gently . The plates were incubated at 37 ° C, 5% CO_2 for 24 hr .

- After incubation, the medium was removed and two fold serial-dilutions of the desired compound (25, 50, 100, 200 and 400 µg/ml) were added to the wells .Triplicates were used per each concentration as well as the controls. cells treated with serum free medium. Plates were incubated at 37 ° C for 48 hr in 5% CO_2 incubator .
- After exposure to SeNPs , 10 µl of the MTT solution was added to each well and the plates were further incubated at 37 ° C in 5% CO_2 for 4 hr .
- The media were carefully removed and 100µl of solubilization solution was added per each well for 5 min .
- The absorbance was determined by using an ELISA reader at a wavelength of 575 nm.
- statistical analysis was performed to calculate the IC50 , through the following equation:

$$Viability(\%) = \frac{optical\ density\ of\ sample}{optical\ density\ of\ control} \times 100\%$$

3.2.20 Effect of SeNPs on gene expression of some virulence factor

The q RT-PCR was performed for quantification expression detection of some virulence factors and biofilm formation genes that normalized by housekeeping (16SrRNA) gene in *Enterococcus faecalis* and *Escherichia coli* isolates. The method was carried out according to (Shakerimoghaddam *et al*., 2017) .Three isolates which formed a strong biofilm were chosen for studying expression of the (*hly* , *fimH* , *luxS* , *qse* and *16SrRNA* gene) in *E. coli* , and (*Esp* , *hly* , *gelE* , *fsrA* and *16SrRNA* gene) in *Enterococcus faecalis*) .

The MIC and sub-MIC of SeNPs concentrations that reduced growth of bacteria and biofilm formation was determined by microtiter-plate methods . For *E. coli* we used three concentration of SeNPs (32 µg , 64µg , 128 µg) , and for *Enterococcus faecalis* we used (16 µg ,32 µg , 64µg).

For gene expression studies , 5 ml of Luria-Bertani broth media was inoculated with tested bacteria and adjusted to (0.5 McFarland) . For each bacteria , three groups was made , the first group treated with sub MIC of SeNPs named as S1 , second group treated with (MIC) of SeNPs and named S2 , the last group was the control which was bacterial growth without any treatment was named (SC) . After adding of Se nanoparticles the tube incubated at 37 C° for 24 h .

3.2.20.1 RNA extraction

Total RNA was extracted from bacterial suspension by using (Total RNA Extraction Kit) according to company instructions as following steps:

- One ml of bacterial suspension that treated with SeNPs were harvested by centrifuge at 13000rpm for 1 min then , supernatant removed .
- The bacterial pellets were suspended by adding 1ml easy-BLUE (Trizol reagent) and vigorously vortex in room temperature for 10 sec.
- Two hundred microliter chloroform was added to each tube and shaken vigorously for 1 min .Then , The mixture was incubated on ice for 5 min . After that centrifuged at 13000 rpm, 4°C, for 15 min .(The mixture was separated into a lower organic phase , interphase , and a color-less upper aqueous phase)
- A color-less upper aqueous phase which contain RNA was transferred into a new 1.5ml microcentrifuge tube .

- For RNA precipitation 500microliter isopropanol was added. Then, mixture mixed by inverting the tube 4-5 times and incubated at 4°C for 10 min . Then, centrifuged at 13000 rpm , 4°C for 10 min .
- Supernatant was discarded, and 1ml (80%) Ethanol was added and mixed by vortex again. Then, centrifuge at 13000 rpm, 4°C for 5 min.
- The supernatant was discarded and the RNA pellet was left to air to dry.
- One hundred microliter free nuclease water was added to each sample to dissolve the RNA pellet, Then, it incubated in a water bath at (55–60) ° C for (10–15) min , the extracted RNA sample was kept at -80 ° C.

3.2.20.2 Estimation and purity of total extracted RNA

The extracted total RNA was checked by using Nanodrop (Thermo Scientific NanoDrop Lite UV Visible Spectrophotometer. USA) that measured RNA concentration (ng/µL) and checked the RNA purity at absorbance (260 /280 nm) as following steps:

- After opening up the Nanodrop software, chosen the appropriate application (Nucleic acid, RNA).
- A dry wipe was taken and cleaned the measurement pedestals several times. Then carefully pipetted 2microliter of free nuclease water and placed onto the surface of the lower measurement pedestals for blank the system.
- The Nanodrop sampling arm was lowered and 1microliter RNA sample were measured .

3.2.20.3 DNase I treatment

The extracted RNA was treated with DNase I enzyme to remove the trace amounts of genomic DNA from the eluted total RNA by using samples

(DNase I enzyme kit) and done according to method described by Promega company, USA instructions as in table (3.11) :

Table (3.11): Treatment of extracted RNA with DNase I enzyme

RT master mix	Volume
Total RNA	10 µl
DNase I enzyme	1 µl
10X buffer	4 µl
DEPC water	5 µl
Total	20 µl

After that , the mixture was incubated at 37°C for 30 min . Then , 1 µl of stop reaction was added and incubated at 65°C for 10 min for inactivation of DNase enzyme action .

3.2.20.4 cDNA synthesis

The DNase treated total extracted RNA samples were used in cDNA synthesis step from mRNA transcripts by using **(AccuPower® RocketScript™ RT PreMix)** and this kit was done according to company instructions as in table (3.12) :

Table (3.12): Reverse transcriptase master mix with their volumes for cDNA synthesis

RT mix	Volume
Total RNA 100µg	10µL
Random Hexamer primer (50pmol)	1µL
DEPC water	9µL
Total	20µl

After that, these RT mix components that mentioned in table above placed in AccuPower® RocketScript™ RT PreMix kit strip tubes that containing all other components which needed to cDNA synthesis such as (Reverse Transcriptase, 5 x Reaction Buffer, DTT, dNTP, and RNase

Inhibitor). Then, all the strip tubes transferred into Exispin vortex centrifuge at 3000rpm for 3 min , and then incubated in Thermocycler (BioRad-USA) as following thermocycler conditions protocol , table (3.13) :

Table (3.13): Thermocycler condition for cDNA synthesis

Step	Temperature	Time
cDNA synthesis (RT step)	42 C°	1 hr
Heat inactivation	95 C°	5 min

3.2.20.5 Real-Time PCR (qPCR) master mix preparation

qPCR master mix was prepared by using **(RealMOD™ Green SF 2X qPCR mix Kit)** based on SYBER green dye amplification in Real-Time PCR system and the qPCR master mix for target genes and housekeeping gene was prepared as in table (3.14):

Table (3.14): qPCR standard master mix protocol

qPCR master mix	Volume
cDNA template (10ng)	5µL
Forward primer(10pmol)	1µL
Reverse primer (10pmol)	1µL
qPCR Master Mix	10µL
Nuclease free water	3µL
Total	20µl

After that, these qPCR master mix component that mentioned above placed in qPCR white plate strip tubes and mixed by Exispin vortex and centrifuge for 5 m , then placed in MiniOpticon Real-Time PCR system.

3.2.20.6 qPCR Thermocycler conditions

qPCR Thermocycler conditions was done according to qPCR kit instruction and used by using **Optimase ProtocolWriter™** online for primers annealing calculation as in table (3.15):

Table (3.15): General thermocycler (RT-PCR) program used in the study

qPCR step	Temperature	Time	Repeat cycle
Initial Denaturation	95 C°	10 min	1
Denaturation	95 C°	30 sec	40
Annealing	60 C°	30 sec	
Extension	72 C°		

The data results of qPCR for target and housekeeping gene were collected and the expression analysis (fold change) used analyzed by using (**The CT Method Using a Reference Gene**) that described by (Livak and Schmittgen, 2001) as following equations:

Gene expression ration (Fold change) = Ratio (reference/target) = 2^CT(reference) – CT(target).

3.2.20.7 Statistical analysis

The data values are presented as the mean ± S.D. Differences in mean values were analyzed by two-way ANOVA followed LSD test with the IBM SPSS Statistics version 27 software (International Business Machines Corp., Armonk, NY, USA). Values with a $P < 0.05$ were considered to indicate statistical significance (Daniel and Cross , 2018) .

Chapter Four

Results

and

Discussion

4 . Results and Discussion

4.1 Isolation and identification of bacterial isolate from UTI

Among of 165 isolates , 115(69.6%) isolates were positive culture , *Escherichia coli* 65(56.52 %) was the predominant and the most common Gram negative bacteria followed by *Enterococcus faecalis* 28(24.34 %), *K. pneumonia* 15 (13.04 %) , and *Staphylococcus saprophyticus* 7(6.1 %) (table 4.1) .

In VITEK2 compact system ,the isolates were identified as *Escherichia coli* with probability of (99) % , *Klebsiella pneumoniae* with probability of (96) % , *Enterococcus faecalis* with probability of (99) % , *Staphylococcus saprophyticus* with probability of (89) % (table 4.1) . Biochemical Characteristics of all bacterial isolates were done also by VITEK2 compact system , appendices (1,2,3,4,5) .These result are similar to (Shilpi *et al.*, 2013) who found that *Escherichia coli* (58.0%) was the most common pathogens ,followed by *Enterococcus faecalis* (15.5%) .

Table (4.1) : Identification of pathogenic bacteria depended on the colonial morphology, microscopically, and Vitek 2 system

Bacteria species	number of isolates	Probability in Vitek 2 system
Escherichia coli	65 (56.5%)	99%
Enterococcus faecalis	28 (24.3 %)	99%
Klebsiella pneumoniae	15 (13.1 %)	96%
Staphylococcus saprophyticus	7 (6.1 %)	89%
Total	115 (100%)	

The morphological examination of *Escherichia coli* on MacConkey agar and nutrient agar after 24 hours of incubation at 37°C produced large, circular, low convex, grayish white, moist, smooth, opaque or partially

translucent colonies **.** *Escherichia coli* produced bright pink flat colonies due to lactose fermentation , and form pink to mauve colonies on chromogenic agar , figure (4.1) .

Urinary tract infection is considered to be one of the most common bacterial infections that affect people in the community and hospitals worldwide **(**Foxman , 2014) . It is well known that the spectrum of pathogens isolated from patients suffering from a UTI is nearly stable, and *Escherichia coli* remains the most common prevalent etiological agent . In the present study, *Escherichia coli* accounted for 56.5% of positive isolates, which is well comparable with the rates reported from some studies conducted in Iraq as 74.32%, Turkey 71.3% , in Iran 65.2% and 51.5% (Aypak *et al*., 2009 ; Mirsoleymani *et al*., 2014; Assafi *et al*., 2015; Pouladfar *et al*., 2017) .

In another study, the most common isolates after *Escherichia coli* was *Enterococcus faecalis* , *Staphylococcus saprophyticus* , *Proteus mirabilis and Klebsiella pneumoniae* (Čeljuska-Tošev *et al*., 2010) . The increased number of enterococcal UTI in this part might be due to the rapid surge in number of diabetic patients; diabetes mellitus is one of the important risk factors of enterococcal UTI (Nitzan *et al*., 2015) .

The increased incidence of enterococcal UTI is alarming; resistance to most commonly used antibacterial agents is a typical characteristic of these bacteria. It is far more difficult to treat enterococcal UTI as compared to UTI caused by other bacteria due to intrinsic resistance to many antibacterials and rapidly increasing acquired resistance (Wisell *et al*., 2008) .

Enterococcus faecalis has greenish-blue color on chromogenic agar , figure (4.1) . It was considered the second prevalent and virulent species causing infections in hospitalized patients .These clones are linked to the hospital by the acquisition of adaptive genetic elements, including the

metabolic genes, the creation of biofilm and antibiotic resistance (Shilpi *et al*., 2013).

The *Klebsiella pneumonia* colonies seemed to be large , spherical , mucoid and glistening pink colonies on a MacConkey agar , and metallic blue on chromogenic agar , figure (4.1) . Microscopic tests of *Klebsiella* alleged isolates showed that had been gram-negative shorter rods (Mahon *et al*., 2018). When cultivated on MacConkey agar from a total of 180 samples taken from two clinical sources in Baghdad Governorate , produced sixty (33.88 %) *klebsiella* isolate (Jasim *et al*., 2017) . In their experiment , they collected 88 (29.33 %) *Klebsiella* isolates of 300 various clinical samples reported on the appearance of pink, mucoid, rounds and wide noted that VITEK 2 is an easy-to-handel system that delivers a fast result (4 to 15 hours) and reasonable for microbial species identification (Ismail , 2017; Abbas , 2020) .

Staphylococcus saprophyticus on nutrient agar were seemed to be circular, cream-colored to white colonies , and are mostly 1mm in diameter with an entire margin , the colonies have raised elevation and a dense center with transparent borders. While in mannitol salt agar , it appeared yellow-colored colonies indicating mannitol fermentation as the color of the media is converted from red to yellow , and the colonies are 1-2 mm in diameter with an entire margin , and appeared turquoise blue on chromogenic agar , figure (4.1) .

Epidemiological studies showed that urinary tract infections caused by *Staphylococcus saprophyticus* are more prevalent during the late summer and fall .These infections are also associated with recent sexual intercourse, hormonal influences related to menstruation, and changes in genital flora caused by candidal infections or spermicides . *Staphylococcus saprophyticus* can cause infections even when it is present in low numbers, For this reason, even low numbers of coagulase-negative

staphylococci in urine cultures should not be dismissed as skin contaminants (Raz *et al*., 2005) .

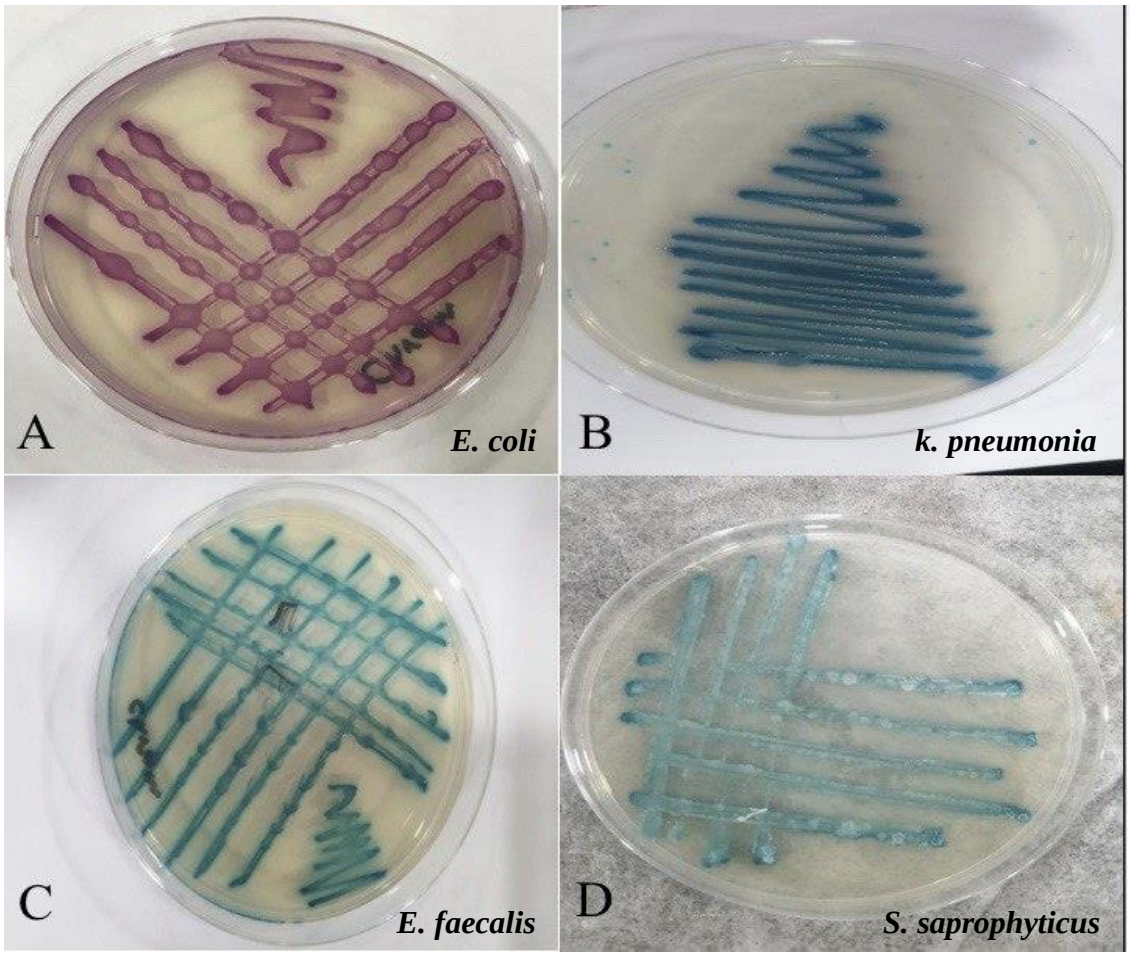

Figure (4.1) : Isolation of pathogenic bacteria on chromogenic agar at 37 º C for 24 hr , A (*E. coli*) , B (*k. pneumonia)* , C (*E. faecalis) , D (S. saprophyticus)*.

4.2 Antibiotic Susceptibility Test (AST)

Lists of antibiotic susceptibility testing were created using documents and breakpoints from the Clinical Laboratory Standards Institute (CLSI , 2020) the European Committee on Antibacterial Susceptibility Testing (EUCAST) and the United States Food and Drug Administration (FDA).

This study included 10 antibiotics was determined by disc-diffusion method , which are Azithromycin , Nitrofurantoin , Imipenem , Amikacin ,

Nalidixic acid , Ciprofloxacin, Doxycycline , Amoxicillin/calvulanic acid , Trimethoprime / sulphamethoxazole , Ampicillin . The results was analyzing sensitivity pattern of antibiotics against (*E.coli , K. pneumoniae , E. faecalis ,S. saprophyticus*) , figure (4.2) .The table below shows the percentages of resistant isolates for antibiotic , table (4.2) .

Table (4.2) : Antibiotic susceptibility test for pathogenic bacteria

antibiotic	Antibiotic susceptibility of pathogenic bacteria (%)			
	E. coli	***K.pnemoniae***	***E . faecalis***	***S. saprophyticus***
	R	**R**	**R**	**R**
AZM	14	15	22	73
AK	5	15	80	9
NA	20	25	66	9
CIP	20	33	9	11
F	45	66	11	38
IPM	40	7	5	0
DO	11	11	56	28
SXT	83	40	88	4
AMC	89	55	74	88
AM	86	60	62	90

Resistance percentages of *E.coli* isolates to Azithromycin were (14%) , Amikacin (5%) , Nalidixic acid (20%) , Ciprofloxacin (20%) Nitrofurantoin (45%) , Imipenem (40%) , Doxycycline (11 %) , Trimethoprime / sulphamethoxazole (83%), Amoxicillin/calvulanic (89%) and Ampicillin (86%) .

This may be attributed to *blaCTX-M type especially blaCTX-M-1, blaCTX-M-2, blaCTX-M-8, blaCTX-M-9 , blaCTX-M-15. blaCTX-M-27* (Birgy *et al*., 2020 ; Hassuna *et al*., 2020) , and attributed to *bla-TEM* , *bla-SHV* , *blaOXA , AmpC* (Esmaeel *et al*., 2020 ; Gajamer *et al*., 2020 ; Naziri *et al*., 2020 ; Pandit *et al*., 2020 ; Sadeghi *et al*., 2020) . Carbapenem-resistant *E. coli* isolates may be due to *blaKPC-2* and *blaNDM-1* (De La Cadena *et al*., 2020). Additionally the resistance to

more than one antibiotics may be attributed to efflux pumps (Al-Zuhairy and Al-Dahmoshi , 2020) .

The percentage of *K. pneumoniae* that resisted to Azithromycin were (15%) , Amikacin (15%) , Nalidixic acid (25%) , Ciprofloxacin (33%) Nitrofurantoin (66%) , Imipenem (7%) , Doxycycline (11%) **,** Trimethoprime / sulphamethoxazole (40%), Amoxicillin/calvulanic (55%) and Ampicillin (60%) .

Resistance of *K. pneumoniae* to beta-lactam also may be mediated by beta-lactamases like *blaOXA-48 , blaKPC , CTX-M-15 , blaAmpC* (Gurung *et al*., 2020 ; Fils *et al*., 2021; Kurittu *et al*., 2021 ; Xiong *et al*., 2021) . ESBL producers represented one-third of *E. coli , K. pneumoniae* UTI episodes (Vachvanichsanong *et al*., 2021) . Current treatment options for UTIs due to ESBL-producing Enterobacteriales include nitrofurantoin, fosfomycin, fluoroquinolones and carbapenems (Bader *et al*., 2020) .

The percentage of *E . faecalis* that resisted to Azithromycin were (22%) , Amikacin (80%) , Nalidixic acid (66%) , Ciprofloxacin (9%) Nitrofurantoin (11%) , Imipenem (5%) , Doxycycline (56%) , Trimethoprime / sulphamethoxazole (88%), Amoxicillin/calvulanic (74%) and Ampicillin (62%) .

Besides their possession of several virulence factors, members of the genus Enterococcus also have inherent capacity to accumulate and dissem-inate antibacterial resistance determinants (Sartelli *et al*., 2016) . The emergence of antibiotics resistant and virulent Enterococci are a major public health concern (Golob and Rao , 2021) . β Lactam antibiotics not have bactericidal action against enterococci as it used as mono therapy, that making the treatment of systemic infections mostly challenging (Reddy *et al*., 2012) . Ciprofloxacin is approved for use for

both uncomplicated and complicated urinary tract infections, including cystitis, pyelonephritis, and chronic bacterial prostatitis (Sattari-Maraji *et al*., 2019 ; Jiang *et al*., 2021) .

The isolates of *S.saprophyticus* that resisted to Azithromycin were (73%) , Amikacin (9%) , Nalidixic acid (9%) , Ciprofloxacin (11%) Nitrofurantoin (38%) , Imipenem (0%) , Doxycycline (28%) , Trimethoprime / sulphamethoxazole (4%) , Amoxicillin/calvulanic (88%) and Ampicillin (90%) .

According to the CLSI, routine susceptibility testing of urinary *S. saprophyticus* isolates to choose antibiotics is not recommended as this microorganism is normally susceptible to trimethoprim/sulfamethoxazole (Jancel and Dudas , 2002) . However, 7 % of the *S. saprophyticus* isolated from UTIs were resistant to sulfamethoxazole/trimethoprim. Similar to our results, 17.6 % of the *S. saprophyticus* isolates were resistant to sulfamethoxazole / trimethoprim (Ferreira *et al*., 2012) . Many researchers reported that isolated *S. saprophyticus* from hospital and farm were resistant to β-lactams, macrolides, lincosamides, and many other antibiotics (Waller *et al*., 2011; Dziri *et al*., 2016) .

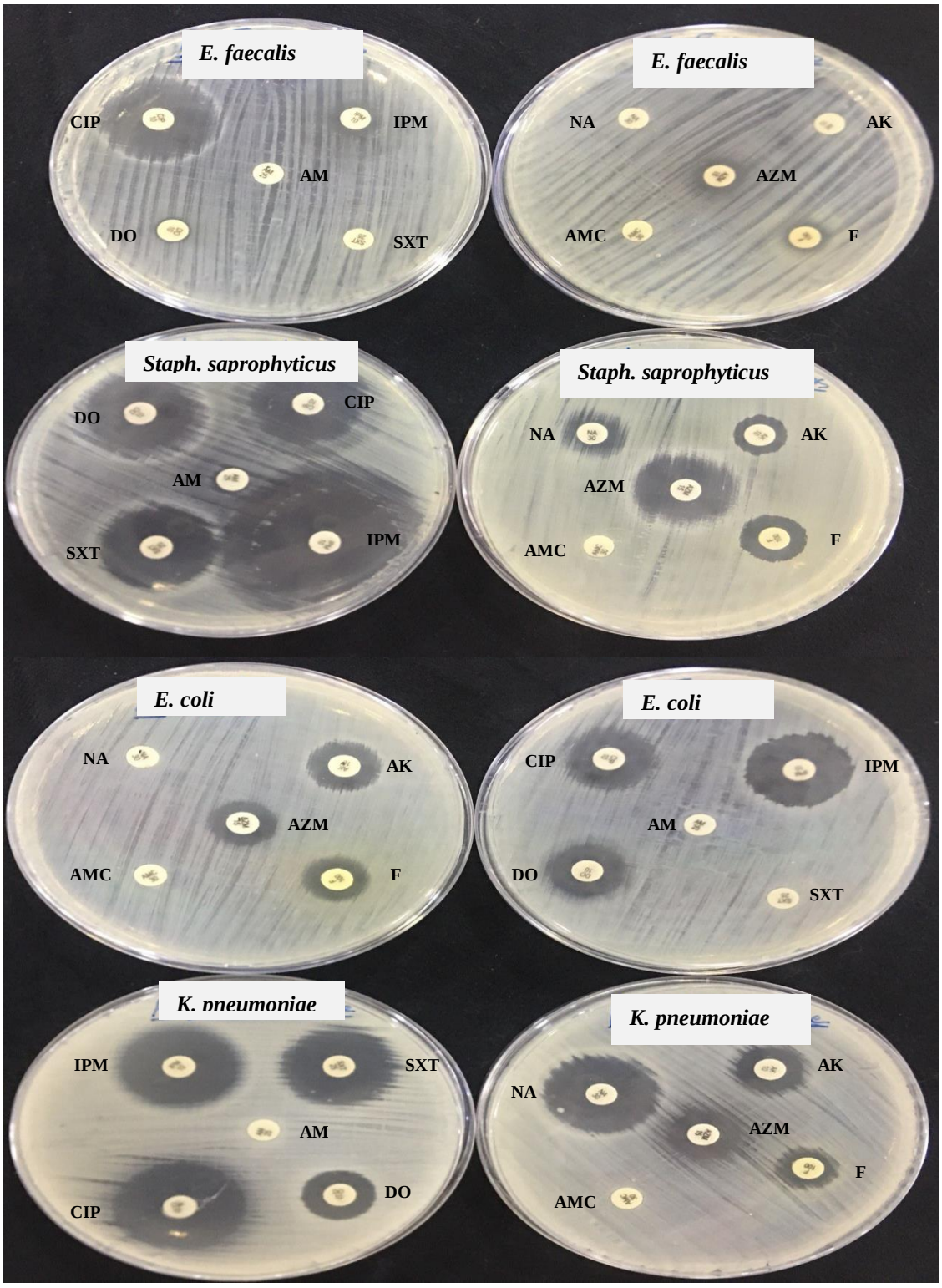

Figure (4.2): Antibacterial activity of antibiotics against pathogenic bacteria on MHA at 37 º C for 24 hr .

4.3 Molecular Identification of *Bacillus clausii*

DNA templates that extracted in (3.2.8.1) were used in the amplification of 16sRNA gene using 16sRNA gene universal primers in (table 3.6). The product then was electrophoresed on agarose gel and documented on gel document. The resulted 16s rRNA bands were 1470bp as shown in (figure 4.3) . After that the sample sent to gene sequence . Sequences for *Bacillus clausii* strain were received online and aligned to NCBI data base using Blast software , multiple aligned to each other using BioEdit software and submitted in fasta format to NCBI through Sequence software as in **(** Berber and Çetinkaya , 2021**)** .

Later pairwise alignment were investigated for *Bacillus calusii* 16sRNA gene sequences . The isolate was found to be nearest and neighbour to *Bacillus clausii* strain (4G219) with Score 1594 bits(863) , Expect 0.0 , Identities(93%) , and Gaps (1%) which rooted to bacillaceae. Accession number: MK496620, GenBank , figure (4.4).

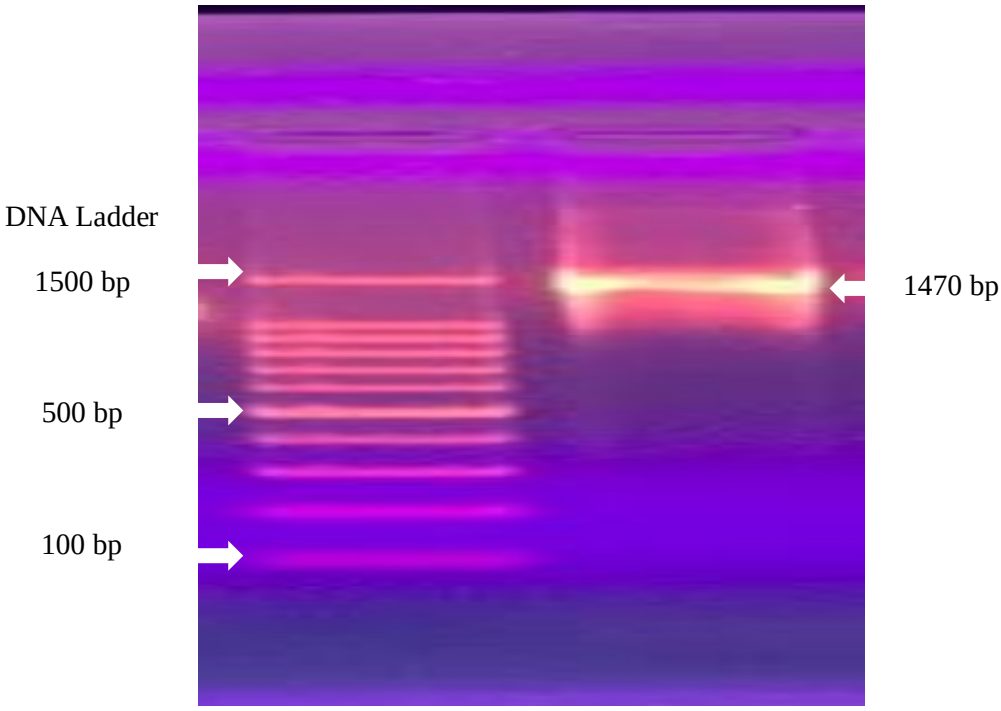

Figure (4.3) : Agarose gel electrophoresis of PCR product for 16S rRNA amplicon bands of *Bacillus clausii* with size 1470bp , at 1.5 % Agarose 75 volt and 40 min .

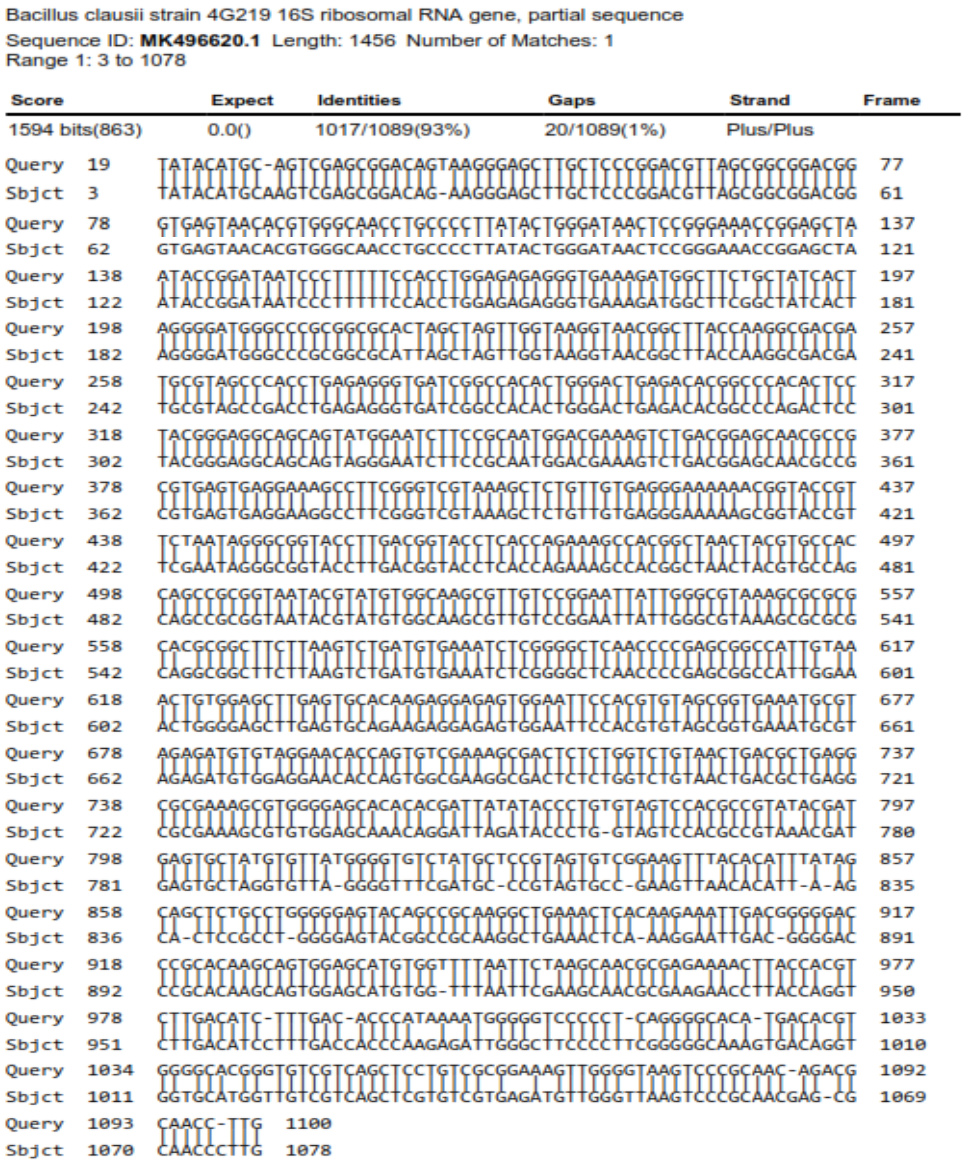

Figure (4.4) : Pair-wised alignment of partial nucleotide sequence of 16S ribosomal RNA gene (Query) to that of *Bacillus clausii* strain 4G219 whose sequence producing highest score (93%) of homology during BLASTn search .

4.4 Biosynthesis of Selenium nanoparticles by using *Bacillus clausii*

Bacillus clausii, which was used in the biosynthesis of SeNPs, demonstrated the ability of extracellular biosynthesis by using cell free supernatant after the addition of Na_2SeO_3 as a substrate under previously optimized conditions. The color changes of the reaction mixture from yellow to red , as in Figure (4.5) after incubation in shaking incubator (150

rpm) at 37 °C for 48 hr , as well as the color change and antibacterial behavior of SeNPs served as indicators for the biosynthesis of SeNPs by *Bacillus clausii* .

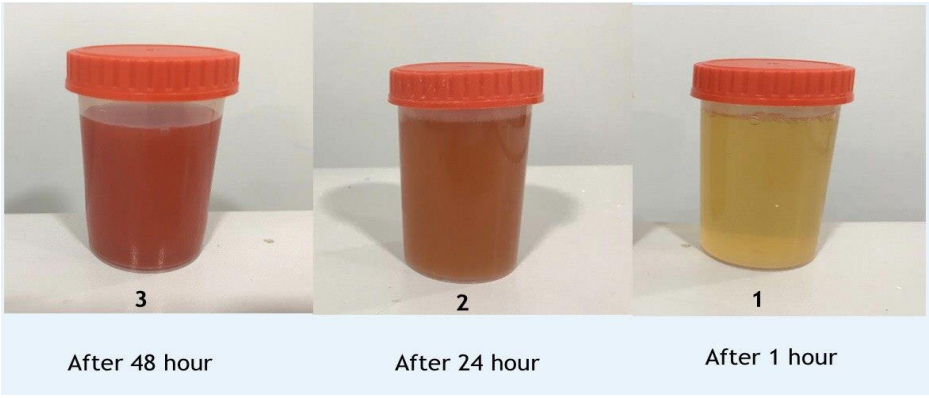

Figure (4.5) :Biosynthesis of SeNPs using *Bacillus clausii* at 37 ° C , 48 hr in aerobic condition .

Partial purification of SeNPs was done through three steps and then dried in oven for further experiment , as in figure (4.6) .

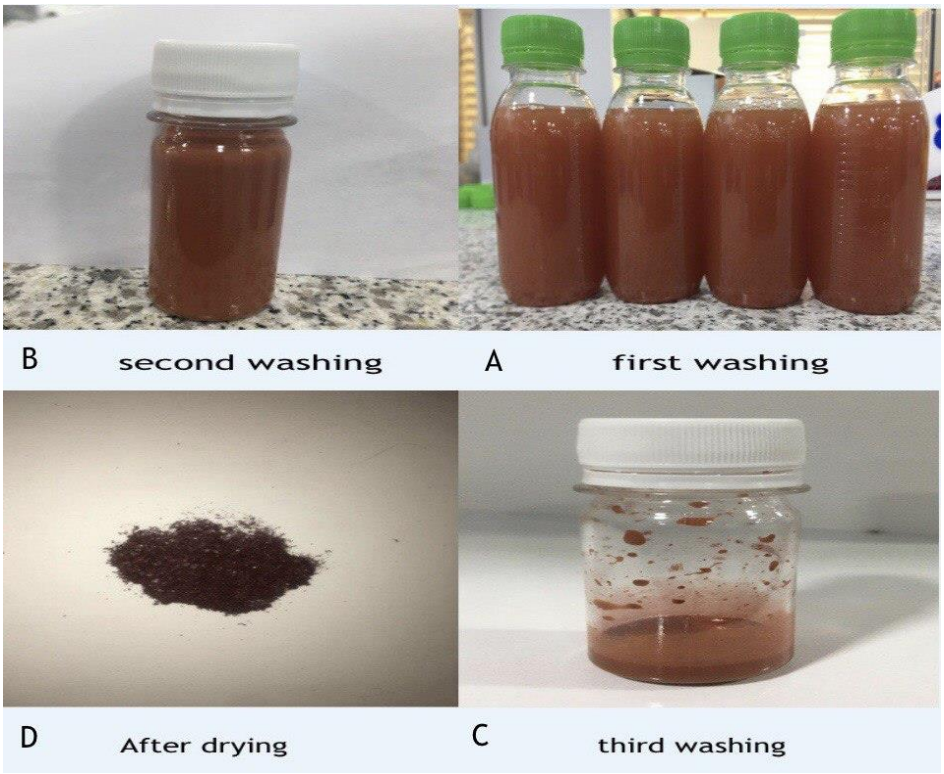

Figure (4.6) : Steps of partial purification of SeNPs .

In the present study , an attempt was made to employ the biosynthesis of SeNPs from *Bacillus clausii* which was recorded in the NCBI as in an economic and easy way. The appearance of color is a clear indication to formation of selenium nanoparticles in the reaction mixture due to reduction of SeO^{2-} ions to red Se^{0} , and it is suggested that the color change was because of the excitation of the SPR (Surface plasmon resonance) . Because of SPR, the reaction mixture color changed from yellow to red . Those findings are similar to the results of (Abbas *et al*., 2021 ; Ullah *et al*., 2021) .

From available reports, these potentially active compounds have been elucidated as reducing and stabilizing agents (Khanna *et al*., 2019) .

Bacillus subtilis BSN313 reduced the soluble, toxic, colorless selenium ions to the insoluble, non-toxic, red elemental SeNPs . It has been recorded that *Bacillus* extracts contain potent biomolecules such as small peptides , proteins, alcohols, phenols, phycocyanins, esters, and amines, which can act as reducing and stabilizing agents (Ullah *et al*., 2021) . These biomolecules, definitely, facilitated and participated in the reaction with SeO_3^{2-} to produce SeNPs (Shirsat *et al*., 2015) .

It is significant to note that selenium nanoparticle producing bacteria are reported in wide range of environments under aerobic and anaerobic conditions including in sludge and sewerage (Mishra *et al*., 2011) . The anaerobic/anoxic bacteria include strains such as *Rhodopseudomonas palustris* N (Li *et al*., 2014), *Veillonella atypica* (Pearce *et al*., 2008), *Shewanella putrefaciens* 200 (Jiang *et al*., 2012), *Shewanella* sp. HN-41 (Ho *et al*., 2021) .

In comparison with the anaerobic bacteria, the phenomenon is mostly cited in aerobic , Gram +ve *Bacillus* species such as *Bacillus laterosporus* (El-Batal *et al*., 2014) , *Bacillus licheniformis* (Khiralla and El-Deeb , 2015) , *Bacillus* sp. MSh-1 (Shakibaie *et al*., 2015) , *Bacillus*

cereus (Kora , 2018) , *Bacillus tropicus* Ism 2 (MK332444)(EL-Baghdady *et al*., 2019) , *Bacillus megaterium* (Hashem *et al*., 2021) , *Bacillus subtilis* 168 (Jia *et al*., 2022) .

4.5 Characterization of selenium nanoparticles

4.5.1 UV-visible Spectroscopy

UV- Visible spectrophotometric is a proven technique for detecting the nanoparticles. After 24 hours of incubation of the reaction mixture, color change was observed which indicated the formation nanoparticles in the reaction mixture .The biosynthesis of nanoparticles can be confirmed by visual observation and measuring the absorbance band using UV-visible spectroscopy in the region of 200-1100 nm. Single peak was at 260 nm (Figure 4.7) .

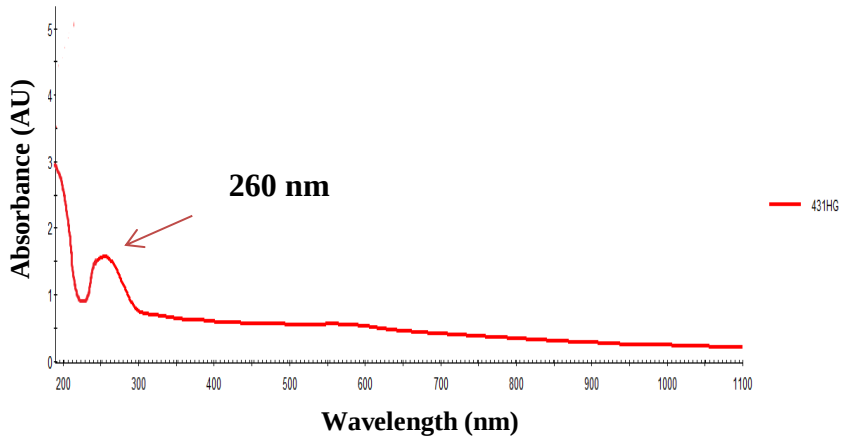

Figure (4.7) : UV- Visible Spectophotometry of the selenium nanoparticles

Various reports have confirmed that the resonance peak of selenium nanoparticles appears around this region, but the accurate position depends on several factors such as particle's size, shape, and material composition, as well as the local environment (Joshi *et al*., 2008) . There were a lot of study about SeNPs formation have various absorption peaks in UV-vis spectra indicate to a presence of SeNPs (Hemalatha *et al*., 2014) .

The peak appeared at nearby 362 nm and have a maximum absorption peak at 650 nm (Ullah *et al*., 2021) , strong absorption band

located at 265 nm , 265.5 nm , respectively (Santanu *et al*., 2015 ; Shubharani *et al*., 2019) , and the peak was seen at around 263 nm confirming the formation of the spherical SeNPs (Satgurunathan *et al*., 2017 ; AbouElmaaty *et al*., 2021). In a study conducted by Tabibi and his colleagues, the light absorption of selenium nanoparticles in the UV-Vis method was 294 nm (Tabibi *et al*., 2020) , while the UV-Visible absorption spectra of SeNPs recovered from the culture broth gave a characteristic peak at 590 nm which corresponds to the large particle size of 182.8 ± 33.2 nm (Lin and Wang , 2005) .

4.5.2 Analysis by Field Emission scanning electron microscopy (FESEM)

SEM was used to confirm the morphology and size of the selenium nanoparticles , rod shape selenium nanoparticle synthesized by *Bacillus clausii* with a size range between 37.58 – 75.16 nm were reported . Figure (4.8) representative SEM micrograph of SeNPs .

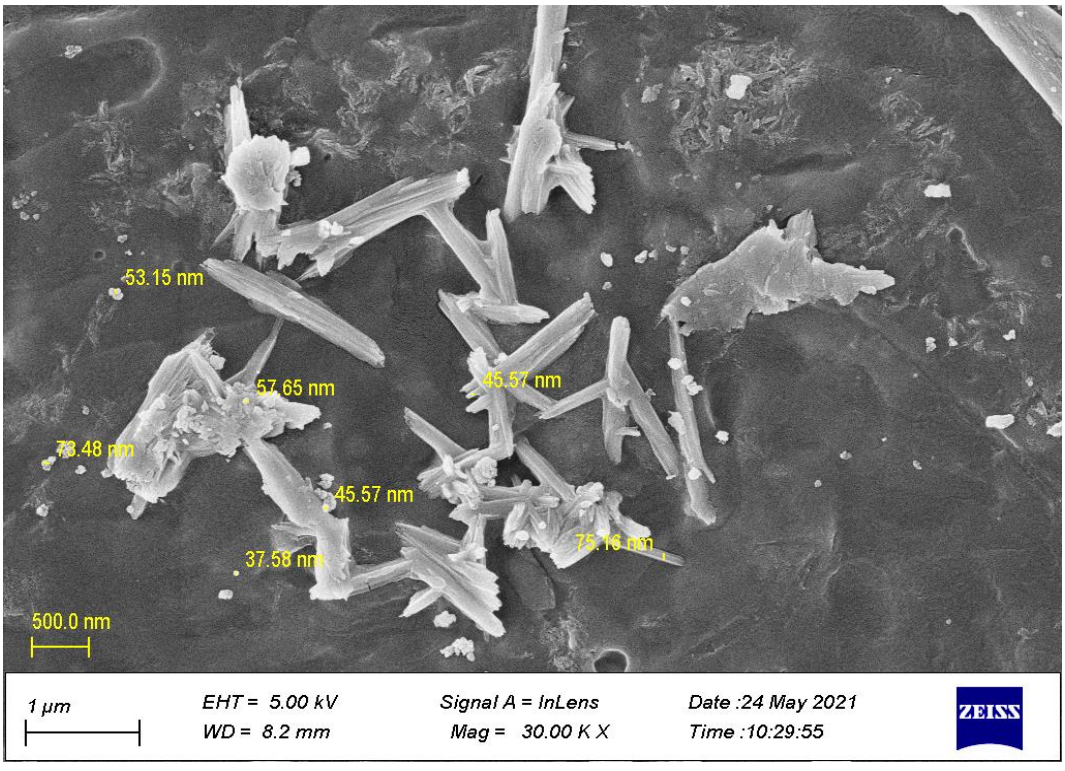

Figure (4.8) : FESEM Micrograph of selenium nanoparticles

SEM is a type of electron microscope that takes the image to the sample by scanning with a high-energy beam of electrons in a raster scan pattern. The electrons interact with atoms that can make up the sample producing signals that hold information about the sample's surface topography, composition, and other properties such as electrical conductivity (Verma and Maheshwari , 2018) .

The sizes and shapes of biogenic metallic nanoparticles can be controlled by exchanging the bio-reduction conditions, including type of culture and organism, nature of the medium and incubation time (Vetchinkina *et al*., 2019) .

Rods-shape of SeNPs showed similarity with result that cited by (Ramamurthy *et al*., 2013 ; Wadhwani *et al.*, 2017 ; Ashengroph and Tozandehjani , 2022) . Whereas spherical shape were reported by (Pouri *et al*., 2018 ; Vetchinkina *et al*., 2019 ; Arunthirumeni *et al*., 2022) . Nowadays, numerous microscopic techniques are commercially available, whenever transmission electron microscopy and SEM are the most popular microscopes for the analysis of the nanoparticles (Verma and Maheshwari, 2018) .

4.5.3 Analysis by energy dispersive X-ray spectroscopy (EDX)

Elemental analysis of SeNPs was established via the EDX coupled SEM. EDX spectrum was presented in table (4.3) , Figure (4.9) . A strong signal appeared from Se atom (53.31 %) , followed by C atom (22.99%) , O atom (18.36%) , P atom (2.27 %) , Ca atom (1.55 %) , K atom (0.39 %) , Mg atom (0.48%) , S (0.43 %) and Na (0.21 %) .

The detection of some atoms as impurities may be related to the presence of remained of *Bacillus clausii* , which was not fully removed after purification . In addition, SeNP oxidation in air before the sample

analysis may be the cause of oxygen detection as sample impurity (Cojocaru *et al*., 2016).

Table (4.3) : signals that observed from the energy-dispersive X-ray analysis .

Element	Line Type	Weight %	Weight % sigma	Atomic %
C	K series	22.99	0.28	4.82
O	K series	18.36	0.35	18.99
Se	L series	53.31	0.50	73.46
P	K series	2.27	0.07	1.21
Ca	K series	1.55	0.06	0.64
K	K series	0.39	0.04	0.17
Mg	K series	0.48	0.05	0.33
S	K series	0.43	0.05	0.22
Na	K series	0.21	0.04	0.15
Total		100.00		100.00

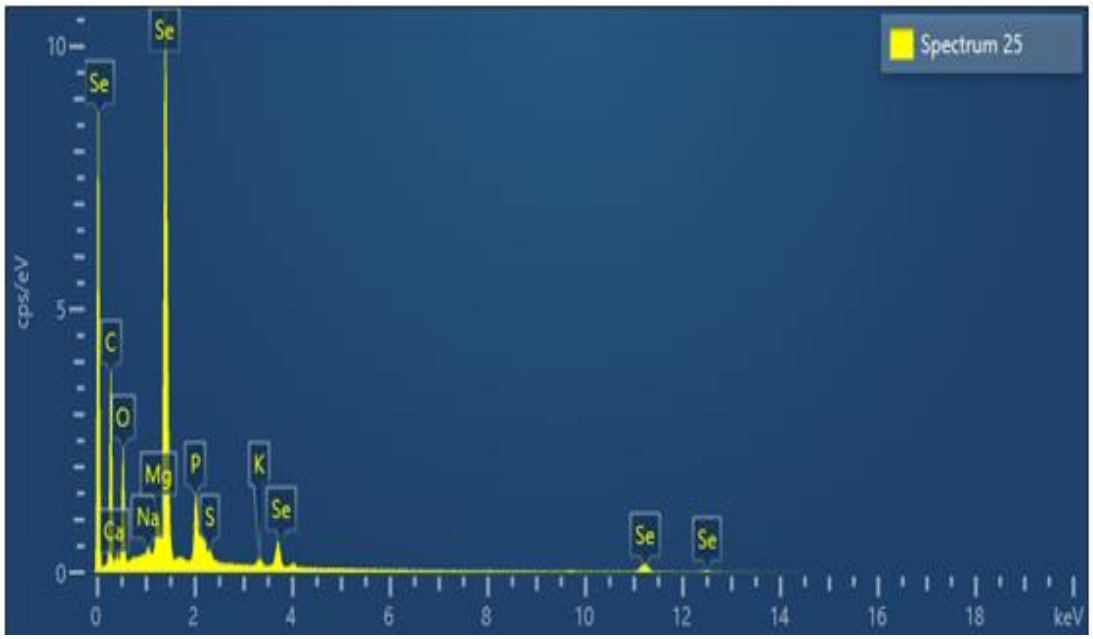

Figure (4.9) : EDX of selenium nanoparticles

Three signals from the energy-dispersive X-ray was found , Se (50.79%) , O (35.55%) and C (13.66%) (Alagesan and Venugopal , 2019) **.** Wherese the EDXS profile showed strong selenium signal 92.76% along with weak sulfur group peaks 7.24% , which confirms the presence of sulfur containing protein/peptide molecules bound to the surface of the nanoparticles (Syed *et al*., 2013) .

4.5.4 Atomic force microscope(AFM)

AFM imaging validated the shape and surface topography of the Selenium NPs. The height measurements were able to provide the elevation of nanoparticles with a high point of precision and accuracy. The average diameter of SeNPs was 19.28 nm which was compatible with the results of (Singh *et al.*, 2014). Three - dimension images, and granularity accumulation distribution charts of SeNPs were shown in (Figure 4.10) .

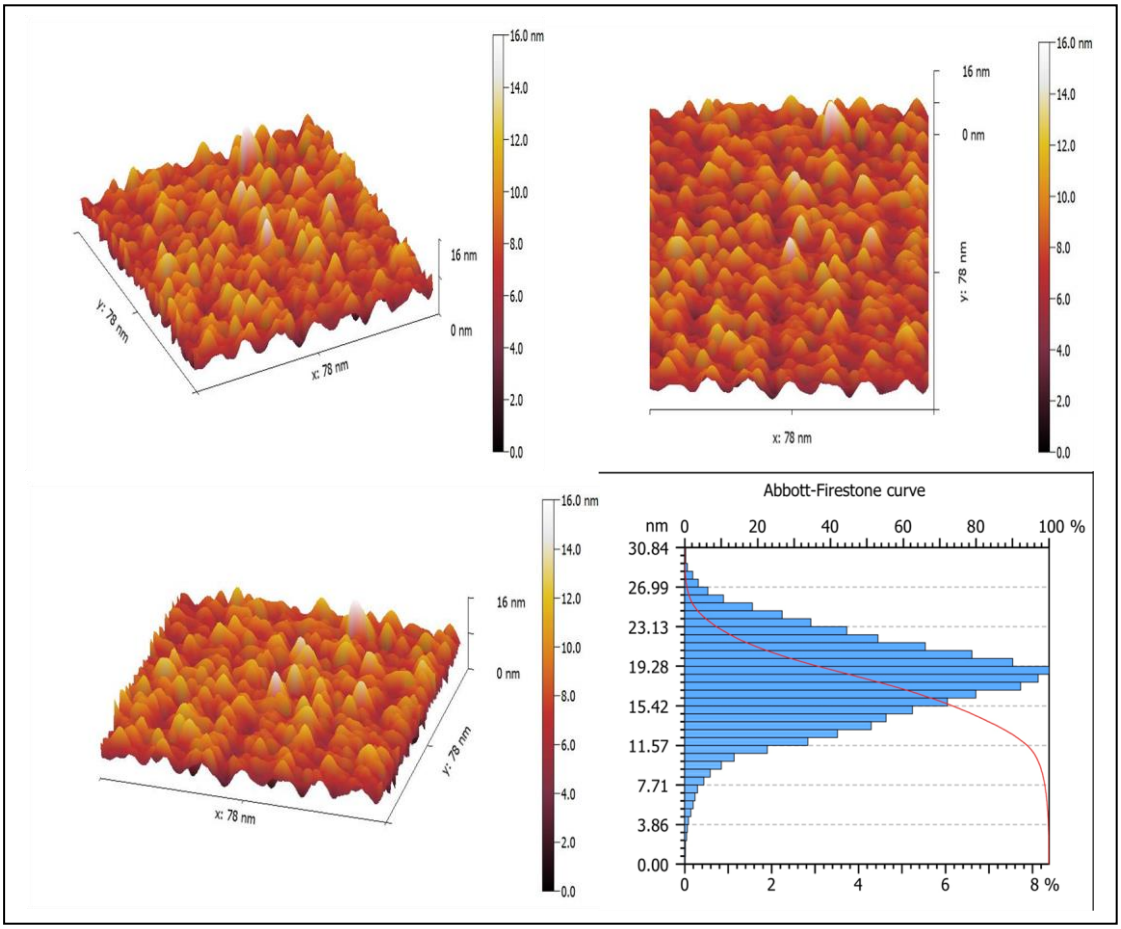

Figure (4.10) : AFM image of selenium nanoparticles

Moreover, the size of the selenium nanoparticles was found to be similar with the data collected from the XRD study , while the variation in size of nanoparticles was commonly found during chemical and biological synthesis . AFM images are obtained by detecting the attractive / repulsive

forces between the sample surface and a sharp probe for bio-effective component of selenium nano-Particles (Khoei *et al*., 2017) .

The image of the atomic force microscope showed the shape of the surface, the shape, and the size of the particles for the samples that have been identified. It also shows a two-dimensional (2D) and three-dimensional (3D) image of the sample (Al-Kazaz *et al*., 2021)

4.5.5. X-ray diffraction (XRD)

The formation of nanoparticles were characterized further by XRD analysis using Powder X-Ray Diffractometer . The studies showed a characteristic peak at 2θ value of 23.601, 29.896 and 44.015 , (appendices 6) , Figure (4.11).

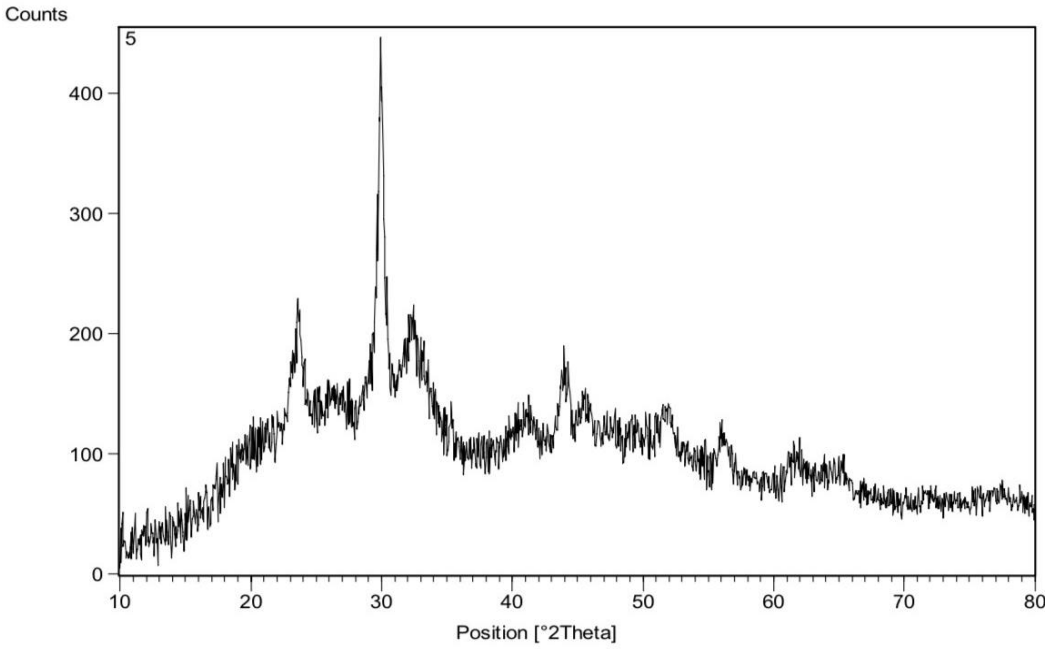

Figure (4.11) : XRD pattern of selenium nanoparticles

Some previous studies related to crystalline phase investigation of selenium nanoparticles suggested that stable amorphous forms (or even low crystallinity) are advantageous for biological applications, as they exhibit better solubility and subsequent adsorption and bioavailability (Cavalu *et al*., 2017).

In another study, XRD results showed that synthetic selenium nanoparticles are crystalline, which is a natural form (Shubharani *et al*., 2019) . However, in other experiments, the results showed that the synthetic selenium nanoparticles did not have any specific crystalline form, and amorphous was seen (Shakibaie *et al*., 2018 ; Borah *et al*., 2021) . The XRD analysis for the extracellular red elemental selenium indicated three intense peaks in the whole spectrum of 2θ values ranging from 5 to 80, the diffractions peak at 2θ value of 23.780, 29.797 and 43.878 can be indexed to the (100), (101) and (102) planes of the face-centered cubic (fcc) red elemental selenium (Singh *et al*., 2014)

The prepared SeNPs calculated crystalline size was 18.215 nm which was lower than the reported value of 41.5 nm by (Mellinas *et al* ., 2019) . The average crystalline size of synthesized SeNPs was calculated by using the Debye–Scherrer equation :

$$D = \frac{\mathrm{K} * \lambda}{\beta * \cos(\theta)}$$

where D is the crystal size , K is a constant whose value is approximately 0.9, λ is the wavelength of the X-ray, β is the full width at half maximum (FWHM) of the peak in radians, and θ is the Bragg's diffraction angle in radians. .

4.5.6. Fourier Transform Infrared Spectroscopy (FTIR)

FTIR analysis was used to obtain information about chemical compounds involved in the reduction and stabilization of SeNPs **.** FTIR spectra of SeNPs showed the present of peak at 3335.96 cm^{-1} can be assigned to hydroxyl (OH) group . 2952.85 cm^{-1} , 2922.50 cm^{-1} and 2853.17 cm^{-1} were assigned to (C-H stretching) , 2726.72 cm^{-1} (present of aldehyde) , 1632.39 cm^{-1} present of (C=C stretch binding carbonyl stretch protein) . 1516.55 cm^{-1} , 1502.78 cm^{-1} associated with aromatic nitro

compounds . 1462.11 cm^{-1} , 1455.69 cm^{-1} and 1376.95 cm^{-1} associated with C-H bend , 1046 cm^{-1} , 721.83 cm^{-1}, 558.51 cm^{-1} , 470.29 cm^{-1} corresponded to (Se−O) , (appendices 7) , Figure (4.12).

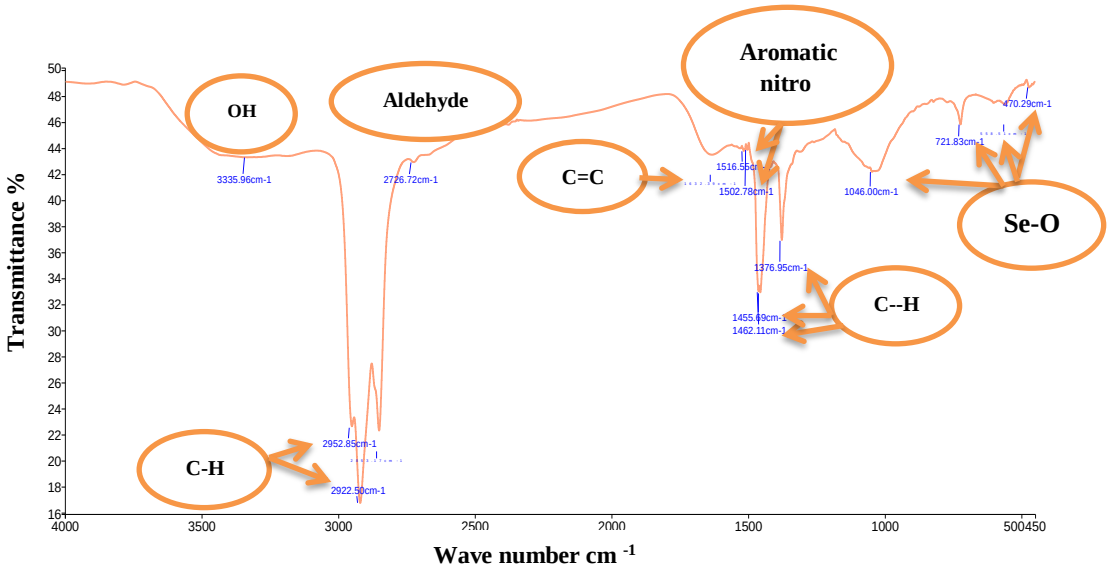

Figure (4.12) : FTIR of selenium nanoparticles

These results indicate the presence of various functional groups as biomolecules such as hydroxyl groups in polyphenols and amide groups in proteins having a key role in the reduction of selenium ions to their element and in the stabilization of the formed SeNPs (Fardsadegh *et al.*, 2019) .With the overall observations, it can be concluded that the proteins might have formed a capping agent over the SeNPs, which may response for their stabilization (Sonkusre *et al.*, 2014) .

In particular, Lenz and co-workers showed that selenium nanoparticles can be bounded with a variety of high-affinity proteins (Lenz *et al.*, 2011). In addition, proteins and other biomolecules such as polysaccharides and fatty acid may play a key role in controlling SeNPs size and morphology (Dobias *et al.*, 2011) . The strong intensity peaks 465 cm^{-1} , 668 cm^{-1} , 1051cm^{-1} which were due to the bending vibration of Se-O bonds were verified by (Cavalu *et al.*, 2017) .

4.6 Influence of Selenium Nanoparticle Against pathogenic bacteria

Biogenic SeNPs synthesized by *Bacillus clausii* were evaluated for their antibacterial activity against some pathogenic bacteria . The agar well diffusion method was used for detecting the antibacterial activity of biogenic SeNPs. SeNPS with different concentrations (100, 300, 500 µg/ml) showed inhibition activities against all tested bacteria. The highest inhibition zone of SeNPs observed in concentration (500 µg/ml), while the lower inhibition zone observed in concentration (100 µg/ml) .This inhibitory effect increased when the SeNPs concentrations were increased from 100µg to 500µg , as in table (4.4).

Table (4.4) : Inhibition zone of SeNPs synthesis by *Bacillus clausii* against different bacteria on MHA at 37 °C for 24 hr .

Bacteria	Inhibition zone (mm)		
	(100 µg/ml)	(300 µg/ml)	(500 µg/ml)
E. coli	15	18	22
K. pneumoniae	18	19	21
E. Faecalis	18	21	25
S. Saprophyticus	17	20	23

After that , the MIC was detected by microtiter plate method . Different concentration of SeNPs ranging from (2 µg/ml -1024 µg/ml) were used .The minimum inhibitory concentration of nanoparticles (MIC) was calculated after the incubation of the microtiter plate for 24 hours at 37 °C (OD 570 nm) . A concentration which prevents growth of bacteria is considered the lowest concentration (MIC) . MIC (32 µg/ml) , MBC (64 µg/ml for *E. Faecalis* and *Staphylococcus saprophyticus*, while MIC and MBC for *Klebsiella pneumoniae* and *Escherichia coli* were (64 µg/ml) and (128 µg/ml) , respectively , table (4.5) .

Table (4.5) :MIC and MBC of SeNPs by microtiter plate against pathogenic bacteria

Test organisms	Minimum Inhibition Concentration (MIC) of SeNPs (µg/ml)	Minimum bactericidal concentration (MBC) of SeNPs (µg/ml)
E. coli	64	128
***K. pneumonia*e**	64	128
E. Faecalis	32	64
S. Saprophyticus	32	64

The application of nanoparticles and metal-based antibacterial strategies is one of the promising approaches to prevent diseases caused by antibiotic-resistant microbes (Chudobova *et al*., 2014). Previous studies indicated that SeNPs have more . Bacteriostatic effect than bactericidal action on microbes (Al Jahdaly *et al.*, 2021) .Our results showed that SeNPs synthesized by *Bacillus clausii* exhibited antibacterial effect towards both Gram-positive and Gram-negative bacteria . The antibacterial activity of chemically and biologically synthesized SeNPs was evaluated before, but with different methodologies and particle sizes , Nevertheless, the chemically synthesized SeNPs showed weaker antibacterial activity than the biogenic SeNPs (Zonaro *et al.*, 2015 ; Cremonini *et al*., 2016) .

Because of the thinner peptidoglycan layer and the presence of porins , selenium nanoparticles have higher antibacterial activity against gram positive bacteria . Moreover, SeNPs were found to have double effect against *Staphylococcus aureus* as silver nanoparticles (7 and 3 mm, respectively) (Chudobova *et al*., 2014) . While other studies demonstrated better antibacterial activity against *Pseudomonas sp*. than *Staphylococcus aureus*, and it failed to demonstrate activity against *Escherichia coli* and *Klebsiella sp* (Singh *et al*., 2014) . Moreover, 200 µg/mL of SeNPs showed antibacterial reactivity against *Escherichia coli* ATCC

8739, *Staphylococcus aureus* ATCC 9027, and *Pseudomonas aeruginosa* ATCC 25923 (Ullah *et al*., 2021) . The morphology of nanoparticles also plays the important role in its effectiveness against microbial species (Hong *et al*., 2016 ; Cheon *et al*., 2019) .

The difference between the findings of different studies is mainly due to the difference in the size of nanoparticles and the type of bacteria used . One of the most important factors affecting the antibacterial properties of nanoparticles is the particle size and concentration. It was considered that smaller nanoparticles had increased the production of ROS than larger surface area to volume ratio inside or out of the cells (Van Khanh and Van Cu , 2019) .

The use of nanoparticles as antibacterial agents is a promising strategy, especially when dealing with chronic and nosocomial infections. The widespread usage of commercial antibiotics has led to the development of multidrug-resistant bacterial strains . Generally, various mechanisms of nanoparticles antibacterial activity were recognized up to now: ROS generation, interaction with cell barrier (cell wall disruption and alteration in permeability), inhibition in the synthesis of proteins and DNA, expression of metabolic genes, etc. (Eleraky *et al*., 2020) .

Negatively charged SeNPs, exhibit more pronounced activity against Gram-positive bacteria, due to the absence of negatively charged LPS particles in their cell walls and thus the absence of the mentioned electrostatic repulsion (Filipović *et al*., 2021) .Given that the same behavior was observed for positively charged formulations of SeNPs, we can conclude that the electrostatic interaction between SeNPs and the bacterial cell barrier is not a critical step in determining their antibacterial activity. Negatively charged regions on Gram-negative bacteria's cell walls are insufficient to ensure the attachment of positively charged SeNPs

(Angeliki , 2021) . However, the low cytotoxic effect of biogenic SeNPs has been reported by (Forootanfar *et al*., 2014 ; Abbas *et al*., 2021).

4.7 Synergistic effect of SeNPs and antibiotic

The synergistic effect of SeNPs was investigated with six antibiotics (Azithromycin , Ciprofloxacin , Trimethoprime / sulphamethoxazole Doxycycline , nitrofurantoin and Ampicillin) against pathogenic bacteria. However, the mechanism for the synergistic activity is not known .

The synergistic effect of Doxycycline with SeNPs in all tested bacteria that sensitive to Doxycycline were decreased , and the isolates that were sensitive to antibiotic became intermediate and intermediate became resistant to antibiotic . while in *E. faecalis* only the effect of SeNPs were appeared when Doxycycline saturated with SeNPs .

The inhibition zone of nitrofurantoin when saturated with SeNPs were decreased in *Escherichia coli* , while in *Klebsiella pneumoniae* , *Enterococcus faecalis and Staphyllococcus Saprophyticus* the sensitivity remained same . As for the other antibiotics, some of them showed a slight increase in the diameters of inhibition , while others did not have any synergistic action between them and SeNPs , figure (4.13) .

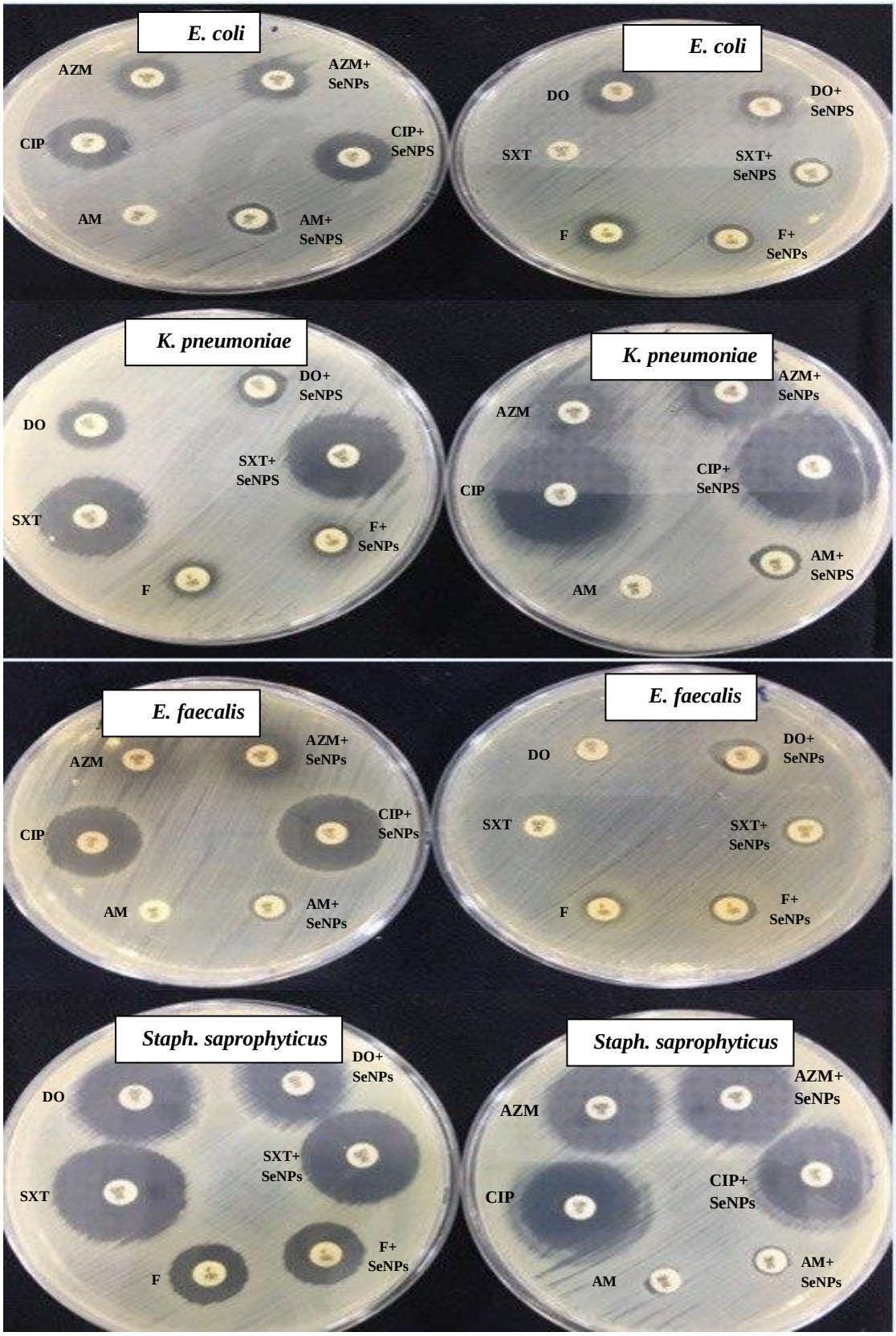

Figure (4.13): Antibacterial activity of SeNPs that combination with antibiotics against pathogenic bacteria on MHA at 37 º C for 24 hr.

Antibacterial combinations are used widely, although most infections in patients with normal defenses can be treated with a single antibacterial agent. Few reasons justify the use of antibacterial combinations: (1) broad-spectrum coverage for the initial therapy of severely infected patients; (2) poly-microbial infections; (3) prevention of selection of resistant microorganisms when a high mutation rate of the causal organism exists to the antibiotic indicated; (4) reduction of dose-related toxicity – this concern is rare and mostly of historical interest, related to the use of sulfonamides; and (5) antibacterial synergistic activity (Acar , 2000) . The emergence of antibiotics resistance in the majority of pathogenic bacterial strains is a cause of utmost concern in infectious bacterial diseases. Therefore, there is an inevitable need to identify the effective antibacterial agents which are more effective against microbial ailments with minimal side effects on host cells (Caruso and Poon , 2018).

Synergism is associated with the generation of hydroxyl radicals, alteration of protective cellular functions and an anti-biofilm potential. The combination of antibiotics with nanoparticles is more effective for enhancing antibiotic efficacy in comparison with the action of antibiotics when used in clinical practice. The combination involves reduced development of bacterial resistance, reduce the duration of treatment and reduce antibiotic dose requirements (Hwang *et al*., 2012) .

Nanoparticles enhanced the reaction rates of antibiotics in a synergistic mode as well as in its own way on different kinds of pathogens (Varak and Priya , 2019). Selenium (Se) is considered a potent antibacterial agent, and its derivative substance like selenium sulfide is extensively used in medicine to treat infections of microorganisms (Sadalage *et al*., 2020). However, overuse of Se causes toxic effects and leads to selenosis, which limits the use of elemental Se for therapeutic purposes (Ungvári *et al*., 2014 ; Gunti *et al*., 2019).

The probable mechanism responsible in enhanced antibacterial activity of antibiotics with selenium nanoparticles may be attributed to the bonding reaction between nanoparticles and antibiotics, then the antibiotic-selenium nanoparticle combination may attach on the cell membrane result in cell wall lysis, which was followed by the entry of SeNPs-antibiotic combination into the cell and may result in the DNA unwinding leads to cell death, the same mechanism suggested with silver nanoparticles and antibiotics (Krishna *et al*., 2015).

Ampicillin, oxacillin and penicillin caused higher inhibitory effects (44%, 8% and 13% respectively) when applied in combination with SeNPs than ATBs alone (Cihalova *et al*., 2015) . SeNPs can target the bacterial cellular membrane of *Staphyllococcus aureus*, SeNPs and LZD would have a synergistic effect (Nguyen *et al*., 2017) .

Tetracyclines such as doxycycline are thought to inhibit translation by binding to the 16S rRNA portion of the ribosome preventing binding of tRNA to the RNA-30S bacterial ribosomal subunit, which is necessary for the delivery of amino acids for protein synthesis. As a result of the above actions, the initiation of protein synthesis by polyribosome formation is blocked. This stops the replication of bacteria and produces a bacteriostatic effect (Suáreza *et al*., 2014 ; Chukwudi , 2016).

The cell walls of gram-negative bacteria are complex than those of gram positive bacteria, both structurally and chemically. The structure of gram-negative microorganisms cell contains two layers outside the cytoplasmic membrane , which represent a greater physical barrier to overcome. This structural complexity explain greater inhibitory effect of the derivatives against gram-positive bacteria (Alvand *et al*., 2022).

Another explanation may be attributed to binding of the hydrophobic groups incorporated into nanoparticle to the teichoic acid, a

structure present in gram positive bacteria, but absent in gram-negative bacteria, which may lead to death (Pasquina *et al*., 2013) .

4.8 Antioxidant assay of SeNPs

The DPPH (2,2-Diphenyl-1-picryl- hydrazyl) radical scavenging assay was used to detect the antioxidant ability of the SeNPs biosynthesized from *B. clausii* in *vitro* by reducing DPPH free radicles . After adding of SeNPs to (0.1 mmol/L) DPPH solution , the absorbance (A) was measured at 517 nm after 30 minutes. The results revealed the ability of nanoparticles to scavenge DPPH free radicals , indicated by observing the color change from the original color of DPPH purple into yellow color in microtiter plate . The activity of SeNPs to reducing DPPH increased with the increas e of SeNPs concentration . It was 39.6 % in 50 µg/ml , 63.1 % in 100 µg/ml, 74.2 % in 150 µg/ml , Figure (4.14).

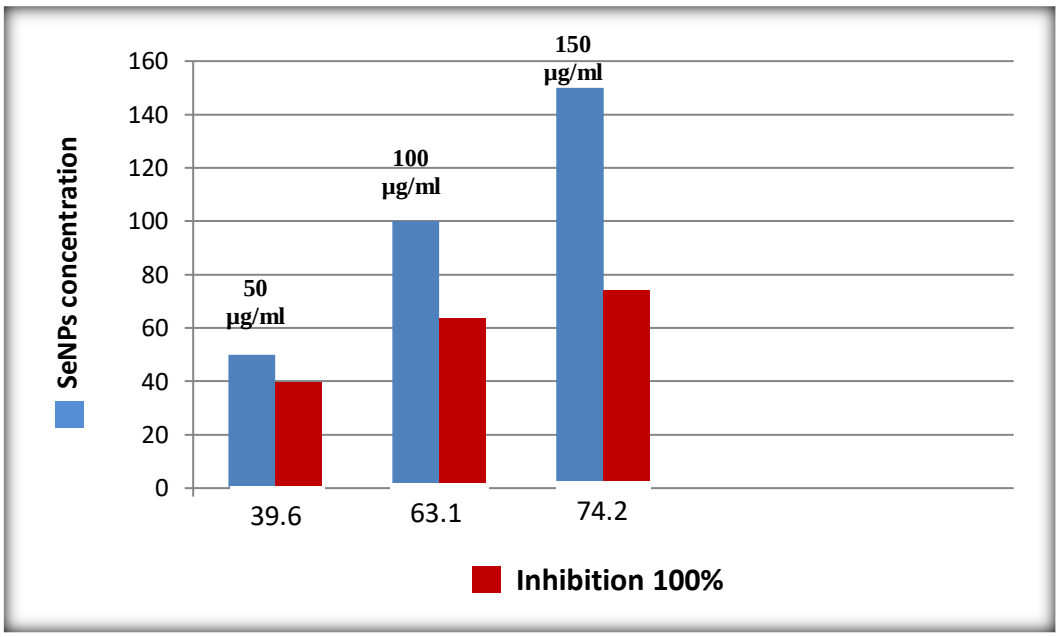

Figure (4.14) : antioxidant activity of Selenium nanoparticles .

According to previous reports, SeNPs have a strong free radical scavengers that can be used as an active form of selenium in food supplements (Boroumand *et al*., 2019 ; Menon *et al*., 2019) . As mentioned before, the antioxidant capacity of NPs increased with the decrease in their dimensions (Shah *et al*., 2017) . This lead to the

hypothesis that, since the cleaning procedure affects the size of the NPs, it also has an impact on their antioxidant capacity. Stable DPPH radicals are widely used to evaluate the antioxidant activity of NPs (Pyrzynska and Pękal , 2013) .

Different mechanisms involved in the radical-antioxidant reactions may explain the difference in scavenging potentials of compounds . The mechanisms of antioxidants are not only by scavenging free radicals, but also by inhibiting production of free radicals (Niki , 2010).

4.9 Haemolysis Effect of SeNPs

The hemolysis was detected by using Triton X-100 as indicators of positive control. Sterile solution of phosphate buffer saline was used as a negative control . SeNPs with all concentration (50, 100,150 µg/ml) did not show any hemolysis for the tested whole blood, as shown in figure (4.15) .

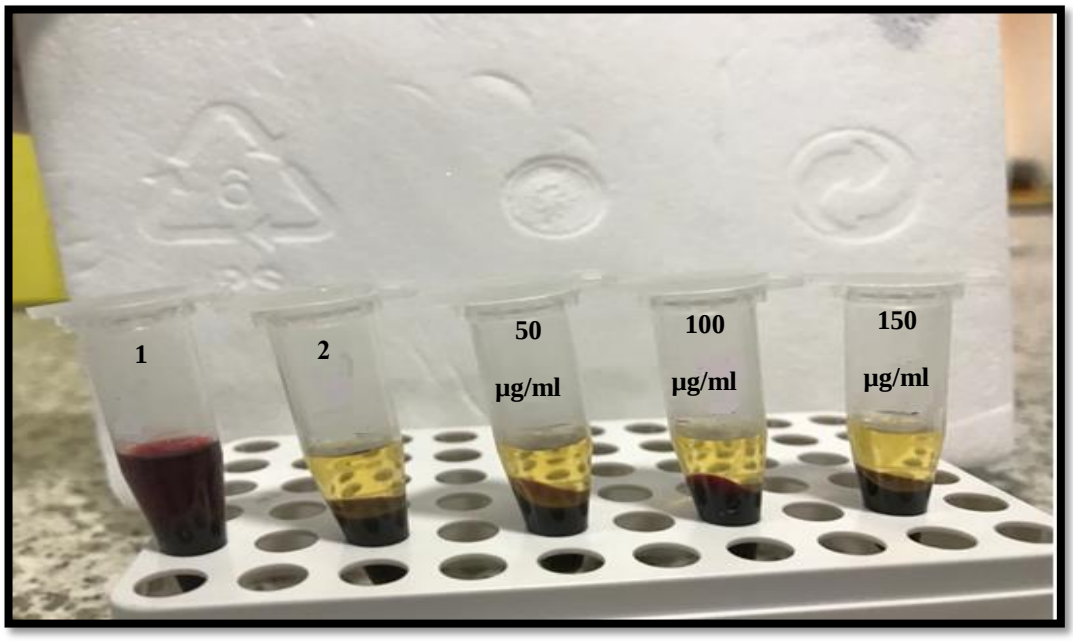

Figure (4.15) : Effect of selenium nanoparticles on hemolysis , 1 (positive control) , 2 (negative control).

Hemolysis is characterized by the rupture of red blood cells (RBCs) and the release of their contents, ultimately leading to anemia, jaundice

and renal failure . All materials entering the blood get in contact with RBCs and so the evaluation of the hemolytic ability of the biomaterials is of utmost importance (Archana *et al.*, 2013 ; Beris and Picard , 2015) .

earlier studies have reported the hemolytic properties of various nanoparticles such as gold , carbon nanotubes , iron oxide, silica , selenium , and silver nanoparticles (Ahn *et al*., 2018 ; Singh *et al*., 2019 ; Liu *et al*., 2020 ; Tsamesidis *et al*., 2020 ; Tang *et al*., 2021; Badmus *et al*., 2022).

SeNPs nanoparticles displayed very modest haemolysis, with only 18% of maximal lysis recorded in vitro (Tran *et al*.,2015) . A very low haemolysis rate (below 5%), showing that all of the produced NPs had good blood compatibility (Zou *et al*., 2021) . While , other research showed that hemolysis and RBC osmotic fragility tests doesn't induce damage to RBC membrane; The hemolysis values demonstrated good bio-compatibility, especially for titanium specimens changed with starch-derived Selenium NPs (Cavalu *et al*., 2018) .

4.10 Biofilm formation assay

By using Congo red method , out of 115 , 60 (52.1%) isolates gave a positive ability to form biofilm , *Klebsiella pneumoniae* (9) , *Escherichia coli* (34) , *Enterococcus. faecalis* **(**14) , *Staphylococcus Saprophyticus* (3) , figure (4.16) . The strength of biofilm formation were investigated by the Microtiter plate method , it is a quantitative method to determine biofilm production by spectrophotometer using an ELISA reader at a wavelength of 620 nm to give a final digital value representing the quantity of biofilms produced by the bacterial suspension in the wells and considered as a standard quantitative method .

Out of 34 isolates of *E.coli* , 25 (73.5 %) were strong biofilm producers , while 6 (17.6 %) were moderate biofilm producers , the remaining 3 isolates accounting for (8.8 %) of the total isolates were weak

biofilm producers . Out of 14 isolates of *E. faecalis* , 9 (64.2 %) were strong biofilm producers , while 3 (21.4 %) were moderate biofilm producers , the remaining 2 isolates accounting for (14.2 %) of the total isolates were weak biofilm producers . Out of 9 isolates of *Klebsiella pneumoniae* , 9 (100 %) were strong biofilm producers , and all 3 (100 %) isolates of *Staphylococcus Saprophyticus* were form strong biofilm , table (4.6) .

Table (4.6): Biofilm Production Capacity (OD 620 nm) of bacterial isolates

Bacteria	Biofilm degree		
	Strong	Moderate	Weak
E. coli	25	6	3
K. pneumonia	9	0	0
E faecalis	9	3	2
Staph. Saprophyticus	3	0	0

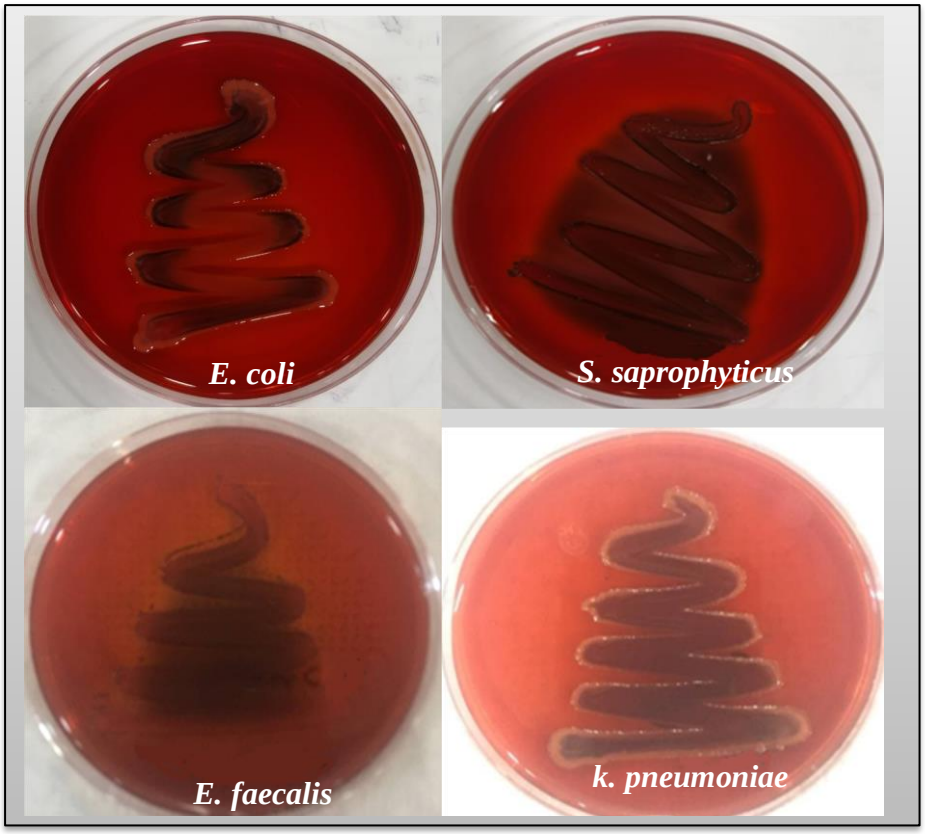

Figure (4.16) :Biofilm formation assay for gram positive and gram negative bacteria on Congo red agar at 37 º C for 24 hr .

Gram negative bacteria are greater than gram positive bacteria in biofilms formation (*Escherichia coli, Klebsiella pneumoniae* , *Enterococcus feacalis* , *Staphylococcus aureus* , *Proteus mirabilis* , *Pseudomonas aeruginosa* and *Citrobacter*) these biofilms were induced by urinary catheter infections (Almalki and Varghese , 2020) . Bacterial biofilms represented a significant source of human infections, which may be acquired through interaction with a wide range of everyday or clinical environments including the consumption of contaminated foods, via hospital environment, medical equipment or devices (Srey *et al*., 2013) .

Most *Klebsiella spp* isolates have potential to be attached in various grades and levels of biofilm production utilizing microtiter Plate methods on the smooth surface (glass and plastic surfaces) (Abood and Ibrahim , 2017) . Biofilms are defined as complex microbial communities enclosed in hydrated extracellular polymeric substances (EPS), which comprise polysaccharides, proteins, phospholipids, teichoic and nucleic acids , that form on a wide variety of surfaces, including living tissues, indwelling medical devices, industrial or potable water systems, food and food-contact surfaces, thereby establishing reservoirs for continuous contaminatio (Costa *et al*., 2018) .

Biofilm production was variable from species to species among the bacterial species , noted that certain bacterial species have a high biofilm forming ratio, while others have poor skills (Lianou *et al*., 2020). Due to their heterogeneous nature, bacterial biofilms are characterized with an enhanced resistance by comparison with their planktonic counterparts to most environmental stresses including nutrient starvation, oxidative stress, antibiotic exposure and other conditions detrimental to bacterial growth (Giaouris *et al*., 2014 ; Bridier *et al*., 2015) .

4.11 Antibiofilm activity of SeNPs

In order to evaluate the anti-biofilm effect of SeNPs , three isolates of each biofilm producer isolates of *Escherichia coli , Klebsiella pneumoniae, Enterococcus faecalis , Staphylococcus Saprophyticus* were tested . SeNPs expressed antibiofilm activity with increasing it´s concentration from (2 to 1024 µg/ml) , the absorbance will decrease with the increasing of SeNPs concentration . The MIC of (*Escherichia coli , Klebsiella pneumoniae*) was (128 µg/ml) , and (64 µg/ml) for *(Staphylococcus Saprophyticus* and *Enterococcus faecalis*) . The MICs of SeNPs against biofilm were found to be twice the MIC in planktonic state.

New strategies other than conventional antibiotic treatments are needed to control biofilm formation in bacterial infections . However, in most cases antibiotics fail to the eradicate these cells, MIC required to eradicate bacteria in biofilms is much higher than MIC of planktonic cells (Chopra *et al*., 2015).

Biofilms are complex bacterial colonies that are resistant to antibiotics as well as the human immune system . To combat the problems, SeNPs have been used to employ antibiofilm activity , a potentially significant potential therapy (Vincent *et al*., 2014) . Selenium nanoparticles either biogenic origin or chemically synthesized have been proven to possess surprising antibacterial and antibiofilm capabilities (Cihalova *et al*., 2015; Cremonini *et al*., 2016; Huang *et al*., 2016).

Although the biogenic SeNPs had antibacterial and antibiofilm effects, they did not show ability to remove the established biofilm up to 50 µg/mL. The concentration of 75 µg/mL showed slight effect on removing the established biofilm (Khiralla and El-Deeb , 2015) .The combined use of MB (Methylene Blue) and SeNPs significantly reduced Colony-Forming Units (CFUs) of one-day-old *Enterococcus*

faecalis biofilm in comparison with the control group (*P value* < 0.05) (Shahmoradi *et al*., 2021) .

The antibiofilm effect of SeNPs was evident at concentrations of 50–200 μg/mL for *V. cholerae* O1 ATCC 14035 strain (Bagheri-Josheghani and Bakhshi , 2022) .The results are consistent with the findings of a previous study which reporting that SeNPs completely eradicated the biofilm structure of *E. coli* at a concentration of 60µg/L (Zonaro *et al*., 2015).

SeNPs that produ^{c}ed by *Providencia vermicola* BGRW under the studied conditions had slight ability to remove established biofilm of different bacteria . 20µg/mL of SeNPs showed a slight effect as a removing agent against the established biofilm developed by all tested strains whereas the strong biofilm turned to moderate biofilm except E.coli whereas, at 24µg/mL, the established biofilm was moderate , while Incorporation of 32µg/mL of SeNPs showed a stronger effect in removing agent against all studied bacteria whereas all established biofilm became weak biofilms. SeNPs are known to have killing effect against S. aureus (El-Deeb *et al*., 2018) .

This could provide an interpretation for the slight removing effect of SeNPs obtained in the present study, where the dead cells could lose their ability to adhere to the surviving cells in the polysaccharide matrix of the established biofilm resulting in the dispersal of a subpopulation of surviving cells (Khiralla and El-Deeb , 2015) .

4.12 Determination the Toxicity of SeNPs on (PC3) Cancer Cell Line and (WRL 68) normal cell line

The cytotoxic response of prostate cancer PC3 cell line and normal hepatic WRL68 cells treated with increasing concentrations of Se NPs (25, 50, 100, 200, 400 µg/mL) was investigated using MTT assay after 24 h exposure. Results in table (4.7) , showed that no significant cytotoxic

effect of Se NPs against PC3 cells at concentrations 25 and 50 µg/mL. Nevertheless, SeNPs at concentration 100, 200 and 400 µg/mL exhibited a dose dependent decrease in PC3 cell viability with maximum inhibition rate of 51.27±2.77% of PC3 cells at 400 µg/mL.

Table (4.7): Multiple comparisons of mean±SD cell inhibition between PC3 and WRL68 treated with Se NPs (25, 50, 100, 200, 400 µg/mL) for 24 hr.

Se NPs	PC3	WRL68	Sig.	*p* Value
	Mean Inhibition ± SD (%)	Mean Inhibition ± SD (%)		
400 µg/mL	51.27±2.77[a]	36.86±3.38[a]	**	<0.00001
200 µg/mL	36.3±2.12[b]	25.54±0.85[b]	**	<0.00001
100 µg/mL	22.38±2.41[c]	9.03±3.3[c]	**	<0.00001
50 µg/mL	8.08±1.36[d]	5.36±1.51[c]	NS	0.5243
25 µg/mL	4.05±0.53[d]	4.71±1.05[c]	NS	0.9981

****: $p < 0.01$, NS: non-significant. Different letters (a, b, c, d) consider significant ($p < 0.05$) in column.**

Regarding WRL68 cells, the sensitivity of the cells to SeNPs treatments was less than that of PC3. Se NPs concentrations at 25, 50 and 100 µg/mL showed no significant differences in pattern of cell inhibition. On the other hand, Se NPs at 200 and 400 µg/mL showed significant ($p < 0.05$) reduction in cell viability with maximum inhibition of 36.86±3.3% at 400 µg/mL.

Multiple comparisons study , table (4.7) between PC3 and WRL68 with regard to SeNPs toxicity showed significant differences ($p = <0.0001$) in the pattern of cell inhibition at 100, 200 and 400 µg/mL, which obviously PC3 cells were more susceptible to SeNPs treatment than WRL68 cells. IC_{50} of Se NPs against PC3 and WRL86 was calculated with values of 164.4 and 175.4 µg/mL, respectively , figure (4.17) .

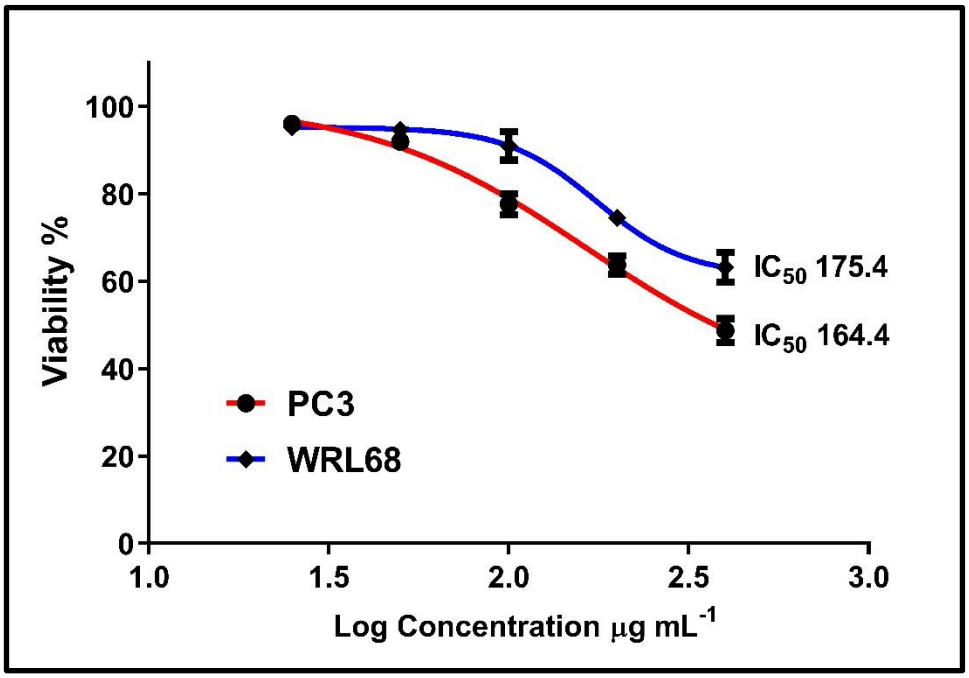

Figure (4.17): (IC_{50}) of SeNPs on PC3 and WRL68 cells treated with NPs at 37°C for 24 hr.

One of the most common materials used in the production of solar cells and photography is selenium, which exhibits a well-known photoelectrical property. It is also an essential component of the human body, as it can protect tissues and cells from free radicals *in vivo* (Alkhudhayri *et al*., 2020). A dose-dependent assessment of the effects of Se NPs on the viability of PC3 cells revealed that the cytotoxic effects of Se NPs were detrimental. The results showed that the presence of Se NPs negatively affected the cell viability of PC3 cells. Depending on their physiochemical characteristics, Se NPs exhibits the tendency to induce the production of reactive oxygen species in exposed cells and thus responsible for the cytotoxic effect (Soltani and Darbemamieh , 2021).

It was indicated that the method of NPs preparation, structure and size of Se nanomaterials have high impact on the antitumoral effect of Se NPs (Siddiqui *et al*., 2020). It was reported that Se NPs in combination with other nano-metals exhibited antiproliferative effect against HepG2

cell line through induction of apoptosis (Cui *et al*., 2018). Moreover, a significant decrease in the viability of prostate LNCaP cell line was observed when treated with different concentrations of Se NPs with signature feature of necrosis due to the decrease in caspases and no LDH release from the cells (Sonkusre , 2020).

Se NPs were found to play an important role in inhibiting numerous types of cancer cells with low effect on normal cells. Similarly, studies have been suggested that Se NPs have potent cytotoxicity against tumor cells, but not against normal cells, like cervical carcinoma, hepatocarcinoma and colorectal cancer (Zhou *et al*., 2016). However, studies confirmed that Se NPs are significantly potent against many cell lines and that their cytotoxicity on prostate cancer cell lines is more convincing than other types of tumor cell lines (Ferro *et al*., 2021; Khurana *et al*., 2019).

The inhibition rate of SeNPs on cancer cells ranged from 46.3% to 77.2% and the most obvious inhibitory effect was observed in prostate cancer cell line after treatment with 100 µg Se NPs (Liao *et al*., 2020) .The molecular mechanism by which Se NPs trigger suppression in tumor cell viability is still not fully understood. In general, Se NPs able to activate tumor cell apoptosis by enhancing cellular uptake and generating reactive oxygen species (Liu *et al*., 2017). Other study reported that Se NPs can stimulate cancer cell autophagy, thus minimizing tumor cell growth and metastasis (Huang *et al*., 2018). Also Se NPs exhibited the ability to induce TNF upregulation, which activate cancer cell necrosis (Sonkusre and Cameotra, 2017).

4.13 : Effect of Se NPs on gene expression of some virulence factor

The results showed that a higher value of *Hly* gene expression was (11.91) in the control group, but a lower value of *Hly* gene expression was (1.51) in Sub-MIC 32 group. There are no significant differences between the Sub-MIC 32 group and MIC 64 group in gene expression of *Hly* gene . However, the control group reveals more significant differences compared with other groups at a significant level (P<0.05) , and a higher value of *FimH* gene expression was (14.31) in the control group, but a lower value of *FimH* gene expression was (2.47) in Sub-MIC 32 group. The findings demonstrated that There are significant differences between the Sub-MIC 32 group , MIC 64 group , and control group in gene expression of *FimH* gene at a significant level (P<0.05) , as shown in (appendices 8) , figure (4.18) .

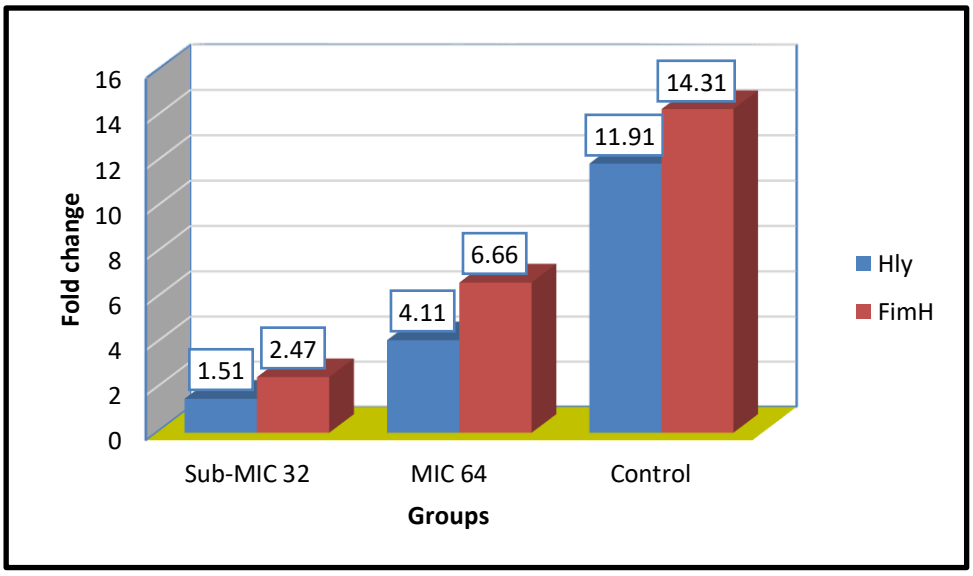

Figure (4.18): Fold change (gene expression) for *Hly* gene and *FimH* gene in *E. coli* .

The results showed that the higher value of *Luxs* gene expression was (15.45) in the control group, but the lower value of *Luxs* gene

expression was (1.38) in Sub-MIC 64 group. There are no significant differences between the Sub-MIC 64 group and the MIC 128 group in gene expression of *Luxs* gene. However, the control group reveals significant differences as compared with other groups at a significant level (P<0.05).

The results showed that a higher value of *qsec* gene expression was (5.52) in the control group, but a lower value of *qsec* gene expression was (0.79) in Sub-MIC 64 group. The findings demonstrated significant differences between Sub-MIC 64 group and MIC 128 group. However, the gene expression of *qsec* gene showed significant positive differences in the control group compared with the other groups at a significant level (P<0.05), as shown in (appendices 9) , figure (4.19) .

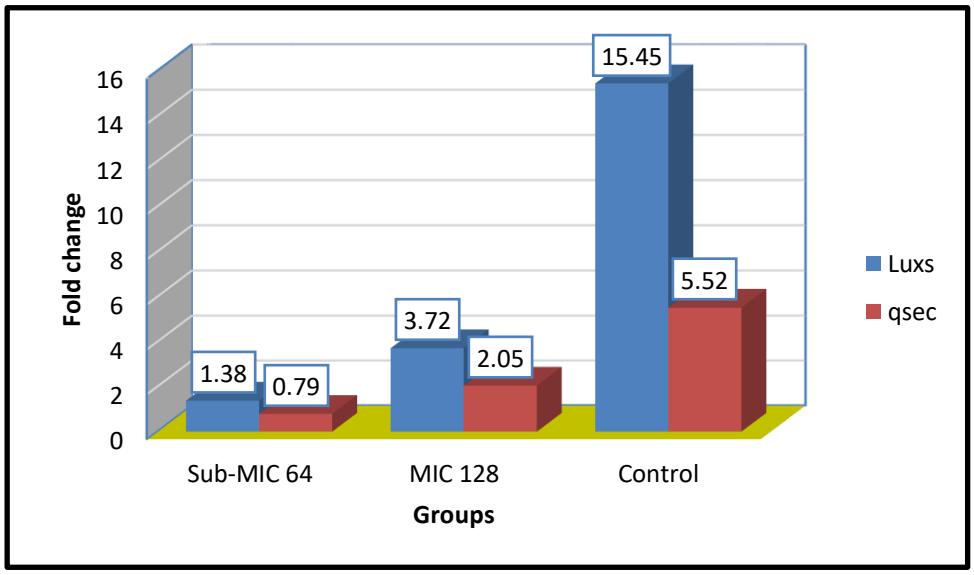

Figure (4.19) : Fold change (gene expression) for *LuxS* gene and *qseC* gene in *E.coli* .

While in *Enterococcus faecalis* the results showed that a higher value of *ESP* gene expression in *Enterococcus faecalis* was (38.13) in the control group, but a lower value of *ESP* gene expression was (1.32) in Sub-MIC 16 group. There are significant differences among the Sub-MIC 16 group, MIC 32 group, and control group in gene expression of the *ESP*

gene, the gene expression of MIC 32 group showed positive significant differences as compared with Sub–MIC 16 group at significant level (P<0.05).

The results showed that a higher value of *HLY* gene expression in *Enterococcus faecalis* was (22.18) in the control group, but a lower value of *HLY* gene expression was (2.21) in Sub-MIC 16 group. The findings demonstrated no significant differences between Sub-MIC 16 group and MIC 32 group. However, the control group showed significant positive differences in gene expression of the *HLY* gene at a significant level (P<0.05), as shown in (appendices 10) , figure (4.20) .

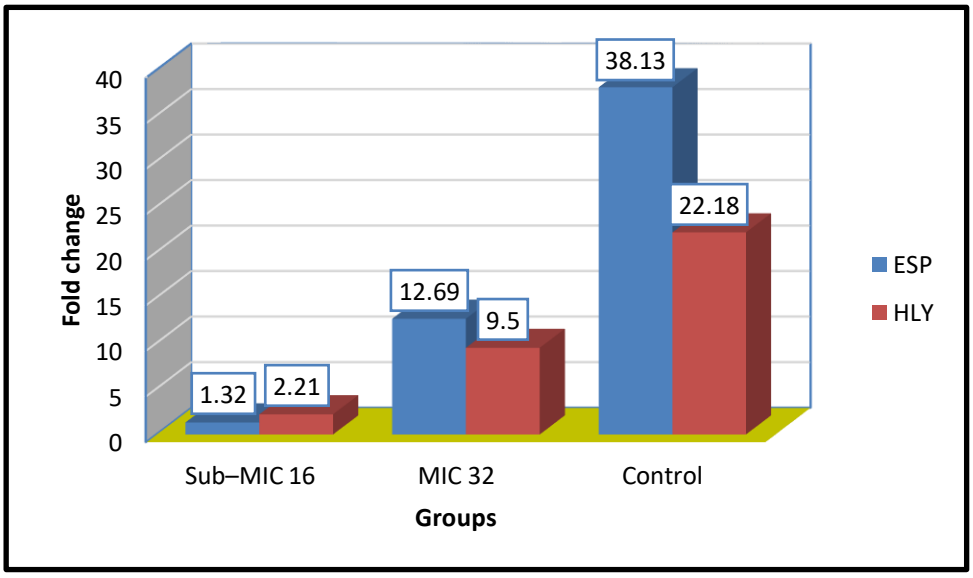

Figure (4.20): Fold change (gene expression) for *ESP* and *HLY* gene in *E. faecalis* .

The higher value of *gelE* gene expression in *Enterococcus faecalis* was (4.70) in the control group, but the lower value of *gelE* gene expression was (0.41) in the Sub-MIC 32 group. There are no significant differences between Sub-MIC 32 group and MIC 64; however, the control group showed significant positive differences as compared with the other groups gene expression of *gelE* gene at a significant level (P<0.05).

The results showed that a higher value of *fsrA* gene expression in *Enterococcus faecalis* was (14.15) in the control group, but a lower value of *fsrA* gene expression was (2.09) in Sub-MIC 32 group. The findings demonstrated that there are significant differences among the Sub-MIC 16 group, the MIC 32 group, and the control group in gene expression of *fsrA* gene at a significant level (P<0.05), as shown in (appendices 11) , figure (4.21) .

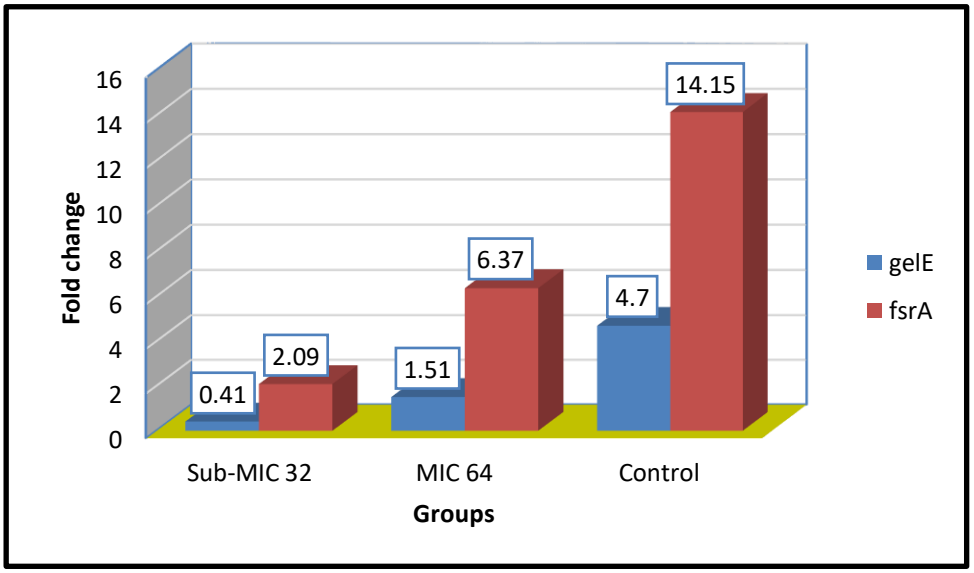

Figure (4.21): Fold change (gene expression) for *gelE* gene and *fsrA* gene in *E. faecalis* .

Studies related to this subject are almost non-existent. Therefore, our study sheds light on this aspect for the first time by studying the effect the Selenium nanoparticles on the gene expression of several genes. It is necessary to refer to many studies that deal with topics related to our topic.

Nanoparticles (NPs) have been widely studied as an alternative to antibiotic use. It is used on many microorganisms such as *Enterococcus faecalis* (Salas-Orozco *et al*., 2022). The enterococcal surface protein , *Esp*, is a high-molecular-weight surface protein of unknown function whose frequency is significantly increased among infection-derived *Enterococcus faecalis* isolates . The presence of the *esp* gene is highly

associated with the capacity of *E. faecalis* to form a biofilm on a polystyrene surface, since 93.5% of the *E. faecalis esp*-positive isolates were capable of forming a biofilm. *Esp* expression in an *E. faecalis esp*-deficient strain promoted primary attachment and biofilm formation. these results reveals that the biofilm formation is widespread among *E. faecalis*, the biofilm formation is restricted to the *E. faecalis* strains harboring *esp*, and *Esp* promotes primary attachment and biofilm formation of *E. faecalis* on abiotic surfaces (Toledo-Arana *et al*., 2001).

ESP expression in *Enterococcus faecalis* is related to the primary adherence and biofilm formation of *E. faecalis*. Twelve *E. faecalis* harboring *esp* gene strains were included, and showed MIC testing and gene expression assay showed that curcumin NPs did not show any inhibitory activity against biofilm formation. these nanoparticles contribute very little, if at all, to inhibition of the *esp* operon (Alizadeh *et al.*, 2019).

NanoZnO/Ze were tested on biofim production of *E. faecalis* and its *esp* gene expression were assessed under nanocomposite treatment . ZnO nanoparticles can effectively inhibited the biofilm formation and affected *esp* gene downregulation of *E. faecalis*. NanoZnO/Zeolite can used against the biofilm infections due to *E. faecalis* and downregulation of *ESP* gene (Partoazar *et al*., 2019).

The application of Selenium nanoparticles as antibacterials are gaining relevance in the medical field . Selenium nanoparticles showed the highest bactericidal and antibacterial properties. The antibacterial effects of selenium nanoparticles were evaluated with respect to growth, biofilm formation of *Staphylococcus aureus* strains (Verma and Maheshwari , 2017).

The strong inhibition effect of SeNPs on biofilms of MERSA isolates , the biofilm formation was intensely inhibited (more than 99%). The use of SeNPs as a tool for the treatment of bacterial infections by induction molecular changes , and increasing resistance of bacteria (Cihalova *et al*., 2015). The most widely application of Se NPs induced apoptosis is to kill cancer cells with the participation of some important signaling events, such as ROS generation, anti-apoptotic gene down-regulation, pro-apoptotic gene up-regulation and caspases activation (Cui *et al*., 2018).

Many studies found that selenium nanoparticles (SeNPs) can influence the genes expression for many genes by management of the transcription factors , and epigenetic DNA methylation . The SeNPs treatments transcriptionally upregulated the bZIP1 transcription factor by an average of 3.5 folds. the upregulation in the expression of the WRKY1 transcription factor. These findings provide that SeNPs associated molecular variations, metabolism and gene expression (parsameher *et al*., 2017 ; Ren *et al*., 2019 ; Sotoodehnia-Korani *et al*., 2020).

Selenium nanoparticles were synthesized with *Bacillus* sp. MSH-1. The ultrastructure of selenium nanoparticles was evaluated with a transmission electron microscope. The antifungal susceptibility test was performed according to the modified Clinical and Laboratory Standards Institute M27-A3 standard protocol. The expression levels of the *CDR1* and *ERG11* genes were analyzed using the quantitative real-time polymerase chain reaction (PCR) assay. The azole-resistant *C. albicans* and wild type *C. albicans* strains were inhibited by 100 and 70 µg/mL of selenium nanoparticle concentrations, respectively. The expression of *CDR1* and *ERG11* genes was significantly down-regulated in these selenium nanoparticle concentrations (Parsameher *et al*., 2017).

Dietary inorganic Se and bacterial organic Se were observed to significantly increase affect levels of gene expression of many genes such as mRNA level in GSH-Px1, GSH-Px4, DIO1, and TXNDR1, while both ADS18 and ADS2 showed high level of mRNA of DIO2 compared to sodium selenite (Dalia *et al*., 2017).

Antibacterial properties of all three nanomaterials were probed against Gram-positive *Enterococcus faecalis*. Se exhibited relatively strong antibacterial activity against both Gram-positive and possible three-pronged approach of bacterial cytotoxicity by these graphene-based materials (Niranjan *et al*., 2022).

Trans-cinnamaldehyde significantly decreased uro-epithelial cell attachment and invasion by uropathogenic *E. coli* ($p < 0.05$). Real-time quantitative polymerase chain reaction revealed that trans-cinnamaldehyde significantly decreased the expression of major genes involved in uropathogenic *E. coli* attachment and invasion of host tissue ($p < 0.05$). The down-regulating effect of trans-cinnamaldehyde on these genes potentially translated into decreased ability of uropathogenic *E. coli* to attach and invade bladder cells (Amalaradjou *et al.*, 2011).

In summary, this study highlights some possible effect of SeNPs on the gene expression of some genes such as *hly*, *FimH*, *Luxs*, *qsec* in *E.coli*, furthermore, *ESP*, *HLY*, *gelE*, and *fsrA* in *Enterococcus faecalis* . We can conclude that , use of higher dose of selenium nanoparticles leads to a decrease in the gene expression of a number of important and vital genes that affect the main functions of the microorganisms used in the study and thus reduce their pathogenicity. This subject come to support the promise of SeNPs in a wide range of medical applications.

Conclusions

and

Recommendations

Conclusions

The present study concludes that

1- The major causative agents of UTIs were *Escherichia coli* (Gram negative bacteria) followed by *Enterococcus faecalis* , *K. pneumonia* , and *Staphylococcus saprophyticus* .
2- SeNPs can be prepared using *Bacillus clausii* through biological method and the nanoparticles showed typical properties and high stability in suspension .
3- In synergistic effect of nanoparticle and antibiotic , all tested bacteria remained resistant to Ampicillin when satiated with SeNPs and only the nano effect appeared , while the synergistic effect of Doxycycline with SeNPs in all tested bacteria that sensitive to Doxycycline were decreased .
4- Selenium nanoparticles showed a high antimicrobial activity against pathogenic bacteria .
5- Antioxidant activity of selenium nanoparticle which are in acceptable range, indicating their ability of reducing free radicles
6- Selenium nanoparticles proved to have a considerable antibiofilm activity against pathogenic tested bacteria .
7- Selenium nanoparticles didn't show hemolysis .
8- Biological SeNPs had low toxicologically parameters on normal cell , so the SeNPs synthesized is safe because of its low toxicity and show anti-cancer effects against PC3 .
9- The results of Gene expression of some virulence factor revealed that SeNPs effective on genes expression by down regulation .

Recommendations

1- Synthesis of selenium nanoparticles using other microorganisms and other method and making a comparative study between them .

2- Compare between commercial selenium nanoparticles and Biological selenium nanoparticles .

3- Using the selenium nanoparticles as antifungal and antiviral , and the effects of SeNPs on some immunological parameters in lab animals and in tissue culture .

4- Further study of antimicrobial effect of SeNPs *in vivo* by using animals lab is needed

5- Detecting the roles of selenium nanoparticles in the industrial and agricultural applications as well as medical application .

6- Extensive studies about gene expression of other virulence factor of pathogenic bacteria treated with SeNPs .

References

References

Abbas, F. M. (2020). Phenotypic and molecular detection of SHV β-lactamase producing *Klebsiella pneumoniae* resistant to carbapenem from Al-Hillah Teaching Hospital environment, Babylon Province, Iraq. *EurAsian Journal of BioSciences*, 14(2), 7351-7355.

Abbas, H. S., Abou Baker, D. H., and Ahmed, E. A. (2021). Cytotoxicity and antimicrobial efficiency of selenium nanoparticles biosynthesized by *Spirulina platensis* . *Archives of Microbiology*, 203(2), 523-532.

Abbrescia, A., Palese, L. L., Papa, S., Gaballo, A., Alifano, P., and M Sardanelli, A. (2014). Antibiotic sensitivity of *Bacillus clausii* strains in commercial preparation. *Clinical Immunology, Endocrine and Metabolic Drugs* (Discontinued), 1(2), 102-110.

Abdal Dayem, A., Hossain, M. K., Lee, S. B., Kim, K., Saha, S. K., Yang, G. M., Choi, H.Y., and Cho, S. G. (2017). The role of reactive oxygen species (ROS) in the biological activities of metallic nanoparticles. *International Journal of Molecular Sciences*, 18(1), 18010120 .

Abobatta, W. F. (2018). Nanotechnology application in agriculture. *Acta Scientific Agriculture*, 2(6) , 99 - 102 .

Abood, S. H., and Ibrahim, I. A. (2017). Comparison of biofilm formation by different species of Klebsiella . *Pakistan Journal of Biotechnology*, 14(4), 531-535.

AbouElmaaty, T., Abdeldayem, S. A., Ramadan, S. M., Sayed-Ahmed, K., and Plutino, M. R. (2021). Coloration and multi-functionalization of polypropylene fabrics with selenium nanoparticles . *Polymers*, 13(15) , 13152483 .

Acar, J. F. (2000). Antibiotic synergy and antagonism. *Medical clinics of north america*, 84(6), 1391-1406.

Ahn, E. Y., Lee, Y. J., Choi, S. Y., Im, A. R., Kim, Y. S., and Park, Y. (2018). Highly stable gold nanoparticles green-synthesized by upcycling cartilage waste extract from yellow-nose skate (Dipturus chilensis) and evaluation of its cytotoxicity, haemocompatibility and antioxidant activity. *Artificial Cells, Nanomedicine, and Biotechnology*, 46(2), 1108-1119.

Al Jahdaly, B. A., Al-Radadi, N. S., Eldin, G. M., Almahri, A., Ahmed, M. K., Shoueir, K., and Janowska, I. (2021). Selenium nanoparticles synthesized using an eco-friendly method: dye decolorization from aqueous solutions, cell viability, antioxidant, and antibacterial effectiveness. *Journal of Materials Research and Technology*, 11, 85-97.

Alagesan, V., and Venugopal, S. (2019). Green synthesis of selenium nanoparticle using leaves extract of *withania somnifera* and its biological applications and photocatalytic activities . *Bionanoscience*, 9(1), 105-116.

Alam, H., Khatoon, N., Khan, M. A., Husain, S. A., Saravanan, M., and Sardar, M. (2020). Synthesis of selenium nanoparticles using probiotic bacteria *Lactobacillus acidophilus* and their enhanced antimicrobial activity against resistant bacteria. *Journal of Cluster Science*, 31(5), 1003-1011.

Alav, I., Sutton, J. M., and Rahman, K. M. (2018). Role of bacterial efflux pumps in biofilm formation. *Journal of Antimicrobial Chemotherapy*, 73(8), 2003-2020.

Ali, E. S., Sharker, S. M., Islam, M. T., Khan, I. N., Shaw, S., Rahman, M. A., Uddin, S.J., Shill, M.C., Rehman, S., Das, N., Ahmad, S., Shilpi, J.A., Tripathi, S., Mishra, S.K., and Mubarak, M. S. (2021).

Targeting cancer cells with nanotherapeutics and nanodiagnostics: Current status and future perspectives. *Seminars in Cancer Biology* , 69, 52-68 .

Aliasgharpour, M., and Rahnamaye Farzami, M. (2013). Trace elements in human nutrition: A review. *International Journal of Medical Investigation*, 2(3), 115-128.

Alizadeh, S. S., Amini, K., and Saffarian, P. (2019). Evaluating the inhibitory effect of Curcumin nanoparticles associated with expression of esp gene in *Enterococcus faecalis* biofilm. *Razi Journal of Medical Science* , 26(9) , 39-46 .

Al-Kazaz, F. F. M., Hussain, D. H., and Khalaf, S. A. (2021). The effect of copper oxide and selenium nanoparticles on vitamin d levels in women with infertility. *Plant Archives*, 21(1), 86-93.

Alkhudhayri, A.A., Wahab, R., Siddiqui, M.A., and Ahmad, J.(2020). Selenium Nanoparticles Induce Cytotoxicity and Apoptosis in Human Breast Cancer (MCF-7) and Liver (HepG2) Cell Lines. *Nanoscience and Nanotechnology Letters* , 12(3), 324-330.

Almalki, M. A., and Varghese, R. (2020). Prevalence of catheter associated biofilm producing bacteria and their antibiotic sensitivity pattern . *Journal of King Saud University-Science*, 32(2), 1427-1433.

Alvand, Z. M., Rahimi, M., and Rafati, H. (2022). Interaction of a Natural Compound Nanoemulsion with Gram Negative and Gram Positive Bacterial Membrane; A Mechanism Based study Using a Microfluidic Chip and DESI Technique. *International Journal of Pharmaceutics*, 122181.

Al-Zuhairy, A. M., and Al-Dahmoshi, H. O. (2020). Aminoglycosides and fluoroquinolones resistant genes among uropathogenic

Escherichia coli in Hilla City, Iraq. *Drug Invention Today*, 13(2) , 307 – 312 .

Amalaradjou, M. A. R., Narayanan, A., and Venkitanarayanan, K. (2011). Trans-cinnamaldehyde decreases attachment and invasion of uropathogenic *Escherichia coli* in urinary tract epithelial cells by modulating virulence gene expression. *The Journal of Urology*, 185(4), 1526-1531.

Amin, K. A., Hashem, K. S., Alshehri, F. S., Awad, S. T., and Hassan, M. S. (2017). Antioxidant and hepatoprotective efficiency of selenium nanoparticles against acetaminophen-induced hepatic damage. *Biological Trace Element Research*, 175(1), 136-145.

Anderson, H. E., Santos, I. C., Hildenbrand, Z. L., and Schug, K. A. (2019). A review of the analytical methods used for beer ingredient and finished product analysis and quality control. *Analytica Chimica Acta*, 1085, 1-20.

Angeliki, K. (2021). Toxicity of Metallic Nanoparticles in the CNS (Doctoral dissertation, National and Kapodistrian University of Athens Greece).

Anjum, S., Hashim, M., Malik, S. A., Khan, M., Lorenzo, J. M., Abbasi, B. H., and Hano, C. (2021). Recent advances in zinc oxide nanoparticles (Zno nps) for cancer diagnosis, target drug delivery, and treatment. *Cancers*, 13(18), 4570.

Archana, D., Dutta, J., and Dutta, P. K. (2013). Evaluation of chitosan nano dressing for wound healing: Characterization, in vitro and in vivo studies. *International Journal of Biological Macromolecules*, 57, 193-203.

Arunthirumeni, M., Veerammal, V., and Shivakumar, M. S. (2022). Biocontrol efficacy of mycosynthesized selenium nanoparticle

using *Trichoderma* sp. on insect pest *Spodoptera litura*. *Journal of Cluster Science*, 33(4), 1645-1653.

Ashengroph, M., and Tozandehjani, S. (2022). Optimized resting cell method for green synthesis of selenium nanoparticles from a new *Rhodotorula mucilaginosa* strain. *Process Biochemistry*, 116, 197-205.

Assafi, M. S., Ibrahim, N. M., Hussein, N. R., Taha, A. A., and Balatay, A. A. (2015). Urinary bacterial profile and antibiotic susceptibility pattern among patients with urinary tract infection in duhok city, kurdistan region, Iraq. *International Journal of Pure and Applied Sciences and Technology*, 30(2), 54 - 63 .

Aypak, C., Altunsoy, A., and Düzgün, N. (2009). Empiric antibiotic therapy in acute uncomplicated urinary tract infections and fluoroquinolone resistance: a prospective observational study. *Annals of Clinical Microbiology and Antimicrobials*, 8(1), 1-7.

Azizi, M., Ghourchian, H., Yazdian, F., Bagherifam, S., Bekhradnia, S., and Nyström, B. (2017). Anti-cancerous effect of albumin coated silver nanoparticles on MDA-MB 231 human breast cancer cell line. *Scientific reports*, *7*(1), 1-18.

Azizi, S., Ahmad, M. B., Namvar, F., and Mohamad, R. (2014). Green biosynthesis and characterization of zinc oxide nanoparticles using brown marine macroalga *Sargassum muticum* aqueous extract. *Materials Letters*, 116, 275-277.

Bader, M. S., Loeb, M., Leto, D., and Brooks, A. A. (2020). Treatment of urinary tract infections in the era of antimicrobial resistance and new antimicrobial agents. *Postgraduate Medicine*, 132(3), 234-250.

……References……

Badmus, J., Oyemomi, S. A., Yekeen, T. A., Adedosu, O. T., Adegbola, P. I., Azeez, M. A., Adebayo, E.A., and Lateef, A. (2022). Haemolytic and cytogenotoxic potential of aqueous leaf extract of *Annona muricata* and its bio-fabricated silver nanoparticles . *Caryologia , International Journal of Cytology, Cytosystematics and Cytogenetics* , 75(1) , 3-13 .

Bag, S., Ghosh, T. S., Banerjee, S., Mehta, O., Verma, J., Dayal, M., Desigamani, A., Kumar, P., Saha, B., Kedia, S., Ahuja, V., Ramamurthy, T., and Das, B. (2019). Molecular insights into antimicrobial resistance traits of commensal human gut microbiota . *Microbial ecology*, 77(2), 546-557.

Bagheri-Josheghani, S., and Bakhshi, B. (2022). Investigation of the Antibacterial and Antibiofilm Activity of Selenium Nanoparticles against *Vibrio cholerae* as a Potent Therapeutics . *Canadian Journal of Infectious Diseases and Medical Microbiology*, 2022 , 1-10 .

Baig, N., Kammakakam, I., and Falath, W. (2021). Nanomaterials: A review of synthesis methods, properties, recent progress, and challenges. *Materials Advances*, 2(6), 1821-1871.

Baker, F. J., and Silverton, R. E. (2014). Introduction to medical laboratory technology. *Butterworth-Heinemann*.

Behzadi, P. (2018). Uropathogenic Escherichia coli and fimbrial adhesins virulome. *Urinary Tract Infection: The Result of the Strength of the Pathogen, or the Weakness of the Host. Croatia: InTechOpen*, 65-83.

Behzadi, P., and Behzadi, E. (2017). Uropathogenic Escherichia coli: An ideal resource for DNA microarray probe designing. *International Conference on Bioinformatics and Biomedical Engineering* . (pp. 12-19). Springer, Cham.

Berber, S., and Çetinkaya, S. (2021). An Isolate of *Bacillus clausii* Appears to Possess Four Distinct Pectinolytic Activities. *Journal of the Institute of Science and Technology*, 11(1), 635-644.

Beris, P., and Picard, V. (2015). Non-immune hemolysis: diagnostic considerations. *In Seminars in Hematology* , 52(4) , 287-303.

Birgy, A., Madhi, F., Jung, C., Levy, C., Cointe, A., Bidet, P., Hobson, C.A., Bechet, S., Sobral, E., Vuthien, H., Ferroni, A., Aberrane, S., Cuzon, G., Beraud, L., Gajdos, V., Launay, E., Pinquier, D., Haas, H., Desmarest, M., Dommergues, M.A., Cohen, R., and Bonacorsi, S. (2020). Diversity and trends in population structure of ESBL-producing Enterobacteriaceae in febrile urinary tract infections in children in France from 2014 to 2017. *Journal of Antimicrobial Chemotherapy*, 75(1), 96-105.

Bizuayehu, H., Bitew, A., Abdeta, A., and Ebrahim, S. (2022). Catheter-associated urinary tract infections in adult intensive care units at a selected tertiary hospital, Addis Ababa, Ethiopia. *Plos One*, 17(3), e0265102.

Borah, S. N., Goswami, L., Sen, S., Sachan, D., Sarma, H., Montes, M., Peralta-Videa, J.R., Pakshirajan, K., and Narayan, M. (2021). Selenite bioreduction and biosynthesis of selenium nanoparticles by *Bacillus paramycoides* SP3 isolated from coal mine overburden leachate. *Environmental Pollution*, 285, 117519.

Bordea, M. A. (2020). The mechanisms responsible for the probiotic effects of *Bacillus* strains against rotavirus infection- tolearn . *Romanian Archives of Microbiology and Immunology*, 79(4), 304-304.

Boroumand, S., Safari, M., Shaabani, E., Shirzad, M., and Faridi-Majidi, R. (2019). Selenium nanoparticles: synthesis, characterization and

study of their cytotoxicity, antioxidant and antibacterial activity. *Materials Research Express*, 6(8), 0850d8.

Bridier, A., Sanchez-Vizuete, P., Guilbaud, M., Piard, J. C., Naitali, M., and Briandet, R. (2015). Biofilm-associated persistence of food-borne pathogens. *Food Microbiology*, 45, 167-178.

Bunu, S. J., Otele, D., Alade, T., and Dodoru, R. T. (2020). Determination of serum DNA purity among patients undergoing antiretroviral therapy using NanoDrop-1000 spectrophotometer and polymerase chain reaction. *Biomedical and Biotechnology Research Journal*, 4(3), 214 – 219 .

Calvo, J., and Martinez-Martinez, L. (2009). Antimicrobial mechanisms of action. *Enfermedades Infecciosas y Microbiologia Clinica*, 27(1), 44-52.

Caruso, S., and Poon, I. K. (2018). Apoptotic cell-derived extracellular vesicles: more than just debris. *Frontiers in immunology* , 9, 1486.

Cavalu, S., Antoniac, I. V., Fritea, L., Mates, I. M., Milea, C., Laslo, V., Vicas, S., and Mohan, A. (2018). Surface modifications of the titanium mesh for cranioplasty using selenium nanoparticles coating. *Journal of Adhesion Science and Technology*, 32(22), 2509-2522 .

Cavalu, S., Kamel, E., Laslo, V., Fritea, L., Costea, T., Antoniac, I. V., Vasile, E., Antoniac, A., Semenescu, A., Mohan, A., Saceleanu, V., and Vicas, S (2017) . Eco-friendly, Facile and Rapid Way for Synthesis of Selenium Nanoparticles. *Revista de Chimie SRL* , 68(12) , 2963 - 2966 .

Čeljuska-Tošev, E., Škerk, V., Markotić, A., Tambić-Andrašević, A., Baršić, B., Andrašević, S., Vargović, M., and Pasini, M. (2010). Struktura i djelatnost Referentnog centra Ministarstva zdravstva i

socijalne skrbi za infekcije mokraćnog sustava u razdoblju od 2005–2010 godine. *Infektološki Glasnik*, 30(2), 75-81.

Chandramohan, S., Sundar, K., and Muthukumaran, A. (2019). Reducing agents influence the shapes of selenium nanoparticles (SeNPs) and subsequently their antibacterial and antioxidant activity. *Materials Research Express*, 6(8), 0850i2.

Chaudhari, S.P., and Nikam, S.A. (2018). Biosynthesis of metallic nanopatricles .

Chawla, R., Filippini, T., Loomba, R., Cilloni, S., Dhillon, K. S., and Vinceti, M. (2020). Exposure to a high selenium environment in Punjab, India: Biomarkers and health conditions. *Science of the Total Environment*, 719, 134541.

Chen, M., Cen, H., Guo, C., Guo, X., and Chen, Z. (2020). Preparation of Cu-MOFs and its corrosion inhibition effect for carbon steel in hydrochloric acid solution. *Journal of Molecular Liquids*, 318, 114328.

Choi, Y. J., Park, J. H., Han, J. W., Kim, E., Jae-Wook, O., Lee, S. Y., ... and Gurunathan, S. (2016). Differential cytotoxic potential of silver nanoparticles in human ovarian cancer cells and ovarian cancer stem cells. *International journal of molecular sciences*, *17*(12), 2077

Chen, Y., Zou, C., Mastalerz, M., Hu, S., Gasaway, C., and Tao, X. (2015). Applications of micro-fourier transform infrared spectroscopy (FTIR) in the geological sciences—a review. *International Journal of Molecular Sciences*, 16(12), 30223-30250.

Cheng, Z., Li, M., Dey, R., and Chen, Y. (2021). Nanomaterials for cancer therapy: Current progress and perspectives. *Journal of Hematology and Oncology*, 14(1), 1-27.

Cheon, J. Y., Kim, S. J., Rhee, Y. H., Kwon, O. H., and Park, W. H. (2019). Shape-dependent antimicrobial activities of silver nanoparticles. *International Journal of Nanomedicine,* 14, 2773–2780.

Chopra, S., Harjai, K., and Chhibber, S. (2015). Potential of sequential treatment with minocycline and *S. aureus* specific phage lysin in eradication of MRSA biofilms: an in vitro study. *Applied Microbiology and Biotechnology*, 99(7), 3201-3210 .

Chudobova, D., Cihalova, K., Dostalova, S., Ruttkay-Nedecky, B., Merlos Rodrigo, M. A., Tmejova, K., Kopel, P., Nejdl, L., Kudr, J., Gumulec, J., Krizkova, S., Kynicky, J., Kizek, R., and Adam, V. (2014). Comparison of the effects of silver phosphate and selenium nanoparticles on Staphylococcus aureus growth reveals potential for selenium particles to prevent infection. FEMS Microbiology Letters, 351(2), 195-201.

Chukwudi, C. U. (2016). rRNA binding sites and the molecular mechanism of action of the tetracyclines. *Antimicrobial Agents and Chemotherapy*, 60(8), 4433-4441.

Chung, Y. C., Su, Y. P., Chen, C. C., Jia, G., Wang, H. L., Wu, J. G., and Lin, J. G. (2004). Relationship between antibacterial activity of chitosan and surface characteristics of cell wall. *Acta Pharmacologica Sinica*, 25(7), 932-936.

Cihalova, K., Chudobova, D., Michalek, P., Moulick, A., Guran, R., Kopel, P., ... and Kizek, R. (2015). *Staphylococcus aureus* and MRSA growth and biofilm formation after treatment with antibiotics and SeNPs . *International Journal of Molecular Sciences*, 16(10), 24656-24672.

CLSI (2020) . Performance standards for antimicrobial susceptibility testing. 29ed. CLSI supplement M100-S29. Wayne, PA: Clinical and laboratory standards institute .

Cojocaru, A., Sin, I., Agapescu, C., Cotarta, A., and Visan, T. (2016). Electrode Processes and SEM/EDX Analysis of Selenium films electro deposited from ionic liquids based on choline chloride. *Chalcogenide Letters*, 13(3) , 127 – 138 .

Collee, J. G., Mackie, T. J., and McCartney, J. E. (1996). Mackie and McCartney practical medical microbiology. *Harcourt Health Sciences.*

Constantinescu-Aruxandei, D., Frîncu, R. M., Capră, L., and Oancea, F. (2018). Selenium analysis and speciation in dietary supplements based on next-generation selenium ingredients. *Nutrients*, 10(10), 1466.

Costa, O. Y., Raaijmakers, J. M., and Kuramae, E. E. (2018). Microbial extracellular polymeric substances: ecological function and impact on soil aggregation. *Frontiers in microbiology*, 9, 1636.

Cremonini, E., Zonaro, E., Donini, M., Lampis, S., Boaretti, M., Dusi, S., Melotti, P., Lleo, M.M., and Vallini, G. (2016). Biogenic selenium nanoparticles: characterization, antimicrobial activity and effects on human dendritic cells and fibroblasts. *Microbial Biotechnology*, 9(6), 758-771.

Cui, D., Yan, C., Miao, J., Zhang, X., Chen, J., Sun, L., Meng, L., Liang, T., and Li, Q. (2018). Synthesis, characterization and antitumor properties of selenium nanoparticles coupling with ferulic acid. *Materials Science and Engineering*, 90, 104-112.

Dalia, A. M., Loh, T. C., Sazili, A. Q., Jahromi, M. F., and Samsudin, A. A. (2017). The effect of dietary bacterial organic selenium on growth performance, antioxidant capacity, and Selenoproteins gene

expression in broiler chickens. *BMC Veterinary Research*, 13(1), 1-11.

Daniel, W. W., and Cross, C. L. (2018). *Biostatistics: a foundation for analysis in the health sciences*. Wiley.

Das, R. K., Pachapur, V. L., Lonappan, L., Naghdi, M., Pulicharla, R., Maiti, S., Cledon, M., Dalila, L.M.A., Sarma, S.J., and Brar, S. K. (2017). Biological synthesis of metallic nanoparticles: plants, animals and microbial aspects. *Nanotechnology for Environmental Engineering* , 2(1), 1-21.

De La Cadena, E., Mojica, M. F., Castillo, N., Correa, A., Appel, T. M., García-Betancur, J. C., Pallares, C.J., and Villegas, M. V. (2020). Genomic analysis of CTX-M-group-1-producing extraintestinal pathogenic E. coli (ExPEc) from patients with urinary tract infections (UTI) from Colombia . *Antibiotics*, 9(12), 9120899 .

Deng, X., Xiong, F., Li, X., Xiang, B., Li, Z., Wu, X., Guo, C., Li, X., Li, Y., Li, G., Xiong, W., and Zeng, Z. (2018). Application of atomic force microscopy in cancer research. *Journal of Nanobiotechnology*, 16(1), 1-15.

Dhanjal, S., and Cameotra, S. S. (2010). Aerobic biogenesis of selenium nanospheres by *Bacillus cereus* isolated from coalmine soil. *Microbial Cell Factories*, 9(1), 1-11.

Dobias, J., Suvorova, E. I., and Bernier-Latmani, R. (2011). Role of proteins in controlling selenium nanoparticle size. *Nanotechnology*, 22 (19) , 195605.

Doron, S., and Snydman, D. R. (2015). Risk and safety of probiotics. *Clinical Infectious Diseases*, 60(2), 129-134.

Duntas, L. (2009). Selenium and inflammation: underlying anti-inflammatory mechanisms . *Hormone and Metabolic Research*, 41(06) , 443-447.

Dziri, R., Klibi, N., Lozano, C., Said, L. B., Bellaaj, R., Tenorio, C., Boudabous, A., Slama, K.B., and Torres, C. (2016). High prevalence of *Staphylococcus haemolyticus* and *Staphylococcus saprophyticus* in environmental samples of a Tunisian hospital. *Diagnostic Microbiology and Infectious Disease,* 85(2), 136-140.

EL-Baghdady, K. Z., Khalil, M. M., El Borhamy, M. I., and Meligi, G. (2019). Biosynthesis, characterization and cytotoxicity of selenium nanoparticles using *Bacillus tropicus* Ism 2. *Egyptian Academic Journal of Biological Sciences, G. Microbiology*, 11(1), 47-57.

El-Batal, A. I., Essam, T. M., El-Zahaby, D. A., and Amin, M. A. (2014). Synthesis of selenium nanoparticles by *Bacillus laterosporus* using gamma radiation. *British Journal of Pharmaceutical Research,* 4(11) , 1364-1386.

El-Deeb, B., Al-Talhi, A., Mostafa, N., and Abou-assy, R. (2018). Biological synthesis and structural characterization of selenium nanoparticles and assessment of their antimicrobial properties. *American Academic Scientific Research Journal for Engineering, Technology and Sciences* , 45(1), 135-170.

Eleraky, N. E., Allam, A., Hassan, S. B., and Omar, M. M. (2020). Nanomedicine fight against antibacterial resistance: an overview of the recent pharmaceutical innovations. *Pharmaceutics*, 12(2), 12020142 .

El-Ghazaly, M. A., Fadel, N., Rashed, E., El-Batal, A., and Kenawy, S. A. (2017). Anti-inflammatory effect of selenium nanoparticles on the inflammation induced in irradiated rats. *Canadian Journal of Physiology and Pharmacology* , 95(2), 101-110.

El-Ramady, H. R., Domokos-Szabolcsy, É., Abdalla, N. A., Alshaal, T. A., Shalaby, T. A., Sztrik, A., Prokisch, J., and Fári, M. (2014).

Selenium and nano-selenium in agroecosystems. *Environmental Chemistry Letters*, 12(4), 495-510.

Esmaeel, N. E., Gerges, M. A., Hosny, T. A., Ali, A. R., and Gebriel, M. G. (2020). Detection of chromosomal and plasmid-mediated quinolone resistance among *Escherichia coli* Isolated from urinary tract infection cases; Zagazig University Hospitals, Egypt. *Infection and Drug Resistance*, 13, 413 - 421.

Fan, A. M., and Vinceti, M. (2015). Selenium and its compounds. *Hamilton and Hardy's Industrial Toxicology; Wiley-Blackwell: Hoboken, NJ, USA*, 205-228.

Fang, X., Li, C. E., Zheng, L., Yang, F., and Chen, T. (2018). Dual-targeted selenium nanoparticles for synergistic photothermal therapy and chemotherapy of tumors. *Chemistry–An Asian Journal*, 13(8), 996-1004.

Fardsadegh, B., and Jafarizadeh-Malmiri, H. (2019). *Aloe vera* leaf extract mediated green synthesis of selenium nanoparticles and assessment of their in vitro antimicrobial activity against spoilage fungi and pathogenic bacteria strains. *Green Processing and Synthesis*, 8(1), 399-407.

Fardsadegh, B., Vaghari, H., Mohammad-Jafari, R., Najian, Y., and Jafarizadeh-Malmiri, H. (2019). Biosynthesis, characterization and antimicrobial activities assessment of fabricated selenium nanoparticles using *Pelargonium zonale* leaf extract. *Green Processing and Synthesis*, 8(1), 191-198.

FDA (2015) . Infant formula: the addition of minimum and maximum levels of selenium to infant formula and related labeling requirements. Final rule. *Federal Register*, 80(120), 35834-35841.

Ferreira, A. M., Bonesso, M. F., Mondelli, A. L., Camargo, C. H., and Maria de Lourdes, R. S. (2012). Oxacillin Resistance and

Antimicrobial Susceptibility Profile of *Staphylococcus saprophyticus* and Other Staphylococci Isolated from Patients with Urinary Tract Infection . *Chemotherapy*, 58(6), 482-491.

Ferro, C., Florindo, H.F., and Santos, H.A. (2021) . Selenium Nanoparticles for Biomedical Applications: From Development and Characterization to therapeutics. *Advanced Healthcare Materials* , 10(16) , 2100598.

Filipović, N., Ušjak, D., Milenković, M. T., Zheng, K., Liverani, L., Boccaccini, A. R., and Stevanović, M. M. (2021). Comparative study of the antimicrobial activity of selenium nanoparticles with different surface chemistry and structure. *Frontiers in Bioengineering and Biotechnology*, 8 , 624621.

Fils, P. E. L., Cholley, P., Gbaguidi-Haore, H., Hocquet, D., Sauget, M., and Bertrand, X. (2021). ESBL-producing *Klebsiella pneumoniae* in a University hospital: Molecular features, diffusion of epidemic clones and evaluation of cross-transmission. *Plos One*, 16(3), e0247875.

Forootanfar, H., Adeli-Sardou, M., Nikkhoo, M., Mehrabani, M., Amir-Heidari, B., Shahverdi, A. R., and Shakibaie, M. (2014). Antioxidant and cytotoxic effect of biologically synthesized selenium nanoparticles in comparison to selenium dioxide. *Journal of Trace Elements in Medicine and Biology*, 28(1), 75-79.

Foxman, B. (2010). The epidemiology of urinary tract infection. *Nature Reviews Urology*, 7(12), 653-660.

Foxman, B. (2014). Urinary tract infection syndromes: occurrence, recurrence, bacteriology, risk factors, and disease burden. *Infectious Disease Clinics*, 28(1), 1-13.

Fu, H., Yuan, J., and Gao, H. (2015). Microbial oxidative stress response: novel insights from environmental facultative anaerobic bacteria. *Archives of Biochemistry and Biophysics*, 584, 28-35.

Gajamer, V. R., Bhattacharjee, A., Paul, D., Ingti, B., Sarkar, A., Kapil, J., Singh, A.K., Pradhan, N., and Tiwari, H. K. (2020). High prevalence of carbapenemase, AmpC β-lactamase and aminoglycoside resistance genes in extended-spectrum β-lactamase-positive uropathogens from Northern India. *Journal of Global Antimicrobial Resistance* , 20, 197-203.

Gajdács, M., Ábrók, M., Lázár, A., and Burián, K. (2019). Comparative epidemiology and resistance trends of common urinary pathogens in a tertiary-care hospital: a 10-year surveillance study. *Medicina*, 55, 356.

Galić, E., Ilić, K., Hartl, S., Tetyczka, C., Kasemets, K., Kurvet, I., Milić, M., Barbir, R., Pem, B., Erceg, I., Sikirić, M.D., Pavičić, I., Roblegg, E., Kahru, A., and Vrček, I. V. (2020). Impact of surface functionalization on the toxicity and antimicrobial effects of selenium nanoparticles considering different routes of entry. *Food and Chemical Toxicology*, 144, 111621.

Gangadoo, S., Stanley, D., Hughes, R. J., Moore, R. J., and Chapman, J. (2017). The synthesis and characterisation of highly stable and reproducible selenium nanoparticles. *Inorganic and Nano-Metal Chemistry*, 47(11), 1568-1576.

Garousi, F. (2015). The toxicity of different selenium forms and compounds–Review. *Acta Agraria Debreceniensis*, (64), 33-38.

Geraghty, R. J., Capes-Davis, A., Davis, J. M., Downward, J., Freshney, R. I., Knezevic, I., Lovell-Badge, R., Masters, J.R.W., Meredith, J., Stacey, G.N., Thraves, P., and Vias, M. (2014). Guidelines for the

use of cell lines in biomedical research. *British Journal of Cancer*, 111(6), 1021-1046.

Ghimire, S., Baral, B. K., Feng, D., Sy, F. S., and Rodriguez, R. (2019). Is selenium intake associated with the presence of depressive symptoms among US adults? Findings from National Health and Nutrition Examination Survey (NHANES) 2011-2014. *Nutrition*, 62, 169-176.

Giaouris, E., Heir, E., Hébraud, M., Chorianopoulos, N., Langsrud, S., Møretrø, T., Habimana, O., Desvaux, M., Renier, S., and Nychas, G. J. (2014). Attachment and biofilm formation by foodborne bacteria in meat processing environments: causes, implications, role of bacterial interactions and control by alternative novel methods. *Meat Science*, 97(3), 298-309.

Goldstein, J. I., Newbury, D. E., Michael, J. R., Ritchie, N. W., Scott, J. H. J., and Joy, D. C. (2017). Scanning electron microscopy and X-ray microanalysis. *Springer*.

Golob, J. L., and Rao, K. (2021). Signal Versus Noise: How to Analyze the Microbiome and Make Progress on Antimicrobial Resistance. *The Journal of Infectious Diseases*, 223(3), 214-221.

Gopinath, V., Priyadarshini, S., Loke, M. F., Arunkumar, J., Marsili, E., MubarakAli, D., Velusamy, P., and Vadivelu, J. (2017). Biogenic synthesis, characterization of antibacterial silver nanoparticles and its cell cytotoxicity. *Arabian Journal of Chemistry*, 10(8), 1107-1117.

Guarino, A., Guandalini, S., and Vecchio, A. L. (2015). Probiotics for prevention and treatment of diarrhea. *Journal of Clinical Gastroenterology*, 49, 37-45.

Gunti, L., Dass, R. S., and Kalagatur, N. K. (2019). Phytofabrication of selenium nanoparticles from Emblica officinalis fruit extract and

exploring its biopotential applications: antioxidant, antimicrobial, and biocompatibility. *Frontiers in Microbiology*, 10, Article 931.

Gurung, S., Kafle, S., Dhungel, B., Adhikari, N., Shrestha, U. T., Adhikari, B., Banjara, M.R., Rijal, K.R., and Ghimire, P. (2020). Detection of OXA-48 gene in carbapenem-resistant *Escherichia coli* and *Klebsiella pneumoniae* from urine samples . *Infection and Drug Resistance*, 13, 2311 – 2321.

Hadrup, N., Loeschner, K., Skov, K., Ravn-Haren, G., Larsen, E. H., Mortensen, A., Lam, H.R., and Frandsen, H. L. (2016). Effects of 14-day oral low dose selenium nanoparticles and selenite in rat—as determined by metabolite pattern determination. *PeerJ*, 4, e2601.

Hashem, A. H., and Salem, S. S. (2022). Green and ecofriendly biosynthesis of selenium nanoparticles using *Urtica dioica* (stinging nettle) leaf extract: Antimicrobial and anticancer activity. *Biotechnology Journal*, 17(2), 2100432.

Hashem, A. H., Abdelaziz, A. M., Askar, A. A., Fouda, H. M., Khalil, A. M., Abd-Elsalam, K. A., and Khaleil, M. M. (2021). *Bacillus megaterium*-mediated synthesis of selenium nanoparticles and their antifungal activity against *Rhizoctonia solani* in Faba Bean Plants. *Journal of Fungi* , 7(3), 195.

Hassuna, N. A., Khairalla, A. S., Farahat, E. M., Hammad, A. M., and Abdel-Fattah, M. (2020). Molecular characterization of Extended-spectrum β lactamase-producing *E. coli* recovered from community-acquired urinary tract infections in Upper Egypt. *Scientific Reports*, 10(1), 1-8.

Hemalatha, T., Krithiga, G., Santhosh Kumar, B., and Sastry, T. P. (2014). Preparation and characterization of hydroxyapatite-coated selenium nanoparticles and their interaction with osteosarcoma

(SaOS-2) cells. *Acta Metallurgica Sinica* (English Letters), 27(6), 1152-1158.

Ho, C. T., Nguyen, T. H., Lam, T. T., Le, D. Q., Nguyen, C. X., Lee, J. H., and Hur, H. G. (2021). Biogenic synthesis of selenium nanoparticles by *Shewanella sp.* HN-41 using a modified bioelectrochemical system. *Electronic Journal of Biotechnology* , 54, 1-7.

Hong, X., Wen, J., Xiong, X., and Hu, Y. (2016). Shape effect on the antibacterial activity of silver nanoparticles synthesized via a microwave-assisted method . *Environmental Science and Pollution Research*, 23(5), 4489-4497.

Hosnedlova, B., Kepinska, M., Skalickova, S., Fernandez, C., Ruttkay-Nedecky, B., Peng, Q., Baron, M., Melcova, M., Opatrilova, R., Zidkova, J., Bjørklund, G., Sochor, J., and Kizek, R. (2018). Nano-selenium and its nanomedicine applications: a critical review. *International Journal of Nanomedicine*, 13, 2107 – 2128 .

Hospodarova, V., Singovszka, E., and Stevulova, N. (2018). Characterization of cellulosic fibers by FTIR spectroscopy for their further implementation to building materials. *American Journal of Analytical Chemistry*, 9(6), 303-310.

Hu, C. H., Li, Y. L., Xiong, L., Zhang, H. M., Song, J., and Xia, M. S. (2012). Comparative effects of nano elemental selenium and sodium selenite on selenium retention in broiler chickens. *Animal Feed Science and Technology*, 177(3-4), 204-210.

Huang, G., Liu, Z., He, L., Luk, K.H., Cheung, S.T., Wong, K.H., and Chen, T. (2018). Autophagy is an important action mode for functionalized selenium nanoparticles to exhibit anti-colorectal cancer activity. *Biomaterials Science*, 6(9) , 2508-2517.

Huang, T., Holden, J. A., Heath, D. E., O'Brien-Simpson, N. M., and O'Connor, A. J. (2019). Engineering highly effective antimicrobial selenium nanoparticles through control of particle size. *Nanoscale*, 11(31), 14937-14951.

Huang, X., Chen, X., Chen, Q., Yu, Q., Sun, D., and Liu, J. (2016). Investigation of functional selenium nanoparticles as potent antimicrobial agents against superbugs. *Acta Biomaterialia*, 30, 397-407.

Husen, A., and Siddiqi, K. S. (2014). Plants and microbes assisted selenium nanoparticles: characterization and application. *Journal of Nanobiotechnology*, 12(1), 1-10.

Hwang, I. S., Hwang, J. H., Choi, H., Kim, K. J., and Lee, D. G. (2012). Synergistic effects between silver nanoparticles and antibiotics and the mechanisms involved. *Journal of Medical Microbiology* , 61 (12) , 1719 – 1726 .

Ikram, M., Javed, B., and Raja, N. I. (2021). Biomedical potential of plant-based selenium nanoparticles: a comprehensive review on therapeutic and mechanistic aspects. *International Journal of Nanomedicine* , 16, 249 – 268 .

Ingale, A. G., and Chaudhari, A. N. (2013). Biogenic synthesis of nanoparticles and potential applications: an eco-friendly approach. *Journal of Nanomedicine and Nanotechnology*, 4(165), 1-7.

Ismail, Z. B. (2017). Pneumonia in dromedary camels (Camelus dromedarius): a review of clinico-pathological and etiological characteristics. *Journal of Camel Practice and Research*, 24(1), 49-54.

Jaffar, M., Pang, Y., Yuan, H., Zou, D., Liu, Y., Zhu, B., ... and Li, X. (2016). Wheat straw pretreatment with KOH for enhancing

biomethane production and ferti-lizer value in anaerobic digestion. *Chinese journal of chemical engineering*, 24(3), 404-409.

Jancel, T., and Dudas, V. (2002). Management of uncomplicated urinary tract infections. *Western Journal of Medicine*, 176(1) , 51- 55.

Jasim, B., Thomas, R., Mathew, J., and Radhakrishnan, E. K. (2017). Plant growth and diosgenin enhancement effect of silver nanoparticles in Fenugreek (*Trigonella foenum-graecum* L.). *Saudi Pharmaceutical Journal*, 25(3), 443 - 447.

Jayanthi, N., and Sudha, R. M. (2015). *Bacillus clausii*-The probiotic of choice in the treatment of diarrhoea. *Journal of Yoga and Physical Therapy*, 5(4), 1.

Jeevanandam, J., Kiew, S. F., Boakye-Ansah, S., Lau, S. Y., Barhoum, A., Danquah, M. K., and Rodrigues, J. (2022). Green approaches for the synthesis of metal and metal oxide nanoparticles using microbial and plant extracts. *Nanoscale*, 14(7), 2534-2571.

Jepson, R. G., Williams, G., and Craig, J. C. (2012). Cranberries for preventing urinary tract infections. *Cochrane Database of Systematic Reviews*, (10) .

Jia, H., Huang, S., Cheng, S., Zhang, X., Chen, X., Zhang, Y., Wang, J., and Wu, L. (2022). Novel mechanisms of selenite reduction in *Bacillus subtilis* 168: Confirmation of multiple-pathway mediated remediation based on transcriptome analysis. *Journal of Hazardous Materials*, 433, 128834.

Jiang, C., Diao, X., Wang, H., and Ma, S. (2021). Diverse and abundant antibiotic resistance genes in mangrove area and their relationship with bacterial communities-A study in Hainan Island, China. *Environmental Pollution*, 276, 116704.

Jiang, S., Ho, C. T., Lee, J. H., Van Duong, H., Han, S., and Hur, H. G. (2012). Mercury capture into biogenic amorphous selenium

nanospheres produced by mercury resistant *Shewanella putrefaciens* 200. *Chemosphere*, 87(6), 621-624.

Johansen, T. B., Bonkat, G., Cai, T., Tandogdu, Z., Wagenlehner, F., and Grabe, M. (2016). Grey zones in the field of urinary tract infections. *European Urology Focus*, 2(4), 460-462.

Johnson, L. A., and Hug, L. A. (2019). Distribution of reactive oxygen species defense mechanisms across domain bacteria. *Free Radical Biology and Medicine,* 140, 93-102.

Jolly, J., Rauf, M. A., and Ahmad, Z. (2020). Selenium nanoparticles: Small is the new big: Mini review. *Open Journal of Chemistry*, 6(1), 013-016.

Joshi, M., Bhattacharyya, A., and Ali, S. W. (2008). Characterization techniques for nanotechnology applications in textiles.

Junior, E. S., Wadt, L. D. O., Silva, K. E., Lima, R. M. B., Batista, K. D., Guedes, M. C., Carvalho, G.S., Carvalho, T.S., Reis, A.R., Lopes, G., and Guilherme, L. R. G. (2017). Natural variation of selenium in Brazil nuts and soils from the Amazon region. *Chemosphere*, 188, 650-658.

Kachuee, R., Moeini, M. M., and Souri, M. (2013). The effect of dietary organic and inorganic selenium supplementation on serum Se, Cu, Fe and Zn status during the late pregnancy in Merghoz goats and their kids. *Small Ruminant Research*, 110(1), 20-27.

Kapil, S., Kumar, T., and Sharma, V. (2020). Mechanism and challenges associated with adaptation and evolution of drug-resistant bacteria: an overview. *AsPac Journal Mol Biol Biotechnol*, 28(2), 1-18.

Karagöz, A., Acar, S., and Körkoca, H. (2015). Characterization of Klebsiella isolates by matrix-assisted laser desorption/ionization time-of-flight mass spectrometry (MALDI-TOF MS) and determination of antimicrobial resistance with VITEK 2 advanced

expert system (AES). *Turkish Journal of Medical Sciences*, 45(6), 1335-1344.

Khanna, P., Kaur, A., and Goyal, D. (2019). Algae-based metallic nanoparticles: Synthesis, characterization and applications. *Journal of Microbiological Methods*, 163, 105656.

Kheradmand, E., Rafii, F., Yazdi, M. H., Sepahi, A. A., Shahverdi, A. R., and Oveisi, M. R. (2014). The antimicrobial effects of selenium nanoparticle-enriched probiotics and their fermented broth against *Candida albicans* . *DARU Journal of Pharmaceutical Sciences*, 22(1), 1-6.

Khiralla, G. M., and El-Deeb, B. A. (2015). Antimicrobial and antibiofilm effects of selenium nanoparticles on some foodborne pathogens. *LWT- Food Science and Technology*, 63(2), 1001-1007.

Khoei, N. S., Lampis, S., Zonaro, E., Yrjälä, K., Bernardi, P., and Vallini, G. (2017). Insights into selenite reduction and biogenesis of elemental selenium nanoparticles by two environmental isolates of *Burkholderia fungorum*. *New Biotechnology*, 34, 1-11.

Khurana, A., Tekula, S., Saifi, M.A., Venkatesh, P., and Godugu, C.(2019). Therapeutic applications of selenium nanoparticles. *Biomedicine and Pharmacotherapy*, 111, 802-812.

Kiehlbauch, J. A., Hannett, G. E., Salfinger, M., Archinal, W., Monserrat, C., and Carlyn, C. (2000). Use of the National Committee for Clinical Laboratory Standards guidelines for disk diffusion susceptibility testing in New York state laboratories. *Journal of Clinical Microbiology*, 38(9), 3341-3348.

Kimura, H., Arima, T. H., Oku, T., and Sakaguchi, T. (2014). Selenium recovery and conversion by a filamentous fungus, *Aspergillus*

oryzae strain RIB40. *Asia Pacific Journal of Sustainable Agriculture, Food and Energy*, 2(2), 5-8.

Kondaparthi, P., Flora, S. J. S., and Naqvi, S. (2019). Selenium nanoparticles: An insight on its Pro-oxidant and antioxidant properties. *Front. Nanoscience Nanotechnology*, 6, 1-5.

Kora, A. J. (2018). *Bacillus cereus*, selenite-reducing bacterium from contaminated lake of an industrial area: A renewable nanofactory for the synthesis of selenium nanoparticles. *Bioresources and Bioprocessing*, 5(1), 1-12.

Krinsky, N. I., Beecher, G. R., Burk, R. F., Chan, A. C., Erdman, J. J., Jacob, R. A., ... and Traber, M. G. (2000). Dietary reference intakes for vitamin C, vitamin E, selenium, and carotenoids. *Institute of Medicine*, 19, 95-185.

Krishna, G. , Kumar, S. S., Pranitha, V., Alha, M., and Charaya, S. (2015). Biogenic synthesis of silver nanoparticles and their synergistic effect with antibiotics: a study against Salmonella sp. *International Journal of Pharmacy and Pharmaceutical Sciences*, 7(11), 84-88.

Krohn, R. M., Lemaire, M., Silva, L. F. N., Lemarié, C., Bolt, A., Mann, K. K., and Smits, J. E. (2016). High-selenium lentil diet protects against arsenic-induced atherosclerosis in a mouse model. *The Journal of Nutritional Biochemistry*, 27, 9-15.

Kumar, A., and Prasad, K. S. (2021). Role of nano-selenium in health and environment. *Journal of Biotechnology*, 325, 152-163.

Kumar, R., Shukla, S. K., Pandey, A., Srivastava, S. K., and Dikshit, A. (2015). Copper oxide nanoparticles: an antidermatophytic agent for Trichophyton spp. *Nanotechnology Reviews*, 4(5), 401-409.

Kurittu, P., Khakipoor, B., Aarnio, M., Nykäsenoja, S., Brouwer, M., Myllyniemi, A. L., Vatunen, E., and Heikinheimo, A. (2021).

Plasmid-borne and chromosomal ESBL/AmpC genes in *Escherichia coli* and *Klebsiella pneumoniae* in global food products. *Frontiers in Microbiology*, 12, 592291.

Lakshmi, S. G., Jayanthi, N., Saravanan, M., and Ratna, M. S. (2017). Safety assesment of Bacillus clausii UBBC07, a spore forming probiotic. *Toxicology Reports*, 4, 62-71.

Lenz, M., Kolvenbach, B., Gygax, B., Moes, S., and Corvini, P. F. (2011). Shedding light on selenium biomineralization: proteins associated with bionanominerals. *Applied and Environmental Microbiology* , 77(13), 4676-4680 .

Li, B., Liu, N., Li, Y., Jing, W., Fan, J., Li, D., Zhang, L., Zhang, X., Zhang, Z., and Wang, L. (2014). Reduction of selenite to red elemental selenium by *Rhodopseudomonas palustris* strain N. *Plos One*, 9(4), e95955.

Li, Y., Lin, Z., Guo, M., Xia, Y., Zhao, M., Wang, C., Xu, T., Chen, T., and Zhu, B. (2017). Inhibitory activity of selenium nanoparticles functionalized with oseltamivir on H1N1 influenza virus. *International Journal of Nanomedicine*, 12, 5733- 5743 .

Li, Y., Lin, Z., Guo, M., Zhao, M., Xia, Y., Wang, C., Xu, T., and Zhu, B. (2018). Inhibition of H1N1 influenza virus-induced apoptosis by functionalized selenium nanoparticles with amantadine through ROS-mediated AKT signaling pathways. *International Journal of Nanomedicine*, 13, 2005 –2016.

Li, Y., Lin, Z., Zhao, M., Xu, T., Wang, C., Xia, H., Wang, H., and Zhu, B. (2016). Multifunctional selenium nanoparticles as carriers of HSP70 siRNA to induce apoptosis of HepG2 cells. *International Journal of Nanomedicine*, 11, 3065 – 3076 .

Lianou, A., Nychas, G. J. E., and Koutsoumanis, K. P. (2020). Strain variability in biofilm formation: A food safety and quality perspective. *Food Research International*, 137, 109424.

Liao, G., Tang, J., Wang, D., Zuo, H., Zhang, Q., Liu, Y., and Xiong, H.(2020) . Selenium nanoparticles (SeNPs) have potent antitumor activity against prostate cancer cells through the upregulation of miR-16. *World Journal of Surgical Oncology*, 18(1) , 1-11.

Lin, Z. H., and Wang, C. C. (2005). Evidence on the size-dependent absorption spectral evolution of selenium nanoparticles. *Materials Chemistry and Physics*, 92(2-3), 591-594.

Liu, C., Fu, Y., Li, C. E., Chen, T., and Li, X. (2017) . Phycocyanin-functionalized selenium nanoparticles reverse palmitic acid-induced pancreatic β cell apoptosis by enhancing cellular uptake and blocking reactive oxygen species (ROS)-mediated mitochondria dysfunction. *Journal of Agricultural and Food Chemistry*, 65(22) , 4405-4413.

Liu, T., Bai, R., Zhou, H., Wang, R., Liu, J., Zhao, Y., and Chen, C. (2020). The effect of size and surface ligands of iron oxide nanoparticles on blood compatibility. *RSC Advances*, 10(13), 7559-7569.

Livak, K. J., and Schmittgen, T. D. (2001). Analysis of relative gene expression data using real-time quantitative PCR and the $2^{-\Delta\Delta CT}$ method. *Methods*, 25(4), 402-408.

Loy, A., Lehner, A., Lee, N., Adamczyk, J., Meier, H., Ernst, J., Schleifer, K. Wagner, M. (2002). Oligonucleotide microarray for 16S rRNA gene-based detection of all recognized lineages of sulfate-reducing prokaryotes in the environment. *Applied and Environmental Microbiology*, 68(10), 5064-5081.

Luo, H., Wang, F., Bai, Y., Chen, T., and Zheng, W. (2012). Selenium nanoparticles inhibit the growth of HeLa and MDA-MB-231 cells through induction of S phase arrest. *Colloids and Surfaces B: Biointerfaces*, 94, 304-308.

Lyu, C., Chen, J., Li, L., Zhao, Z., and Liu, X. (2022). Characteristics of Se in water-soil-plant system and threshold of soil Se in seleniferous areas in Enshi, China. *Science of The Total Environment*, 827, 154372.

MacFaddin, J. F. (2000). Biochemical tests for identification of medical bacteria, williams and wilkins. *Philadelphia, PA*, 113.

Magesh, H., Kumar, A., Alam, A., and Sekar, U. (2013). Identification of natural compounds which inhibit biofilm formation in clinical isolates of Klebsiella pneumoniae. *Indian Journal of Experimental Biology* , 51(09) , 764-772.

Mahon, C. R., Lehman, D. C., and Manuselis, G. (2018). Textbook of diagnostic microbiology-e-book. *Elsevier Health Sciences*.

Maiyo, F., and Singh, M. (2017). Selenium nanoparticles: Potential in cancer gene and drug delivery. *Nanomedicine*, 12(9), 1075-1089.

Makabenta, J. M. V., Nabawy, A., Li, C. H., Schmidt-Malan, S., Patel, R., and Rotello, V. M. (2021). Nanomaterial-based therapeutics for antibiotic-resistant bacterial infections. *Nature Reviews Microbiology*, 19(1), 23-36.

Mancuso, G., Midiri, A., Gerace, E., and Biondo, C. (2021). Bacterial antibiotic resistance: the most critical pathogens. *Pathogens* , 10 (10), 1310.

Mann, J., and Truswell, A. S. (2017) . Essentials of human nutrition. *Oxford University Press.*

Mathur T, S Singhal, S Khan.(2006) . Detection of biofilm formation among the clinical isolates of staphylococci: an evaluation of three different screening methods. *Indian journal* , l24, 0255-0857.

Maveyraud, L., and Mourey, L. (2020). Protein X-ray crystallography and drug discovery. *Molecules*, 25(5), 1030.

Medina Cruz, D., Mi, G., and Webster, T. J. (2018). Synthesis and characterization of biogenic selenium nanoparticles with antimicrobial properties made by Staphylococcus aureus, methicillin-resistant Staphylococcus aureus (MRSA), Escherichia coli, and Pseudomonas aeruginosa. *Journal of Biomedical Materials Research Part A*, 106(5), 1400-1412.

Mellinas, C., Jiménez, A., and Garrigós, M. D. C. (2019). Microwave-assisted green synthesis and antioxidant activity of selenium nanoparticles using Theobroma cacao L. bean shell extract. *Molecules*, 24(22), 24224048 .

Menon, S., KS, S. D., Agarwal, H., and Shanmugam, V. K. (2019). Efficacy of biogenic selenium nanoparticles from an extract of ginger towards evaluation on anti-microbial and anti-oxidant activities. *Colloid and Interface Science Communications*, 29, 1-8.

Mesdaghinia, A., Pourpak, Z., Naddafi, K., Nodehi, R. N., Alizadeh, Z., Rezaei, S., Mohammadi, A., and Faraji, M. (2019). An in vitro method to evaluate hemolysis of human red blood cells (RBCs) treated by airborne particulate matter (PM10). *MethodsX*, 6, 156-161.

Miglani, S., and Tani-Ishii, N. (2021). Biosynthesized selenium nanoparticles: characterization, antimicrobial, and antibiofilm activity against *Enterococcus faecalis*. *PeerJ*, 9, e11653.

Mirsoleymani, S. R., Salimi, M., Shareghi Brojeni, M., Ranjbar, M., and Mehtarpoor, M. (2014). Bacterial pathogens and antimicrobial

resistance patterns in pediatric urinary tract infections: a four-year surveillance study (2009–2012). *International Journal of Pediatrics* , 2014 , 126142 .

Mishra, P. K., Mishra, S., Bisht, S. C., Selvakumar, G., Kundu, S., Bisht, J. K., and Gupta, H. S. (2009). Isolation, molecular characterization and growth-promotion activities of a cold tolerant bacterium Pseudomonas sp. NARs9 (MTCC9002) from the Indian Himalayas. *Biological Research*, 42(3), 305-313.

Mishra, R. R., Prajapati, S., Das, J., Dangar, T. K., Das, N., and Thatoi, H. (2011). Reduction of selenite to red elemental selenium by moderately halotolerant Bacillus megaterium strains isolated from Bhitarkanika mangrove soil and characterization of reduced product. *Chemosphere*, 84(9), 1231-1237.

Mojarad-Jabali, S., Farshbaf, M., Walker, P. R., Hemmati, S., Fatahi, Y., Zakeri-Milani, P., Sarfraz, M., and Valizadeh, H. (2021). An update on actively targeted liposomes in advanced drug delivery to glioma. *International Journal of Pharmaceutics*, 602, 120645.

Motiei Pour, M., Moghbeli, M. R., Larijani, B., and Akbari Javar, H. (2022). pH-Sensitive mesoporous bisphosphonate-based TiO2 nanoparticles utilized for controlled drug delivery of dexamethasone. *Chemical Papers* , 76(1), 439-451.

Munita, J. M., and Arias, C. A. (2016). Mechanisms of antibiotic resistance. *Microbiology Spectrum*, 4(2), 4-2.

Munoz-Dávila, M. J., Roig, M., Yagüe, G., Blázquez, A., Salvador, C., and Segovia, M. (2013). Comparative evaluation of Vitek 2 identification and susceptibility testing of urinary tract pathogens directly and isolated from chromogenic media. *European Journal of Clinical Microbiology and Infectious Diseases*, 32(6), 773-780.

Murugesan, G., Nagaraj, K., Sunmathi, D., and Subramani, K. (2019). Methods involved in the synthesis of selenium nanoparticles and their different applications-a review. *European Journal of Biomedical AND Pharmaceutical Sciences*, 6(4), 189-194.

Nayak, V., Singh, K. R., Singh, A. K., and Singh, R. P. (2021). Potentialities of selenium nanoparticles in biomedical science. *New Journal of Chemistry*, 45(6), 2849-2878.

Naziri, Z., Derakhshandeh, A., Borchaloee, A. S., Poormaleknia, M., and Azimzadeh, N. (2020). Treatment failure in urinary tract infections: a warning witness for virulent multi-drug resistant ESBL-producing *Escherichia coli*. *Infection and Drug Resistance*, 13, 1839 –1850.

Ndwandwe, B. K., Malinga, S. P., Kayitesi, E., and Dlamini, B. C. (2021). Advances in green synthesis of selenium nanoparticles and their application in food packaging. *International Journal of Food Science and Technology*, 56(6), 2640-2650.

Nguyen, T. H., Vardhanabhuti, B., Lin, M., and Mustapha, A. (2017). Antibacterial properties of selenium nanoparticles and their toxicity to Caco-2 cells. *Food Control*, 77, 17-24.

Niki, E. (2010). Assessment of antioxidant capacity in vitro and in vivo. *Free Radical Biology and Medicine*, 49(4), 503-515.

Nikzamir, M., Hanifehpour, Y., Akbarzadeh, A., and Panahi, Y. (2021). Applications of dendrimers in nanomedicine and drug delivery: A review. *Journal of Inorganic and Organometallic Polymers and Materials*, 31(6) , 2246-2261.

Niranjan, R., Zafar, S., Lochab, B., and Priyadarshini, R. (2022). Synthesis and characterization of sulfur and sulfur-selenium nanoparticles loaded on reduced graphene oxide and their

antibacterial activity against gram-positive pathogens. *Nanomaterials*, 12(2), 191.

Nitzan, O., Elias, M., Chazan, B., and Saliba, W. (2015). Urinary tract infections in patients with type 2 diabetes mellitus: review of prevalence, diagnosis, and management. *Diabetes, Metabolic Syndrome and Obesity: Targets and Therapy*, 8, 129 - 136.

Oake, A., Bhatt, P., and Pathak, Y. V. (2019). Understanding surface characteristics of nanoparticles. In Surface modification of nanoparticles for targeted drug delivery (pp. 1-17). *Springer*, Cham.

Okojie, R. O., and Omorokpe, V. O. (2018). A survey on urinary tract infection associated with two most common uropathogenic bacteria. *African Journal of Clinical and Experimental Microbiology*, 19(3) , v19i3.3 .

Oliveira, B. E. C., dos Santos Ré, A. C., Aires, C. P., and Ricomini Filho, A. P. (2022). Polysaccharides in Bacterial Biofilm 27. *Polysaccharides of Microbial Origin*, 599.

Öztürk, R., and Murt, A. (2020). Epidemiology of urological infections: a global burden. *World Journal of Urology*, 38(11), 2669-2679.

Pandit, R., Awal, B., Shrestha, S. S., Joshi, G., Rijal, B. P., and Parajuli, N. P. (2020). Extended-spectrum β-lactamase (ESBL) genotypes among multidrug-resistant uropathogenic *Escherichia coli* clinical isolates from a teaching hospital of Nepal. *Interdisciplinary Perspectives on Infectious Diseases*, 2020 , 5826 .

Paparo, L., Tripodi, L., Bruno, C., Pisapia, L., Damiano, C., Pastore, L., and Berni Canani, R. (2020). Protective action of Bacillus clausii probiotic strains in an in vitro model of Rotavirus infection. *Scientific Reports*, 10(1), 1-10.

Parsameher, N., Rezaei, S., Khodavasiy, S., Salari, S., Hadizade, S., Kord, M., and Mousavi, S. A. A. (2017). Effect of biogenic selenium nanoparticles on ERG11 and CDR1 gene expression in both fluconazole-resistant and-susceptible Candida albicans isolates. *Current Medical Mycology*, 3(3), 16-20.

Partoazar, A., Talaei, N., Bahador, A., Pourhajibagher, M., Dehpour, S., Sadati, M., and Bakhtiarian, A. (2019). Antibiofilm activity of natural zeolite supported NanoZnO: inhibition of *Esp* gene expression of *Enterococcus faecalis*. *Nanomedicine,* 14(6), 675-687.

Parvej, M. S., Khan, M. I., and Hossain, M. K. (2022). Preparation of nanoparticle-based polymer composites. *In Nanoparticle-Based Polymer Composites* (pp. 55-94).

Pasquina, L. W., Santa Maria, J. P., and Walker, S. (2013). Teichoic acid biosynthesis as an antibiotic target. *Current Opinion in Microbiology*, 16(5), 531-537.

Patil, N. A., Gade, W. N., and Deobagkar, D. D. (2016). Epigenetic modulation upon exposure of lung fibroblasts to TiO2 and ZnO nanoparticles: alterations in DNA methylation. *International journal of nanomedicine*, *11*, 4509.

Patel, J. K., Patel, A., and Bhatia, D. (2021). Introduction to nanomaterials and nanotechnology. *In Emerging Technologies for Nanoparticle Manufacturing* (pp. 3-23). Springer, Cham.

Patrone, V., Molinari, P., and Morelli, L. (2016). Microbiological and molecular characterization of commercially available probiotics containing Bacillus clausii from India and Pakistan. *International Journal of Food Microbiology*, 237, 92-97.

Pearce, C. I., Coker, V. S., Charnock, J. M., Pattrick, R. A., Mosselmans, J. F. W., Law, N., Beveridge, T.J., and Lloyd, J. R. (2008).

Microbial manufacture of chalcogenide-based nanoparticles via the reduction of selenite using Veillonella atypica: an in situ EXAFS study. *Nanotechnology,* 19(15), 155603.

Pouladfar, G., Basiratnia, M., Anvarinejad, M., Abbasi, P., Amirmoezi, F., and Zare, S. (2017). The antibiotic susceptibility patterns of uropathogens among children with urinary tract infection in Shiraz. *Medicine*, 96(37), e7834.

Purohit, M. P., Verma, N. K., Kar, A. K., Singh, A., Ghosh, D., and Patnaik, S. (2017). Inhibition of thioredoxin reductase by targeted selenopolymeric nanocarriers synergizes the therapeutic efficacy of doxorubicin in MCF7 human breast cancer cells. *ACS Applied Materials and Interfaces*, 9(42), 36493-36512.

Pyrzynska, K., and Pękal, A. (2013). Application of free radical diphenylpicrylhydrazyl (DPPH) to estimate the antioxidant capacity of food samples. *Anal Methods* , 5: 4288–4295.

Pyrzynska, K., and Sentkowska, A. (2021). Biosynthesis of selenium nanoparticles using plant extracts. *Journal of Nanostructure in Chemistry*, 1-14.

Rahimi, H. R., and Doostmohammadi, M. (2019). Nanoparticle synthesis, applications, and toxicity. *In Applications of Nanobiotechnology* (pp. 1-16) . London , UK: IntechOpen .

Rahimi, M., Charmi, G., Matyjaszewski, K., Banquy, X., and Pietrasik, J. (2021). Recent developments in natural and synthetic polymeric drug delivery systems used for the treatment of osteoarthritis. *Acta Biomaterialia* , 123, 31-50.

Ralston, N. V., and Raymond, L. J. (2010). Dietary selenium's protective effects against methylmercury toxicity. *Toxicology*, 278(1), 112-123.

Ramamurthy, C. H., Sampath, K. S., Arunkumar, P., Kumar, M. S., Sujatha, V., Premkumar, K., and Thirunavukkarasu, C. (2013). Green synthesis and characterization of selenium nanoparticles and its augmented cytotoxicity with doxorubicin on cancer cells. *Bioprocess and Biosystems Engineering*, 36(8), 1131-1139 .

Ranjitha, V. R., and Ravishankar, V. R. (2018). Extracellular synthesis of selenium nanoparticles from an actinomycetes streptomyces griseoruber and evaluation of its cytotoxicity on HT-29 cell line. *Pharmaceutical Nanotechnology*, 6(1), 61-68.

Raz, R., Colodner, R., and Kunin, C. M. (2005). Who are you—Staphylococcus saprophyticus?. *Clinical Infectious Diseases*, 40(6), 896-898.

Rebelo, A., Mourão, J., Freitas, A. R., Duarte, B., Silveira, E., Sanchez-Valenzuela, A., Almeida, A., Baquero, F., Coque, T.M., Peixe, L., Antunes, P., and Novais, C. (2021). Diversity of metal and antibiotic resistance genes in Enterococcus spp. from the last century reflects multiple pollution and genetic exchange among phyla from overlapping ecosystems. *Science of The Total Environment*, 787, 147548.

Reddy, S. M., Datta, K. K. R., Sreelakshmi, C., Eswaramoorthy, M., and Reddy, B. V. (2012). Honey mediated green synthesis of Pd nanoparticles for suzuki coupling and hydrogenation of conjugated olefins. *Nanoscience and Nanotechnology Letters*, 4(4), 420-425.

Ren, S. X., Zhang, B., Lin, Y., Ma, D. S., and Yan, H. (2019). Selenium nanoparticles dispersed in phytochemical exert anti-inflammatory activity by modulating catalase, GPx1, and COX-2 gene expression in a rheumatoid arthritis rat model. Medical science monitor: *International Medical Journal of Experimental and Clinical Research*, 25, 991-1000 .

Ricciotti, E., and FitzGerald, G. A. (2011). Prostaglandins and inflammation. *Arteriosclerosis, Thrombosis, and Vascular Biology*, 31(5), 986-1000.

Ruchi, T., Sujata, B., and Anuradha, D. (2015). Comparison of phenotypic methods for the detection of biofilm production in uro-pathogens in a tertiary care hospital in India. *International Journal of Current Microbiology* , 4(9), 840-849.

Rumbaugh, K. P., and Sauer, K. (2020). Biofilm dispersion. *Nature Reviews Microbiology*, 18(10), 571-586.

Sadalage, P. S., Nimbalkar, M. S., Sharma, K. K. K., Patil, P. S., and Pawar, K. D. (2020). Sustainable approach to almond skin mediated synthesis of tunable selenium microstructures for coating cotton fabric to impart specific antibacterial activity. *Journal of Colloid and Interface Science*, 569, 346-357.

Sadeghi, M., Ebrahim-Saraie, H. S., Mojtahedi, A., Nikokar, I., and Roushan, Z. A. (2020). Genetic diversity and prevalence of aminoglycoside modifying enzymes among Escherichia coli strains isolated from inpatients with urinary tract infections. *Gene Reports*, 21, 100957.

Salas-Orozco, M. F., Niño-Martínez, N., Martínez-Castañón, G. A., Méndez, F. T., Morán, G. M. M., Bendaña-Piñeiro, A. E., Ruiz, F., and Bach, H. (2022). Proteomic analysis of an Enterococcus faecalis mutant generated against the exposure to silver nanoparticles. *Journal of Applied Microbiology*, 132(1), 244-255.

Saleh, T. A. (2021). Protocols for synthesis of nanomaterials, polymers, and green materials as adsorbents for water treatment technologies. *Environmental Technology and Innovation*, 24, 101821.

Sánchez-López, E., Gomes, D., Esteruelas, G., Bonilla, L., Lopez-Machado, A. L., Galindo, R., Cano, A., Espina, M., Ettcheto, M., Camins , A., Silva, A.M., Durazzo, A., Santini, A., Garcia, M.L., and Souto, E. B. (2020). Metal-based nanoparticles as antimicrobial agents: an overview. *Nanomaterials*, 10(2), 10020292 .

Santanu, S., Sowmiya, R., and Balakrishnaraja, R. (2015). Biosynthesis of selenium nanoparticles using citrus reticulata peel extract. *World Journal of Pharmaceutical Research*, 4(1), 1322-1330.

Sartelli, M., Weber, D. G., Ruppé, E., Bassetti, M., Wright, B. J., Ansaloni, L., ... and Siribumrungwong, B. (2016). Antimicrobials: a global alliance for optimizing their rational use in intra-abdominal infections (AGORA). *World Journal of Emergency Surgery*, 11(1), 1-32.

Satgurunathan, T., Bhavan, P. S., and Komathi, S. (2017). Green synthesis of selenium nanoparticles from sodium selenite using garlic extract and its enrichment on Artemia nauplii to feed the freshwater prawn Macrobrachium rosenbergii post-larvae . *Research Journal of Chemistry and Environment*, 21(10), 1-12.

Sattar, R., Shahzad, F., Ishaq, T., Mukhtar, R., and Naz, A. (2022). Nano-Drug Carriers: A Potential Approach towards Drug Delivery Methods. *Chemistry Select* , 7(22), e202200884.

Sattari-Maraji, A., Jabalameli, F., Node Farahani, N., Beigverdi, R., and Emaneini, M. (2019). Antimicrobial resistance pattern, virulence determinants and molecular analysis of Enterococcus faecium isolated from children infections in Iran. *BMC microbiology*, 19(1), 1-8.

Schomburg, L. (2021). Selenium Deficiency Due to Diet, Pregnancy, Severe Illness, or COVID-19—A Preventable Trigger for

Autoimmune Disease. *International Journal of Molecular Sciences*, 22(16), 22168532 .

Sentkowska, A., and Pyrzyńska, K. (2022). The Influence of Synthesis Conditions on the Antioxidant Activity of Selenium Nanoparticles. *Molecules*, 27(8), 2486.

Shah, S. T., Yehye, W. A., Saad, O., Simarani, K., Chowdhury, Z. Z., Alhadi, A. A., and Al-Ani, L. A. (2017). Surface functionalization of iron oxide nanoparticles with gallic acid as potential antioxidant and antimicrobial agents. *Nanomaterials*, 7(10), 306.

Shahbaz, M., Akram, A., Raja, N. I., Mukhtar, T., Mashwani, Z. U., Mehak, A., ... and Yousaf, T. (2022). Green synthesis and characterization of selenium nanoparticles and its application in plant disease management : A review . *Pakistan Journal of Phytopathology*, 34(1), 189-102.

Shahmoradi, S., Shariati, A., Zargar, N., Yadegari, Z., Asnaashari, M., Amini, S. M., and Darban-Sarokhalil, D. (2021). Antimicrobial effects of selenium nanoparticles in combination with photodynamic therapy against *Enterococcus faecalis* biofilm. *Photodiagnosis and Photodynamic Therapy*, 35, 102398.

Shakerimoghaddam, A., Ghaemi, E. A., and Jamalli, A. (2017). Zinc oxide nanoparticle reduced biofilm formation and antigen 43 expressions in uropathogenic *Escherichia coli*. *Iranian Journal of Basic Medical Sciences*, 20(4), 451- 456 .

Shakibaie, M., Forootanfar, H., Golkari, Y., Mohammadi-Khorsand, T., and Shakibaie, M. R. (2015). Anti-biofilm activity of biogenic selenium nanoparticles and selenium dioxide against clinical isolates of Staphylococcus aureus, Pseudomonas aeruginosa, and Proteus mirabilis. *Journal of Trace Elements in Medicine and Biology*, 29, 235-241.

Shakibaie, M., Jafari, M., Ameri, A., Rahimi, H. R., and Forootanfar, H. (2018). Biosynthesis and physicochemical characterization, and cytotoxic evaluation of selenium nanoparticles produced by streptomyces lavendulae FSHJ9 against MCF-7 cell line. *Journal of Rafsanjan University of Medical Sciences*, 17(7), 625-638.

Sharma, G., Sharma, A. R., Bhavesh, R., Park, J., Ganbold, B., Nam, J. S., and Lee, S. S. (2014). Biomolecule-mediated synthesis of selenium nanoparticles using dried Vitis vinifera (raisin) extract. *Molecules*, 19(3), 2761-2770.

Sharma, J., and Chauhan, D. S. (2014). Inhibition of Pseudomonas aeruginosa by antibiotics and probiotics combinations–In vitro study. *European Journal of Experimental Biology*, 4(6), 10-14.

Shilpi, T., Ahmed, M. N., Huq, S. A., Baul, S. K., and Khatun, M. (2013). Isolation of bacteria causing urinary tract infections and their antibiotic susceptibility profile at Anwer Khan Modern Medical College Hospital. *Anwer Khan Modern Medical College Journal*, 4(2), 23-27.

Shirley, B., and Jarochowska, E. (2022). Chemical characterisation is rough: the impact of topography and measurement parameters on energy-dispersive X-ray spectroscopy in biominerals. *Facies*, 68(2), 1-15.

Shirsat, S., Kadam, A., Naushad, M., and Mane, R. S. (2015). Selenium nanostructures: microbial synthesis and applications. *Rsc Advances*, 5(112), 92799-92811.

Shubharani, R., Mahesh, M., and Yogananda Murthy, V. (2019). Biosynthesis and characterization, antioxidant and antimicrobial activities of selenium nanoparticles from ethanol extract of Bee Propolis. *Journal of Nanomedicine and Nanotechnology*, 10:522, 1-7 .

Siddiqui, M. A., Wahab, R., Ahmad, J., Farshori, N. N., and Al-Khedhairy, A. A. (2020). Single and Multi-metal Oxide Nanoparticles Induced Cytotoxicity and ROS Generation in Human Breast Cancer (MCF-7) Cells. *Journal of Inorganic and Organometallic Polymers and Materials*, 30(10) , 4106-4116.

Silhavy, T. J., Kahne, D., and Walker, S. (2010). The bacterial cell envelope. *Cold Spring Harbor perspectives in biology*, 2(5), a000414.

Singh, N., Saha, P., Rajkumar, K., and Abraham, J. (2014). Biosynthesis of silver and selenium nanoparticles by Bacillus sp. JAPSK2 and evaluation of antimicrobial activity. *Der Pharmacia Lettre*, 6(6), 175-181.

Singh, V., Basu, A., Shivapriya, P. M., Varadwaj, P. K., Samanta, S. K., and Sahoo, A. K. (2019). Exploration of interactions of 'blood-nano interface'of carbon-based nanomaterials for biomedical applications. *Journal of Materials Research*, 34(11), 1950-1964.

Skalickova, S., Milosavljevic, V., Cihalova, K., Horky, P., Richtera, L., and Adam, V. (2017). Selenium nanoparticles as a nutritional supplement. *Nutrition*, 33, 83-90.

Slavin, Y. N., Asnis, J., Häfeli, U. O., and Bach, H. (2017). Metal nanoparticles: understanding the mechanisms behind antibacterial activity. *Journal of Nanobiotechnology*, 15(1), 1-20.

Solovyev, N., Drobyshev, E., Bjørklund, G., Dubrovskii, Y., Lysiuk, R., and Rayman, M. P. (2018). Selenium, selenoprotein P, and Alzheimer's disease: is there a link?. *Free Radical Biology and Medicine*, 127, 124-133.

Soltani, L., and Darbemamieh, M. (2021). Anti-proliferative, apoptotic potential of synthesized selenium nanoparticles against breast

cancer cell line (MCF7). *Nucleosides, Nucleotides and Nucleic acids*, 40(9), 926-941.

Sonkusre, P. (2020) . Specificity of Biogenic Selenium Nanoparticles for Prostate Cancer Therapy With Reduced Risk of Toxicity: An in vitro and in vivo Study. *Frontiers in Oncology*, 9, 1541.

Sonkusre, P., and Cameotra, S.S. (2017). Biogenic selenium nanoparticles induce ROS-mediated necroptosis in PC-3 cancer cells through TNF activation. *Journal of Nanobiotechnology*, 15(1) , 1-12.

Sonkusre, P., Nanduri, R., Gupta, P., and Cameotra, S. S. (2014). Improved extraction of intracellular biogenic selenium nanoparticles and their specificity for cancer chemoprevention. *Journal of Nanomedicine and Nanotechnology*, 5(2), 194.

Sotoodehnia-Korani, S., Iranbakhsh, A., Ebadi, M., Majd, A., and Ardebili, Z. O. (2020). Selenium nanoparticles induced variations in growth, morphology, anatomy, biochemistry, gene expression, and epigenetic DNA methylation in Capsicum annuum; an in vitro study. *Environmental Pollution*, 265, 114727.

Spiliopoulou, M., Valmas, A., Triandafillidis, D. P., Kosinas, C., Fitch, A., Karavassili, F., and Margiolaki, I. (2020). Applications of X-ray powder diffraction in protein crystallography and drug screening. *Crystals*, 10(2), 54.

Srey, S., Jahid, I. K., and Ha, S. D. (2013). Biofilm formation in food industries: a food safety concern. *Food Control*, 31(2), 572-585.

Srinivas, A. (2020). Original Research Article Anti-microbial susceptibility pattern of spores used in Bacillus clausii suspension: an in vitro study. *International Journal of Contemporary Pediatrics*, 7(5), 1.

Srivastava, N., and Mukhopadhyay, M. (2015). Green synthesis and structural characterization of selenium nanoparticles and assessment of their antimicrobial property. *Bioprocess and Biosystems Engineering*, 38(9), 1723-1730.

Suáreza, D. F., Consuegrab, J., Trajanoc, V. C., Gontijoc, S. M., Guimarãesa, P. P.G., Cortésc, M. E., Denadai, A.L., and Sinisterraa, R. D. (2014). Structural and thermodynamic characterization of doxycycline/-cyclodextrin supramolecular complex and its bacterial membrane interactions. *Colloids and Surfaces B: Biointerfaces*, 118, 194-201.

Sudha, M. R., Bhonagiri, S., and Kumar, M. A. (2013). Efficacy of Bacillus clausii strain UBBC-07 in the treatment of patients suffering from acute diarrhoea. *Beneficial Microbes*, 4(2), 211-216.

Suwanjinda, D., Eames, C., and Panbangred, W. (2007). Screening of lactic acid bacteria for bacteriocins by microbiological and PCR methods. *Biochemistry and Molecular Biology Education*, 35(5), 364-369.

Syed, A., Saraswati, S., Kundu, G. C., and Ahmad, A. (2013). Biological synthesis of silver nanoparticles using the fungus Humicola sp. and evaluation of their cytoxicity using normal and cancer cell lines. *Spectrochimica Acta Part A: Molecular and Biomolecular Spectroscopy*, 114, 144-147.

Tabibi, M., Agaei, S. S., Amoozegar, M. A., Nazari, R., and Zolfaghari, M. R. (2020). Antibacterial, antioxidant, and anticancer activities of biosynthesized selenium nanoparticles using two indigenous halophilic bacteria. *Archives of Hygiene Sciences*, 9(4), 275-286.

Tang, L., Luo, X., Wang, M., Wang, Z., Guo, J., Kong, F., and Bi, Y. (2021). Synthesis, characterization, in vitro antioxidant and hypoglycemic activities of selenium nanoparticles decorated with

polysaccharides of Gracilaria lemaneiformis. *International Journal of Biological Macromolecules*, 193, 923-932.

Toledo-Arana, A., Valle, J., Solano, C., Arrizubieta, M. J., Cucarella, C., Lamata, M., Amorena, B., Leiva, J., Penadés, J.R., and Lasa, I. (2001). The enterococcal surface protein, *Esp*, is involved in *Enterococcus faecalis* biofilm formation . *Applied and Environmental Microbiology*, 67(10), 4538-4545.

Tran, P. A., O'Brien-Simpson, N., Reynolds, E. C., Pantarat, N., Biswas, D. P., and O'Connor, A. J. (2015). Low cytotoxic trace element selenium nanoparticles and their differential antimicrobial properties against *S. aureus* and *E. coli*. *Nanotechnology*, 27(4), 045101.

Trüeb, R. M. (2020). Nutritional Disorders of the Hair and Their Management. *In Nutrition for Healthy Hair* (111-223). Springer, Cham.

Tsamesidis, I., Pouroutzidou, G. K., Lymperaki, E., Kazeli, K., Lioutas, C. B., Christodoulou, E., Perio, P., Reybier, K., Pantaleo, A., and Kontonasaki, E. (2020). Effect of ion doping in silica-based nanoparticles on the hemolytic and oxidative activity in contact with human erythrocytes. *Chemico-Biological Interactions*, 318, 108974.

Tugarova, A. V., Mamchenkova, P. V., Dyatlova, Y. A., and Kamnev, A. A. (2018). FTIR and Raman spectroscopic studies of selenium nanoparticles synthesised by the bacterium Azospirillum thiophilum. Spectrochimica Acta Part A: *Molecular and Biomolecular Spectroscopy*, 192, 458-463.

Ullah, A., Yin, X., Wang, F., Xu, B., Mirani, Z. A., Xu, B., Chan, M.W.H., Ali, A., Usman, M., Ali, N., and Naveed, M. (2021). Biosynthesis of selenium nanoparticles (via Bacillus subtilis

bsn313), and their isolation, characterization, and bioactivities. *Molecules*, 26(18), 26185559 .

Ungvári, É., Monori, I., Megyeri, A., Csiki, Z., Prokisch, J., Sztrik, A., Jávor, A., and Benkő, I. (2014). Protective effects of meat from lambs on selenium nanoparticle supplemented diet in a mouse model of polycyclic aromatic hydrocarbon-induced immunotoxicity. *Food and Chemical Toxicology*, 64, 298-306.

Upadrasta, A., Pitta, S., and Madempudi, R. S. (2016). Draft genome sequence of *Bacillus clausii* UBBC07, a spore-forming probiotic strain. *Genome Announcements*, 4(2), e00235-16.

Vachvanichsanong, P., McNeil, E. B., and Dissaneewate, P. (2021). Extended-spectrum beta-lactamase Escherichia coli and Klebsiella pneumoniae urinary tract infections. *Epidemiology and Infection*, 149 , e12, 1–7.

Van Khanh, N., and Van Cu, P. (2019). Antibacterial activity of silver nanoparticles against aeromonas spp. and Vibrio spp. isolated from aquaculture water environment in Thua Thien Hue. *Hue University Journal of Science: Agriculture and Rural Development*, 128(3B), 5-16.

Van Malderen, S. (2017). Optimization of methods based on laser ablation-ICP-mass spectrometry (LA-ICP-MS) for 2-D and 3-D elemental mapping (Doctoral dissertation, Ghent University).

Vandepitte, J., Verhaegen, J., Engbaek, K., Piot, P., Heuck, C. C., Rohner, P., and Heuck, C. C. (2003). Basic laboratory procedures in clinical bacteriology. *World Health Organization*.

Varak, K., and Priya, P. K. (2019). Synergistic Effect Of Selenium Nanoparticles (Senps) With Various Antibiotics As An Antimicrobial Activity". *Think India Journal*, 22(4), 1707-1712.

Verma, P., and Maheshwari, S. K. (2017). Minimum biofilm eradication concentration (MBEC) assay of Silver and Selenium nanoparticles against biofilm forming Staphylococcus aureus. *Journal of Medical Science And Clinical Research*, 5(4), 20213-20222.

Verma, P., and Maheshwari, S. K. (2018). Preparation of sliver and selenium nanoparticles and its characterization by dynamic light scattering and scanning electron microscopy. *Journal of Microscopy and Ultrastructure*, 6(4), 182 - 187.

Vetchinkina, E., Loshchinina, E., Kupryashina, M., Burov, A., and Nikitina, V. (2019). Shape and size diversity of gold, silver, selenium, and silica nanoparticles prepared by green synthesis using fungi and bacteria. *Industrial and Engineering Chemistry Research*, 58(37), 17207-17218.

Vincent, M. G., John, N. P., Narayanan, P. M., Vani, C., and Murugan, S. (2014). In vitro study on the efficacy of zinc oxide and titanium dioxide nanoparticles against metallo beta-lactamase and biofilm producing Pseudomonas aeruginosa. *Journal of Applied Pharmaceutical Science*, 4(7), 041-046.

Wadhwani, S. A., Gorain, M., Banerjee, P., Shedbalkar, U. U., Singh, R., Kundu, G. C., and Chopade, B. A. (2017). Green synthesis of selenium nanoparticles using Acinetobacter sp. SW30: Optimization, characterization and its anticancer activity in breast cancer cells. *International Journal of Nanomedicine*, 12, 6841–6855.

Waller, K. P., Aspán, A., Nyman, A., Persson, Y., and Andersson, U. G. (2011). CNS species and antimicrobial resistance in clinical and subclinical bovine mastitis. *Veterinary Microbiology*, 152(1-2), 112-116.

Wang, H., Wei, W., Zhang, S. Y., Shen, Y. X., Yue, L., Wang, N. P., and Xu, S. Y. (2005). Melatonin-selenium nanoparticles inhibit oxidative stress and protect against hepatic injury induced by Bacillus Calmette–Guérin/lipopolysaccharide in mice. *Journal of Pineal Research*, 39(2), 156-163.

Wang, H., Zhang, J., and Yu, H. (2007). Elemental selenium at nano size possesses lower toxicity without compromising the fundamental effect on selenoenzymes: comparison with selenomethionine in mice. *Free Radical Biology and Medicine*, 42(10), 1524-1533.

Wang, K., Taylor, K. G., and Ma, L. (2021). Advancing the application of atomic force microscopy (AFM) to the characterization and quantification of geological material properties. *International Journal of Coal Geology*, 247, 103852.

Wang, L., Hu, C., and Shao, L. (2017). The antimicrobial activity of nanoparticles: present situation and prospects for the future. *International Journal of Nanomedicine*, 12, 1227 –1249.

Wang, Y., Xue, D., Li, Y., Pan, X., Zhang, X., Kuang, B., Zhou, M., Li, X., Xiong, W., Li, G., Zeng, Z., and Yang, T. (2016). The long noncoding RNA MALAT-1 is a novel biomarker in various cancers: a meta-analysis based on the GEO database and literature. *Journal of Cancer*, 7(8), 991-1001.

WHO (2019) . Ten threats to global health .

Wisell, K. T., Kahlmeter, G., and Giske, C. G. (2008). Trimethoprim and enterococci in urinary tract infections: new perspectives on an old issue. *Journal of Antimicrobial Chemotherapy*, 62(1), 35-40.

Xia, Y., Lin, Z., Li, Y., Zhao, M., Wang, C., Guo, M., Zhang, B., and Zhu, B. (2017). Targeted delivery of siRNA using RGDfC-conjugated functionalized selenium nanoparticles for anticancer therapy. *Journal of Materials Chemistry B*, 5(33), 6941-6952.

Xiong, Y., Zhang, C., Gao, W., Ma, Y., Zhang, Q., Han, Y., Jiang, S., Zhao, Z., Wang, J., and Chen, Y. (2021). Genetic diversity and co-prevalence of ESBLs and PMQR genes among plasmid-mediated AmpC β-lactamase-producing *Klebsiella pneumoniae* isolates causing urinary tract infection. *The Journal of Antibiotics*, 74(6), 397-406.

Yang, F., Tang, Q., Zhong, X., Bai, Y., Chen, T., Zhang, Y., Li, Y., and Zheng, W. (2012). Surface decoration by Spirulina polysaccharide enhances the cellular uptake and anticancer efficacy of selenium nanoparticles. *International Journal of Nanomedicine*, 7, 835 – 844.

Yazdi, M. H., Mahdavi, M., Kheradmand, E., and Shahverdi, A. R. (2012). The preventive oral supplementation of a selenium nanoparticle-enriched probiotic increases the immune response and lifespan of 4T1 breast cancer bearing mice. *Arzneimittelforschung*, 62(11), 525-531.

Zafar, S. (2022). Review on synthesis and applications of nanomaterials. *SBK Journal of Basic Sciences and Innovative Research*, 1(2), 1-53.

Zayed, M. F., Eisa, W. H., El-Kousy, S. M., Mleha, W. K., and Kamal, N. (2019). Ficus retusa-stabilized gold and silver nanoparticles: controlled synthesis, spectroscopic characterization, and sensing properties. Spectrochimica Acta Part A: *Molecular and Biomolecular Spectroscopy*, 214, 496-512.

Zhai, X., Zhang, C., Zhao, G., Stoll, S., Ren, F., and Leng, X. (2017). Antioxidant capacities of the selenium nanoparticles stabilized by chitosan. *Journal of Nanobiotechnology*, 15(1), 1-12.

Zhang, H., Li, Z., Dai, C., Wang, P., Fan, S., Yu, B., and Qu, Y. (2021). Antibacterial properties and mechanism of selenium nanoparticles

synthesized by Providencia sp. DCX. *Environmental Research*, 194, 110630.

Zhang, H., Xia, M., and Hu, C. (2007). Effect of nano-selenium on the activities of glutathione peroxidase and type-I deiodinase in the liver of weanling pigs. *Journal of Biomedical Engineering* , 24(1), 153-156.

Zhang, H., Zhou, H., Bai, J., Li, Y., Yang, J., Ma, Q., and Qu, Y. (2019). Biosynthesis of selenium nanoparticles mediated by fungus Mariannaea sp. HJ and their characterization. Colloids and Surfaces A: *Physicochemical and Engineering Aspects*, 571, 9-16.

Zhao, S., Yu, Q., Pan, J., Zhou, Y., Cao, C., Ouyang, J. M., and Liu, J. (2017). Redox-responsive mesoporous selenium delivery of doxorubicin targets MCF-7 cells and synergistically enhances its anti-tumor activity. *Acta Biomaterialia*, 54, 294-306.

Zheng, W., Cao, C., Liu, Y., Yu, Q., Zheng, C., Sun, D., Ren, X., and Liu, J. (2015). Multifunctional polyamidoamine-modified selenium nanoparticles dual-delivering siRNA and cisplatin to A549/DDP cells for reversal multidrug resistance. *Acta Biomaterialia*, 11, 368-380.

Zhou, Y., Xu, M., Liu, Y., Bai, Y., Deng, Y., Liu, J., and Chen, L.(2016) . Green synthesis of Se/Ru alloy nanoparticles using gallic acid and evaluation of theiranti-invasive effects in HeLa cells. *Colloids and Surfaces B: Biointerfaces*, 144, 118-124.

Zhu, C., Zhang, S., Song, C., Zhang, Y., Ling, Q., Hoffmann, P. R., Li, J., Chen, T., Zheng, W., and Huang, Z. (2017). Selenium nanoparticles decorated with Ulva lactuca polysaccharide potentially attenuate colitis by inhibiting NF-κB mediated hyper inflammation. *Journal of Nanobiotechnology*, 15(1), 1-15.

Zonaro, E., Lampis, S., Turner, R. J., Qazi, S. J. S., and Vallini, G. (2015). Biogenic selenium and tellurium nanoparticles synthesized by environmental microbial isolates efficaciously inhibit bacterial planktonic cultures and biofilms. *Frontiers in Microbiology* , 6, 584.

Zou, X., Jiang, Z., Li, L., and Huang, Z. (2021). Selenium nanoparticles coated with pH responsive silk fibroin complex for fingolimod release and enhanced targeting in thyroid cancer. *Artificial Cells, Nanomedicine, and Biotechnology*, 49(1), 83-95.

Zwolak, I. (2020). The role of selenium in arsenic and cadmium toxicity: an updated review of scientific literature. *Biological Trace Element Research*, 193(1), 44-63.

Appendices

Appendix 1: Identification of E.coli by Vitek 2 compact system.

Selected Organism			99% Probability **Escherichia coli** **Bionumber:** 0405610550524610														
ID Analysis Messages																	
Biochemical Details																	
2	APPA	-	3	ADO	-	4	PyrA	-	5	lARL	-	7	dCEL	-	9	BGAL	+
10	H2S	-	11	BNAG	-	12	AGLTp	-	13	dGLU	+	14	GGT	-	15	OFF	+
17	BGLU	-	18	dMAL	+	19	dMAN	+	20	dMNE	+	21	BXYL	-	22	BAlap	-
23	ProA	-	26	LIP	-	27	PLE	-	29	TyrA	+	31	URE	-	32	dSOR	+
33	SAC	+	34	dTAG	-	35	dTRE	+	36	CIT	-	37	MNT	-	39	5KG	-
40	lLATk	+	41	AGLU	-	42	SUCT	+	43	NAGA	-	44	AGAL	+	45	PHOS	-
46	GlyA	-	47	ODC	-	48	LDC	+	53	lHISa	-	56	CMT	+	57	BGUR	+
58	O129R	+	59	GGAA	-	61	lMLTa	-	62	ELLM	-	64	lLATa	-			

Appendix 2: Identification of Enterococcus faecalis by Vitek 2 system.

Selected Organism			99% Probability **Enterococcus faecalis** **Bionumber:** 156002661773431														
ID Analysis Messages																	
Biochemical Details																	
2	AMY	+	4	PIPLC	-	5	dXYL	-	8	ADH1	+	9	BGAL	-	11	AGLU	+
13	APPA	-	14	CDEX	+	15	AspA	+	16	BGAR	-	17	AMAN	-	19	PHOS	-
20	LeuA	-	23	ProA	-	24	BGURr	-	25	AGAL	-	26	PyrA	+	27	BGUR	-
28	AlaA	-	29	TyrA	+	30	dSOR	+	31	URE	-	32	POLYB	+	37	dGAL	+
38	dRIB	+	39	lLATk	-	42	LAC	-	44	NAG	+	45	dMAL	+	46	BACI	+
47	NOVO	+	50	NC6.5	+	52	dMAN	+	53	dMNE	+	54	MBdG	+	56	PUL	-
57	dRAF	-	58	O129R	-	59	SAL	+	60	SAC	+	62	dTRE	+	63	ADH2s	-
64	OPTO	+															

Appendix 3: Identification of Klebsiella pneumoniae by Vitek 2 system.

Selected Organism			96% Probability **Klebsiella pneumoniae ssp pneumoniae** **Bionumber:** 6607734553564610 **Confidence:** Excellent identification														
SRF Organism																	
Analysis Organisms and Tests to Separate:																	
Analysis Messages:																	
Contraindicating Typical Biopattern(s) Klebsiella pneumoniae ssp pneumoniae BGUR(3),																	
Biochemical Details																	
2	APPA	-	3	ADO	+	4	PyrA	+	5	lARL	-	7	dCEL	+	9	BGAL	+
10	H2S	-	11	BNAG	-	12	AGLTp	-	13	dGLU	+	14	GGT	+	15	OFF	+
17	BGLU	+	18	dMAL	+	19	dMAN	+	20	dMNE	+	21	BXYL	+	22	BAlap	-
23	ProA	-	26	LIP	-	27	PLE	+	29	TyrA	+	31	URE	(-)	32	dSOR	+
33	SAC	+	34	dTAG	-	35	dTRE	+	36	CIT	+	37	MNT	+	39	5KG	-
40	lLATk	+	41	AGLU	-	42	SUCT	+	43	NAGA	-	44	AGAL	+	45	PHOS	+
46	GlyA	-	47	ODC	-	48	LDC	+	53	lHISa	-	56	CMT	+	57	BGUR	+
58	O129R	+	59	GGAA	-	61	lMLTa	-	62	ELLM	-	64	lLATa	-			

Appendix 4: Identification of Staphylococcus saprophyticus by Vitek 2 system.

Selected Organism				89% Probability **Bionumber:**		**Staphylococcus saprophyticus** 070002057771271											
ID Analysis Messages																	
Biochemical Details																	
2	AMY	-	4	PIPLC	-	5	dXYL	-	8	ADH1	+	9	BGAL	+	11	AGLU	+
13	APPA	-	14	CDEX	-	15	AspA	-	16	BGAR	-	17	AMAN	-	19	PHOS	-
20	LeuA	-	23	ProA	-	24	BGURr	-	25	AGAL	-	26	PyrA	+	27	BGUR	-
28	AlaA	-	29	TyrA	-	30	dSOR	-	31	URE	+	32	POLYB	-	37	dGAL	+
38	dRIB	+	39	lLATk	+	42	LAC	+	44	NAG	+	45	dMAL	+	46	BACI	+
47	NOVO	+	50	NC6.5	+	52	dMAN	+	53	dMNE	+	54	MBdG	-	56	PUL	-
57	dRAF	-	58	O129R	+	59	SAL	-	60	SAC	+	62	dTRE	+	63	ADH2s	+
64	OPTO	+															

Appendix 5: Identification of Bacillus clausii by Vitek 2 system.

Bionumber: 5373331317447671
Organism Quantity: **Selected Organism: Bacillus claussi**

Biochemical Details																	
1	BXYL	+	3	LysA	-	4	AspA	+	5	LeuA	+	7	PheA	+	8	ProA	-
9	BGAL	+	10	PyrA	+	11	AGAL	+	12	AlaA	+	13	TyrA	+	14	BNAG	-
15	APPA	(+)	18	CDEX	+	19	dGAL	-	21	GLYG	+	22	INO	+	24	MdG	(-)
25	ELLM	+	26	MdX	-	27	AMAN	-	29	MTE	+	30	GlyA	+	31	dMAN	-
32	dMNE	+	34	dMLZ	-	36	NAG	-	37	PLE	+	39	IRHA	+	41	BGLU	+
43	BMAN	(-)	44	PHC	-	45	PVATE	+	46	AGLU	(-)	47	dTAG	-	48	dTRE	+
50	INU	+	53	dGLU	+	54	dRIB	+	56	PSCNa	-	58	NaCl 6.5%	+	59	KAN	+
60	OLD	+	61	ESC	+	62	TTZ	+	63	POLYB_B	+						

Appendix 6 : XRD values of selenium nanoparticles .

	2-Theta (degree)	Theta	FWHM (degree)	Crystallite size(nm)	D(nm)
1	23.601	14.94835	0.7872	10.31472	**18.215**
2	29.8967	11.8005	0.246	33.44077	
3	44.0156	22.0078	0.7872	10.88965	

Appendix 7 : Functional groups values of FTIR .

Peak Number	X (cm-1)	Y (%T)
1	3335.96	43.40
2	2952.85	22.64
3	2922.50	16.72
4	2853.17	22.31
5	2726.72	43.02
6	1632.39	43.60
7	1516.55	43.88
8	1502.78	43.98
9	1462.11	33.05
10	1455.69	32.97
11	1376.95	37.01
12	1046.00	42.28
13	721.83	45.94
14	558.51	47.48
15	470.29	48.79

Appendix 8: Gene expression (Mean ± SE) for Hly gene and FimH gene in E.coli

Groups	*Hly* gene	*FimH* gene
Sub-MIC 32	1.51±0.98Aa	2.47±1.93Aa
MIC 64	4.11±0.98Aa	6.66±2.52Ba
Control	11.91±3.09Ba	14.31±3.73Ca

Means with different big letters in the same column and small letters in the same row are significantly different (P<0.05) .

Appendix 9 : Gene expression (Mean ± SE) for LuxS gene and qseC gene in E. coli (biofilm production and regulation)

Groups	*LuxS* gene	*qseC* gene
Sub-MIC 64	1.38±0.21Aa	0.79±0.18Aa
MIC 128	3.72±1.15Aa	2.05±0.55Aa
Control	15.45±4.43Ba	5.52±1.2Bb

Means with different big letters in the same column and small letters in the same row are significantly different (P<0.05) .

Appendix 10 : Gene expression (Mean ± SE) for ESP gene and HLY gene in E. faecalis .

Groups	*ESP* gene	*HLY* gene
Sub–MIC 16	1.32±0.15Aa	2.21±0.15Aa
MIC 32	12.69±2.52Ba	9.5±0.81Ba
Control	38.13±6.86Ca	22.18±9.03Cb

Means with different big letters in the same column and small letters in the same row are significantly different (P<0.05) .

Appendix 11 : Gene expression (Mean ± SE) of gelE and fsrA gene in E. faecalis (biofilm production and regulation)

Groups	*gelE* gene	*fsrA* gene
Sub-MIC 32	0.41±0.05Aa	2.09±0.43Aa
MIC 64	1.51±0.51Aa	6.37±1.29Bb
Control	4.70±1.33Ba	14.15±2.99Cc

Means with different big letters in the same column and small letters in the same row are significantly different (P<0.05).

الخلاصـــــــــة :

تحتل الطريقة البيولوجية لتصنيع الجسيمات النانوية مجالًا مهمًا نظرا لفائدتها الاقتصادية وكونها صديقة للبيئة عند مقارنتها بطرق التخليق الفيزيائية والكيميائية . لذلك , فان هذه الدراسة هدفت الى تصنيع جسيمات السيلينيوم النانوية (SeNPs) من خلال طريقه بايلوجية باستخدام بكتريا *Bacillus clausii* من سلاله (4G219) والتي شخصت باستخدام نظام VITEK 2 وباستخدام سلسلة مورث الحمض النووي الرايبوزي 16SrRNA . تم تحديد الخصائص الشكلية والهيكلية لجسيمات السيلينيوم النانوية بِاستخدام اِلقياس اِلطيفي اِلمرئي لِلأشعة فِوقِ البنفسجيةِ – UV visible ولن ذروة الامتصاص كانت عند الطول الموجي (260) نانومتر , المجهر الالكتروني الماسح SEM (تراوحت اقطار الجزيئات النانوية بين (37.58 - 75.16) نانومتر , حيث تبين ان الجسيمات النانوية المصنعة كانت بلورية ومستقرة الى حد ما وذات شكل قضيبي , والتحليل الطيفي للطاقة المشتتة من الاشعة السينية (EDXS) كشف ان اكثر الاشارات الحادة تعود لجزيئات السيلينيوم النانوية . في فحص XRD ، وجد أن حجم جسيمات السيلينيوم النانوية متشابه مع البيانات التي تم الحصول عليها من (AFM) مع الحجم (18.215 نانومتر ، 19. 28 نانومتر) على التوالي. اما مطياف الأشعة تحت الحمراء FTIR لجزيئات السيلينيوم النانوية فقد اظهر وجود عدد من المجاميع الوظيفية .

تم جمع مائة وخمسة وستين عينة ادرار من مرضى يعانون من أعراض سريرية ويشتبه في إصابتهم بالتهاب المسالك البولية داخل مستشفيات مختلفة في محافظة بابل للفترة من (اذار – تشرين الاول) 2021 . 115 (69.6٪) عزلة كانت موجبة الفحص ، تم تشخيص أربعة أنواع من البكتيريا الممرضة (*Escherichia coli* , *Enterococcus faecalis* , *Klebsiella pneumoniae* , *Staphyllococcus saprophyticus*) , معظمها كان مقاوم للمضادات الحيوية وبالأخص *Enterococcus faecalis* . تم فحص النشاط المضاد البكتيري لجسيمات السيلينيوم النانوية ضد الانواع الاربعه للبكتريا المرضية . تم استخدام عشرة تركيزات مختلفة من SeNPs (2 , 4 , 8 , 16 , 32 , 64 , 128 , 256 , 512 , 1024) ميكروغرام / مل . وجد ان التركيز المثبط الادنى لجزيئات السيلينيوم النانوية (MIC) هو (32 ميكروغرام / مل) والتركيز القاتل الادنى لجزيئات السيلينيوم النانوية (MBC) هو (64 ميكروغرام / مل) لكل من *Staphylococcus Saprophyticus* و *Enterococcus faecalis* ، بينما

التركيز المثبط الادنى (MIC) و التركيز القاتل الادنى (MBC) لـ *Klebsiella pneumoniae* و *Escherichia coli* فقد كان (64 ميكروغرام / مل) و (128 ميكروغرام / مل) على التوالي .

تم دراسة التأثير التآزري لـ SeNPs باستخدام ستة مضادات حيوية (Azithromycin، Ciprofloxacin، Trimethoprime / sulphamethoxazole , Doxycycline، nitrofurantoin and Ampicillin) ضد البكتيريا المرضية . انخفض التأثير التآزري لـ Doxycycline مع SeNPs في جميع البكتيريا المُختبرة الحساسة للدوكسيسايكلين ، وأصبحت العزلات التي كانت حساسة للمضاد الحيوي متوسطة المقاومة والمتوسطة المقاومة اصبحت مقاومة للمضادات الحيوية. تم تحديد النشاط المضاد للأكسدة لجزيئات السيلينيوم النانوية باستخدام (DPPH) (2,2-Diphenyl-1-picryl- hydrazyl) . حيث كان للجسيمات النانوية اعلى نشاط مضاد للأكسدة (% 39.6 , 63.1% , % 74.2) عند التراكيز (50 , 100 , 150) ميكروغرام / مل , على التوالي . لم تظهر جسيمات السيلينيوم النانوية بكل التراكيز المستخدمة أي انحلال كامل للدم الذي تم اختباره .

اما في اختبار تكوين الاغشية الحيوية الرقيقة (Biofilm) , من اصل 115 عزله , كانت 60 عزلة لها القدرة على تكوين الاغشية الحيوية . اما في اختبار ضدية تكوين الاغشية الحيوية الرقيقة (Antibiofilm) فقد تم قياس قدرة بعض انواع البكتريا على تكوين الاغشية الحيوية الرقيقة بوجود جزيئات السيلينيوم النانوية باستخدام طريقة صفيحة 96 حفرة . وجد ان التركيز المثبط الادنى (MIC) لجزيئات السيلينيوم النانوية لتكوين الاغشية الحيوية هو (128 ميكروغرام / مل) لبكتريا *Escherichia coli* and *Klebsiella pneumoniae)* و(64 ميكروغرام / مل) لبكتريا *Staphylococcus Saprophyticus* (and *Enterococcus faecalis*) , فقد وجد ان التركيز المثبط الادنى MIC لجزيئات السيلينيوم النانوية ضد تكوين الاغشية الحيوية هو ضعف التركيز المثبط الادنى MIC لجزيئات السيلينيوم النانوية في حاله البكتريا العالقه .

أظهر فحص الاستجابة السمية للخلايا لخط خلايا سرطان البروستات PC3 والخلايا الكبدية البشرية الطبيعية WRL68 عدم وجود تأثير سام لـ Se NPsعلى خلايا PC3 بتركيز 25 و 50 ميكروغرام / مل . ومع ذلك فقد اظهر الـ SeNPs بتركيز (100 , 200 , 400 ميكروغرام / مل) انخفاض في معدل بقاء خلايا PC3 مع اقصى معدل تثبيط بلغ (51.27±2.77%) لخط خلايا PC3 بتركيز (400 ميكروغرام / مل) . اما فيما يتعلق بخط خلايا (WRL68) فقد كانت حساسية الخلايا لل SeNPs اقل من تلك الموجودة في خط خلايا ال PC3 .

تم تقييم التعبير الجيني لعوامل الضراوة للجينات (*Hly*، *FimH*، *Luxs*، *qsec*) لبكتريا *E.coli* و جينات (*ESP*، *HLY*، *gelE*، *fsrA*) لبكتريا *E.faecalis* عن طريق تفاعل البلمرة المتسلسل الكمي في الوقت الحقيقي (RT- qPCR) قبل وبعد المعاملة بـالـ SeNPs , اذ كشفت النتائج أن SeNPs يؤثر على التعبير الجيني لهذه الجينات عن طريق تقليل التعبير الجيني (down regulation) .

استنتجت هذه الدراسة قدرة *Bacillus clausii* على تخليق جسيمات السيلينيوم النانوية. وقد ثبت قدرة هذه الجسيمات كمضاد بكتيري , مضاد لتكوين الغشاء الحيوي , مضادات الأكسدة , النشاط المضاد للسرطان في خط خلايا PC3 و WRL 68 واخيرا تقليل التعبير الجيني لجينات عوامل الضراوة .

جمهورية العراق
وزارة التعليم العالي والبحث العلمي
جامعة بابل
كلية العلوم
قسم علوم الحياة

التخليق الحيوي لجسيمات السيلينيوم النانوية من *Bacillus clausii* وتقيم فعاليته المضادة للبكتريا وللاغشيه الحيويه الرقيقه وفحص السمية الخلوية

اطروحة مقدمة الى
مجلس كلية العلوم / جامعة بابل
وهي جزء من متطلبات نيل درجة الدكتوراه فلسفة
في العلوم / علوم الحياة

من قبل

حوراء جواد كاظم عمران
بكالوريوس احياء مجهرية / جامعة بابل (2007)
ماجستير احياء مجهرية / جامعة بابل (2014)

بأشراف

أ.د وجدان رضا تاج الدين

2022م 1444 هـ

Republic of Iraq
Ministry of Higher Education and Scientific Research
University of Babylon
College of Science
Department of Biology

Biosynthesis of Selenium Nanoparticles from *Bacillus clausii* and Evalution of Antibacterial , Antibiofilm and Cytotoxicity Assay

A Dissertation

Submitted to the Council of the College of Science University of Babylon, in Partial Fulfillment of the Requirements for the Degree Doctor of Philosophy In Sciences / Biology

By

Hawraa Jawad Kadhim omran

B.Sc. Microbiology /University of Babylon (2007)

M.Sc. Microbiology/University of Babylon (2014)

Supervised By

Prof. Dr.Wejdan Ridha Taj- Aldeen

2022 A.D 1444 A.H

The Supervisor's Certification

I certify that this thesis entitled " **Biosynthesis of Selenium Nanoparticles from *Bacillus clausii* and Evalution of Antibacterial , Antibiofilm and Cytotoxicity Assay** " was prepared by " ***Hawraa Jawad Kadhim omran*** " under our supervision in the University of Babylon /College of Science /Department of Biology as a partial fulfillment of the requirements for the Degree of Doctor of Philosophy in Biology .

Signature :

Prof. Dr. Wejdan Ridha Taj-Aldeen

Department of Biology / College of Science

University of Babylon

Data : / / 2022

In view of the available recommendation, I put forward this thesis for debate by the examining committee .

Signature:

Assist. Prof. Dr. Adi Jassim Abd AL-Razzaq

Head of Biology Department

Data : / / 2022

Examination Committee

We, the examiner committee , certify that we have read the thesis entitled **" Biosynthesis of Selenium Nanoparticles from *Bacillus clausii* and Evalution of Antibacterial , Antibiofilm and Cytotoxicity Assay "** and have examined the student **" *Hawraa Jawad Kadhim omran* "** in its contents, and that in our opinion it is accepted as a thesis for the degree of Doctor in Philosophy of Biology - Microbiology with **" Excellent "** estimation .

Signature:
Prof. Dr. Abeer Fauzi Murad AL-Rubaye
College of Science for women
University of Babylon
Chairman

Signature:
Prof. Dr. Shaimaa Jassim AL-Sultany
College of Science
University of Babylon
Member

Signature:
Assist. Prof. Dr. Yazi Abdullah Jassim
College of Science
University of Babylon
Member

Signature:
Assist. Prof. Dr. Mais Emad Ahmad
College of Science
University of Baghdad
Member

Signature:
Assist. Prof. Dr. Iman Fadhel Abdul-Hussin
College of Biotechnology
Al-Qasim Green University
Member

Signature:
Prof. Dr. Wejdan Ridha Taj-Aldeen
College of Science
University of Babylon
Member & Supervisor

Approved for the College Committee of graduate studies

Signature:
Prof. Dr. Mohammed Mansour Kadhum AL Kafaji
Dean of College of Science
University of Babylon

Dedication

If the Dedication expresses even part of the fulfillment, then the Dedication is due …

To the soul of (grandmother's)

To the source of tender, love and advice..

(Mother & Father)

To whom I hold my dearest in life , my brothers and my dear sister **(Rawaa)**

To my dear children (Qaswar , Hawraa , Asal) and my husband (Dhiya)

To every knowledge student
I dedicate this study

Hawraa

Acknowledgements

***Initially** , I thank Almighty God for giving me the strength and the will to complete this work for the required degree*

My deepest thanks to University of Babylon and I would like to thank the staff of College of Science / Department of Biology , for their kind assistance

It is my pleasure to express my deep thanks and gratitude to my supervisor Professor Dr. Wejdan Ridha Taj- Aldeen who has provided me with valuable scientific guidance and continuous support throughout the period of preparation, and has devoted a large part of her time for the purpose of writing this dissertation.

Sincere thanks are due to the Dr. Nawfal Al-Dujaily, Dr. Hassan Hachim , Mrs. Zahraa , Mrs. Helen . Thanks to every teacher who contributed to my education in my life.

I would like to thank my family for their support in all times .

***Finally** , thanks and appreciation are to my colleagues and to all those who helped me in completing this work*

Hawraa

Summary

The biological method for the synthesis of nanoparticles occupies an important area due to economic and ecofriendly benefits when compared with physical and chemical synthesis methods. Hence ,this study aims to prepare selenium nanoparticles through the biological method from *Bacillus clausii* strain (4G219) that was diagnosed by VITEK2 system and 16srRNA gene sequencing .

The morphological and structural properties of selenium naanoparticles were determined by UV – visible spectroscopy and the absorption peak was observed at 260 nm wavelength , Field Emission Scanning Electron Microscope (FESEM) (diameters of SeNPs ranging from 37.58 – 75.16 nm) showing that the synthesized nanoparticles were crystalline, moderately stable and have rod shape , energy dispersive X-ray spectroscopy (EDX) revealed that the most principal sharp signal observed was belong to selenium nanoparticles . In XRD , the size of selenium nanoparticle was found to be similar with data obtained from (AFM) with size (18.215 nm , 19. 28 nm) respectively . Fourier Transform Infrared Spectroscopy(FTIR) spectra of SeNPs showed the present of some functional groups .

One hundred – sixty five sample of urine were collected from patients with clinical symptoms and suspected to Urinary Tract Infection (UTI) admitted in Al-Hilla teaching hospital and Public health laboratory in Babylon province during a period from (March - October) 2021 . 115(69.6%) isolates were positive culture , four type of pathogenic bacteria were diagnosed (*Escherichia coli , Enterococcus faecalis , Klebsiella pneumoniae , Staphyllococcus saprophyticus)* , most of them were resistant to antibiotics especially *Enterococcus faecalis* .

The antibacterial activity of selenium nanoparticles examined against these four pathogenic bacteria . Ten different concentrations of SeNPs (2, 4,

8, 16, 32,64,128, 256,512 and 1024 µg/ml) were used . Minimum inhibitory concentration (MIC) 32 µg/ml , Minimum bactericidal concentration (MBC) 64 µg/ml for both *Enterococcus faecalis* and *Staphylococcus Saprophyticus* , while MIC and MBC for *Klebsiella pneumoniae* and *Escherichia coli* were 64 µg/ml and 128 µg/ml , respectivily .

The synergistic effect of SeNPs was investigated with six antibiotics (Azithromycin , Ciprofloxacin , Trimethoprime / sulphamethoxazole Doxycycline , nitrofurantoin and Ampicillin) against pathogenic bacteria. The synergistic effect of Doxycycline with SeNPs in all tested bacteria that sensitive to Doxycycline were decreased , and the isolates that were sensitive to antibiotic became intermediate and intermediate became resistant to antibiotic .

Antioxidant activity of SeNPs was determined using (2,2-Diphenyl-1-picryl- hydrazyl)(DPPH) . The selenium nanoparticles had the highest antioxidant activity 39.6 % , 63.1% and 74.2 % at concentration 50, 100 and 150 µg/ml , respectivily . Selenium nanoparticles with all concentration did not show any hemolysis for the tested whole blood .

In biofilm formation assay out of all positive culture (115) isolates , 60 (52.1%) isolates gave a positive ability to form biofilm . The antibiofilm activity of selenium nanoparticles on some pathogenic bacteria formation biofilm was quantified in plate 96 well assay , The MIC of SeNPs on biofilm formation in (*Escherichia coli* and *Klebsiella pneumoniae*) was 128 µg/ml , and 64 µg/ml for *Staphylococcus Saprophyticus* and *Enterococcus faecalis* . The MICs of SeNPs against biofilm were found to be twice the MIC of planktonic state .

The cytotoxic response of prostate cancer PC3 cell line and normal hepatic WRL68 cells showed that no significant cytotoxic effect of Se NPs against PC3 cells at concentrations 25 and 50 µg/ ml . Nevertheless, Se NPs

at 100, 200 and 400 µg/mL exhibited a dose dependent decrease in PC3 cell viability with maximum inhibition rate of 51.27±2.77% of PC3 cells at 400 µg/ml. Regarding WRL68 cells, the sensitivity of the cells to SeNPs treatments was less than that of PC3.

Gene expression of virulence factor of (*Hly* , *FimH* , *Luxs* , *qsec*) genes of *E.coli* and (*ESP* , *HLY* , *gelE* , *fsrA*) genes of *E.faecalis* were evaluated by Real- time quantitive polymerase chain reaction (RT- qPCR) before and after treatment with SeNPs The results revealed that SeNPs effective on genes expression by down regulation .

The conclusion of this study found the ability of *Bacillus clausii* to synthesis of selenium nanoparticle . These SeNPs were proved to be antibacterial, antibiofilm, antioxidant, anticancer activity of PC3 and WRL 68 , and down regulation for virulence factor .

List of Contents

List of Appendices

List of Figures

List of Tables

List of Abbreviations

Abbreviation	Meaning
16S rRNA	16S Ribosomal Ribonucleic acid
AFM	Atomic Force Microscope
Akr1B10	Aldo-ketoreductase1B10
AMR	antimicrobial resistance
AST	Antibiotic Susceptibility Test
ATP	Adenosine Triphosphate
BHIB	Brian Heart Infusion Broth
CDC	Centers for Disease Control
cDNA	complementary- DNA
CLSI	Clinical and Laboratory Standards Institute
CT	cycle threshold
DMSO	Dimethyl sulfoxide
DPPH	1,1-Diphenyl-2-picrylhydrazyl
EDTA	Ethylene diamine tetraacetic acid
EDXS	Energy Dispersive X-Ray Spectroscopy
EPS	extracellular polymeric substances
EUCAST	European Committee on Antimicrobial Susceptibility Testing
FDA	Food and Drug Administration
FT IR	Fourier transform infrared spectrophotometer
GSH-Px	Glutathione Peroxidase
IDD	Iodothyronine Deiodinases
MB	Methylene Blue
MBC	Minimum bactericidal concentration
MHA	Mueller Hinton Agar
MIC	Minimum inhibitory concentration
NCBI	National center for biotechnology Information
NCCLS	national committee for clinical laboratory standards
NNI	National Nanotechnology Initiative
NP	Nanoparticle

OD	Optical density
PBS	Phosphate buffer saline
PCR	Polymerase chain reaction
RNA	Ribonucleic Acid
ROS	Reactive Oxygen Species
RPMI	Roswell Park Memorial Institute Medium
RT-PCR	Real-Time Polymerase chain reaction
Se	selenium
SeC	selenocysteine
SEM	Scanning Electron Microscopes
SeNPs	Selenium nanoparticles
SPR	Surface Plasmon resonance
TCP	Tissue Culture Plate
TNF-α	Tumor nicrosis factor - α
TR	Thioredoxin Reductase
UTI	Urinary tract infection
WHO	World Health Organization
XRD	X ray diffraction

Chapter One

Introduction

1. Introduction

Urinary tract infections (UTIs) are the most common infection in a clinical setting and the second most prevalent infection after respiratory tract infections (Bizuayehu *et al*., 2022) . Worldwide , UTIs affect about 150 million people every year (Öztürk and Murt , 2020) . In most cases the infectious agents are *Enterobacteriaceae* ,including *Escherichia coli* , *Klebsiella* sp. , *Enterobacter* sp. and *Proteus* sp., and Gram-positive bacteria such as *Enterococcus faecalis* , *Streptococcus agalactiae* and *Staphylococcus* spp . *Staphylococcus saprophyticus* is a member of the coagulase-negative staphylococci , which are commonly responsible for 5%–10% of UTIs (Gajdács *et al*., 2019) .

Bacterial resistance is the capability of bacterial cells to prevent antibiotic bacteriostatic or bactericidal effects (Munita and Arias , 2016) . Resistance of antibiotic is one of the most serious global public health issues; it has the capacity to kill 700,000 people and might rise to ten million in 2050 (Mancuso *et al*., 2021). In 2019, due to its impact on human health , the World Health Organization included antimicrobial resistance (AMR) as one of the top ten threats to global health (WHO , 2019) . According to the evidence , The rising threat of multidrug-resistant bacteria and biofilm-associated illnesses necessitates the development of new bactericidal methods . As a result, new and emerging nanoparticle-based materials in the field of antimicrobial chemotherapy have received a lot of attention (Makabenta *et al*., 2021) .

The formation of microbial biofilms enables single planktonic cells to assume a multicellular mode of growth. During dispersion, the final step of the biofilm life cycle, single cells egress from the biofilm to resume a planktonic lifestyle. As the planktonic state is considered to be more vulnerable to antimicrobial agents and immune responses, dispersion

is being considered a promising avenue for biofilm control (Rumbaugh and Sauer , 2020) . Biofilm form through a complex cascade of events that encapsulate bacteria within self-assembled (EPS) . Viscous layer that prevents the entry of chemo-therapeutic agents , leading to the recalcitrance of bacteria . Bacteria inside the biofilm are resistant to external stress and evade the host immune system Biofilm- associated tissue infections are the sole cause of nosocomial infections(Oliveira *et al*., 2022) .

Nanotechnology is a new field of study that combines nanotechnology and biotechnology to give nano science . The diameter of the nanoparticles ranges between (1-100) nm , their chemical activity , large surface area , charge density and ability to interact with the bacterial-cell enabled them to enhance the antimicrobial activity by generating reactive oxygen species or free toxic metal ions (Fardsadegh and Jafarizadeh-Malmiri , 2019 ; Alam *et al*., 2020).

Nanoparticles are manufactured by physical , chemical and biological methods. In biological methods plants , fungi and bacteria were used to prepare nanomaterials . One of the benefits of this method is that it is environmentally friendly, economical , and less toxic when compared to other methods . As for the physical and chemical methods which that used in manufacturing , they produce high radiation and toxic reducing materials , which have the ability to affect human and other living organisms (Jeevanandam *et al*., 2022 ; Parvej *et al*., 2022) .

In biological systems , Selenium nanoparticles have many nanomedicine applications due to their anti-cancer , anti-microbial and anti-oxidant properties , and the cytotoxicity of selenium nanoparticles was lower than that of silver nanoparticles (Hosnedlova *et al*., 2018) . Polymers , dendrimers , liposomes , silicon and metal NPs (Zn , Fe , Au ,

Ti , Se and others) have all been employed as effective therapeutic agents and drug delivery carriers (Anjum *et al*., 2021 ; Ikram *et al*., 2021 ; Mojarad-Jabali *et al*., 2021; Nikzamir *et al*., 2021 ; Rahimi *et al*., 2021; Motiei Pour *et al*., 2022 ; Sattar *et al*., 2022) . Because of their high stability and low toxicity , SeNPs are now widely accepted and recommended for use in a variety of scientific branches (Gunti *et al*., 2019) .

Bacillus have the obvious benefit over other prospective probiotics in that they can be generated easily and economically effectively by drying and last well through shelf life. They will also survive gastric acidity and make it into the intestine, the rumored location of action (Upadrasta *et al*., 2016) . *Bacillus clausii*, a spore-forming probiotic, is able to colonize the gut. It is a rod-shaped, nonpathogenic, aerobic, Gram-positive bacterium, able to survive transit through the acidic environment of the stomach and colonize the intestine even in the presence of antibiotics (Bordea , 2020) .

The present work aims to biosynthesis of selenium nanoparticles by non-pathogenic bacteria , and then study the antibacterial , antioxidant , haemolysis , anticancer activity of SeNPs and finally study the action mode of selenium nanoparticles on pathogenic bacteria by the following :

- Biosynthesis of selenium Nanoparticles by *Bacillus clausii* and purification partially .
- Characterization of biosynthesized selenium Nanoparticles by UV-visible spectrophotometer, FESEM, EDS , XRD, AFM and FTIR .
- Antibacterial activities of selenium Nanoparticles against bacteria that caused UTI infections.

- Detection the antibiotics susceptibility test and the synergetic effect of SeNPs with antibiotic against gram negative and gram positive bacteria .
- Anticancer activity of SeNPs aganist PC3 cell line and cytotoxicity against WRL 68 cell line .
- Biological assay of selenium nanoparticle such as antibiofilm , antioxidant and hemolysis
- Measurement the gene expression of gene encoding to hemolysin, attachment, biofilm production and biofilm regulation with and without selenium nanoparticles .

Chapter Two

Literature Review

2. Literature review

2.1 Urinary tract infection

Urinary tract infection (UTI), the second-ranked infectious diseases, are recognized as a big concern relating to global healthcare systems (Behzadi and Behzadi , 2017) . UTIs are known as multi-microbial infectious diseases, which can be happened by bacteria (Gram-positive and/or Gram-negative strains) and fungi. Among Gram-negative bacteria, the member of Enterobacteriaceae , in particular, *Escherichia coli* and *Klebsiella pneumoniae* are the most common uropathogenic bacterial agents, which may cause different types of UTIs (Behzadi , 2018) .

Furthermore G $^{-ve}$ bacteria , including Streptococci , Staphylococci and Enterococci, are involved in UTIs in humans . On the other hand, fungi and particularly *Candida albicans* strains may act as opportunistic pathogenic fungi for causing UTIs. However, the non - *C. albicans* such as *C. glabrata* and *C. tropicalis* are reported from some countries as the predominant species of the causative agents of UTIs (Okojie and Omorokpe , 2018) .

There are different types of UTIs including acute and/or chronic, asymptomatic and/or symptomatic (mild/moderate and/or severe), complicated and/or uncomplicated, and community and/or nosocomial acquired infections . If the UTIs occur ≥ three times in a year or ≥ two times continuously after disappearance (treatment) of the first infection in a half year, they are recognized as recurrent UTIs (rUTIs) (Johansen *et al*., 2016) .

In addition to this diversity, as the human's urinary tract is divided into two parts of lower and upper sections, the UTIs may occur in the lower part of the UT (known as cystitis) and/or upper part of the UT (known as nephritis) . These characteristics are in association with microbial pathogenomics, duration of infection , and the abilities of human host (Foxman, 2010) .The threshold of microbial population for UTIs is reported as ≥100,000 living cells or colony-forming unit (CFU) per urine milliliter (ml); however, it varies from 100 to 1000 to 100,000 CFU/ml. Of course, the UTIs without syndromes and with syndromes are recognized as asymptomatic and symptomatic UTIs, respectively (Jepson *et al*., 2012) .

2.2 Nanomaterials

The term nanometer was first used in 1914 by Richard Adolf Zsigmondy . The American physicist and Nobel Prize laureate Richard Feynman introduced the specific concept of nanotechnology in 1959 in his speech during the American Physical Society's annual meeting . This is considered to be the first academic talk about nanotechnology (Zafar , 2022) . Due to the nanoscale dimension , nanomaterials exhibit exceptional properties that differ from those of their bulk counter parts (Baig *et al*., 2021) .

Medical nanotechnology uses materials with nano range size, which is generally1–100 nm . These materials are applied in the design , fabrication , regulation , and application of therapeutic drugs or devices (Ali *et al*., 2021) . Typical nanomaterials possess several common characteristics : high surface-to-volume ratio , enhanced electrical conductivity , superparamagnetic behavior , spectral shift of optical absorption , and unique fluorescence properties . In the medical field , nanomaterials can be applied in drug transportation , increased

permeability enabling crossing through biological barriers and improved biocompatibility are also noticeable features (Nayak *et al*., 2021) . The high surface-to-volume ratio of some nanomaterials can assemble with biomolecules or residues , which can enhance the specificity of chemical drug complex in targeted therapy , thereby enhancing the efficacy of nanomaterial-based treatment while reducing its toxicity to normal cells (Cheng *et al*., 2021) .

Many researchers have used the term nanomaterial if the size is a few nanometers or smaller than a few tens of nanometers , whereas others have even used the term nanomaterial for anything less than a micrometer (Baig *et al*., 2021) .

The physical and chemical properties of nanomaterials depend upon their precise composition , shape , and size . The effects of nanomaterial on health and the environment also depend upon their size, shape, etc. A single internationally accepted definition of nanomaterials is challenging to find , and a rigorous definition of nanomaterials is still under discussion in the scientific community (Patel *et al*., 2021).

2.3 Nanoparticle synthesis approaches

The nanomaterials prepared through two basic methods :first **(Top-down)** systems: where tiny manipulations of little number of atoms or molecules fashion elegant patterns, through mechanical- physical methods like grinding, milling and crushing for producing nanoparticles, this method was used for producing Nano composites and Nano-grained bulk materials like metallic and ceramic nanomaterials in extensive size distribution (10 - 1000 nm) , while second method was **(Bottom-up)** system , numerous molecules were self-assembled in parallel steps, as a function of their molecular recognition characters, this processing produced more complex structures from atoms or molecules, also, this

method produce a uniform controlling sizes, shapes and size ranges of nano materials , figure (2.1) (Abobatta , 2018) .

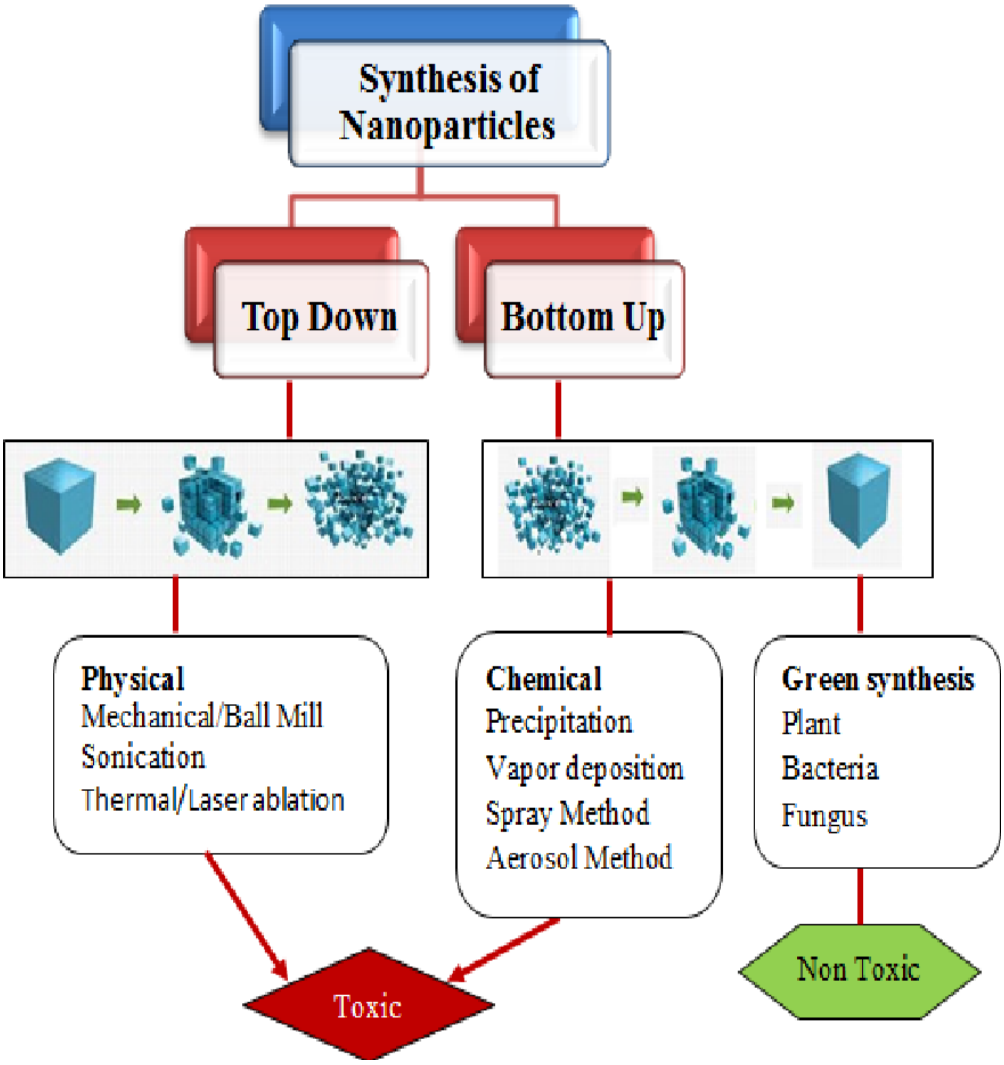

Figure (2.1): Schematic diagram for top-down and bottom – up synthesis of nanoparticle (Chaudhari and Nikam, 2018) .

Nanoparticles can be synthesized by several methods such as physical ,chemical and biological method. The nanoparticles can be synthesized using the top-down in physical approach and bottom-up in chemical and biological approach (Saleh , 2021). Different types of physical and chemical methods are employed for the synthesis of nanoparticles but the use of these methods requires both strong and weak chemical reducing agents and protective agents which are mostly toxic,

flammable, cannot be easily disposed due to environmental issues and , a low production rate and elevated temperatures for synthesis process in addition these are capital intensive and are inefficient in materials and energy use (Rahimi and Doostmohammadi, 2019).

Although the chemical and physical methods are able to produce small quantities of nanoparticles with a defined size and shape in a relatively long time, they are complicated, outdated, costly, inefficient and produce hazardous toxic wastes that are harmful not only to the environment but also to human health (Murugesan *et al*., 2019 ; Kumar and Prasad , 2021) .

The biological method for the synthesis of nanoparticles employs biological agents such , fungi (Zhang *et al*., 2019) , bacteria (Alam *et al*., 2020) , actinomycetes (Ranjitha and Ravishankar , 2018) , and plant extracts (Pyrzynska and Sentkowska , 2021) . The biological agents secrete a large amount of enzymes, which are capable of hydrolyzing metals and thus bring about enzymatic reduction of metals ions (Das *et al*., 2017) . Moreover, leaf extracts , seed extracts , root extracts , bulbs , and latex of plants were used to synthesize gold , silver, and palladium nanoparticles (Azizi *et al*., 2014) Biological materials such as honey, starch, and ascorbic acid were used to synthesize gold , silver , palladium, carbon, and platinum nanoparticles (Reddy *et al*., 2012) .

The purpose of highlighting the biological synthesis of nanoparticles was because of its easiness of rapid synthesis, controlled toxicity, controlling size characteristics, reasonable, and ecofriendly approach (Ingale and Chaudhari , 2013) . Biological method of nanoparticles synthesis would help to remove harsh processing conditions by enabling the synthesis at physiological, temperature, pressure, and at the same time at lower cost. One of the options to achieve this goal is to use microorganisms to synthesize nanoparticles (Ndwandwe *et al*., 2021).

2.4 Characterization of nanoparticles

2.4.1 UV-visible Spectroscopy

The technique of spectrophotometry is generally used for the qualitative and quantitative estimation of biomolecules such as proteins, sugar, carbohydrates, amino acids, nucleic acids and vitamins. UV–visible spectroscopy has proven to be extremely useful for analyzing various nanoparticles like : selenium , gold , silver , etc (Anderson *et al*., 2019 ; Hashem and Salem , 2022). The observation of high large surface plasmon peaks at visible regions (400–600 nm) for different metal nanoparticles with sizes varying from 2 to 100 nm has been well reported. A UV–visible spectrophotometer is made up of two parts: a spectrometer for producing light of various wavelengths and a photometer for measuring light intensity(Zayed *et al*., 2019).

2.4.2 Scanning electron microscopy (SEM)

Scanning electron microscopy (SEM) offers the topographical and elemental knowledge of NPs with an almost infinite field depth for useful amplifications. In the evaluation of elementary structure, grain size, roughness of the surface , porosity, distribution of dimensions, homogeneity, inter-metal distribution and diffusion of NP, scanning electron microscopy can also be used (Van Malderen , 2017).

The mechanism of action is based on the passage of finely focused scanned electron beam across the surface of the sample; this generates backscattered electrons, secondary electrons, and characteristic X-rays. When collected by detectors, These signals form images of the scanned sample displayed on a cathode ray tube screen(Goldstein *et al*., 2017).

2.4.3 Energy-Dispersive X-ray Spectroscopy (EDX)

Energy dispersive spectroscopy investigates surface analysis and elemental characterization of the sample. Basic principle involves the

study of the emitted X-rays of different energies coming from the sample when a beam of electron strikes its elements. The amount and composition of metal nanoparticles can be easily identified from the surface of the given sample (Shirley and Jarochowska , 2022).

The rays issued have been observed and their energy analysed. Since the energy of x-rays is distinctive for any aspect, it could be used to analyze the sample components(Shahbaz *et al*., 2022).

2.4.4 Atomic force microscope(AFM)

Atomic force microscopy (AFM) is a tool of exceptionally high resolution that can be used to study the morphology of a sample as well as quantify its mechanical properties at atomic resolution (Wang *et al*., 2021). AFM employs a microscopic physical probe to "grope" the microcosm and analyze the morphology of the sample under study in three-dimensional space, extracting information from the very slight interaction between the probe and the sample surface. AFM images can be collected in an aqueous medium, making it an important method of studying the action of nanoparticles in a biological context (Deng *et al*., 2018) .

The functionalized probe can be used to classify individual molecules or interactions powers like ligand-receptor interactions. As a result, AFM has a good future in biomedicine and clinical medicine, especially in cancer diagnosis and treatment. Cell dynamics is an important biomarker for identifying cell states(Wang *et al*., 2016).

2.4.5 X-ray diffraction (XRD)

The X Ray Crystallography is a strong technique for the analysis of the three-dimensional structure of macromolecules like protein or nucleic acids in the crystal phase. The technology is also known as a method of radiation diffraction (Spiliopoulou *et al*., 2020). There are many methods

for the three-dimensional structure analysis , the most effective methods was x-ray crystallography. Along with amorphous compounds such as polymers, X-ray diffraction is used to determine the atomic arrangements and thickness of thin films (Maveyraud and Mourey, 2020).

Two steps are involved in the use of the microscope. At the beginning , light is incident on the target and is diffracted in a variety of directions , then the lens captures and reassembles the diffracted rays to create an image . X-rays was used to detect diffraction from molecules , and a screen to reassemble the picture (Oake *et al*., 2019).

2.4.6 Fourier Transform Infrared Spectroscopy (FTIR)

FTIR technique is a vibrational spectroscopic technique that has various uses in the study of excavated textiles. For organic compounds, molecular vibrations result in the formation of distinct absorption bands in the spectra, which may aid in their detection (Hospodarova *et al*., 2018) **.**

FTIR is used to assess the heterogeneous structure and surface behavior of materials by gathering data on the maximum values at particular lambda values in absorption and reflection spectra. A Fourier transform (mathematical operation) is used to convert the data collected from all wavelengths traveling through the sample to the real spectrum. The FTIR technique is used to study the vibrational structures of solids(Chen *et al*., 2015).

2.5 Selenium

Selenium (Se) is an essential dietary trace element which presents in human beings (Fang *et al.*, 2018). Selenium which is a building block of the selenocysteine, that mainly involved in the synthesis and catalytic function of selenoproteins such as peroxidases and reductases (Hadrup *et al*., 2016) .

Many selenoproteins believed to be having oxidoreductase activity which plays an important role in regulation of the physiological redox balance. Due to the narrow therapeutic window and toxicity margins , selenium is widely replaced by the selenium nanoparticle which is believed to be having a wide therapeutic window and reduced toxicity which is also having the optimized body distribution (Khurana *et al*., 2019).

Selenium is a metalloid having different oxidation states : selenium (0) , selenide (-2), selenite (+4), and selenate (+6) , inorganic selenium mainly founds in the soil , while organic selenium mostly founds in soil, air and plants . Presently there are 25 selenium proteins which are known to play a role as antioxidants, with selenite, selenomethionine, methylselenocysteine and selenocysteine are the compounds which are mostly studied , because of their application in disease prevention and therapy. Many Studies revealed that the elemental selenium is less toxic and preferential biological activity compared with its other forms (Maiyo and Singh , 2017) .

The elemental selenium mainly involved in the antioxidant defines system that play a vital role in protecting against oxidative stress. In several studies they showed that the Selenium can upregulates the level of enzymes such as Glutathione peroxidase (GPx) , with the supply of Selenium and reducing the cellular damage by preventing the accumulation of free radical species . Se^0 is believed to be having more attention due to its low toxicity and more bioavailability when compared with Se (4) and Se (6), meanwhile they both have free radicals capturing ability (Kondaparthi *et al*., 2019) .

It is difficult to apply of selenium in food and medicine fields because of its poor water solubility and their ability to convert into a grey analogue . The water solubility of the selenium nanoparticle can be

enhanced by reducing their size and increasing their surface area with application of the nanotechnology (Zhai *et al*., 2017) .

The selenium can improve the cell mediated immune responses when it is supplied in the form of sodium selenite to head and neck cancer patients during radiation and surgery. The selenoproteins are required for the normal function of the activated T cells and the T cells are sensitive to Reactive Oxygen Species (ROS) when the deficiency of selenoproteins occurs, it leads to ROS elevation, so selenoproteins, cannot proliferate in response to the T cell receptor stimulation. Selenium depletion leads to irreversible brain injury. The Selenium can deliver to brain by specific selenoprotein called selenoprotein P , which is believed to be improving the neuronal survival and also prevent cell death caused by beta-amyloid accumulation (Solovyev *et al*., 2018) .

2.6 Nano-selenium

Nano-Se could be defined as nano-elemental selenium or nano-Se manufactured for use in nutritional supplements and developed for applications in medical therapy (Hu *et al*., 2012) . It is bright red, highly stable, and of nano-size in the redox state of zero (Se^0). Nano-Se has a higher efficiency in upregulating selenoenzymes and exhibits less toxicity than selenite (Hosnedlova *et al*., 2018).

From three allotropes of Se^0 , the gray and the black ones are biologically inert, which is due to their insolubility (El-Ramady *et al*., 2014) . A variety of bacteria , fungi and plant extracts have been used to synthesize Se nanoparticles of different size and morphology (Kimura *et al*., 2014 ; Sharma *et al*., 2014 ; Srivastava and Mukhopadhyay, 2015) .

Biogenic Se nanoparticles could be synthesized from Se salts especially selenite and selenates in the presence of reducing agents (biomolecules) such as phenols, alcohols, proteins, and amines. These previous biomolecules can be used to reduce Se salts in vitro, but the by-

products released in the environment may be hazardous to flora and fauna (Husen and Siddiqi , 2014).

2.7 Therapeutic applications of SeNPs

Based on the improved properties of SeNPs over Se, they have been explored in various disease conditions. SeNPs offer improved bioavailability with the added advantage of decreased toxicity. The pro-oxidant, as well as the antioxidant effects provide different avenues for exploration in a variety of pathological conditions. Some studies focused on the role of SeNPs as antimicrobial , antioxidant , anticancer agent , in drug delivery , in reducing inflammation (Jolly *et al*., 2020) .

2.7.1 Role of SeNPS as antimicrobial

SeNPs possess the antimicrobial activity thus inhibiting the growth of microbes such as bacteria, fungi, and viruses. Biologically synthesized SeNPs (from bacterium *Ralstonia eutropha*) has been showed to possess antimicrobial activity at a concentration of 100, 100, 250, and 100 µg/mL by inhibiting 99% growth of *Pseudomonas aeruginosa, Staphylococcus aureus, Escherichia coli*, and *Streptococcus pyogenes* respectively. Furthermore, it has been observed that SeNPs at a concentration of 500µg/mL inhibits the growth of pathogenic fungi *Aspergillus clavatus* (Srivastava and Mukhopadhyay, 2015) .

Lactobacillus plantarum and *Lactobacillus johnsonii* reduced selenium dioxide to cell-associated elemental selenium nanoparticles. The cell-free spent culture media, from both *Lactobacillus* species that had been grown with selenium dioxide for 48 h, showed enhanced antifungal activity against *Candida albicans* (Kheradmand *et al*., 2014) . The antiviral activity of SeNPs has been investigated on H1N1 influenza virus and was found that the combined use of oseltamivir and amantadine-

loaded SeNPs strongly inhibits the generation of ROS and activation of p53 phosphorylation and AKT (Li *et al*., 2017 ; Li *et al*., 2018) .

2.7.2 Role of SeNPS as antioxidant

Selenium was playing an important role in forming selenoproteins that help synthesize glutathione peroxidase enzymes . More specifically, Selenium nanoparticles are noted to upregulate the expression of peroxidase (GPx) by forming selenophosphate (Kondaparthi *et al*., 2019). ROS such as superoxide anion (O_2^-), 1,1-diphenyl-2-picrylhydrazyl, singlet oxygen ($^1O_2$) , and carbon-centered free radicals were scavenged by Selenium NPs (Kumar and Prasad , 2021) . According to some studies, the activity of glutathione peroxidase (GSH - Px) in the liver of weanling pigs increases significantly when the animals are fed a Nano-Selenium diet (concentration range of 0.50 and 1.0 mg/kg) instead of an inorganic form of selenium (Zhang *et al*., 2007) .

Another study found that Nano-Selenium protects against acetaminophen (APAP) which induced hepatotoxicity by improving liver function and oxidative stress mediated by catalase, SOD, and GSH, as well as decreasing hepatic DNA fragmentation and hepatic biomarker of cell death (Amin *et al*., 2017). Similarly, Selenium NPs protect against K2Cr2O7-induced thyroid damage by correcting free T3 and T4 levels as well as GSH, catalase, SOD, and MDA levels (Khurana *et al*., 2019) .

2.7.3 Role of SeNPS as an anticancer agent

The anticancer property of SeNPs is due to that selenium inducing glutathione S-transferase (GST) (Wang *et al*., 2007) . SeNPs mitigates the problems of drug resistance and toxicities connected with chemotherapeutic agents. SeNPs have the potential to suppress the growth of cancer cells via the induction of cell cycle arrest at S phase (Luo *et al*., 2012) .

Cancer cells selectively incorporate SeNPs via endocytosis, and then these SeNPs induces the apoptosis of cancer cell by triggering apoptotic signal transduction pathways (Hosnedlova *et al*., 2018) . SeNPs have been observed to inhibit the growth of prostate LNCaP cancer cells moderately via caspases mediated apoptosis *in vitro* (Kong *et al*., 2011) . Furthermore, it has been observed that SeNPs, along with *Lactobacillus Brevis*, stimulates the immune response via enhancing the production of interferon and delayed-type hypersensitivity response in a metastatic breast cancer mice model (Yazdi *et al*., 2012) .

Introduction of biologically synthesized SeNPs (concentration as low as 2 μg Se·mL-1) were competent enough to suppress the proliferation and induce caspase-independent necrosis in human prostate adenocarcinoma cells (PC3) (Sonkusre *et al*., 2014) . In addition to their anticancer potential alone, SeNPs when used in combination with 5-Flourouracil (5-FU) has been shown to enhance the anticancer potential of the drug in A375 human melanoma cells . Figure (2.2) demonstrates the mode of SeNPs action as an potential anticancer agent and carrying out the apoptosis (Jolly *et al*., 2020) .

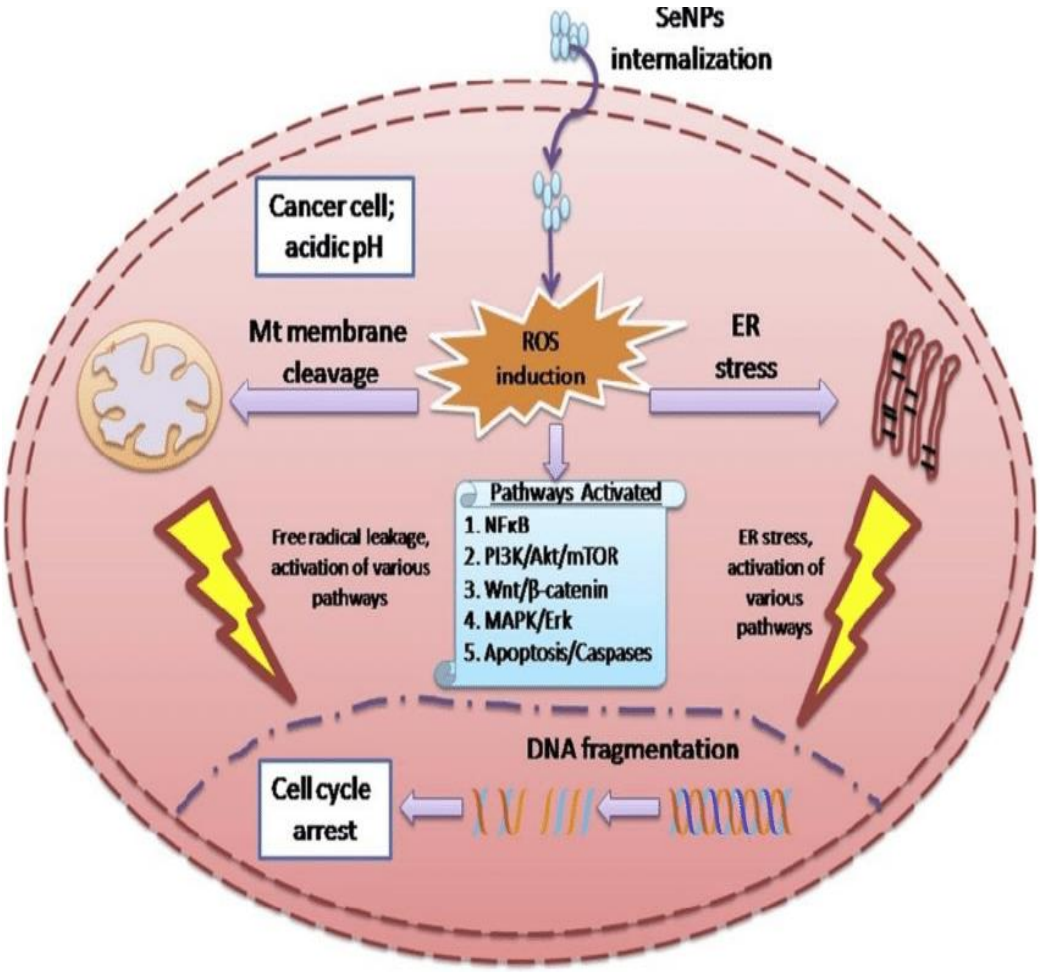

Figure (2.2) : The mechanism of SeNPs as an anticancer agent (Nayak *et al.*, 2021) .

2.7.4 Role of SeNPs in drug delivery

SeNPs have been used as a drug delivery system for anticancer drugs/agents, for active immunization via carrying antigens and also for genes to the appropriate site , figure (2.3) (Khurana *et al.*, 2019) . The selective/effective uptake and drug accumulation at the target site are possible because of the nanosize of these particles. SeNPs have been found to deliver siRNA against specific oncogenic gene (Sonkusre *et al.*, 2014) .

The usage of several surface decorators increases the cellular uptake and anticancer potential of nanoparticles (Yang *et al.*, 2012). SeNPs were functionalized with *Spirulina* polysaccharides (SPS) , SPS

surface decoration markedly increased the cellular uptake and cytotoxicity of SeNPs against various cancer cell lines. The SPS-SeNPs was observed to suppress the growth of cancer cell via apoptosis, as manifested by an increment of the sub-G1 cell population, fragmentation of DNA, condensation of chromatin, and translocation of phosphatidyl-serine (Li *et al.*, 2016) .

Many research reported that polyamidoamine dendrimer-modified SeNPs efficiently deliver the siRNA and cisplatin to A549/DDP cells for reversal multidrug resistance. This combination induces apoptosis of cells via PI3K/Akt/mTOR and MAPK/ERK pathways in A549/DDP cells . Furthermore, SeNPs has proved to be as a carrier for the delivery of doxorubicin for targeting breast cancer with lesser toxicity and improved anticancer potential (Yang *et al* ., 2012 ; Zheng *et al*., 2015) .

The delivery of siRNA using RGDfC-conjugated functionalized SeNPs is successful against liver carcinoma (Xia *et al*., 2017) . It activates Wnt/β-catenin signaling and sparks Bcl-2 mediated apoptosis (Zhao *et al*., 2017) .

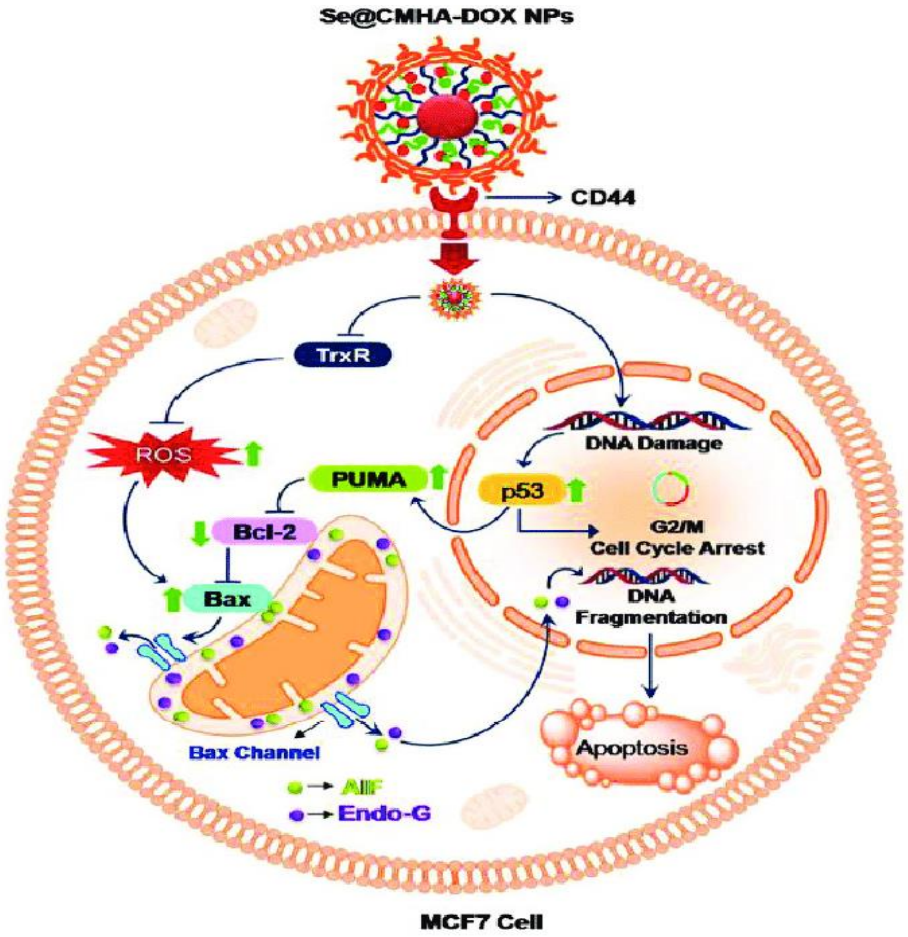

Figure (2.3) : Role of SeNPs in drug delivery (purohit *et al.*, 2017)

2.7.5 Role of SeNPS in reducing inflammation

Inflammation is the earliest step in the onset of a disease/injury leading to accretion of body fluids, white blood cells and release of prostaglandins and several inflammatory mediators (Ricciotti and FitzGerald , 2011). The nuclear factor kappa-B (NF-κB) signaling pathway has been associated with enhanced inflammatory response and its activation has been significantly correlated with interleukin-6 and TNF-α production. Selenium may inhibit the activation of NF-κB by modulating selenoprotein genes expression , figure (2.4) (Duntas , 2009) .

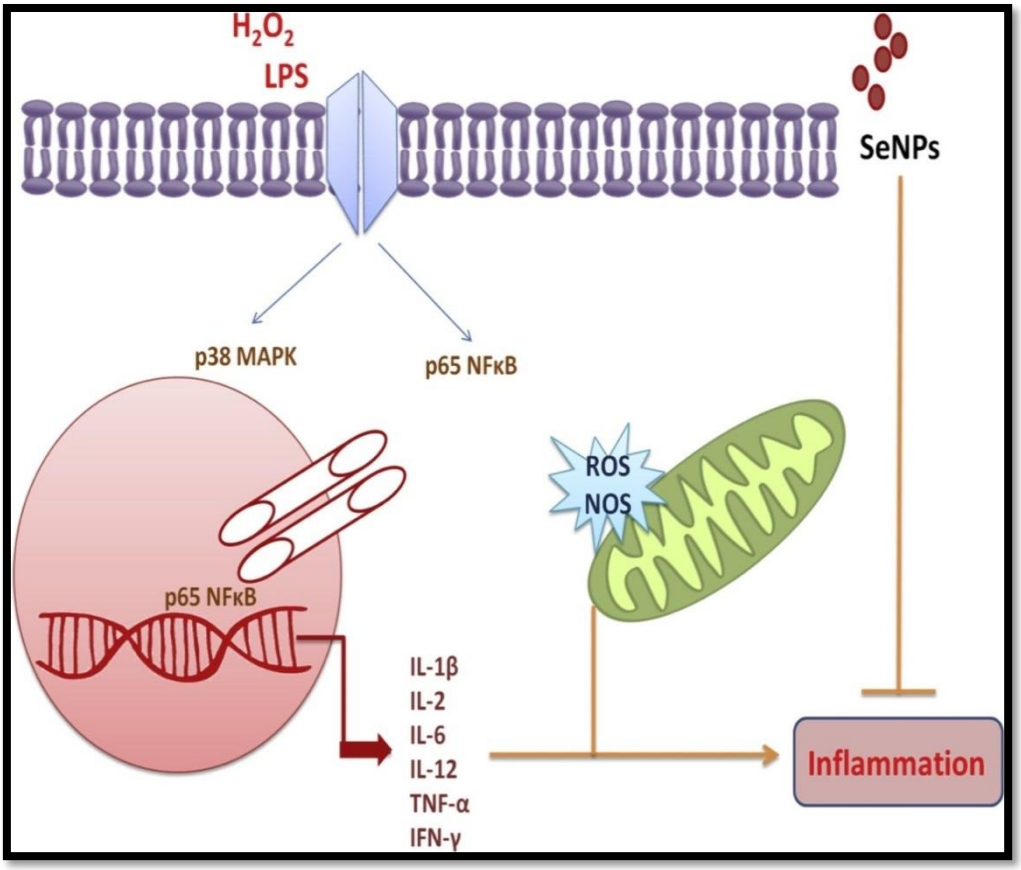

Figure (2.4) : Anti-inflammatory effects of SeNPs (Khurana *et al.*, 2019) .

It has been observed that SeNPs decorated with Ulva lactuca polysaccharide (ULP) (ULP-SeNPs) significantly inhibited the proinflammatory cytokines (IL-6 and TNF-α) and the nuclear factor kappa-B(NFκB) signalling in dextran sodium sulphate induced colitis (Zhu *et al.*, 2017) . Similarly, it has been recently found that SeNPs decreases the expression of genes of pro inflammatory mediators like tumor necrosis factor-α (TNF-α), prostaglandin E_2 ($PGE_{2)}$ and thiobarbituric acid reactive substances (TBAR) in inflammation induced irradiated rats (El-Ghazaly *et al.*, 2017) .

Administered of melatonin-SeNPs (MT-se) at doses of 5, 10, or 20 mg/kg to Bacillus Calmette–Guérin (BCG)/lipopolysaccharide (LPS) (BCG/LPS) treated mice for 10 days, significantly reduced the increase in plasma aminotransferase, reduced the severe extent of hepatic cell

damage and the immigration of inflammatory cells. The MT-Se particles also attenuated the increase in the content of thiobarbituric acid-reactive substances and enhanced the decrease in reduced activities of superoxide dismutase and glutathione peroxidase (GPx). However, treatment with MT-Se suppressed the increase in nitric oxide levels both in plasma and liver tissue. Furthermore, supplementation with MT-Se at the dose of 10 mg/kg (composed of 9.9 mg/kg melatonin and 0.1 mg/kg selenium) had great capability to protect against hepatocellular damage than a similar dose of melatonin (10 mg/kg) or selenium (0.1 mg/kg) alone. This effect may relate to its higher antioxidant efficacy in decreasing lipid peroxidation and increasing GPx activity (Wang *et al*., 2005) .

2.8 Nutritional sources of selenium

Dietary selenium comes from meat, nuts, cereals and mushrooms. Brazil nuts are the richest dietary source (though this is soil-dependent, since the Brazil nut does not require high levels of the element for its own needs) (Junior *et al*., 2017) .The US Recommended Dietary allowance of selenium for teenagers and adults is 55 μg/day (Ghimire *et al*., 2019) . Selenium as a dietary supplement is available in many forms, including multi-vitamins/mineral supplements, which typically contain 55 or 70 μg/serving . Selenium-specific supplements typically contain either 100 or 200 μg/serving (Constantinescu-Aruxandei *et al*., 2018 ; Trüeb , 2020).

In June 2015, the US Food and Drug Administration (FDA) published its final rule establishing there quirement of minimum and maximum levels of selenium in infant formula (FDA , 2015) .The selenium content in the human body is believed to be in the 13–20 mg range (Aliasgharpour and Rahnamaye Farzami , 2013) .

2.9 High and Low level of Selenium

Although selenium is an essential trace element, it is toxic if taken in excess. Exceeding the tolerable upper intake level of 400 micrograms per day was considered harmless and lead to selenosis (Krohn *et al*., 2016). This 400 μg tolerable upper intake level is based primarily on a 1986 study of five Chinese patients who exhibited overt signs of selenosis and a follow up study on the same five people in 1992(Krinsky *et al*., 2000).

Se concentration in edible parts of main crops ranged from 0.005 mg kg^{-1} to 4.17 mg kg^{-1}, and cereal plants had a higher Se-enrichment ability than tuber plants. The probable dietary intake of Se in high-Se areas was decreased to 959.3 μg d^{-1} in recent years, which might be attributed to tap water as drinking water in recent year rather than well water-dependent and changes in dietary structure, but still far above the permissible value of 400 μg d^{-1} (Lyu *et al*., 2022) .

Serum selenium showed limited association with consumption of locally produced foods, while pulses and vegetables, along with cereals and pulses, were associated with higher hair and nail selenium contents, respectively. Association of a number of adverse health endpoints with serum and hair selenium was stronger than for nail selenium contents. Such endpoints included higher prevalence of nausea and vomiting, bad breath, worm infestation, breathlessness exert and bad breath, chest pain, hair and nail abnormalities and loss, garlic odor, edema, spontaneous abortion, and overall selenosis. In contrast, we gathered no evidence of dermatitis or loss of appetite in residents most exposed to selenium (Chawla *et al*., 2020) .

Elemental selenium and most metallic selenides have relatively low toxicities because of low bioavailability (Garousi, 2015) . Arsenic (As) and cadmium (Cd) are elements arousing major public health

concerns associated with environmental pollution, high toxicity potential, and carcinogenic nature. However, selenium (Se) at low doses and incorporated into enzymes and proteins has antioxidant properties and protects animals and humans from the risk of various diseases . In general, recent reports show that Se, regardless of its form (as selenite, selenomethionine, nanoSe, or Se from lentils), can reduce As- or Cd-mediated toxicity in the liver, kidney, spleen, brain, or heart in animal models and in cell culture studies. Se antagonizes the toxicity of As and Cd mainly through sequestration of these elements into biologically inert complexes and/or through the action of Se-dependent antioxidant enzymes (Zwolak , 2020) .

Hydrogen selenide is an extremely toxic, corrosive gas. Selenium also occurs in organic compounds, such as dimethyl selenide, seleno-methionine, seleno-cysteine and methylseleno-cysteine, all of which have high bioavailability and are toxic in large doses (Fan and Vinceti , 2015). Biomarkers of Se status decline strongly in pregnancy, severe illness, or COVID-19, reaching critically low concentrations. Notably, these conditions are associated with an increased risk for autoimmune disease (AID). Positive effects on the immune system are observed with Se supplementation in pregnancy, autoimmune thyroid disease, and recovery from severe illness (Schomburg , 2021) .

Selenium deficiency, defined by low (<60% of normal) selenoenzyme activity levels in brain and endocrine tissues, occurs only when a low selenium level is linked with an additional stress, such as high exposures to mercury or increased oxidant stress from vitamin E deficiency (Ralston and Raymond , 2010) .

Selenium interacts with other nutrients, such as iodine and vitamin E , and other minerals, such as zinc and copper (Mann and Truswell , 2017) . High doses of Se supplements in pregnant animals might disturb

the Zn:Cu ratio and lead to Zn reduction; in such treatment cases, Zn levels should be monitored. Further studies are needed to confirm these interactions (Kachuee *et al*., 2013) .

2.10 *Bacillus clausii*

Classification

Kingdom ; (Eubacteria)

Domain ; (Bacteria)

Phylum ; (Firmicutes)

Class ; (Bacilli)

Order ; (Bacillales)

Family ; (Bacillaceae)

Genus ; (*Bacillus*)

Species ; (*clausii*)

Bacillus clausii is a gram-positive, the cell wall is made up of the peptidoglycan murien , spore forming rod , *B. clausii* cells tend to line up into chain-like formation ,observable as a long rod cell. *B. clausii* is an endospore producing microbe that creates ellipsoidal spored located sub-terminally or para-centrally in the sporangium , widely used as probiotic (Paparo *et al*., 2020) .

Probiotics have been used for hundreds of years to treat different diseases. They have been used since the 1960s to treat viral diarrhea in children and the side effects of antibiotic administration (Jayanthi and Sudha , 2015) . Antibiotic-associated side effects with Clostridioides difficile diarrhea are well known scenarios , therefor probiotics were proven to be efficient in treatment (Guarino *et al*., 2015) .

Recent research on safety of *Bacillus clausii* administration has concluded that it has intrinsic resistance mechanisms to some antibiotics (e.g. macrolides) , but it does not have toxin producing genes or transferrable antimicrobial resistance, making it very safe (Upadrasta *et*

al., 2016 ; Lakshmi *et al*., 2017). Since then, several studies have been carried out demonstrating no related side effects linked to its use (Sudha *et al*., 2013).

Side effects have been inconsistently reported and have not been adequately assessed. In spite of this, according to the World Health Organization, probiotics might be responsible for systemic infections and deleterious metabolic activities (Doron and Snydman , 2015) .

B. clausii was found to be resistant to broad-spectrum antibiotic chloramphenicol, anti-mycobacterial rifampicin, beta-lactamase inhibitor amoxiclav, first-generation antibiotic cefaloridine, penicillin ampicillin, and tetracycline. *B. clausii* was resistant to both the aminoglycoside antibiotics (streptomycin and kanamycin) . Off first-generation fluoroquinolones studied, *B. clausii* was resistant to ciprofloxacin but partially sensitive to norfloxacin, ofloxacin and to macrolide azithromycin (Srinivas , 2020) .

Spores of *Bacillus* are heat stable, capable of surviving the low pH of the gastric barrier, additionally products made on them can be stored at room temperature without any deleterious effect on viability (Abbrescia *et al*., 2014) .

2.11 Mechanism of resistance to antibiotics

The treatment of infections is increasingly complicated by the ability of bacteria to develop resistance to antibiotics. Bacteria may be intrinsically resistant to one or more classes of antibiotics, or may acquire resistance by de novo mutation or by the acquisition of resistance genes from other organisms. Better understanding of mechanisms of antibiotic resistance would allow the development of control strategies to reduce the spread of resistant bacteria and their evolution. Bacteria may be intrinsically resistant to a class of antibiotics or may acquire resistance

(Sartelli *et al*., 2016) . Main mechanisms of resistance to antibiotics that illustrated in figure (2.5) can be caused by :

- inactivation of the antibiotic through hydrolysis or modification
- an alteration or the protection of the target site of the antibiotic that reduces its binding capacity
- the modification of metabolic pathways to circumvent the antibiotic effect
- the reduced intracellular antibiotic accumulation by decreasing permeability and/or increasing active efflux of the antibiotic from the cell by a series of membrane-associated pumping proteins .

Bacteria can develop resistance to antibiotics by mutating existing genes (vertical evolution) or by acquiring new genes from other strains or species (horizontal gene transfer) (Kapil *et al*., 2020) . Many of the antibiotic resistance genes are carried on genetic elements (plasmids, transposons or phages) that act as vectors that transfer these genes to other members of the same bacterial species, as well as to bacteria in another genus or species (Bag *et al*., 2019) .

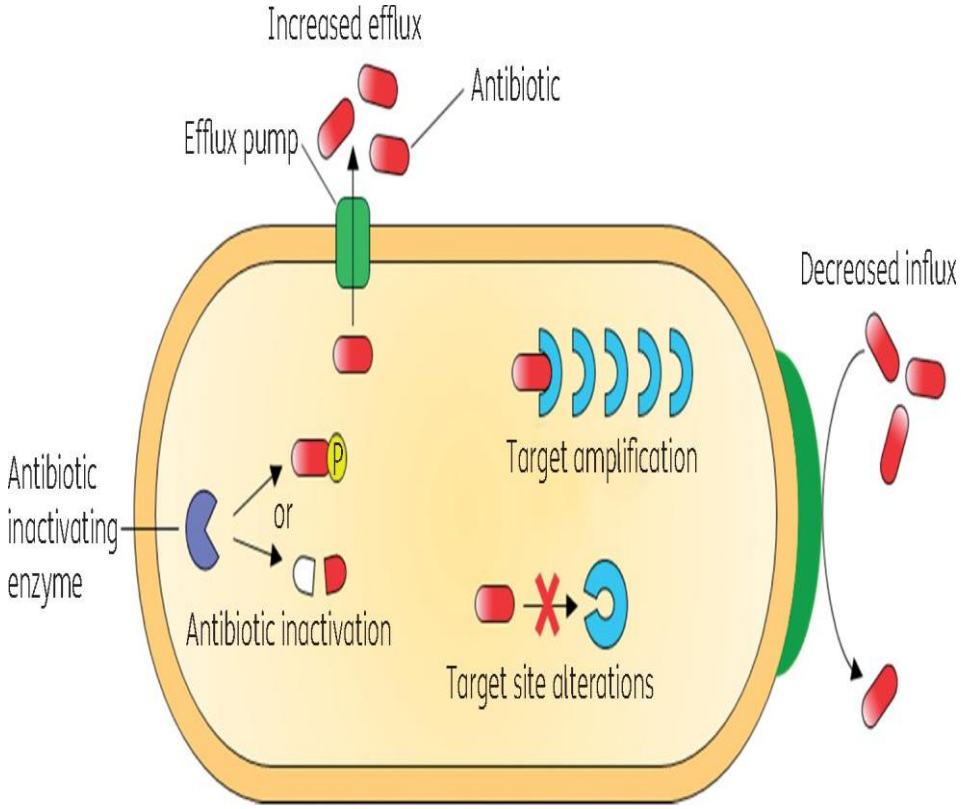

Figure (2.5) : Antibiotic resistance mechanisms of bacteria (Alav *et al*., 2018).

2.12 Antimicrobial Action Mechanisms of SeNPs

Antimicrobial activity of SeNPs, alone or in combination with standard antibiotics , has been tested against a wide range of microorganisms, including Gram-negative , Gram-positive bacteria, and fungi (El-Deeb *et al*., 2018 ; Medina Cruz *et al*., 2018) . However, studies are rare about the mechanisms of antimicrobial action of these nanoparticles. In general, it has been proposed that some nanoparticles can follow three mechanisms: (i) cell wall and membrane damage, (ii) intracellular penetration, and (iii) oxidative stress(Sánchez-López *et al*., 2020 ; Zhang *et al*., 2021) .

2.12.1 cell wall and membrane damage

Cell wall and membrane components could be involved in different adhesion pathways for nanoparticles. One of the functions of the cell wall and membrane is to protect the microorganism against environmental

threats while maintaining its homeostasis, allowing nutrients transport within the cell . The cell wall of Gram-negative bacteria has a thin layer of peptidoglycan with an additional outer membrane consisting of lipopolysaccharide. On the other hand, the cell wall of Gram-positive bacteria is typically thicker and is mainly composed of peptidoglycans (Slavin *et al*., 2017) . These structures are changed by the physical interaction between cell wall and nanoparticles and more affecting against gram-negative bacteria (Calvo and Martinez-Martinez , 2009).

Cell wall confers a negative charge on both Gram-positive and negative bacteria at neutral pH (Chung *et al*., 2004) . However, Gram-negative bacteria represent the set of microorganisms with the highest negative charge. In addition, Gram-negative bacteria have an outer membrane composed of phospholipids with partially phosphorylated lipopolysaccharides that increase the negative charge of their cell envelope (Gopinath *et al*., 2017) .

This negative charge is supposed to influence the interactions between the bacterium cell wall and the NPs or ions released from them. When SeNPs are interacted with bio-organic compounds positively charged, such as proteins or amino acids, they are attracted to the cell negative wall binding by electrostatic interactions. These nanoparticles lead to the formation of a strong bond with membranes, causing cell wall rupture and permeability (Galić *et al*., 2020 ; Filipović *et al*., 2021).

Thus, the interaction between SeNPs and microorganisms begins with their adhesion to the microbial wall and cell membrane. This binding is based on the electrostatic attraction between the negatively charged microbial cell membrane and the positive or less negatively charged SeNPs (Zhang *et al*., 2021) . After the attraction and interaction of SeNPs with the microorganism, structural and morphological changes are caused by the SeNPs, leading to the interruption of both membrane permeability

and respiratory functions. This effect takes place through membrane depolarization, disruption of cell integrity, and finally, cell death (Huang *et al*., 2016 ; Chandramohan *et al*., 2019) .

As a result of increased membrane permeability and cell wall disruption, cell contents, including proteins, enzymes, DNA, ions, metabolites and energy reserves, seep into the environment (Zhang *et al*., 2021 ; Nguyen *et al*., 2017) . SEM and TEM analyses showed that when bacteria are treated with SeNPs, they have a cellular contraction and take an irregular shape compared to a control group of bacteria (Huang *et al* ., 2016 ; Nguyen *et al*., 2017 ; Chandramohan *et al*., 2019 ; Huang *et al*., 2019) .

For example, after incubation of *E. coli* and *S. aureus* with coated SeNPs, cell lysis and intracellular leakage were observed in *E. coli*, while in *S. aureus*, there were sunken cell walls and cytoplasmic release, including cell wall disorganization (Huang *et al*., 2016) .

In addition, the mechanism by which SeNPs damage bacteria cytoplasmic membrane is by producing a rapid depolarization of the membrane (Calvo and Martinez- Martinez , 2009) . On the other hand SeNPs have a related mechanism to metabolic interference through the alteration of intracellular concentrations of adenosine triphosphate (ATP) (Huang *et al*., 2019) .

2.12.2 Intracellular penetration and damage

Metabolic functions of the cell are affected since NPs penetrate through the membrane , especially when it presents a certain level of damage interacting with DNA and proteins (Fu *et al*., 2015) . This action represents one of the proposed mechanisms for the antimicrobial activity of NPs, which is based on the release of ions (Skalickova *et al*., 2017) .

In this sense, several researchers have reported that Se^0 is soluble in trace concentrations in aqueous environments . Therefore, the amount

of Se ions released from SeNPs is likely to be very small. In other words, the antimicrobial effects of Se ions may be too weak, representing a non significant mechanism of SeNPs (Huang *et al*., 2019 ; Galić *et al*., 2020).

Although the studies are very recent, they mark a trend in research proposals to encompass the entire set of antimicrobial mechanisms associated with the penetration of compounds through the cell membrane of bacteria and their subsequent interaction within their metabolism.

2.12.3 Oxidative Stress

Reactive oxygen species (ROS) are oxygen-containing molecules that have a strong redox potential. Under normal conditions, the production of ROS and the antioxidant capacity of the cell are balanced. However, if there is an imbalance between the antioxidant mechanism and the excessive production of ROS, the redox balance of the cell favours oxidation, and this causes oxidative stress. Furthermore, oxidative stress is a cellular process involved in many aspects of cell signalling, although when it occurs excessively, it causes irreversible damage to cell metabolism, affecting viability (Abdal Dayem *et al*., 2017; Johnson and Hug , 2019 ; Sánchez-López *et al*., 2020) .

Many researcher reports that after the addition of SeNPs, these are absorbed on the surface of bacteria and trigger cellular oxidative stress (Abdal Dayem *et al*., 2017 ; Wang *et al*., 2017 ; Zhang *et al*., 2021) . To overcome this stress, cells exhibit protective responses that include enzymatic or non-enzymatic defence mechanisms (Fu *et al*., 2015) .

When oxidative stress overcomes defence mechanisms, the cell wall and biomolecules such as proteins, lipids and DNA are subjected to damage caused by ROS and free radicals such as hypochlorous acid (HOCl), hydrogen peroxide (H_2O_2), hydroxyl radical (OH), superoxide anion (O_2^-) and singlet oxygen ($^1O_2$) (Abdal Dayem *et al*., 2017 ; Wang *et al*., 2017).

ROS generation is responsible for antibacterial activity when Bio-SeNPs were tested against Gram-positive and Gram-negative bacteria (Zhang *et al*., 2021) .

2.13 The selective toxicity of nanomaterials on in vitro cancer cell models

Several mechanisms are involved in NP-mediated in vitro toxicity in normal (i.e. noncancerous) and cancerous cells. Cellular responses to NP exposure might include those at cell , organelle and gene level or a combination of them (Patil *et al*., 2016). Direct cytotoxic effects might be apoptosis or necrosis (or both) mediated , with a number of mechanisms leading to cell death, changes in proliferation patterns and effects on cell differentiation. High levels of reactive oxygen species (ROS) production , downregulation of antioxidant enzyme coding genes , lipid peroxidation and genotoxic effects, may be involved in the integrated cellular response to NPs (Choi *et al*., 2016 ; Abdal Dayem *et al*., 2017) .

Apoptosis is a common response of cells to NP treatment . Azizi and colleagues found that albumin-coated silver NPs (AgNPs) LD50 were several times lower for breast cancer cells than for normal white blood cells. Apoptosis assays such as Annexin V and microscopy counts of apoptotic bodies demonstrated that albumin-coated AgNPs exert pro-apoptotic selective effects on breast cancer cells while normal blood cells remained viable at the tested concentrations and times of exposure (Azizi *et al*., 2017) .

Chapter Three

Materials
and
Methods

3. Materials and Methods

3.1 Materials

3.1.1 Equipments and instruments

Equipments and instruments used in this study are listed in (table 3.1).

Table (3.1): Equipments and instruments used in this study.

Equipment and Instruments	Manufacture company	Origin
Atomic Force Microscope (AFM) , X ray diffraction (XRD)	Broker	Germany
Autoclave	Labtech	Korea
Balance (electrical)	Denver	Canada
Centrifuge	Hitachi	Japan
Deep freezer , VITEK 2- Compact system1	Biomerieux	France
Digital camera	Sony	Japan
Distillator	GFL	Germany
ELISA system	Beekman	Austria
Fourier Transform Infrared (FT-IR)	Perkin-Elmer 1725x	Japan
Hood	Bio Lab	Korea
Incubator , Oven	Memmert	Germany
Light Microscope	Olympus	Japan
Micro and cooling centrifuge	Hermle Labortechnik	Germany
Micropipette	Eppendrof	Germany
pH meter	Orient	USA
Refrigerator	Beko	Korea
Scanning electron microscope	FEI	Netherland
Shaking incubater	Gallenkamp	England
Thermocycler	Bio- Rad	USA
UV-visible spectrophotometer	Shimadzu	Japan
Vortex mixer	Thermolyne	USA

3.1.2 Chemical and biological materials

The Chemical and biological materials used in present study are listed in (table 3.2)

Table (3.2): Chemical and biological materials used in this study .

Materials	Manufacture company	Origin
2,2-diphenyl-1-picrylhydrazyl	Sigma-Aldrich	USA
Ethanol (96%)	BDH	England
Glycerol	Sigma	USA
Hydrochloric acid (HCl)	EMC	Germany
Methanol	BDH	England
Phosphate buffer saline (PBS)	Bioworld	USA
Sodium selenite (Na_2SeO_3)	Sigma	USA
Sodium hydroxide (NaOH)	EMC	Germany
Gram stain	Himedia	India
Ethidium Bromide Solution	Bio Basic	Canada
DNA Ladder 100 bp	Promega	USA
DNA loading dye	Promega	USA
Agarose	Conda	USA
Crystal violet powder	BDH	England
Sucrose	Himedia	India
Tris-EDTA (TE) buffer	Bio Basic	Canada

3.1.3 Culture Media

The culture media which used in the present study and the purpose from used it listed in table (3.3).

Table (3.3) : Culture media that used in this study with their purpose .

Culture Media	Company/origin	Purpose
Nutrient agar	Himedia /India	used for the growth and isolate bacterial types
Brain heart infusion broth	Himedia /India	Used for preservation of bacteria
Brain heart infusion agar	Himedia /India	Used for growth ,activation and maintenance of bacteria
Chromogenic Agar	Orientation/ France	used for the growth and differentiate between bacterial types in urine
Luria Bertani broth	Lab /USA	Used for maintenance and propagation of UPEC
Muller Hinton agar	Lab /USA	Determine the sensitivity test of bacteria to antibiotic
MacConky agar	Lab /USA	Growth of G-ve bacteria and determination their ability to lactose fermentation
Mannitol salt agar	Himedia/ India	Growth and isolate of staphylococci and determination the bacterial ability to mannitol fermentation
RPMI-1640 Medium	Gibco/ U.K	Used for cell growth and viability
Serum-medium	Gibco/ U.K	Used for growth cell and inactivate Trypsin EDTA

3.1.4 Antibiotic discs

The antibiotics used in this study are listed in table (3.4).

Table (3.4): Antibiotic Disc , Symbol and Potency

Antibiotic class	Antimicrobial agent	Symbol	Disk content (µg) (potency)	Mode of action
Penicillins	Ampicillin	AM	10	Cell wall synthesis inhibitors
B-LACTAM COMBINATION AGENT	Amoxicillin/calvulanic	AMC	30	Cell wall synthesis inhibitors
Carbapenems	Imipenem	IPM	10	Cell wall synthesis inhibitors
Aminoglycosides	Amikacin	AK	30	Protein synthesis inhibitor
Macrolides	Azithromycin	AZM	15	Protein synthesis inhibitor
Tetracyclin	Doxycycline	DO	30	Protein synthesis inhibitor
Fluoroquinolones	Ciprofloxacin	CIP	5	DNA synthesis inhibitor
Quinolones	Nalidixic acid	NA	30	DNA synthesis inhibitor
Nitrofurans	Nitrofurantoin	F	300	DNA synthesis inhibitor
Folate pathway Antagonistic	Trimethoprim / Sulfamethoxazole	SXT	25	Folic acid Synthesis inhibitor

3.1.5 Kits :

The commercial kits used in the present study are shown in table (3.5)

Table (3.5): kits for identification of bacteria and extraction of RNA

No.	Kit	Company	Country
1	**VITEK-2 compact system kit**	Biomerieux,	France
2	**Total RNA Extraction Kit**	iNtRON	Korea
	Trizol reagent 100ml		
3	**RealMOD™ Green SF 2X qPCR mix**	iNtRON	Korea
	RealMODTM Green SF 2X qPCR mix (1ml)		
4	**Go Taq® G2 Green Master Mix Kit**	iNtRON	Korea
5	**DNase I enzyme kit**	Promega	USA
	DNase I enzyme		
	10x buffer		
	Free nuclease water		
	Stop reaction		
6	**AccuPower® RocketScript™ RT PreMix**	Bioneer	Korea
	RocketScript Reverse Transcriptase (200U)		
	5X reaction buffer		
	dNTP 250µM		
	DTT 0.25mM		
	RNase Inhibitor (1U)		
7	**Wizard® SV Gel and PCR Clean-Up System**	Promega	USA
	Membrane Binding Solution		
	Membrane Wash Solution (concentrated)		
	Nuclease-Free Water		
	Wizard® SV Minicolumns		
	Collection Tubes (2ml)		

8	**MTT kit**	Intron	Korea
	MTT solution 3-(4,5-dimethylthiazol-2yl) 2,5diphenyl -2H- tetrazolium bromide		
	Solubilization solution		

3.1.6 Primers

Real Time PCR primers for quantification gene expression detection in Enterococcus faecalis and Escherichia coli were designed in this study by using NCBI Genbank database and Primer3 plus primer design software. These primers were provided by Macrogen company from Korea as following table (3.6) , (3.7) :

Table (3.6): *Enterococcus faecalis* qPCR detection gene primers with their nucleotide sequence .

Primer	Sequence (5'-3')		Product Size	Genbank code
Esp gene	F	TAAAGAAGAGAGCGGAGACACG	135 bp	KF550185.1
	R	ACAAGTTGCGCTTTGTGACC		
hly gene	F	GCATCAGCAGGAAATGAGTCG	90 bp	KF020739.1
	R	AGCTCCGACGGTAATTACAGAC		
gelE gene	F	AGGCGGTTACGTTTTAGCTG	143 bp	DQ845100.1
	R	TTTTGAATCCGTCCCAGTCG		
fsrA gene	F	TTGAACAACTGCATCCAGATTTG	128 bp	HE574483.1
	R	TGAGACTGGTACTTCCGTTCC		
16rRNA gene	F	GCAGCAAACGCATTAAGCAC	125 bp	LT844634.1
	R	AAGGTTCTTCGCGTTGCTTC		

Table (3.7): *Escherichia coli* qPCR detection gene primers with their nucleotide sequence .

Primer	Sequence (5'-3')		Product Size	Genbank code
hly gene	F	CTGGATGTTGTCTCCGGAATTC	78bp	MN708341.1
	R	TGTTCCTGTATGTGCGTCAC		
fimH gene	F	ATGCGGGCAACTCGATTTTC	94bp	JX847135.1
	R	GCTGGAATAATCGTACCGTTGC		
luxS gene	F	AAGACGTGCTGAAAGTGCAG	148bp	NC_000913.3
	R	TCTTCGTTGCTGTTGATGCG		
qseC gene	F	TCGCCTGGAAACAAACAACG	75bp	NC_000913.3
	R	TTAACCGCTTGGCAAACAGC		
16rRNA gene	F	TTCGATGCAACGCGAAGAAC	122 bp	AJ567540.1
	R	TTTCACAACACGAGCTGACG		

3.2 Methods

3.2.1 Study Design

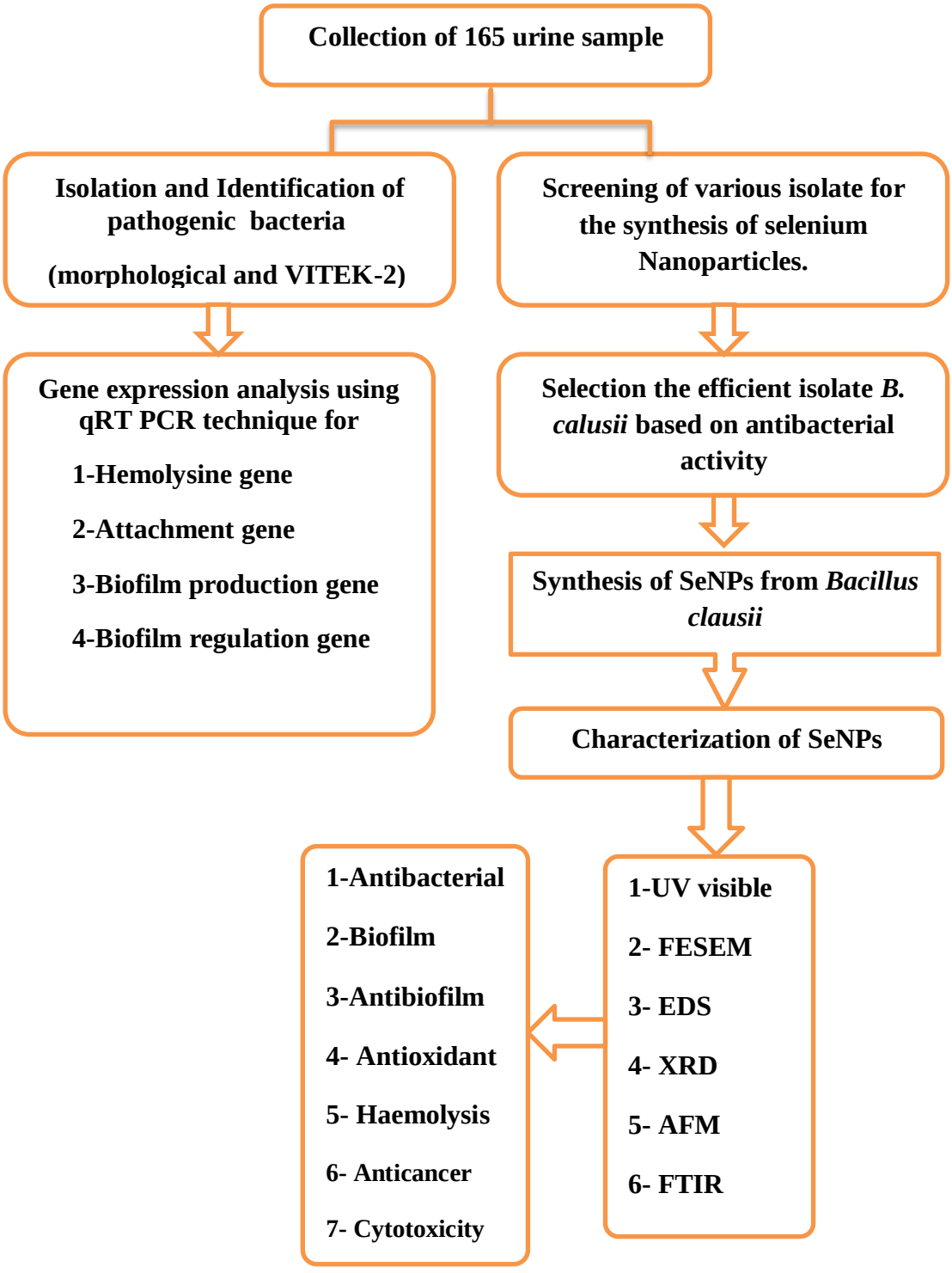

3.2.2 Collection of sample

A 165 samples of urine were collected from patients with clinical symptoms and suspected to UTI admitted in Al-Hilla Teaching Hospital and Public Health Laboratory in Babylon province during a period from (March - October 2021) . About 10 ml of Clean-Catch midstream urine of the patients that were diagnosed by a physician depending on clinical manifestation as patient with UTI was collected in the morning in sterile containers , ensure that the patient has not taken any drug for three days before collection of urine samples . Samples were transported to the laboratory in the college of science .

3.2.3 Media preparation and sterilization technique

All culture media presented in table (3.3) were prepared according to the manufacturing company instructions .The constituents were dissolved in distilled water completely , sterilized by autoclaving at 121Cº for 15min at 15 pound/inch^2. After cooling to 45-50 C° each medium was dispensed into sterile petri dishes in case of agar media and in sterilized screw tubes in the case of broth media . The work performed in laminar flow cabinets . Then , poured media were incubated for 24hr at 37 C° to ensure sterility. (MacFaddin , 2000).

3.2.4 Preparation of Reagents & Solution

3.2.4.1 Phosphate Buffer Saline (PBS)

Phosphate buffer saline was prepared by dissolving 1 tablet of (PBS), PH 7.2 in 100 ml deionized distilled water (DDW) . It was used in biofilm and antibiofilm experiments (Collee *et al*., 1996).

3.2.4.2 Hydrochloric acid (0.25 M)

It was prepared by adding 20.444 ml of 37.5% hydrochloric acid , and slowly dilute to 1 liters D.W. in a volumetric flask. Then allowed the

solution to cool to ambient temperature and properly mix it (Chen *et al*., 2020).

3.2.4.3 Sodium Hydroxide (NaOH) Solution (1M)

Sodium hydroxide (1M) was prepared by dissolving 4g of NaOH up to 50 ml of distilled water; this solution was used to adjust the pH during pH optimization step (Baker and Silverton, 2014).

3.2.4.4 DPPH Solution (0.1mM)

2,2-Diphenyl-1-picrylhydrazyl solution prepared by dissolving 0.00394 g. of 2,2-Diphenyl-1-picrylhydrazyl in 100ml ethanol (99.8%). The solution was used for detection of antioxidant activity of SeNPs (Sentkowska and Pyrzyńska , 2022).

3.2.4.5 TBE Solution

TBE buffer was prepared as 10x by Promega company. Tris-borate-EDTA buffer used at concentration of 1 X (1: 10 dilution of the concentration stock). The stock solution was diluted by D.W. and stored at room temperature.

3.2.4.6 Crystal Violet Solution(1%)

Crystal violet solution was prepared by dissolving 1gm of crystal violet in 100 ml Distilled water (Vandepitte *et al*., 2003).

3.2.4.7 Trypsin-(EDTA) solution

It was prepared by dissolving 15gm of trypsin-EDTA in 125 ml of D.W and constantly added by stirring the volume completed to 1 liter, and then filtration by using 0.22 μm Millipore filters and stored at (- 80˚C). These solution was used to detach and disaggregate the adherent monolayer cells from the bottom of the culture vessel in cytotoxicity assay .

3.2.5 Preservation and maintenance of bacterial isolate

The preservation and maintenance of isolates were done according to (Silhavy *et al*., 2010) as follows:

3.2.5.1 Short term preservation

The positive cultures were stored on nutrient agar at 4C° until further testing.

3.2.5.2 Long term preservation

Fresh 24 hr nutrient agar cultured isolates frozen in 20% glycerol brain –heart infusion broth and stored at -20 C° until required.

3.2.6 Morphological Identification of Isolates

The collected specimens were inoculated on nutrient agar and incubated for 24 hr at 37 C°. Dishes that did not appear grow within 24 hr were incubated for another 24 hr before counting negative result . After that, the isolated colonies were further subjected to subculture and purification on MacConkey agar, mannitol salt agar and Chromogenic agar , all positive culture subjected to VITEK-2 compact system to confirm the result (Munoz-Dávila *et al*., 2013).

3.2.7 Identification of bacteria by VITEK-2 Compact System

Suspension of bacteria was prepared according to the manufacturer's instructions. An adequate number of colonies was obtained by transferring an overnight pure culture and suspending it in 3.0 ml of sterile saline in (polystyrene) test tube. Adjustment of turbidity to 0.5 McFarland was made. Employing a Densi-Chek turbidity meter. Finally, the vitek-2 chamber with the specimen suspension tubes was loaded with the Gram negative -ID, and Gram positive -ID cassette (Karagöz *et al*., 2015).

3.2.8 Selection the efficient isolate that producing SeNPs

Eight isolates of bacteria (*Lactobacillus plantarium , Lactobacillus casei , Lactobacillus lactis , Lactobacillus bulgaricus , Bacillus cereus ,*

Bacillus subtilis , Bacillus clausii , Bacillus licheniformis) obtained from the laboratories of the Faculty of Science were screened for biosynthesis of selenium nanoparticles. These isolates were grown in brain heart infusion broth for 24 hr at 37 ° C. After incubation , the colloidal suspension was centrifuged at 10,000 rpm for 15 min , 4° C . The precipitate was discarded , and the supernatant was applied to the Na_2SeO_3 . An efficient isolate (*Bacillus clausii*) was selected based on colour change , antibacterial activity and absorption spectrum .

3.2.9 Molecular Identification of *Bacillus clausii*

Sequencing the 16sRNA gene has been used in this study for the identification of *Bacillus clausii* (Patrone *et al*., 2016).

3.2.9.1 Extraction of Bacterial Genomic DNA

Total DNA was extracted from culture broth, 1.5 ml of culture broth pipetted into Eppendorf tubes then centrifuged at 4,300 rpm for 5 min and the supernatant discarded , 200 µl of TE buffer was added , vortexes well , boiled for 15 min in water-bath , and then put on ice immediately for 1 min , this was centrifuged again at 6,700 rpm for 10 min and the supernatant was collected, which contains DNA for use as DNA template (Suwanjinda *et al*., 2007). DNA concentration and purity was estimated by nanodrop at absorbance (260 /280 nm) , DNA integrity was detected in Agarose gel electrophoresis (Bunu *et al*., 2020) .

3.2.9.2 The mixture of PCR reaction.

The polymerase chain reaction (PCR) was used to amplify fragments of DNA using Go Taq® G2 Green Master Mix Kit (promega/ USA). The reaction mixture of the specific interaction used for gene diagnosis is listed in table (3.8) and Primers that used in this study listed in table (3.9) .

Table (3.8): Contents of the Reaction Mixture of PCR

Contents of reaction mixture	Volume
Master Mix (2X)	12.5 µl
Template DNA	5 µl
Forward primer (10pmol/microliter)	2 µl
Reverse primer (10pmol/microliter)	2 µl
Nuclease free water	3.5 µl
Total	25 µl

Table (3.9): 16S rRNA primer pair

Primer name	Sequence(5-3)	Product Size (bp)	Reference
CF	5-AGAGTTTGATCCTGGCTCAG-3	1470	Loy *et al*., 2002
CR	5-GGTTACCTTGTTACGACTT-3		

PCR assay was carried out upon molecular identification using universal primers that was shown in table (3.9) . These primers synthesized by (Macrogen/Korea).Primers were dissolved using sterile DNAase free ddH_2O (PCR grade water). The stock solution (100 pmol/microliter) was prepared by adding ddH_2O to the vial containing lyophilized primer while working solution of 10 pmol/microliter was made by mixing 10 microliter of the stock primer and 90 microliter of free ddH_2O to reach a final volume 100 microliter ,the stock and working solution were stored in (-20) C° . .

3.2.9.3 PCR Program

The following parameters were used for PCR cycle independently of different researches .The optimum conditions applied in the thermo cycler are clarified in table (3.10) .

Table (3.10) : PCR conditions for amplification of 16S rRNA gene

Step	Phase	Temperature (°C)	Time	No. of cycles
1	**Initial Denaturation**	95	5 min	1
2	**Denaturation**	95	30 sec	35
3	**Annealing**	53	45 sec	
4	**Extension**	72	100 sec	
5	**Final extension**	72	5 min	1
6	**Storage**	4	Hold	1

3.2.9.4 Detection of Amplified Products by Agarose Gel Electrophoresis

Gel electrophoresis was used for detection of DNA , 1.5 gm of Agarose was weighted and applied to 100 ml of TBE (1X) buffer and microwaved until the solution became clear. After cooling the agarose to 50 C°, 5 microliter of ethidium bromide dye was added to 100 ml of melted agarose gel , and poured on preparing tray. Comb was removed after the hardening of agarose leaving wells , 5-10 microliter of DNA was mixed with 1-2 microliter of loading dye , TBE (1X) buffer was added to the electrophoresis tank. A tray with agarose was immersed in electrophoresis tank. Each well was loaded with 6microliter of DNA sample and standard molecular weight of DNA ladder (100-1500 bp) were loaded in a first well. Electrophoreses ran at 75 volt for 40 min . Gel was visualized with UV transilluminator at 280 nm and photographed by using digital Camera (Mishra *et al*., 2009).

3.2.9.5 Clean – up the gel slice to sending for sequencing

DNA purification was done by using (Wizard® SV Gel and PCR Clean-Up System) (Promega /USA) . To prepare membrane washing solution ,75 milliliters of ethanol (95%) was mixed with 15 milliliters of membrane wash solution (concentrated) . After each usage , the bottle top was carefully closed to avoid evaporation.

Agarose gel slice containing relevant DNA fragments was excised and the extra agarose removed to minimize the size of the gel slice , these steps were done by using a clean scalpel . Membrane binding solution was added at ratio of 10 µl per 10 mg of agarose gel slice . The mixture was vortexed and heated at 65 C° until the gel slice has been completely dissolved .The tube was vortexed every few minute to speed up the melting of gel slice . The tube was centrifuged quickly at room temperature , to guarantee that the content are at the bottom of the tube . The DNA fragment purification steps as following :

- In the collecting tube , SV Minicolumn was placed . After that the dissolved gel mixture was transferred to the SV Minicolumn assembly and incubated for 1 min at room temperature .
- The SV Minicolumn assembly was centrifuged at 13500 rpm for 1 min , discard flowthrough and reinsert Minicolumn into collection tube .
- The SV Minicolumn was washed by adding 700 µl of membrane wash solution (previously diluted with ethanol 95%) , centrifuged for 1 min at 13500 rpm , discard flowthrough and reinsert Minicolumn into collection tube , then repeated washing again by centrifuging for 5 min at 13500 rpm with 500 µl of membrane wash solution .
- The collecting tube was emptied , and the SV Minicolumn assembly was centrifuged for 1 min to evaporate any leftover ethanol.
- Carefully transfer SV Minicolumn to a clean 1.5 ml microcentrifuge tube , 50µl of nuclease free water was pipetted directly into the center of column without contacting the membrane . Then , incubated for 1 min at room temperature and centrifuged for 1 min at 13500 rpm .

- The SV Minicolumn has been removed and the eluted DNA was kept in a micro-centrifuge tube at -20 C° and then sent to gene sequence

3.2.9.6 Similarity Search by BLASTN

DNA sequence was analyzed for the sequence similarity to the existing DNA sequences available in the database at National Center for Biotechnology Information (NCBl), website (www.ncbi.nlm.nih.gov/blast). National Library of Medicine (NLM), and National institute of Health (NIH) .

3.2.10 Biosynthesis of Selenium nanoparticles by using *Bacillus clausii*

The pure culture of *Bacillus clausii* 5 ml were inoculated in flask containing 500 ml of brian heart infusion broth and incubated at 37 C° for 24hr . After incubation , the colloidal suspension was centrifuged at 10,000 rpm for 15 min at 4C° , the precipitate was removed and the supernatant was then passed through millipore filter (0.2 µm) to get rid of impurities . 3 mM of Na_2SeO_3 were prepared and added to 250 ml of supernatant , pH of supernatant was adjusted to (8) and then incubated for 48 hr at 37C^o in a shaking incubator (150 rpm) in aerobic condition (Singh *et al*., 2014) .

After that the reaction mixture was centrifuged at (10000 rpm , 4 C° for 10 min) , the supernatant was discarded and the sediment was taken . In order to purify selenium nanoparticles , these sediment was washed with DDW , these step were repeated three times. The final suspension was dried in oven at 40 C° for 18-24 hr . The dried powder was collected carefully and stored in sample vials for further analysis (Dhanjal and Cameotra , 2010) .

3.2.11 Characterization of Biosynthesized selenium nanoparticles

The physical characteristics of selenium nanoparticles were characterized by UV-Visible absorption spectroscopy, SEM coupled with EDXS , XRD , AFM and FTIR .

3.2.11.1 UV-Visible Spectra analysis

UV-vis spectroscopy was used for the determination of selenium nanoparticles in solution . Two ml of a aliquot selenium nanoparticles was measured in a 1 cm path-length quartz cuvette and scanned at a medium scan rate 2 nm / second , in the range of (200 – 800) nm, The absorbance at which the peak was formed was noted (Gangadoo *et al*., 2017) .

3.2.11.2 Analysis by Field Emission scanning electron microscopy (FESEM)

Field Emission Scanning electron microscope (FESEM) was used for characterization the morphological and size of selenium nanoparticles in electron microscope unit , / University of Kashan . The SEM was carried by smearing the sample on a small piece of adhesive carbon tape that was fixed on a brass stub. The sample was then subjected to gold coating using a sputtering unit for 10 sec at 10 mA of current. The gold coated sample placed in the SEM chamber and secondary electron/back scattered electron images were recorded. The microscope operated with different magnification ranging from 15000 x to 35000 x and voltage 20-30 KV (Ramamurthy *et al*., 2013) .

3.2.11.3 Analysis by energy dispersive X-ray spectroscopy (EDX)

Energy dispersive spectroscopy (EDS) was performed to confirm the conversion of selenium ions into elemental selenium (Se) using a FEI Tecnai

F20 TEM/STEM operated at 200 kV. A small aliquot of the sample was pipetted onto a carbon coated 200 mesh copper grid (Gangadoo *et al*., 2017).

3.2.11.4 X-ray diffraction (XRD)

The X-ray diffraction was used for characterization of selenium nanoparticle at University of kashan , the powder of selenium nanoparticle was used for test. The nanoparticle sample was dispersed on a low background noise sample holder and analyzed in a Bruker D8 Advance X-Ray diffractometer equipped with a LynxEYE detector. X ray diffraction analysis was operated at a voltage of 40 kV, with current of 40 mA, with copper radiation of 1.54060 Å. The scanning was performed in the 2θ range of 10° to 40° at 0.02°/min with time constant of 1.2 s. (Gangadoo *et al*., 2017) .

3.2.11.5 Atomic force microscope(AFM)

Atomic force microscope(AFM) was used for characterization the selenium nanoparticle in University of Kashan , A drop of (SeNPs) was placed on a slide and a thin smear was made. The smear was air-dried and the slide was scanned and observed under Atomic Force Microscope (Model- Nanosurf easyscan 2 AFM , Switzerland) (Singh *et al*., 2014).

3.2.11.6 Fourier Transform Infrared Spectroscopy (FTIR)

The transmittance of the prepared formulations was accomplished by FT-IR spectrophotometer , in a spectral range of 400-4000 cm^{-1} at 2 cm^{-1} resolution. The data sets were averaged over 64 scans (Tugarova *et al*., 2018) .

3.2.12 Influence of Selenium Nanoparticle Against pathogenic bacteria

3.2.12.1 Antibacterial activity of selenium nanoparticles

This method was done on Muller Hinton agar as described in (Boroumand *et al*., 2019) **:**

- Turbidity of each bacterial isolates compared to McFarland 0.5 standard to get the right concentration for each of them .
- A 0.1 ml of each bacterial isolates were added to petri dish containing Muller Hinton agar and spread by spreader and left the dishes for an 1 hr.
- Wells were made by using cork borer (5 mm diameter) as it was equal distance between the well and the other.
- The SeNPs were dissolved with deionized water to get various concentrations (100 , 300 , 500) µg/ ml.
- A 40 microliter of each concentration of Se NPs were added to each well and incubated in the incubator at 37 ° C for 24 hr .
- Nanoparticles inhibition zones were measured by a ruler .

3.2.12.2 Detection of Minimum inhibitory concentration (MIC) of nanoparticle

The MIC is a lowest selenium nanoparticles concentration that inhibited completely the bacterial growth can be detected by using micro-titerplate method , The turbidity of bacterial suspension was compared and matched with the turbidity of 0.5 McFarland units . The McFarland 0.5 standard corresponds approximately to a homogeneous suspension of 1.5×10^8 cells/ml , An amount of 100 µl of BHI media was transferred to each well , 100 µl of SeNPs (2048 µg/ml) was added in each well of Column 2 . Serial dilutions were performed from Column 2 to Column 11, to obtain the final NPs concentrations, which varied from 1024µg/ml in (2^{nd} well) to 2 µg /ml in (11th well).

A 10 microliter of bacterial inoculum were added to each well , except all wells of (column 1). NPs free well (Column 12) containing medium and inoculum and (column 1) contained media only . The microtiter plate incubated at 37°C for 24 hr . OD at 570 nm was recorded

spectrophotometrically . MIC was determined as the lowest NP concentration showing absence of growth as compared with the growth in the SeNPs -free well (Kumar *et al*., 2015) .

3.2.13 Antibiotic Susceptibility Test (AST)

The antibiotic resistance of bacterial isolates was assessed using disc diffusion method , according to the national committee for clinical laboratory standards (NCCLS) guidelines(Kiehlbauch *et al*., 2000). The bacterial suspension 0.5 McFarland standard was inoculated by swabbing the MHA surface 3 times by rotating to ensure an even distribution , after 10 min antibiotic discs of Azithromycin (15 μg), Nitrofurantion (300 μg), Imipenem (10 μg), Amikacin (30 μg) , Nalidixic acid (30 μg) , Ciprofloxacin(5 μg) , Doxycycline (30 μg) , Amoxicillin/calvulanic acid (30 μg) , Trimethoprime / sulphamethoxazole (25 μg) , Ampicillin (10 μg) were placed on Mueller Hinton agar (MHA) surface and kept at 37 C° for 24 h (Sharma and Chauhan, 2014).

3.2.14 Synergistic effect of nanoparticle and antibiotic

The antagonistic activity of antibiotic and selenium nanoparticles combination were determined by the modified disc diffusion method according to the NCCLS guidelines . The MHA plates were seeded with the above antibiotic disc impregnated with selenium nanoparticle (32 μg /ml) for (*E. faecalis* and *S. saprophyticus*) and (64 μg /ml) for (*K. pneumoniae and E.coli*) along with plain antibiotic disc taking as positive control , the MHA plates were kept at 4C° for 1 hr to allow the proper diffusion , after that kept at 37 C° for 24 hr . The zones of inhibition were measured by using a caliper micrometer against the back of the petri plates (Varak and Priya, 2019).

3.2.15Antioxidant assay of SeNPs

Antioxidant activities of SeNPs synthesized from *Bacillus clausii* were detected by using DPPH (2,2-Diphenyl-1-picryl- hydrazyl) radical

scavenging assay according to the procedure described by (Sentkowska and Pyrzyńska, 2022) as the following :

100 µl of SeNPs with different concentration (50 , 100 , 150 µg/ml) was mixed with 100 µl of DPPH (final DPPH concentration : 0.1 mmol/L) in a 96 well microplate . The reaction mixture was incubated in dark at room temperature for 30 min . The absorbance of the mixture was recorded at 517 nm spectrophotometrically using ELISA reader. The negative control consisted of methanol-DMSO mixture and DPPH solution, while ascorbic acid was used as a reference .The inhibition of the DPPH radical by selenium was calculated according to the following special formula:

$$inhibition\ (\%) = \frac{(Abs\ of\ control - Abs\ of\ test)}{(\text{Abs of control})}\ X\ 100$$

3.2.16 Haemolysis Effect of SeNPs

Haemolysis assays were performed on the human red blood cells of one healthy donor and collected in anticoagulant EDTA tube : 2 ml of blood was applied to each tube and incubated for 30 m with SeNPs (50, 100 , 150 µg/ml) which suspended in tyrode .Triton X- 100 1% was used as positive control , Tyrode as negative control. The suspension was incubated at room temperature on a shaking plate during 1 hr , 4 hr and 24 hr . After the incubation time, the suspension was centrifuged at 10 000 xg over 5 min and then read OD in spectrophotometer at 550 nm. Positive and negative controls induced 100% and 0% of lysis, respectively (Mesdaghinia *et al*., 2019) .

3.2.17 Biofilm formation assay

3.2.17.1 Congo red method

Congo red method is used for qualitative assessment of biofilm formation. The result was recorded as changing the color of a colony from

red to black on the Congo red agar . Congo red agar is a specially formulated medium consisting of brain heart infusion broth (37 gm/L), sucrose (5 gm/L), agar (10 gm/L), and Congo red (8 gm/L) . To obtain Congo red agar we prepared a Congo red stain as stock solution, autoclaved at 121 C° for 20 min then applied to autoclaved BHI agar supplemented with sucrose at a temperature of 55 Cº. The bacterial strains were inoculated and incubated at 37 C° for (24 – 48) hr , then read the result as following: if the bacteria formed black colonies with a dry crystalline consistency that was mean it biofilm producer isolates while if it formed red colonies that was mean the non-biofilm producer isolates (Ruchi *et al*., 2015).

3.2.17.2 Microtiter Plate Method (MTP)

Microtiter plate (MTP) is a quantitative method to determine biofilm production by microtiter plate reader as described by (Jaffar *et al.,* 2016) in following steps:

- Cultured isolates and incubated overnight at 37 Cº.
- Bacterial suspension was prepared in Mueller-Hinton Broth (MHB) supplemented with 1% glucose and adjusted to 0.5 McFarland.
- Then , 180µl of Mueller-Hinton Broth (MHB) that supplemented with 1% glucose and 20µl of bacterial suspensions are inoculated into 96-well flat-bottomed sterile polystyrene micro titer plate (3 wells for each strain) .
- Microtiter plate was incubated in 24 hr at 37C° .
- The sessile isolates of which biofilms formed on the walls of micro titer plate are stained with only 150 µl of 0.1% crystal violet for 10 min , after planktonic cells in wells of micro titer plate are discharged by washing twice with phosphate-buffered saline (PBS) (pH 7.2) and wells are dried at 60°C for 1hr .

- After drying wells of microplate , dye of biofilms that lined the walls of the microplate was resolubilized by 150µl of 95% ethanol.
- Then, microtiter plate was measured at 620 nm by a microtiter plate reader.

Each assay was performed in triplicate and the average optical density was considered . According to their optical densities, the adherence capability of each bacterial cell was classified into three categories: above the mean optical density of the negative control (containing broth only) were considered the cut-off optical density (ODc) (Mathur *et al.,* 2006) . Isolates were classified as follows :

(ODc < OD < 2×ODc)…….... Weakly-adherent.
(2×ODc < OD < 4×OD)……. Moderately-adherent.
(4×OD < OD)……. Strongly-adherent.

3.2.18 Antibiofilm activity of SeNPs

The antibiofilm effect of SeNPs against various pathogens was determined in vitro by using 96 wells polystyrene microtiter-plates method (Khiralla and El-deeb, 2015 ; Miglani and Tani-Ishii , 2021) , Antibiofilm procedure include :

- Bacterial cell suspension (0.1ml) have been inoculated in 1.9 ml BHI broth and adjusted to 0.5 McFarland .
- One hundred microliter of the cultured BHI broth which supplemented with 1% glucose transferred into each well of 96- well microtiter-plate .
- One hundred microliter of SeNPs (2048 µg/ml) was added in each well of column 2 . Serial dilutions were performed from column 2 to column 11, to obtain the final NPs concentrations, which varied from 1024µg/ml in (2^{nd} well) to 2 µg /ml in (11th well).

- Ten microliter of bacterial cell suspension that prepared in step 1 was added from column 2 to column 12 . column 1 contain (BHIB+1% glucose) serve as negative control , column 12 contain (BHIB+1% glucose) and stimulated culture act as positive control . Plates were incubated at 37 C° for 24 hr .
- After the incubation period, contents of the microtiter-plates were emptied and the wells were washed three times with 200 microliter of phosphate buffered saline (PBS, pH 7.2).
- The remaining adhered bacteria were fixed with 200 microliter of methanol (99 %) per well . After 15 min , the microtiter-plates were stained with 200 microliter per well of 0.1 % crystal violet for 5 min .
- The surplus of stain was rinsed off by placing the microtiter-plates under slow running tap water. After drying , 200 microliter of 33% acetic acid was added to the wells.
- The biofilm growth was read at 620 nm using micro plate reader . Therefore , varying amount of biofilm formation by various isolates could be quantitated by comparing OD values of stained adherent

cells . Isolates which gave an OD <0.120 were classified as non-adherent and weak biofilm producers ; OD values of 0.120 to 0.240 were classified as moderately adherent and moderate biofilm producers ; OD value of > 0.240 was classified as strongly adherent and high biofilm producers (Magesh *et al.*, 2013) .

3.2.19 Determination the Toxicity of SeNPs on (PC3) Cancer Cell Line and (WRL 68) normal cell line.

This method was performed in vitro to investigate the possible cytotoxic effect of different SeNPs concentration on Prostat cancer cell line (PC3) and normal hepatic cell line (WRL 68).

3.2.19.1Cell Line Maintenance:

When the cells in the vessel formed confluent monolayer, the following protocol was performed (Geraghty *et al*., 2014) :

- The growth medium was aspirated and the cell sheet washed with PBS.
- Two to three ml trypsin/EDTA solution was added to the cell. The vessel was turned over to cover the monolayer completely with gentle, rocking. The vessel allowed incubation at 37 C° for (1 – 2) min until the cells were detached from the vessel.
- Fresh complete RPMI medium (15-20 ml) was added and cells were dispersed from the wedding surface into growth medium by pipetting.
- Cells were redistributed at required concentration into culture vessels, flasks or plates whatever needed and incubated at 37 C° in 5% CO_2 Incubator.

Cell concentration was achieved by counting the cells using the haemocytometer and applying the formula:

$$Total\ cell\ \frac{count}{ml} = cell\ count \times dilution\ factor(sample\ volume) \times 10^4$$

3.2.19.2 MTT Cytotoxicity Assay

The cytotoxic effect of SeNPs in different concentration (25 ,50 ,100, 200 and 400 µg/ml) was performed by using MTT kit (Intron Biotech) as following :

- Cancer cells ($1x10^{4}$ – $1x10^{6}$ cells/ml) were grown in 96 flat well micro- titer plates, in a final volume of 200µl complete culture medium per each well. The microplate was covered by sterilized

parafilm and shacked gently . The plates were incubated at 37 ° C, 5% CO_2 for 24 hr .

- After incubation, the medium was removed and two fold serial-dilutions of the desired compound (25, 50, 100, 200 and 400 µg/ml) were added to the wells .Triplicates were used per each concentration as well as the controls. cells treated with serum free medium. Plates were incubated at 37 ° C for 48 hr in 5% CO_2 incubator .
- After exposure to SeNPs , 10 µl of the MTT solution was added to each well and the plates were further incubated at 37 ° C in 5% CO_2 for 4 hr .
- The media were carefully removed and 100µl of solubilization solution was added per each well for 5 min .
- The absorbance was determined by using an ELISA reader at a wavelength of 575 nm.
- statistical analysis was performed to calculate the IC50 , through the following equation:

$$Viability(\%) = \frac{optical\ density\ of\ sample}{optical\ density\ of\ control} \times 100\%$$

3.2.20 Effect of SeNPs on gene expression of some virulence factor

The q RT-PCR was performed for quantification expression detection of some virulence factors and biofilm formation genes that normalized by housekeeping (16SrRNA) gene in *Enterococcus faecalis* and *Escherichia coli* isolates. The method was carried out according to (Shakerimoghaddam *et al*., 2017) .Three isolates which formed a strong biofilm were chosen for studying expression of the (*hly* , *fimH* , *luxS* , *qse* and *16SrRNA* gene) in *E. coli* , and (*Esp* , *hly* , *gelE* , *fsrA* and *16SrRNA* gene) in *Enterococcus faecalis*) .

The MIC and sub-MIC of SeNPs concentrations that reduced growth of bacteria and biofilm formation was determined by microtiter-plate methods . For *E. coli* we used three concentration of SeNPs (32 µg , 64µg , 128 µg) , and for *Enterococcus faecalis* we used (16 µg ,32 µg , 64µg).

For gene expression studies , 5 ml of Luria-Bertani broth media was inoculated with tested bacteria and adjusted to (0.5 McFarland) . For each bacteria , three groups was made , the first group treated with sub MIC of SeNPs named as S1 , second group treated with (MIC) of SeNPs and named S2 , the last group was the control which was bacterial growth without any treatment was named (SC) . After adding of Se nanoparticles the tube incubated at 37 C° for 24 h .

3.2.20.1 RNA extraction

Total RNA was extracted from bacterial suspension by using (Total RNA Extraction Kit) according to company instructions as following steps:

- One ml of bacterial suspension that treated with SeNPs were harvested by centrifuge at 13000rpm for 1 min then , supernatant removed .
- The bacterial pellets were suspended by adding 1ml easy-BLUE (Trizol reagent) and vigorously vortex in room temperature for 10 sec.
- Two hundred microliter chloroform was added to each tube and shaken vigorously for 1 min .Then , The mixture was incubated on ice for 5 min . After that centrifuged at 13000 rpm, 4°C, for 15 min .(The mixture was separated into a lower organic phase , interphase , and a color-less upper aqueous phase)
- A color-less upper aqueous phase which contain RNA was transferred into a new 1.5ml microcentrifuge tube .

- For RNA precipitation 500microliter isopropanol was added. Then, mixture mixed by inverting the tube 4-5 times and incubated at 4°C for 10 min . Then, centrifuged at 13000 rpm , 4°C for 10 min .
- Supernatant was discarded, and 1ml (80%) Ethanol was added and mixed by vortex again. Then, centrifuge at 13000 rpm, 4°C for 5 min.
- The supernatant was discarded and the RNA pellet was left to air to dry.
- One hundred microliter free nuclease water was added to each sample to dissolve the RNA pellet, Then, it incubated in a water bath at (55–60) ° C for (10–15) min , the extracted RNA sample was kept at -80 ° C.

3.2.20.2 Estimation and purity of total extracted RNA

The extracted total RNA was checked by using Nanodrop (Thermo Scientific NanoDrop Lite UV Visible Spectrophotometer. USA) that measured RNA concentration (ng/µL) and checked the RNA purity at absorbance (260 /280 nm) as following steps:

- After opening up the Nanodrop software, chosen the appropriate application (Nucleic acid, RNA).
- A dry wipe was taken and cleaned the measurement pedestals several times. Then carefully pipetted 2microliter of free nuclease water and placed onto the surface of the lower measurement pedestals for blank the system.
- The Nanodrop sampling arm was lowered and 1microliter RNA sample were measured .

3.2.20.3 DNase I treatment

The extracted RNA was treated with DNase I enzyme to remove the trace amounts of genomic DNA from the eluted total RNA by using samples

(DNase I enzyme kit) and done according to method described by Promega company, USA instructions as in table (3.11) :

Table (3.11): Treatment of extracted RNA with DNase I enzyme

RT master mix	Volume
Total RNA	10 µl
DNase I enzyme	1 µl
10X buffer	4 µl
DEPC water	5 µl
Total	20 µl

After that , the mixture was incubated at 37°C for 30 min . Then , 1 µl of stop reaction was added and incubated at 65°C for 10 min for inactivation of DNase enzyme action .

3.2.20.4 cDNA synthesis

The DNase treated total extracted RNA samples were used in cDNA synthesis step from mRNA transcripts by using **(AccuPower® RocketScript™ RT PreMix)** and this kit was done according to company instructions as in table (3.12) :

Table (3.12): Reverse transcriptase master mix with their volumes for cDNA synthesis

RT mix	Volume
Total RNA 100µg	10µL
Random Hexamer primer (50pmol)	1µL
DEPC water	9µL
Total	20µl

After that, these RT mix components that mentioned in table above placed in AccuPower® RocketScript™ RT PreMix kit strip tubes that containing all other components which needed to cDNA synthesis such as (Reverse Transcriptase, 5 x Reaction Buffer, DTT, dNTP, and RNase

Inhibitor). Then, all the strip tubes transferred into Exispin vortex centrifuge at 3000rpm for 3 min , and then incubated in Thermocycler (BioRad-USA) as following thermocycler conditions protocol , table (3.13) :

Table (3.13): Thermocycler condition for cDNA synthesis

Step	Temperature	Time
cDNA synthesis (RT step)	42 C°	1 hr
Heat inactivation	95 C°	5 min

3.2.20.5 Real-Time PCR (qPCR) master mix preparation

qPCR master mix was prepared by using **(RealMOD™ Green SF 2X qPCR mix Kit)** based on SYBER green dye amplification in Real-Time PCR system and the qPCR master mix for target genes and housekeeping gene was prepared as in table (3.14):

Table (3.14): qPCR standard master mix protocol

qPCR master mix	Volume
cDNA template (10ng)	5µL
Forward primer(10pmol)	1µL
Reverse primer (10pmol)	1µL
qPCR Master Mix	10µL
Nuclease free water	3µL
Total	20µl

After that, these qPCR master mix component that mentioned above placed in qPCR white plate strip tubes and mixed by Exispin vortex and centrifuge for 5 m , then placed in MiniOpticon Real-Time PCR system.

3.2.20.6 qPCR Thermocycler conditions

qPCR Thermocycler conditions was done according to qPCR kit instruction and used by using **Optimase ProtocolWriter™** online for primers annealing calculation as in table (3.15):

Table (3.15): General thermocycler (RT-PCR) program used in the study

qPCR step	Temperature	Time	Repeat cycle
Initial Denaturation	95 C°	10 min	1
Denaturation	95 C°	30 sec	40
Annealing	60 C°	30 sec	
Extension	72 C°		

The data results of qPCR for target and housekeeping gene were collected and the expression analysis (fold change) used analyzed by using (**The CT Method Using a Reference Gene**) that described by (Livak and Schmittgen, 2001) as following equations:

Gene expression ration (Fold change) = Ratio (reference/target) = 2^CT(reference) – CT(target).

3.2.20.7 Statistical analysis

The data values are presented as the mean ± S.D. Differences in mean values were analyzed by two-way ANOVA followed LSD test with the IBM SPSS Statistics version 27 software (International Business Machines Corp., Armonk, NY, USA). Values with a $P < 0.05$ were considered to indicate statistical significance (Daniel and Cross , 2018) .

Chapter Four

Results

and

Discussion

4 . Results and Discussion

4.1 Isolation and identification of bacterial isolate from UTI

Among of 165 isolates , 115(69.6%) isolates were positive culture , *Escherichia coli* 65(56.52 %) was the predominant and the most common Gram negative bacteria followed by *Enterococcus faecalis* 28(24.34 %), *K. pneumonia* 15 (13.04 %) , and *Staphylococcus saprophyticus* 7(6.1 %) (table 4.1) .

In VITEK2 compact system ,the isolates were identified as *Escherichia coli* with probability of (99) % , *Klebsiella pneumoniae* with probability of (96) % , *Enterococcus faecalis* with probability of (99) % , *Staphylococcus saprophyticus* with probability of (89) % (table 4.1) . Biochemical Characteristics of all bacterial isolates were done also by VITEK2 compact system , appendices (1,2,3,4,5) .These result are similar to (Shilpi *et al.*, 2013) who found that *Escherichia coli* (58.0%) was the most common pathogens ,followed by *Enterococcus faecalis* (15.5%) .

Table (4.1) : Identification of pathogenic bacteria depended on the colonial morphology, microscopically, and Vitek 2 system

Bacteria species	number of isolates	Probability in Vitek 2 system
Escherichia coli	65 (56.5%)	99%
Enterococcus faecalis	28 (24.3 %)	99%
Klebsiella pneumoniae	15 (13.1 %)	96%
Staphylococcus saprophyticus	7 (6.1 %)	89%
Total	115 (100%)	

The morphological examination of *Escherichia coli* on MacConkey agar and nutrient agar after 24 hours of incubation at 37°C produced large, circular, low convex, grayish white, moist, smooth, opaque or partially

translucent colonies **.** *Escherichia coli* produced bright pink flat colonies due to lactose fermentation , and form pink to mauve colonies on chromogenic agar , figure (4.1) .

Urinary tract infection is considered to be one of the most common bacterial infections that affect people in the community and hospitals worldwide **(**Foxman , 2014) . It is well known that the spectrum of pathogens isolated from patients suffering from a UTI is nearly stable, and *Escherichia coli* remains the most common prevalent etiological agent . In the present study, *Escherichia coli* accounted for 56.5% of positive isolates, which is well comparable with the rates reported from some studies conducted in Iraq as 74.32%, Turkey 71.3% , in Iran 65.2% and 51.5% (Aypak *et al*., 2009 ; Mirsoleymani *et al*., 2014; Assafi *et al*., 2015; Pouladfar *et al*., 2017) .

In another study, the most common isolates after *Escherichia coli* was *Enterococcus faecalis* , *Staphylococcus saprophyticus* , *Proteus mirabilis and Klebsiella pneumoniae* (Čeljuska-Tošev *et al*., 2010) . The increased number of enterococcal UTI in this part might be due to the rapid surge in number of diabetic patients; diabetes mellitus is one of the important risk factors of enterococcal UTI (Nitzan *et al*., 2015) .

The increased incidence of enterococcal UTI is alarming; resistance to most commonly used antibacterial agents is a typical characteristic of these bacteria. It is far more difficult to treat enterococcal UTI as compared to UTI caused by other bacteria due to intrinsic resistance to many antibacterials and rapidly increasing acquired resistance (Wisell *et al*., 2008) .

Enterococcus faecalis has greenish-blue color on chromogenic agar , figure (4.1) . It was considered the second prevalent and virulent species causing infections in hospitalized patients .These clones are linked to the hospital by the acquisition of adaptive genetic elements, including the

metabolic genes, the creation of biofilm and antibiotic resistance (Shilpi *et al*., 2013).

The *Klebsiella pneumonia* colonies seemed to be large , spherical , mucoid and glistening pink colonies on a MacConkey agar , and metallic blue on chromogenic agar , figure (4.1) . Microscopic tests of *Klebsiella* alleged isolates showed that had been gram-negative shorter rods (Mahon *et al*., 2018). When cultivated on MacConkey agar from a total of 180 samples taken from two clinical sources in Baghdad Governorate , produced sixty (33.88 %) *klebsiella* isolate (Jasim *et al*., 2017) . In their experiment , they collected 88 (29.33 %) *Klebsiella* isolates of 300 various clinical samples reported on the appearance of pink, mucoid, rounds and wide noted that VITEK 2 is an easy-to-handel system that delivers a fast result (4 to 15 hours) and reasonable for microbial species identification (Ismail , 2017; Abbas , 2020) .

Staphylococcus saprophyticus on nutrient agar were seemed to be circular, cream-colored to white colonies , and are mostly 1mm in diameter with an entire margin , the colonies have raised elevation and a dense center with transparent borders. While in mannitol salt agar , it appeared yellow-colored colonies indicating mannitol fermentation as the color of the media is converted from red to yellow , and the colonies are 1-2 mm in diameter with an entire margin , and appeared turquoise blue on chromogenic agar , figure (4.1) .

Epidemiological studies showed that urinary tract infections caused by *Staphylococcus saprophyticus* are more prevalent during the late summer and fall .These infections are also associated with recent sexual intercourse, hormonal influences related to menstruation, and changes in genital flora caused by candidal infections or spermicides . *Staphylococcus saprophyticus* can cause infections even when it is present in low numbers, For this reason, even low numbers of coagulase-negative

staphylococci in urine cultures should not be dismissed as skin contaminants (Raz *et al*., 2005) .

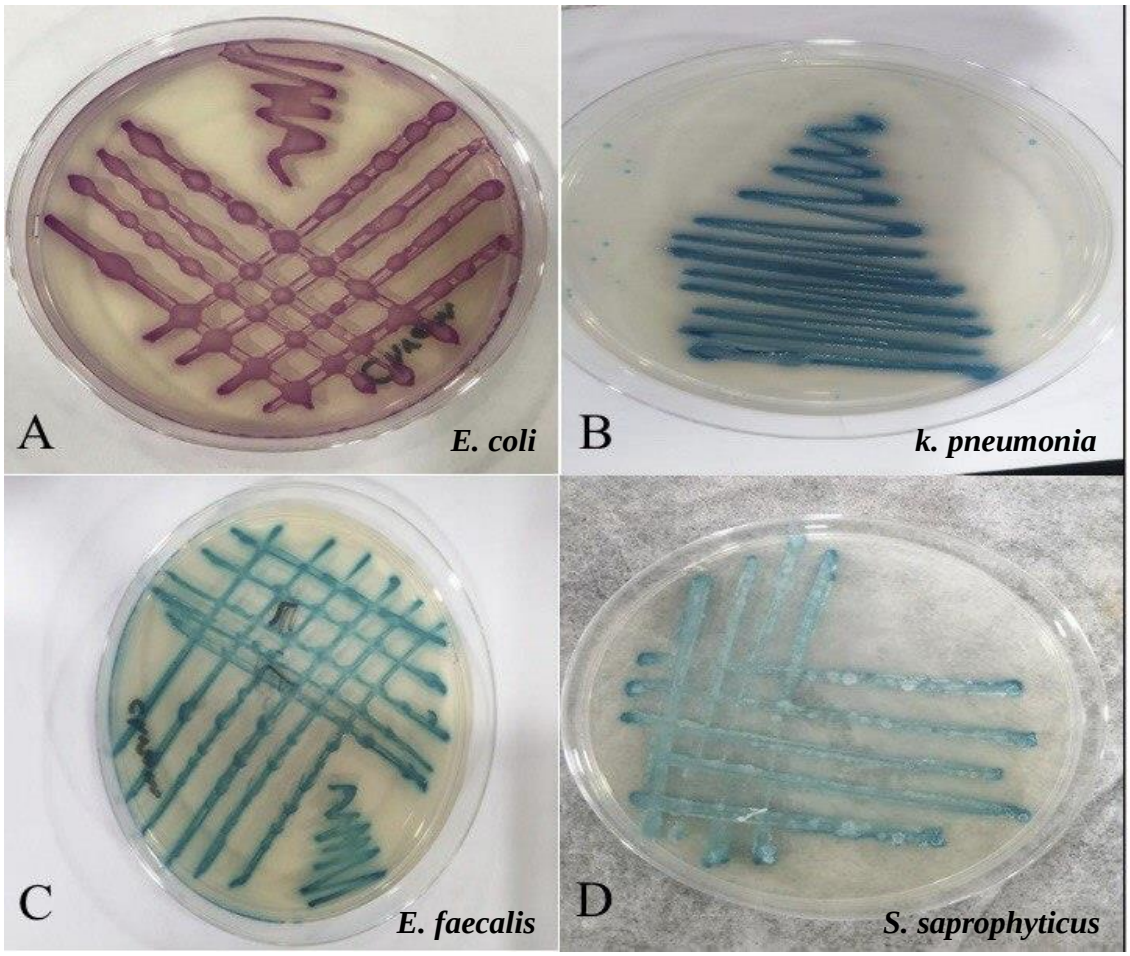

Figure (4.1) : Isolation of pathogenic bacteria on chromogenic agar at 37 º C for 24 hr , A (*E. coli*) , B (*k. pneumonia)* , C (*E. faecalis) , D (S. saprophyticus)*.

4.2 Antibiotic Susceptibility Test (AST)

Lists of antibiotic susceptibility testing were created using documents and breakpoints from the Clinical Laboratory Standards Institute (CLSI , 2020) the European Committee on Antibacterial Susceptibility Testing (EUCAST) and the United States Food and Drug Administration (FDA).

This study included 10 antibiotics was determined by disc-diffusion method , which are Azithromycin , Nitrofurantoin , Imipenem , Amikacin ,

Nalidixic acid , Ciprofloxacin, Doxycycline , Amoxicillin/calvulanic acid , Trimethoprime / sulphamethoxazole , Ampicillin . The results was analyzing sensitivity pattern of antibiotics against (*E.coli , K. pneumoniae , E. faecalis ,S. saprophyticus*) , figure (4.2) .The table below shows the percentages of resistant isolates for antibiotic , table (4.2) .

Table (4.2) : Antibiotic susceptibility test for pathogenic bacteria

antibiotic	Antibiotic susceptibility of pathogenic bacteria (%)			
	E. coli	***K.pnemoniae***	***E . faecalis***	***S. saprophyticus***
	R	**R**	**R**	**R**
AZM	14	15	22	73
AK	5	15	80	9
NA	20	25	66	9
CIP	20	33	9	11
F	45	66	11	38
IPM	40	7	5	0
DO	11	11	56	28
SXT	83	40	88	4
AMC	89	55	74	88
AM	86	60	62	90

Resistance percentages of *E.coli* isolates to Azithromycin were (14%) , Amikacin (5%) , Nalidixic acid (20%) , Ciprofloxacin (20%) Nitrofurantoin (45%) , Imipenem (40%) , Doxycycline (11 %) , Trimethoprime / sulphamethoxazole (83%), Amoxicillin/calvulanic (89%) and Ampicillin (86%) .

This may be attributed to *blaCTX-M type especially blaCTX-M-1, blaCTX-M-2, blaCTX-M-8, blaCTX-M-9 , blaCTX-M-15. blaCTX-M-27* (Birgy *et al*., 2020 ; Hassuna *et al*., 2020) , and attributed to *bla-TEM* , *bla-SHV* , *blaOXA , AmpC* (Esmaeel *et al*., 2020 ; Gajamer *et al*., 2020 ; Naziri *et al*., 2020 ; Pandit *et al*., 2020 ; Sadeghi *et al*., 2020) . Carbapenem-resistant *E. coli* isolates may be due to *blaKPC-2* and *blaNDM-1* (De La Cadena *et al*., 2020). Additionally the resistance to

more than one antibiotics may be attributed to efflux pumps (Al-Zuhairy and Al-Dahmoshi , 2020) .

The percentage of *K. pneumoniae* that resisted to Azithromycin were (15%) , Amikacin (15%) , Nalidixic acid (25%) , Ciprofloxacin (33%) Nitrofurantoin (66%) , Imipenem (7%) , Doxycycline (11%) **,** Trimethoprime / sulphamethoxazole (40%), Amoxicillin/calvulanic (55%) and Ampicillin (60%) .

Resistance of *K. pneumoniae* to beta-lactam also may be mediated by beta-lactamases like *blaOXA-48 , blaKPC , CTX-M-15 , blaAmpC* (Gurung *et al*., 2020 ; Fils *et al*., 2021; Kurittu *et al*., 2021 ; Xiong *et al*., 2021) . ESBL producers represented one-third of *E. coli , K. pneumoniae* UTI episodes (Vachvanichsanong *et al*., 2021) . Current treatment options for UTIs due to ESBL-producing Enterobacteriales include nitrofurantoin, fosfomycin, fluoroquinolones and carbapenems (Bader *et al*., 2020) .

The percentage of *E . faecalis* that resisted to Azithromycin were (22%) , Amikacin (80%) , Nalidixic acid (66%) , Ciprofloxacin (9%) Nitrofurantoin (11%) , Imipenem (5%) , Doxycycline (56%) , Trimethoprime / sulphamethoxazole (88%), Amoxicillin/calvulanic (74%) and Ampicillin (62%) .

Besides their possession of several virulence factors, members of the genus Enterococcus also have inherent capacity to accumulate and dissem-inate antibacterial resistance determinants (Sartelli *et al*., 2016) . The emergence of antibiotics resistant and virulent Enterococci are a major public health concern (Golob and Rao , 2021) . β Lactam antibiotics not have bactericidal action against enterococci as it used as mono therapy, that making the treatment of systemic infections mostly challenging (Reddy *et al*., 2012) . Ciprofloxacin is approved for use for

both uncomplicated and complicated urinary tract infections, including cystitis, pyelonephritis, and chronic bacterial prostatitis (Sattari-Maraji *et al*., 2019 ; Jiang *et al*., 2021) .

The isolates of *S.saprophyticus* that resisted to Azithromycin were (73%) , Amikacin (9%) , Nalidixic acid (9%) , Ciprofloxacin (11%) Nitrofurantoin (38%) , Imipenem (0%) , Doxycycline (28%) , Trimethoprime / sulphamethoxazole (4%) , Amoxicillin/calvulanic (88%) and Ampicillin (90%) .

According to the CLSI, routine susceptibility testing of urinary *S. saprophyticus* isolates to choose antibiotics is not recommended as this microorganism is normally susceptible to trimethoprim/sulfamethoxazole (Jancel and Dudas , 2002) . However, 7 % of the *S. saprophyticus* isolated from UTIs were resistant to sulfamethoxazole/trimethoprim. Similar to our results, 17.6 % of the *S. saprophyticus* isolates were resistant to sulfamethoxazole / trimethoprim (Ferreira *et al*., 2012) . Many researchers reported that isolated *S. saprophyticus* from hospital and farm were resistant to β-lactams, macrolides, lincosamides, and many other antibiotics (Waller *et al*., 2011; Dziri *et al*., 2016) .

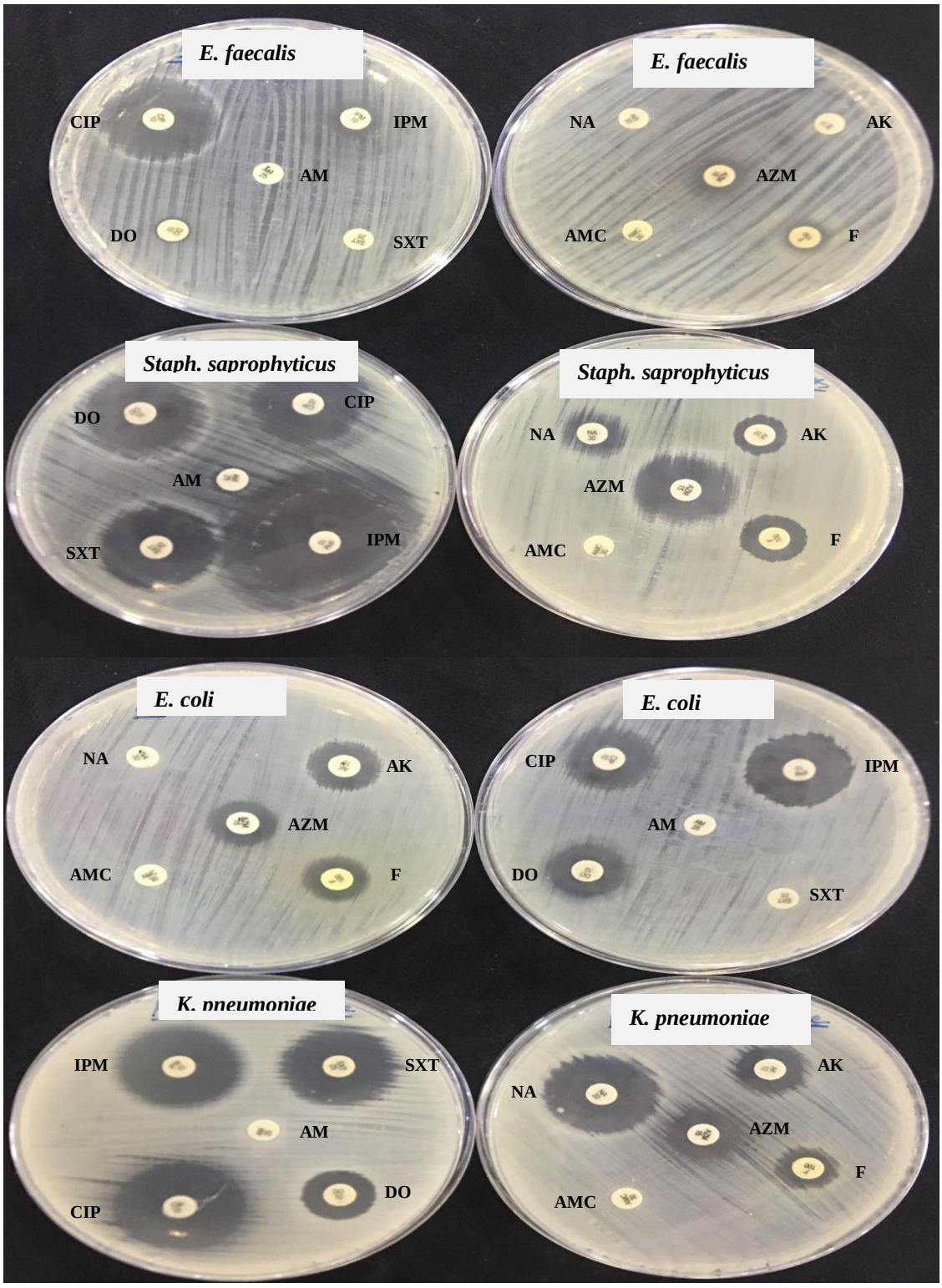

Figure (4.2): Antibacterial activity of antibiotics against pathogenic bacteria on MHA at 37 º C for 24 hr .

4.3 Molecular Identification of *Bacillus clausii*

DNA templates that extracted in (3.2.8.1) were used in the amplification of 16sRNA gene using 16sRNA gene universal primers in (table 3.6). The product then was electrophoresed on agarose gel and documented on gel document. The resulted 16s rRNA bands were 1470bp as shown in (figure 4.3) . After that the sample sent to gene sequence . Sequences for *Bacillus clausii* strain were received online and aligned to NCBI data base using Blast software , multiple aligned to each other using BioEdit software and submitted in fasta format to NCBI through Sequence software as in **(** Berber and Çetinkaya , 2021**)** .

Later pairwise alignment were investigated for *Bacillus calusii* 16sRNA gene sequences . The isolate was found to be nearest and neighbour to *Bacillus clausii* strain (4G219) with Score 1594 bits(863) , Expect 0.0 , Identities(93%) , and Gaps (1%) which rooted to bacillaceae. Accession number: MK496620, GenBank , figure (4.4).

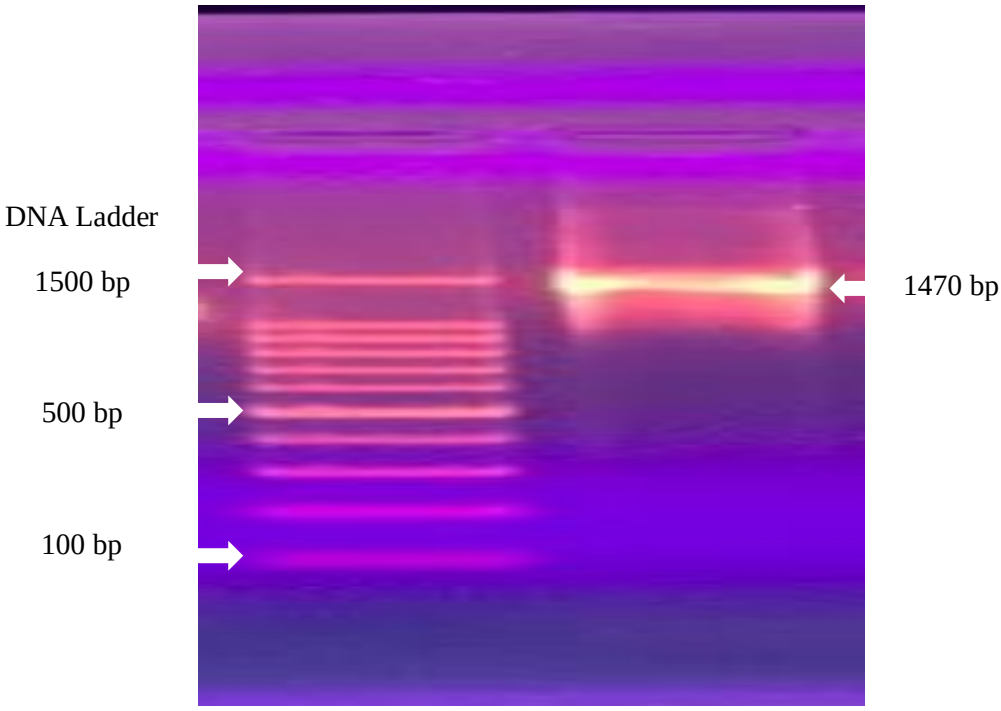

Figure (4.3) : Agarose gel electrophoresis of PCR product for 16S rRNA amplicon bands of *Bacillus clausii* with size 1470bp , at 1.5 % Agarose 75 volt and 40 min .

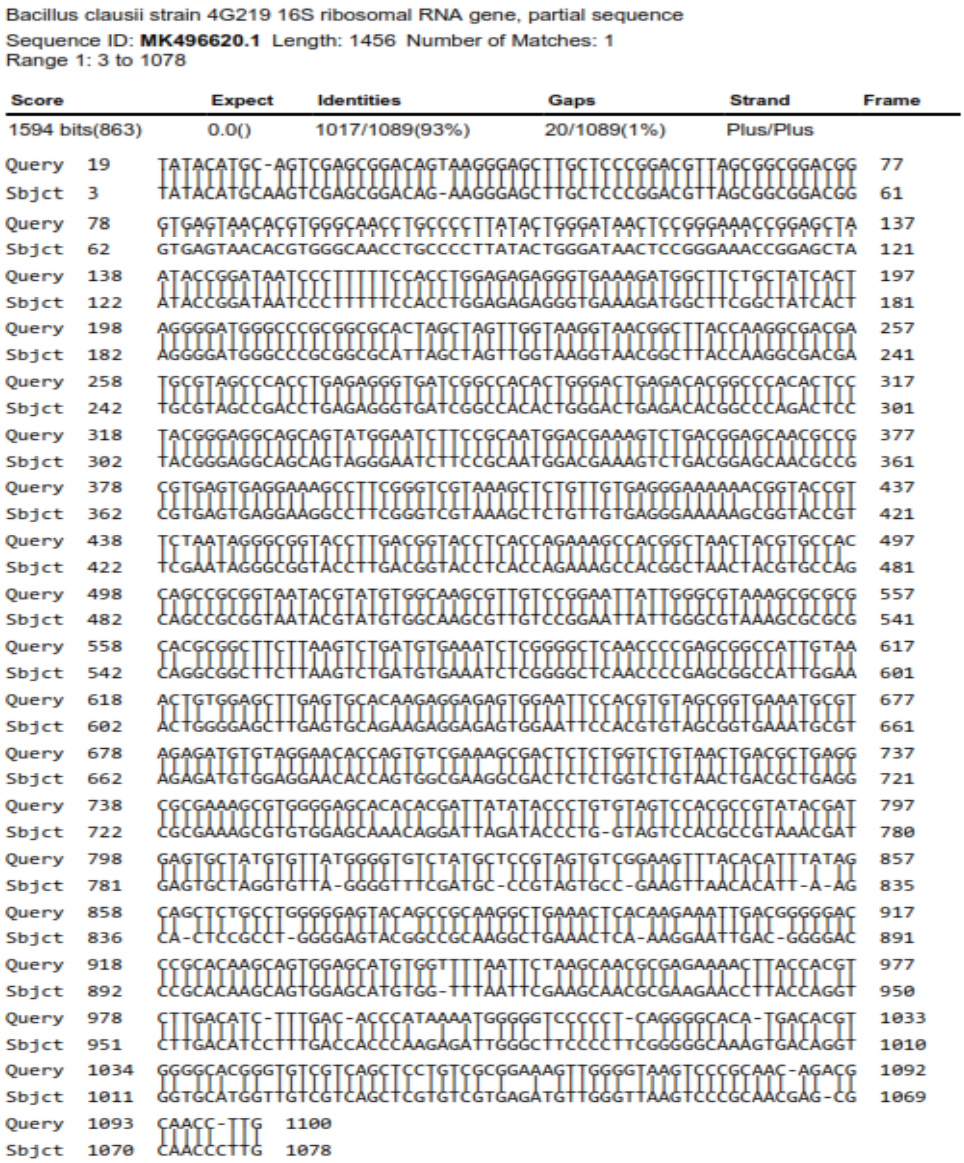

Figure (4.4) : Pair-wised alignment of partial nucleotide sequence of 16S ribosomal RNA gene (Query) to that of *Bacillus clausii* strain 4G219 whose sequence producing highest score (93%) of homology during BLASTn search .

4.4 Biosynthesis of Selenium nanoparticles by using *Bacillus clausii*

Bacillus clausii, which was used in the biosynthesis of SeNPs, demonstrated the ability of extracellular biosynthesis by using cell free supernatant after the addition of Na_2SeO_3 as a substrate under previously optimized conditions. The color changes of the reaction mixture from yellow to red , as in Figure (4.5) after incubation in shaking incubator (150

rpm) at 37 °C for 48 hr , as well as the color change and antibacterial behavior of SeNPs served as indicators for the biosynthesis of SeNPs by *Bacillus clausii* .

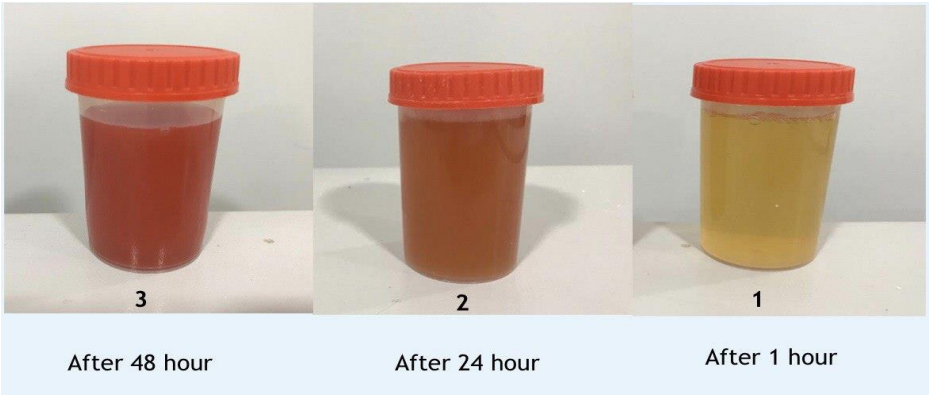

Figure (4.5) :Biosynthesis of SeNPs using *Bacillus clausii* at 37 ° C , 48 hr in aerobic condition .

Partial purification of SeNPs was done through three steps and then dried in oven for further experiment , as in figure (4.6) .

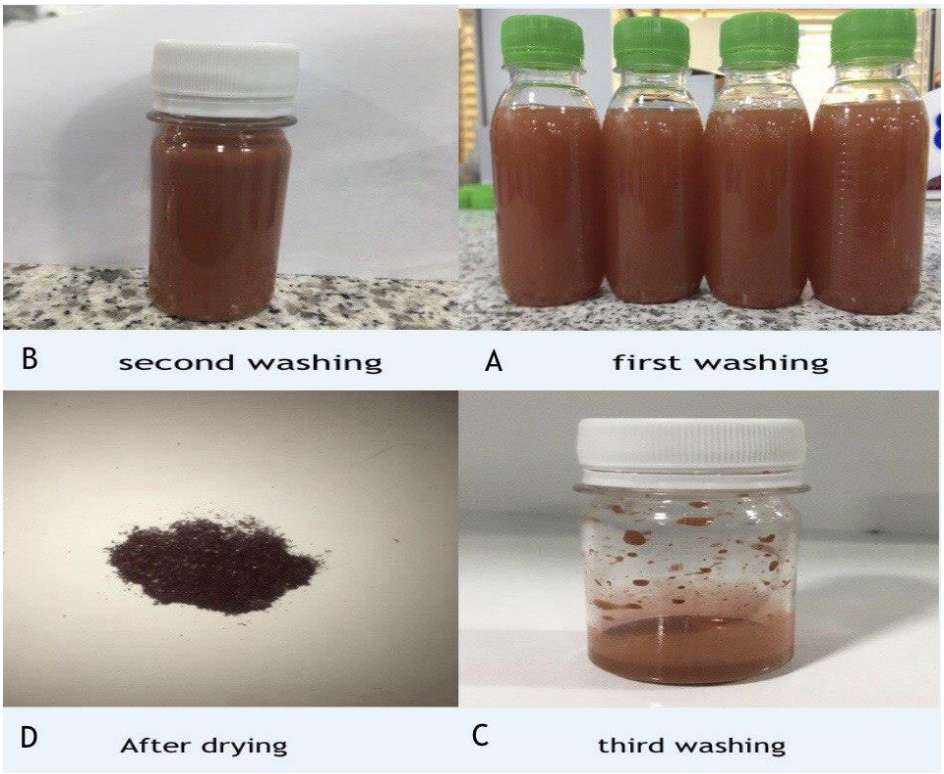

Figure (4.6) : Steps of partial purification of SeNPs .

In the present study , an attempt was made to employ the biosynthesis of SeNPs from *Bacillus clausii* which was recorded in the NCBI as in an economic and easy way. The appearance of color is a clear indication to formation of selenium nanoparticles in the reaction mixture due to reduction of SeO^{2-} ions to red Se^{0} , and it is suggested that the color change was because of the excitation of the SPR (Surface plasmon resonance) . Because of SPR, the reaction mixture color changed from yellow to red . Those findings are similar to the results of (Abbas *et al*., 2021 ; Ullah *et al*., 2021) .

From available reports, these potentially active compounds have been elucidated as reducing and stabilizing agents (Khanna *et al*., 2019) .

Bacillus subtilis BSN313 reduced the soluble, toxic, colorless selenium ions to the insoluble, non-toxic, red elemental SeNPs . It has been recorded that *Bacillus* extracts contain potent biomolecules such as small peptides , proteins, alcohols, phenols, phycocyanins, esters, and amines, which can act as reducing and stabilizing agents (Ullah *et al*., 2021) . These biomolecules, definitely, facilitated and participated in the reaction with SeO_3^{2-} to produce SeNPs (Shirsat *et al*., 2015) .

It is significant to note that selenium nanoparticle producing bacteria are reported in wide range of environments under aerobic and anaerobic conditions including in sludge and sewerage (Mishra *et al*., 2011) . The anaerobic/anoxic bacteria include strains such as *Rhodopseudomonas palustris* N (Li *et al*., 2014), *Veillonella atypica* (Pearce *et al*., 2008), *Shewanella putrefaciens* 200 (Jiang *et al*., 2012), *Shewanella* sp. HN-41 (Ho *et al*., 2021) .

In comparison with the anaerobic bacteria, the phenomenon is mostly cited in aerobic , Gram +ve *Bacillus* species such as *Bacillus laterosporus* (El-Batal *et al*., 2014) , *Bacillus licheniformis* (Khiralla and El-Deeb , 2015) , *Bacillus* sp. MSh-1 (Shakibaie *et al*., 2015) , *Bacillus*

cereus (Kora , 2018) , *Bacillus tropicus* Ism 2 (MK332444)(EL-Baghdady *et al*., 2019) , *Bacillus megaterium* (Hashem *et al*., 2021) , *Bacillus subtilis* 168 (Jia *et al*., 2022) .

4.5 Characterization of selenium nanoparticles

4.5.1 UV-visible Spectroscopy

UV- Visible spectrophotometric is a proven technique for detecting the nanoparticles. After 24 hours of incubation of the reaction mixture, color change was observed which indicated the formation nanoparticles in the reaction mixture .The biosynthesis of nanoparticles can be confirmed by visual observation and measuring the absorbance band using UV-visible spectroscopy in the region of 200-1100 nm. Single peak was at 260 nm (Figure 4.7) .

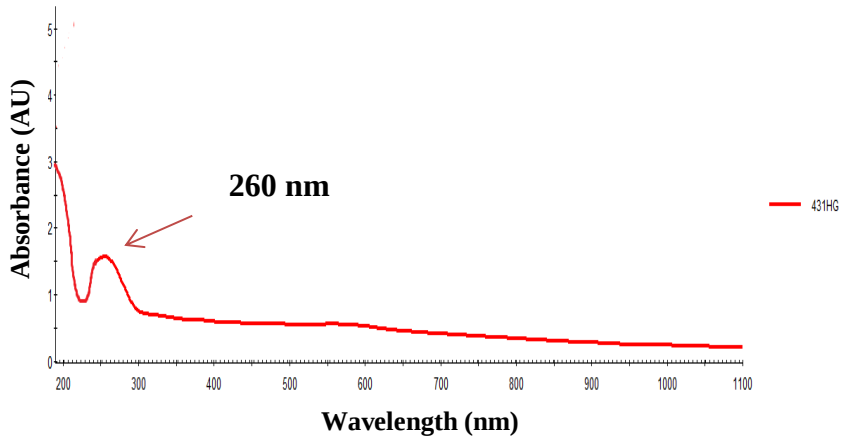

Figure (4.7) : UV- Visible Spectophotometry of the selenium nanoparticles

Various reports have confirmed that the resonance peak of selenium nanoparticles appears around this region, but the accurate position depends on several factors such as particle's size, shape, and material composition, as well as the local environment (Joshi *et al*., 2008) . There were a lot of study about SeNPs formation have various absorption peaks in UV-vis spectra indicate to a presence of SeNPs (Hemalatha *et al*., 2014) .

The peak appeared at nearby 362 nm and have a maximum absorption peak at 650 nm (Ullah *et al*., 2021) , strong absorption band

located at 265 nm , 265.5 nm , respectively (Santanu *et al*., 2015 ; Shubharani *et al*., 2019) , and the peak was seen at around 263 nm confirming the formation of the spherical SeNPs (Satgurunathan *et al*., 2017 ; AbouElmaaty *et al*., 2021). In a study conducted by Tabibi and his colleagues, the light absorption of selenium nanoparticles in the UV-Vis method was 294 nm (Tabibi *et al*., 2020) , while the UV-Visible absorption spectra of SeNPs recovered from the culture broth gave a characteristic peak at 590 nm which corresponds to the large particle size of 182.8 ± 33.2 nm (Lin and Wang , 2005) .

4.5.2 Analysis by Field Emission scanning electron microscopy (FESEM)

SEM was used to confirm the morphology and size of the selenium nanoparticles , rod shape selenium nanoparticle synthesized by *Bacillus clausii* with a size range between 37.58 – 75.16 nm were reported . Figure (4.8) representative SEM micrograph of SeNPs .

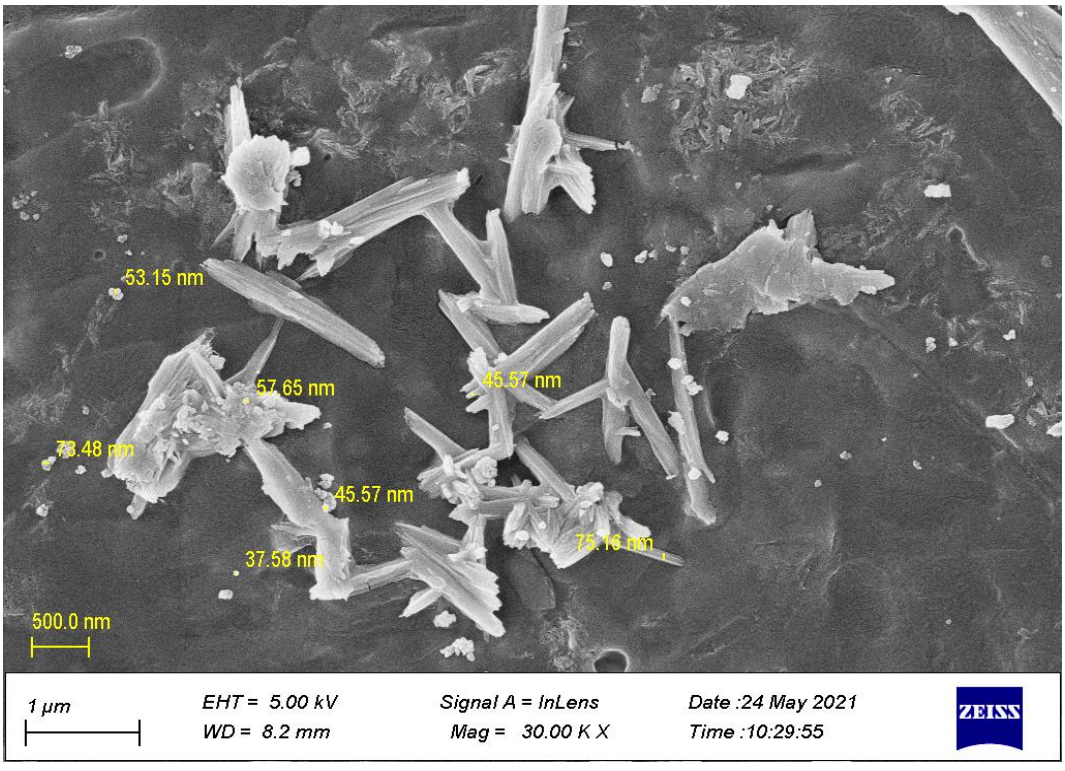

Figure (4.8) : FESEM Micrograph of selenium nanoparticles

SEM is a type of electron microscope that takes the image to the sample by scanning with a high-energy beam of electrons in a raster scan pattern. The electrons interact with atoms that can make up the sample producing signals that hold information about the sample's surface topography, composition, and other properties such as electrical conductivity (Verma and Maheshwari , 2018) .

The sizes and shapes of biogenic metallic nanoparticles can be controlled by exchanging the bio-reduction conditions, including type of culture and organism, nature of the medium and incubation time (Vetchinkina *et al*., 2019) .

Rods-shape of SeNPs showed similarity with result that cited by (Ramamurthy *et al*., 2013 ; Wadhwani *et al.*, 2017 ; Ashengroph and Tozandehjani , 2022) . Whereas spherical shape were reported by (Pouri *et al*., 2018 ; Vetchinkina *et al*., 2019 ; Arunthirumeni *et al*., 2022) . Nowadays, numerous microscopic techniques are commercially available, whenever transmission electron microscopy and SEM are the most popular microscopes for the analysis of the nanoparticles (Verma and Maheshwari, 2018) .

4.5.3 Analysis by energy dispersive X-ray spectroscopy (EDX)

Elemental analysis of SeNPs was established via the EDX coupled SEM. EDX spectrum was presented in table (4.3) , Figure (4.9) . A strong signal appeared from Se atom (53.31 %) , followed by C atom (22.99%) , O atom (18.36%) , P atom (2.27 %) , Ca atom (1.55 %) , K atom (0.39 %) , Mg atom (0.48%) , S (0.43 %) and Na (0.21 %) .

The detection of some atoms as impurities may be related to the presence of remained of *Bacillus clausii* , which was not fully removed after purification . In addition, SeNP oxidation in air before the sample

analysis may be the cause of oxygen detection as sample impurity (Cojocaru *et al*., 2016).

Table (4.3) : signals that observed from the energy-dispersive X-ray analysis .

Element	Line Type	Weight %	Weight % sigma	Atomic %
C	K series	22.99	0.28	4.82
O	K series	18.36	0.35	18.99
Se	L series	53.31	0.50	73.46
P	K series	2.27	0.07	1.21
Ca	K series	1.55	0.06	0.64
K	K series	0.39	0.04	0.17
Mg	K series	0.48	0.05	0.33
S	K series	0.43	0.05	0.22
Na	K series	0.21	0.04	0.15
Total		100.00		100.00

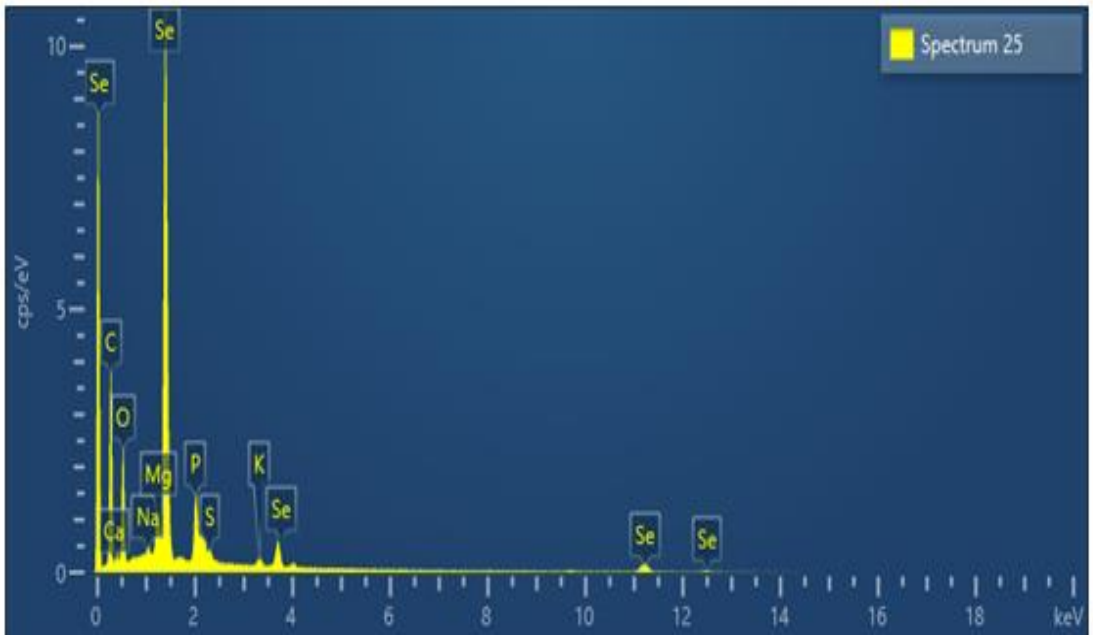

Figure (4.9) : EDX of selenium nanoparticles

Three signals from the energy-dispersive X-ray was found , Se (50.79%) , O (35.55%) and C (13.66%) (Alagesan and Venugopal , 2019) **.** Wherese the EDXS profile showed strong selenium signal 92.76% along with weak sulfur group peaks 7.24% , which confirms the presence of sulfur containing protein/peptide molecules bound to the surface of the nanoparticles (Syed *et al*., 2013) .

4.5.4 Atomic force microscope(AFM)

AFM imaging validated the shape and surface topography of the Selenium NPs. The height measurements were able to provide the elevation of nanoparticles with a high point of precision and accuracy. The average diameter of SeNPs was 19.28 nm which was compatible with the results of (Singh *et al.*, 2014). Three - dimension images, and granularity accumulation distribution charts of SeNPs were shown in (Figure 4.10) .

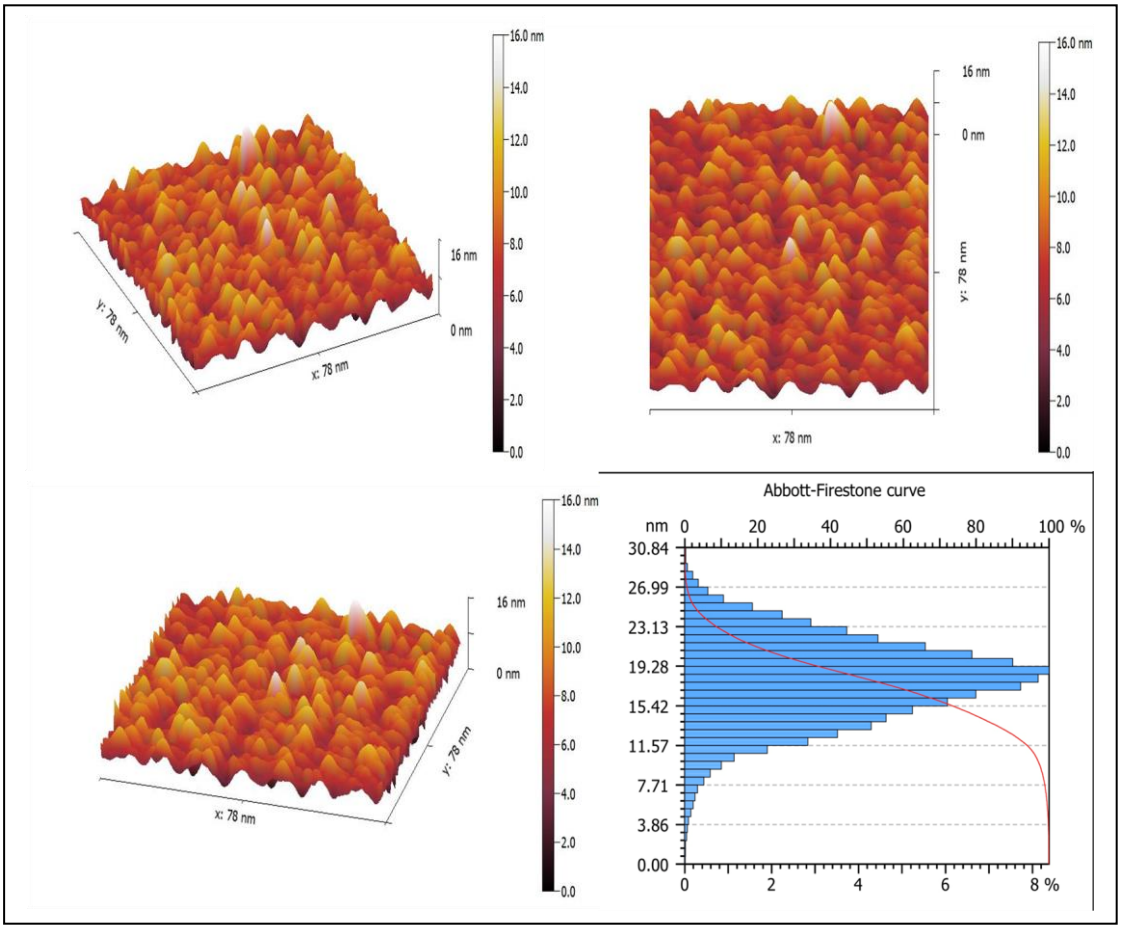

Figure (4.10) : AFM image of selenium nanoparticles

Moreover, the size of the selenium nanoparticles was found to be similar with the data collected from the XRD study , while the variation in size of nanoparticles was commonly found during chemical and biological synthesis . AFM images are obtained by detecting the attractive / repulsive

forces between the sample surface and a sharp probe for bio-effective component of selenium nano-Particles (Khoei *et al*., 2017) .

The image of the atomic force microscope showed the shape of the surface, the shape, and the size of the particles for the samples that have been identified. It also shows a two-dimensional (2D) and three-dimensional (3D) image of the sample (Al-Kazaz *et al*., 2021)

4.5.5. X-ray diffraction (XRD)

The formation of nanoparticles were characterized further by XRD analysis using Powder X-Ray Diffractometer . The studies showed a characteristic peak at 2θ value of 23.601, 29.896 and 44.015 , (appendices 6) , Figure (4.11).

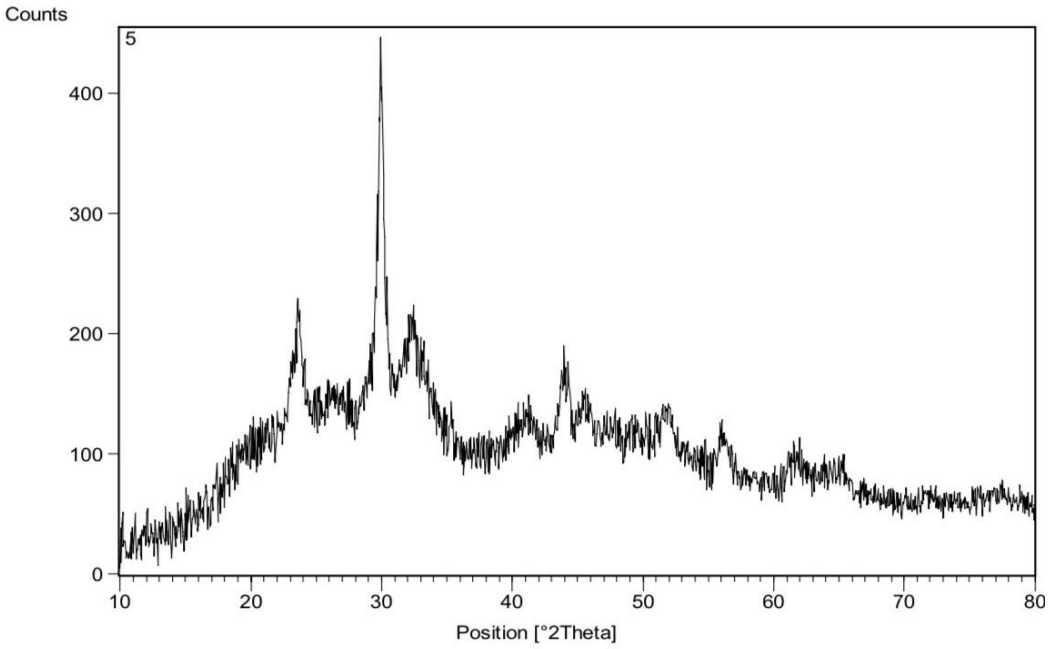

Figure (4.11) : XRD pattern of selenium nanoparticles

Some previous studies related to crystalline phase investigation of selenium nanoparticles suggested that stable amorphous forms (or even low crystallinity) are advantageous for biological applications, as they exhibit better solubility and subsequent adsorption and bioavailability (Cavalu *et al*., 2017).

In another study, XRD results showed that synthetic selenium nanoparticles are crystalline, which is a natural form (Shubharani *et al*., 2019) . However, in other experiments, the results showed that the synthetic selenium nanoparticles did not have any specific crystalline form, and amorphous was seen (Shakibaie *et al*., 2018 ; Borah *et al*., 2021) . The XRD analysis for the extracellular red elemental selenium indicated three intense peaks in the whole spectrum of 2θ values ranging from 5 to 80, the diffractions peak at 2θ value of 23.780, 29.797 and 43.878 can be indexed to the (100), (101) and (102) planes of the face-centered cubic (fcc) red elemental selenium (Singh *et al*., 2014)

The prepared SeNPs calculated crystalline size was 18.215 nm which was lower than the reported value of 41.5 nm by (Mellinas *et al* ., 2019) . The average crystalline size of synthesized SeNPs was calculated by using the Debye–Scherrer equation :

$$D = \frac{\mathrm{K} * \lambda}{\beta * \cos(\theta)}$$

where D is the crystal size , K is a constant whose value is approximately 0.9, λ is the wavelength of the X-ray, β is the full width at half maximum (FWHM) of the peak in radians, and θ is the Bragg's diffraction angle in radians. .

4.5.6. Fourier Transform Infrared Spectroscopy (FTIR)

FTIR analysis was used to obtain information about chemical compounds involved in the reduction and stabilization of SeNPs **.** FTIR spectra of SeNPs showed the present of peak at 3335.96 cm^{-1} can be assigned to hydroxyl (OH) group . 2952.85 cm^{-1} , 2922.50 cm^{-1} and 2853.17 cm^{-1} were assigned to (C-H stretching) , 2726.72 cm^{-1} (present of aldehyde) , 1632.39 cm^{-1} present of (C=C stretch binding carbonyl stretch protein) . 1516.55 cm^{-1} , 1502.78 cm^{-1} associated with aromatic nitro

compounds . 1462.11 cm^{-1} , 1455.69 cm^{-1} and 1376.95 cm^{-1} associated with C-H bend , 1046 cm^{-1} , 721.83 cm^{-1}, 558.51 cm^{-1} , 470.29 cm^{-1} corresponded to (Se−O) , (appendices 7) , Figure (4.12).

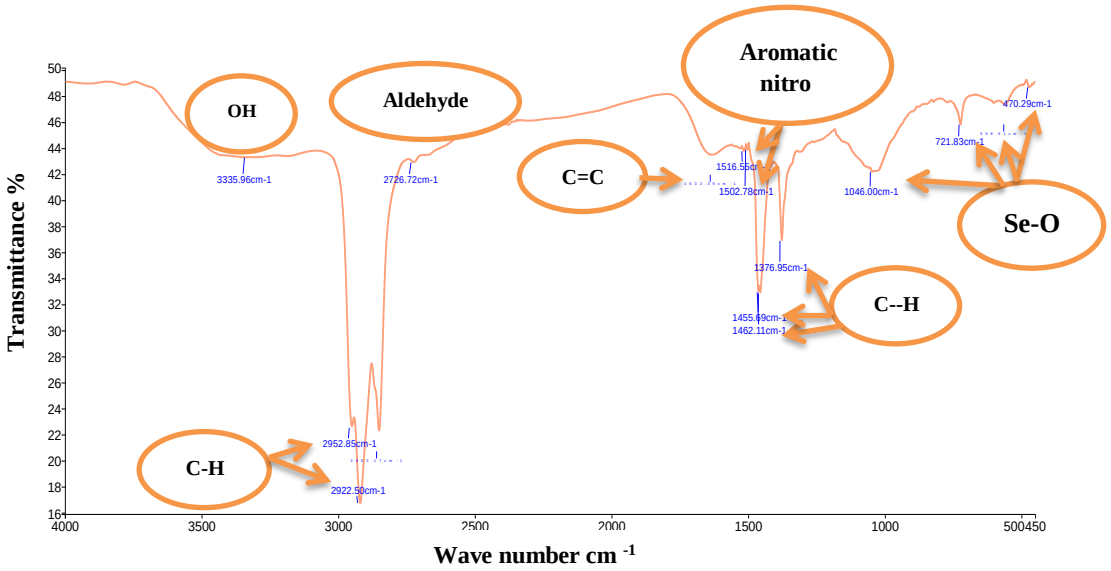

Figure (4.12) : FTIR of selenium nanoparticles

These results indicate the presence of various functional groups as biomolecules such as hydroxyl groups in polyphenols and amide groups in proteins having a key role in the reduction of selenium ions to their element and in the stabilization of the formed SeNPs (Fardsadegh *et al.*, 2019) .With the overall observations, it can be concluded that the proteins might have formed a capping agent over the SeNPs, which may response for their stabilization (Sonkusre *et al.*, 2014) .

In particular, Lenz and co-workers showed that selenium nanoparticles can be bounded with a variety of high-affinity proteins (Lenz *et al.*, 2011). In addition, proteins and other biomolecules such as polysaccharides and fatty acid may play a key role in controlling SeNPs size and morphology (Dobias *et al.*, 2011) . The strong intensity peaks 465 cm^{-1} , 668 cm^{-1} , 1051cm^{-1} which were due to the bending vibration of Se-O bonds were verified by (Cavalu *et al.*, 2017) .

4.6 Influence of Selenium Nanoparticle Against pathogenic bacteria

Biogenic SeNPs synthesized by *Bacillus clausii* were evaluated for their antibacterial activity against some pathogenic bacteria . The agar well diffusion method was used for detecting the antibacterial activity of biogenic SeNPs. SeNPS with different concentrations (100, 300, 500 µg/ml) showed inhibition activities against all tested bacteria. The highest inhibition zone of SeNPs observed in concentration (500 µg/ml), while the lower inhibition zone observed in concentration (100 µg/ml) .This inhibitory effect increased when the SeNPs concentrations were increased from 100µg to 500µg , as in table (4.4).

Table (4.4) : Inhibition zone of SeNPs synthesis by *Bacillus clausii* against different bacteria on MHA at 37 °C for 24 hr .

Bacteria	Inhibition zone (mm)		
	(100 µg/ml)	(300 µg/ml)	(500 µg/ml)
E. coli	15	18	22
K. pneumoniae	18	19	21
E. Faecalis	18	21	25
S. Saprophyticus	17	20	23

After that , the MIC was detected by microtiter plate method . Different concentration of SeNPs ranging from (2 µg/ml -1024 µg/ml) were used .The minimum inhibitory concentration of nanoparticles (MIC) was calculated after the incubation of the microtiter plate for 24 hours at 37 °C (OD 570 nm) . A concentration which prevents growth of bacteria is considered the lowest concentration (MIC) . MIC (32 µg/ml) , MBC (64 µg/ml for *E. Faecalis* and *Staphylococcus saprophyticus*, while MIC and MBC for *Klebsiella pneumoniae* and *Escherichia coli* were (64 µg/ml) and (128 µg/ml) , respectively , table (4.5) .

Table (4.5) :MIC and MBC of SeNPs by microtiter plate against pathogenic bacteria

Test organisms	Minimum Inhibition Concentration (MIC) of SeNPs (µg/ml)	Minimum bactericidal concentration (MBC) of SeNPs (µg/ml)
E. coli	64	128
***K. pneumonia*e**	64	128
E. Faecalis	32	64
S. Saprophyticus	32	64

The application of nanoparticles and metal-based antibacterial strategies is one of the promising approaches to prevent diseases caused by antibiotic-resistant microbes (Chudobova *et al*., 2014). Previous studies indicated that SeNPs have more . Bacteriostatic effect than bactericidal action on microbes (Al Jahdaly *et al.*, 2021) .Our results showed that SeNPs synthesized by *Bacillus clausii* exhibited antibacterial effect towards both Gram-positive and Gram-negative bacteria . The antibacterial activity of chemically and biologically synthesized SeNPs was evaluated before, but with different methodologies and particle sizes , Nevertheless, the chemically synthesized SeNPs showed weaker antibacterial activity than the biogenic SeNPs (Zonaro *et al.*, 2015 ; Cremonini *et al*., 2016) .

Because of the thinner peptidoglycan layer and the presence of porins , selenium nanoparticles have higher antibacterial activity against gram positive bacteria . Moreover, SeNPs were found to have double effect against *Staphylococcus aureus* as silver nanoparticles (7 and 3 mm, respectively) (Chudobova *et al*., 2014) . While other studies demonstrated better antibacterial activity against *Pseudomonas sp*. than *Staphylococcus aureus*, and it failed to demonstrate activity against *Escherichia coli* and *Klebsiella sp* (Singh *et al*., 2014) . Moreover, 200 µg/mL of SeNPs showed antibacterial reactivity against *Escherichia coli* ATCC

8739, *Staphylococcus aureus* ATCC 9027, and *Pseudomonas aeruginosa* ATCC 25923 (Ullah *et al*., 2021) . The morphology of nanoparticles also plays the important role in its effectiveness against microbial species (Hong *et al*., 2016 ; Cheon *et al*., 2019) .

The difference between the findings of different studies is mainly due to the difference in the size of nanoparticles and the type of bacteria used . One of the most important factors affecting the antibacterial properties of nanoparticles is the particle size and concentration. It was considered that smaller nanoparticles had increased the production of ROS than larger surface area to volume ratio inside or out of the cells (Van Khanh and Van Cu , 2019) .

The use of nanoparticles as antibacterial agents is a promising strategy, especially when dealing with chronic and nosocomial infections. The widespread usage of commercial antibiotics has led to the development of multidrug-resistant bacterial strains . Generally, various mechanisms of nanoparticles antibacterial activity were recognized up to now: ROS generation, interaction with cell barrier (cell wall disruption and alteration in permeability), inhibition in the synthesis of proteins and DNA, expression of metabolic genes, etc. (Eleraky *et al*., 2020) .

Negatively charged SeNPs, exhibit more pronounced activity against Gram-positive bacteria, due to the absence of negatively charged LPS particles in their cell walls and thus the absence of the mentioned electrostatic repulsion (Filipović *et al*., 2021) .Given that the same behavior was observed for positively charged formulations of SeNPs, we can conclude that the electrostatic interaction between SeNPs and the bacterial cell barrier is not a critical step in determining their antibacterial activity. Negatively charged regions on Gram-negative bacteria's cell walls are insufficient to ensure the attachment of positively charged SeNPs

(Angeliki , 2021) . However, the low cytotoxic effect of biogenic SeNPs has been reported by (Forootanfar *et al*., 2014 ; Abbas *et al*., 2021).

4.7 Synergistic effect of SeNPs and antibiotic

The synergistic effect of SeNPs was investigated with six antibiotics (Azithromycin , Ciprofloxacin , Trimethoprime / sulphamethoxazole Doxycycline , nitrofurantoin and Ampicillin) against pathogenic bacteria. However, the mechanism for the synergistic activity is not known .

The synergistic effect of Doxycycline with SeNPs in all tested bacteria that sensitive to Doxycycline were decreased , and the isolates that were sensitive to antibiotic became intermediate and intermediate became resistant to antibiotic . while in *E. faecalis* only the effect of SeNPs were appeared when Doxycycline saturated with SeNPs .

The inhibition zone of nitrofurantoin when saturated with SeNPs were decreased in *Escherichia coli* , while in *Klebsiella pneumoniae* , *Enterococcus faecalis and Staphyllococcus Saprophyticus* the sensitivity remained same . As for the other antibiotics, some of them showed a slight increase in the diameters of inhibition , while others did not have any synergistic action between them and SeNPs , figure (4.13) .

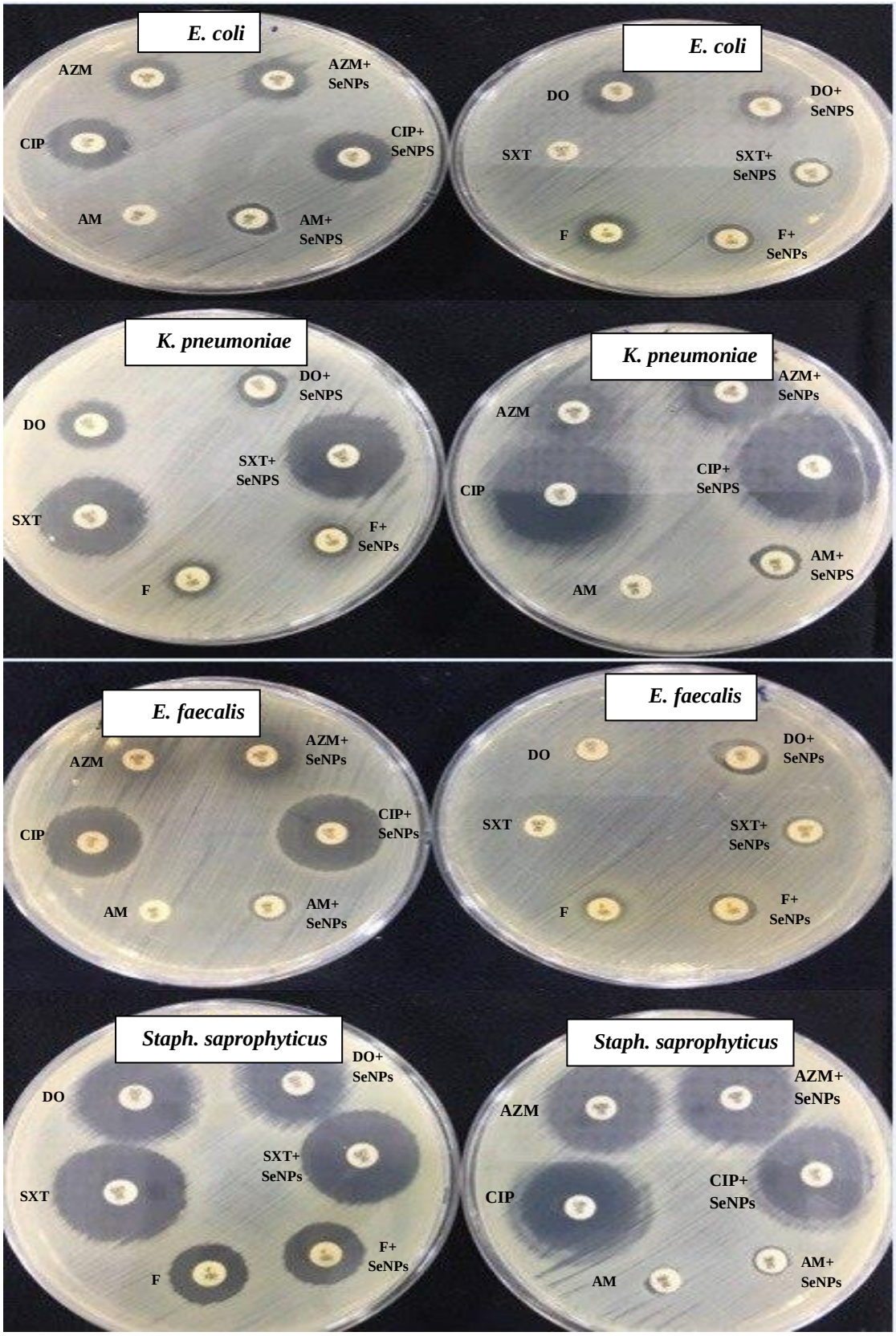

Figure (4.13): Antibacterial activity of SeNPs that combination with antibiotics against pathogenic bacteria on MHA at 37 º C for 24 hr.

Antibacterial combinations are used widely, although most infections in patients with normal defenses can be treated with a single antibacterial agent. Few reasons justify the use of antibacterial combinations: (1) broad-spectrum coverage for the initial therapy of severely infected patients; (2) poly-microbial infections; (3) prevention of selection of resistant microorganisms when a high mutation rate of the causal organism exists to the antibiotic indicated; (4) reduction of dose-related toxicity – this concern is rare and mostly of historical interest, related to the use of sulfonamides; and (5) antibacterial synergistic activity (Acar , 2000) . The emergence of antibiotics resistance in the majority of pathogenic bacterial strains is a cause of utmost concern in infectious bacterial diseases. Therefore, there is an inevitable need to identify the effective antibacterial agents which are more effective against microbial ailments with minimal side effects on host cells (Caruso and Poon , 2018).

Synergism is associated with the generation of hydroxyl radicals, alteration of protective cellular functions and an anti-biofilm potential. The combination of antibiotics with nanoparticles is more effective for enhancing antibiotic efficacy in comparison with the action of antibiotics when used in clinical practice. The combination involves reduced development of bacterial resistance, reduce the duration of treatment and reduce antibiotic dose requirements (Hwang *et al*., 2012) .

Nanoparticles enhanced the reaction rates of antibiotics in a synergistic mode as well as in its own way on different kinds of pathogens (Varak and Priya , 2019). Selenium (Se) is considered a potent antibacterial agent, and its derivative substance like selenium sulfide is extensively used in medicine to treat infections of microorganisms (Sadalage *et al*., 2020). However, overuse of Se causes toxic effects and leads to selenosis, which limits the use of elemental Se for therapeutic purposes (Ungvári *et al*., 2014 ; Gunti *et al*., 2019).

The probable mechanism responsible in enhanced antibacterial activity of antibiotics with selenium nanoparticles may be attributed to the bonding reaction between nanoparticles and antibiotics, then the antibiotic-selenium nanoparticle combination may attach on the cell membrane result in cell wall lysis, which was followed by the entry of SeNPs-antibiotic combination into the cell and may result in the DNA unwinding leads to cell death, the same mechanism suggested with silver nanoparticles and antibiotics (Krishna *et al*., 2015).

Ampicillin, oxacillin and penicillin caused higher inhibitory effects (44%, 8% and 13% respectively) when applied in combination with SeNPs than ATBs alone (Cihalova *et al*., 2015) . SeNPs can target the bacterial cellular membrane of *Staphyllococcus aureus*, SeNPs and LZD would have a synergistic effect (Nguyen *et al*., 2017) .

Tetracyclines such as doxycycline are thought to inhibit translation by binding to the 16S rRNA portion of the ribosome preventing binding of tRNA to the RNA-30S bacterial ribosomal subunit, which is necessary for the delivery of amino acids for protein synthesis. As a result of the above actions, the initiation of protein synthesis by polyribosome formation is blocked. This stops the replication of bacteria and produces a bacteriostatic effect (Suáreza *et al*., 2014 ; Chukwudi , 2016).

The cell walls of gram-negative bacteria are complex than those of gram positive bacteria, both structurally and chemically. The structure of gram-negative microorganisms cell contains two layers outside the cytoplasmic membrane , which represent a greater physical barrier to overcome. This structural complexity explain greater inhibitory effect of the derivatives against gram-positive bacteria (Alvand *et al*., 2022).

Another explanation may be attributed to binding of the hydrophobic groups incorporated into nanoparticle to the teichoic acid, a

structure present in gram positive bacteria, but absent in gram-negative bacteria, which may lead to death (Pasquina *et al*., 2013) .

4.8 Antioxidant assay of SeNPs

The DPPH (2,2-Diphenyl-1-picryl- hydrazyl) radical scavenging assay was used to detect the antioxidant ability of the SeNPs biosynthesized from *B. clausii* in *vitro* by reducing DPPH free radicles . After adding of SeNPs to (0.1 mmol/L) DPPH solution , the absorbance (A) was measured at 517 nm after 30 minutes. The results revealed the ability of nanoparticles to scavenge DPPH free radicals , indicated by observing the color change from the original color of DPPH purple into yellow color in microtiter plate . The activity of SeNPs to reducing DPPH increased with the increas e of SeNPs concentration . It was 39.6 % in 50 µg/ml , 63.1 % in 100 µg/ml, 74.2 % in 150 µg/ml , Figure (4.14).

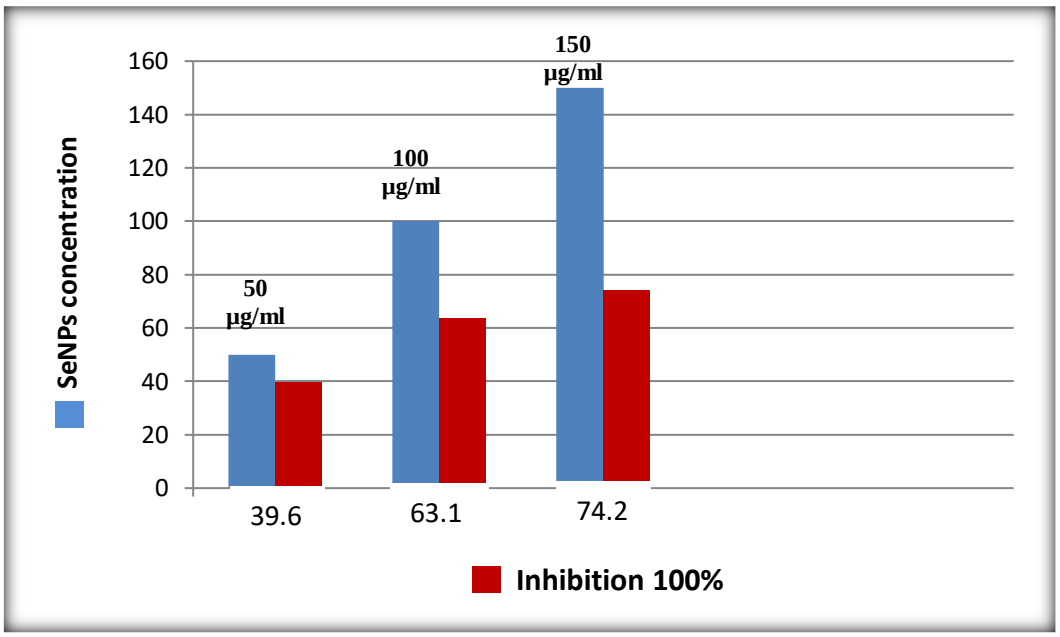

Figure (4.14) : antioxidant activity of Selenium nanoparticles .

According to previous reports, SeNPs have a strong free radical scavengers that can be used as an active form of selenium in food supplements (Boroumand *et al*., 2019 ; Menon *et al*., 2019) . As mentioned before, the antioxidant capacity of NPs increased with the decrease in their dimensions (Shah *et al*., 2017) . This lead to the

hypothesis that, since the cleaning procedure affects the size of the NPs, it also has an impact on their antioxidant capacity. Stable DPPH radicals are widely used to evaluate the antioxidant activity of NPs (Pyrzynska and Pękal , 2013) .

Different mechanisms involved in the radical-antioxidant reactions may explain the difference in scavenging potentials of compounds . The mechanisms of antioxidants are not only by scavenging free radicals, but also by inhibiting production of free radicals (Niki , 2010).

4.9 Haemolysis Effect of SeNPs

The hemolysis was detected by using Triton X-100 as indicators of positive control. Sterile solution of phosphate buffer saline was used as a negative control . SeNPs with all concentration (50, 100,150 µg/ml) did not show any hemolysis for the tested whole blood, as shown in figure (4.15) .

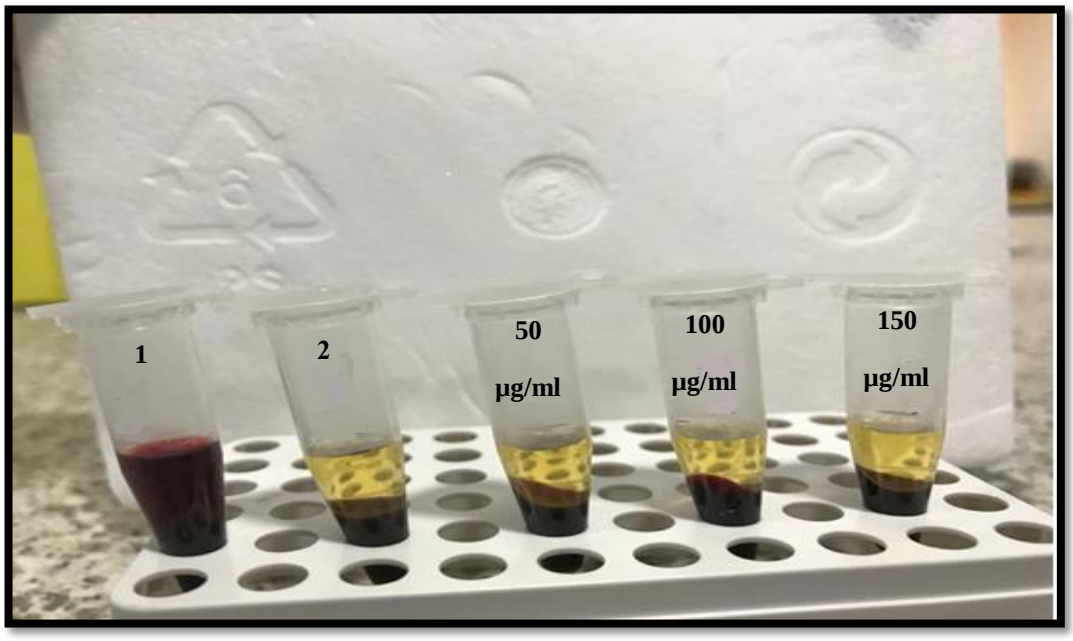

Figure (4.15) : Effect of selenium nanoparticles on hemolysis , 1 (positive control) , 2 (negative control).

Hemolysis is characterized by the rupture of red blood cells (RBCs) and the release of their contents, ultimately leading to anemia, jaundice

and renal failure . All materials entering the blood get in contact with RBCs and so the evaluation of the hemolytic ability of the biomaterials is of utmost importance (Archana *et al.*, 2013 ; Beris and Picard , 2015) .

earlier studies have reported the hemolytic properties of various nanoparticles such as gold , carbon nanotubes , iron oxide, silica , selenium , and silver nanoparticles (Ahn *et al*., 2018 ; Singh *et al*., 2019 ; Liu *et al*., 2020 ; Tsamesidis *et al*., 2020 ; Tang *et al*., 2021; Badmus *et al*., 2022).

SeNPs nanoparticles displayed very modest haemolysis, with only 18% of maximal lysis recorded in vitro (Tran *et al*.,2015) . A very low haemolysis rate (below 5%), showing that all of the produced NPs had good blood compatibility (Zou *et al*., 2021) . While , other research showed that hemolysis and RBC osmotic fragility tests doesn't induce damage to RBC membrane; The hemolysis values demonstrated good bio-compatibility, especially for titanium specimens changed with starch-derived Selenium NPs (Cavalu *et al*., 2018) .

4.10 Biofilm formation assay

By using Congo red method , out of 115 , 60 (52.1%) isolates gave a positive ability to form biofilm , *Klebsiella pneumoniae* (9) , *Escherichia coli* (34) , *Enterococcus. faecalis* **(**14) , *Staphylococcus Saprophyticus* (3) , figure (4.16) . The strength of biofilm formation were investigated by the Microtiter plate method , it is a quantitative method to determine biofilm production by spectrophotometer using an ELISA reader at a wavelength of 620 nm to give a final digital value representing the quantity of biofilms produced by the bacterial suspension in the wells and considered as a standard quantitative method .

Out of 34 isolates of *E.coli* , 25 (73.5 %) were strong biofilm producers , while 6 (17.6 %) were moderate biofilm producers , the remaining 3 isolates accounting for (8.8 %) of the total isolates were weak

biofilm producers . Out of 14 isolates of *E. faecalis* , 9 (64.2 %) were strong biofilm producers , while 3 (21.4 %) were moderate biofilm producers , the remaining 2 isolates accounting for (14.2 %) of the total isolates were weak biofilm producers . Out of 9 isolates of *Klebsiella pneumoniae* , 9 (100 %) were strong biofilm producers , and all 3 (100 %) isolates of *Staphylococcus Saprophyticus* were form strong biofilm , table (4.6) .

Table (4.6): Biofilm Production Capacity (OD 620 nm) of bacterial isolates

Bacteria	Biofilm degree		
	Strong	Moderate	Weak
E. coli	25	6	3
K. pneumonia	9	0	0
E faecalis	9	3	2
Staph. Saprophyticus	3	0	0

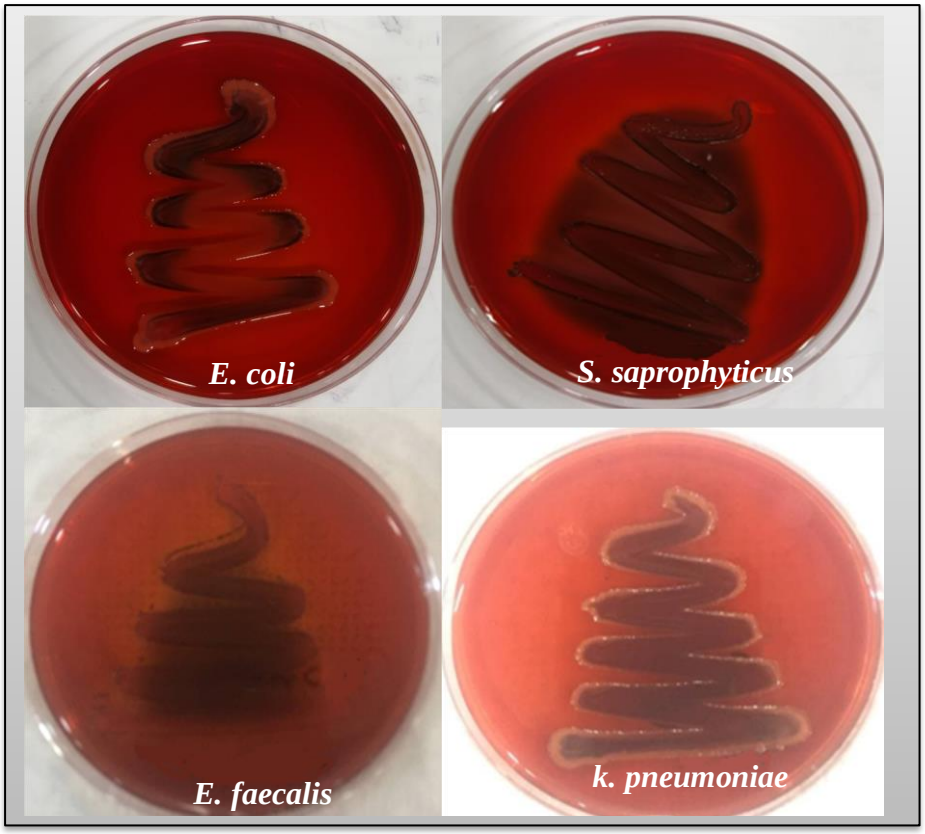

Figure (4.16) :Biofilm formation assay for gram positive and gram negative bacteria on Congo red agar at 37 º C for 24 hr .

Gram negative bacteria are greater than gram positive bacteria in biofilms formation (*Escherichia coli, Klebsiella pneumoniae* , *Enterococcus feacalis* , *Staphylococcus aureus* , *Proteus mirabilis* , *Pseudomonas aeruginosa* and *Citrobacter*) these biofilms were induced by urinary catheter infections (Almalki and Varghese , 2020) . Bacterial biofilms represented a significant source of human infections, which may be acquired through interaction with a wide range of everyday or clinical environments including the consumption of contaminated foods, via hospital environment, medical equipment or devices (Srey *et al*., 2013) .

Most *Klebsiella spp* isolates have potential to be attached in various grades and levels of biofilm production utilizing microtiter Plate methods on the smooth surface (glass and plastic surfaces) (Abood and Ibrahim , 2017) . Biofilms are defined as complex microbial communities enclosed in hydrated extracellular polymeric substances (EPS), which comprise polysaccharides, proteins, phospholipids, teichoic and nucleic acids , that form on a wide variety of surfaces, including living tissues, indwelling medical devices, industrial or potable water systems, food and food-contact surfaces, thereby establishing reservoirs for continuous contaminatio (Costa *et al*., 2018) .

Biofilm production was variable from species to species among the bacterial species , noted that certain bacterial species have a high biofilm forming ratio, while others have poor skills (Lianou *et al*., 2020). Due to their heterogeneous nature, bacterial biofilms are characterized with an enhanced resistance by comparison with their planktonic counterparts to most environmental stresses including nutrient starvation, oxidative stress, antibiotic exposure and other conditions detrimental to bacterial growth (Giaouris *et al*., 2014 ; Bridier *et al*., 2015) .

4.11 Antibiofilm activity of SeNPs

In order to evaluate the anti-biofilm effect of SeNPs , three isolates of each biofilm producer isolates of *Escherichia coli , Klebsiella pneumoniae, Enterococcus faecalis , Staphylococcus Saprophyticus* were tested . SeNPs expressed antibiofilm activity with increasing it´s concentration from (2 to 1024 µg/ml) , the absorbance will decrease with the increasing of SeNPs concentration . The MIC of (*Escherichia coli , Klebsiella pneumoniae*) was (128 µg/ml) , and (64 µg/ml) for *(Staphylococcus Saprophyticus* and *Enterococcus faecalis*) . The MICs of SeNPs against biofilm were found to be twice the MIC in planktonic state.

New strategies other than conventional antibiotic treatments are needed to control biofilm formation in bacterial infections . However, in most cases antibiotics fail to the eradicate these cells, MIC required to eradicate bacteria in biofilms is much higher than MIC of planktonic cells (Chopra *et al*., 2015).

Biofilms are complex bacterial colonies that are resistant to antibiotics as well as the human immune system . To combat the problems, SeNPs have been used to employ antibiofilm activity , a potentially significant potential therapy (Vincent *et al*., 2014) . Selenium nanoparticles either biogenic origin or chemically synthesized have been proven to possess surprising antibacterial and antibiofilm capabilities (Cihalova *et al*., 2015; Cremonini *et al*., 2016; Huang *et al*., 2016).

Although the biogenic SeNPs had antibacterial and antibiofilm effects, they did not show ability to remove the established biofilm up to 50 µg/mL. The concentration of 75 µg/mL showed slight effect on removing the established biofilm (Khiralla and El-Deeb , 2015) .The combined use of MB (Methylene Blue) and SeNPs significantly reduced Colony-Forming Units (CFUs) of one-day-old *Enterococcus*

faecalis biofilm in comparison with the control group (*P value* < 0.05) (Shahmoradi *et al*., 2021) .

The antibiofilm effect of SeNPs was evident at concentrations of 50–200 μg/mL for *V. cholerae* O1 ATCC 14035 strain (Bagheri-Josheghani and Bakhshi , 2022) .The results are consistent with the findings of a previous study which reporting that SeNPs completely eradicated the biofilm structure of *E. coli* at a concentration of 60µg/L (Zonaro *et al*., 2015).

SeNPs that produ^{c}ed by *Providencia vermicola* BGRW under the studied conditions had slight ability to remove established biofilm of different bacteria . 20µg/mL of SeNPs showed a slight effect as a removing agent against the established biofilm developed by all tested strains whereas the strong biofilm turned to moderate biofilm except E.coli whereas, at 24µg/mL, the established biofilm was moderate , while Incorporation of 32µg/mL of SeNPs showed a stronger effect in removing agent against all studied bacteria whereas all established biofilm became weak biofilms. SeNPs are known to have killing effect against S. aureus (El-Deeb *et al*., 2018) .

This could provide an interpretation for the slight removing effect of SeNPs obtained in the present study, where the dead cells could lose their ability to adhere to the surviving cells in the polysaccharide matrix of the established biofilm resulting in the dispersal of a subpopulation of surviving cells (Khiralla and El-Deeb , 2015) .

4.12 Determination the Toxicity of SeNPs on (PC3) Cancer Cell Line and (WRL 68) normal cell line

The cytotoxic response of prostate cancer PC3 cell line and normal hepatic WRL68 cells treated with increasing concentrations of Se NPs (25, 50, 100, 200, 400 µg/mL) was investigated using MTT assay after 24 h exposure. Results in table (4.7) , showed that no significant cytotoxic

effect of Se NPs against PC3 cells at concentrations 25 and 50 µg/mL. Nevertheless, SeNPs at concentration 100, 200 and 400 µg/mL exhibited a dose dependent decrease in PC3 cell viability with maximum inhibition rate of 51.27±2.77% of PC3 cells at 400 µg/mL.

Table (4.7): Multiple comparisons of mean±SD cell inhibition between PC3 and WRL68 treated with Se NPs (25, 50, 100, 200, 400 µg/mL) for 24 hr.

Se NPs	PC3	WRL68	Sig.	*p* Value
	Mean Inhibition ± SD (%)	Mean Inhibition ± SD (%)		
400 µg/mL	51.27±2.77[a]	36.86±3.38[a]	**	<0.00001
200 µg/mL	36.3±2.12[b]	25.54±0.85[b]	**	<0.00001
100 µg/mL	22.38±2.41[c]	9.03±3.3[c]	**	<0.00001
50 µg/mL	8.08±1.36[d]	5.36±1.51[c]	NS	0.5243
25 µg/mL	4.05±0.53[d]	4.71±1.05[c]	NS	0.9981

****: $p < 0.01$, NS: non-significant. Different letters (a, b, c, d) consider significant ($p < 0.05$) in column.**

Regarding WRL68 cells, the sensitivity of the cells to SeNPs treatments was less than that of PC3. Se NPs concentrations at 25, 50 and 100 µg/mL showed no significant differences in pattern of cell inhibition. On the other hand, Se NPs at 200 and 400 µg/mL showed significant ($p < 0.05$) reduction in cell viability with maximum inhibition of 36.86±3.3% at 400 µg/mL.

Multiple comparisons study , table (4.7) between PC3 and WRL68 with regard to SeNPs toxicity showed significant differences ($p = <0.0001$) in the pattern of cell inhibition at 100, 200 and 400 µg/mL, which obviously PC3 cells were more susceptible to SeNPs treatment than WRL68 cells. IC_{50} of Se NPs against PC3 and WRL86 was calculated with values of 164.4 and 175.4 µg/mL, respectively , figure (4.17) .

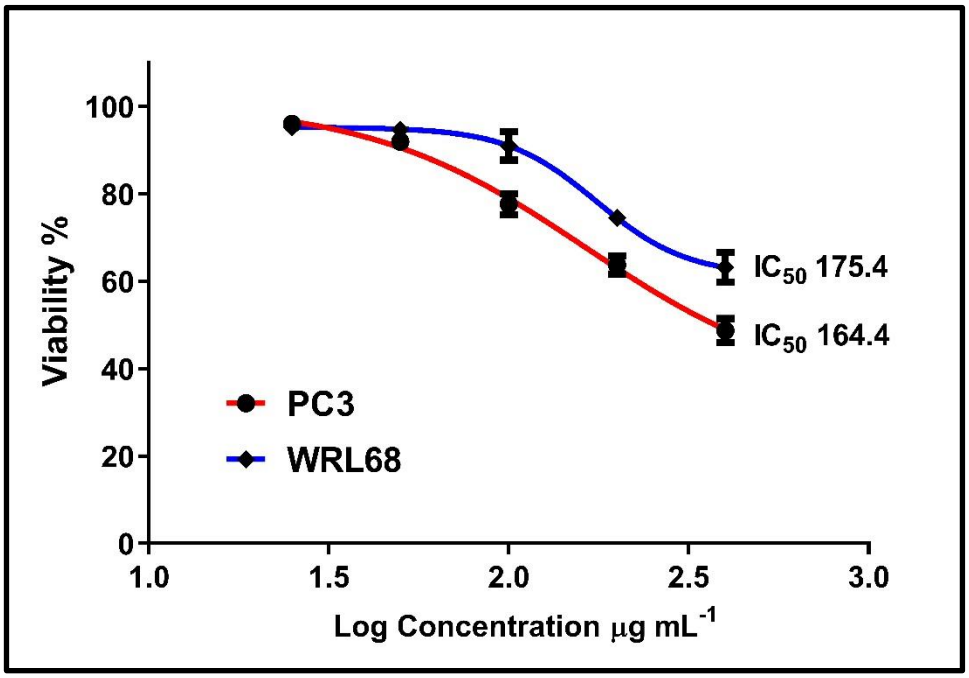

Figure (4.17): (IC_{50}) of SeNPs on PC3 and WRL68 cells treated with NPs at 37°C for 24 hr.

One of the most common materials used in the production of solar cells and photography is selenium, which exhibits a well-known photoelectrical property. It is also an essential component of the human body, as it can protect tissues and cells from free radicals *in vivo* (Alkhudhayri *et al*., 2020). A dose-dependent assessment of the effects of Se NPs on the viability of PC3 cells revealed that the cytotoxic effects of Se NPs were detrimental. The results showed that the presence of Se NPs negatively affected the cell viability of PC3 cells. Depending on their physiochemical characteristics, Se NPs exhibits the tendency to induce the production of reactive oxygen species in exposed cells and thus responsible for the cytotoxic effect (Soltani and Darbemamieh , 2021).

It was indicated that the method of NPs preparation, structure and size of Se nanomaterials have high impact on the antitumoral effect of Se NPs (Siddiqui *et al*., 2020). It was reported that Se NPs in combination with other nano-metals exhibited antiproliferative effect against HepG2

cell line through induction of apoptosis (Cui *et al*., 2018). Moreover, a significant decrease in the viability of prostate LNCaP cell line was observed when treated with different concentrations of Se NPs with signature feature of necrosis due to the decrease in caspases and no LDH release from the cells (Sonkusre , 2020).

Se NPs were found to play an important role in inhibiting numerous types of cancer cells with low effect on normal cells. Similarly, studies have been suggested that Se NPs have potent cytotoxicity against tumor cells, but not against normal cells, like cervical carcinoma, hepatocarcinoma and colorectal cancer (Zhou *et al*., 2016). However, studies confirmed that Se NPs are significantly potent against many cell lines and that their cytotoxicity on prostate cancer cell lines is more convincing than other types of tumor cell lines (Ferro *et al*., 2021; Khurana *et al*., 2019).

The inhibition rate of SeNPs on cancer cells ranged from 46.3% to 77.2% and the most obvious inhibitory effect was observed in prostate cancer cell line after treatment with 100 µg Se NPs (Liao *et al*., 2020) .The molecular mechanism by which Se NPs trigger suppression in tumor cell viability is still not fully understood. In general, Se NPs able to activate tumor cell apoptosis by enhancing cellular uptake and generating reactive oxygen species (Liu *et al*., 2017). Other study reported that Se NPs can stimulate cancer cell autophagy, thus minimizing tumor cell growth and metastasis (Huang *et al*., 2018). Also Se NPs exhibited the ability to induce TNF upregulation, which activate cancer cell necrosis (Sonkusre and Cameotra, 2017).

4.13 : Effect of Se NPs on gene expression of some virulence factor

The results showed that a higher value of *Hly* gene expression was (11.91) in the control group, but a lower value of *Hly* gene expression was (1.51) in Sub-MIC 32 group. There are no significant differences between the Sub-MIC 32 group and MIC 64 group in gene expression of *Hly* gene . However, the control group reveals more significant differences compared with other groups at a significant level (P<0.05) , and a higher value of *FimH* gene expression was (14.31) in the control group, but a lower value of *FimH* gene expression was (2.47) in Sub-MIC 32 group. The findings demonstrated that There are significant differences between the Sub-MIC 32 group , MIC 64 group , and control group in gene expression of *FimH* gene at a significant level (P<0.05) , as shown in (appendices 8) , figure (4.18) .

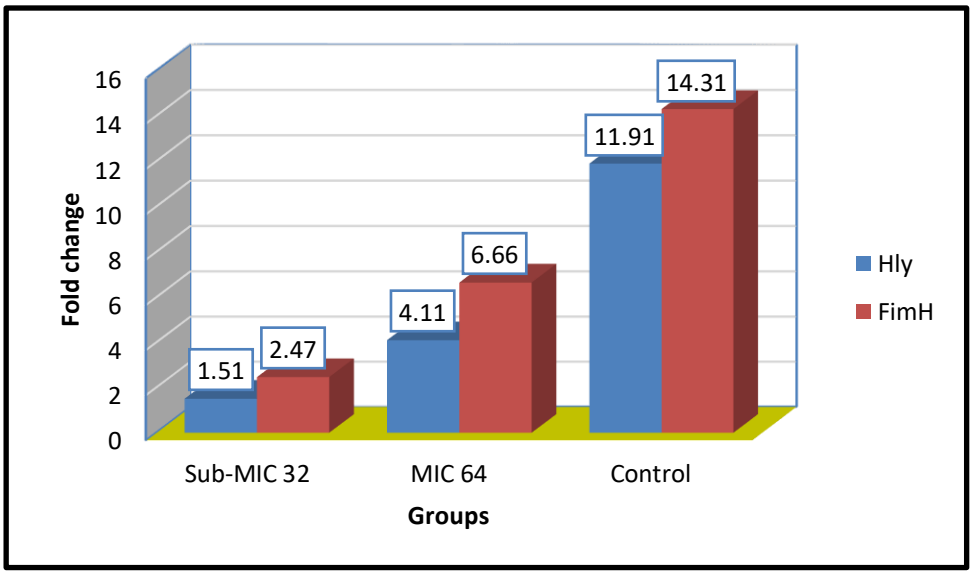

Figure (4.18): Fold change (gene expression) for *Hly* gene and *FimH* gene in *E. coli* .

The results showed that the higher value of *Luxs* gene expression was (15.45) in the control group, but the lower value of *Luxs* gene

expression was (1.38) in Sub-MIC 64 group. There are no significant differences between the Sub-MIC 64 group and the MIC 128 group in gene expression of *Luxs* gene. However, the control group reveals significant differences as compared with other groups at a significant level (P<0.05).

The results showed that a higher value of *qsec* gene expression was (5.52) in the control group, but a lower value of *qsec* gene expression was (0.79) in Sub-MIC 64 group. The findings demonstrated significant differences between Sub-MIC 64 group and MIC 128 group. However, the gene expression of *qsec* gene showed significant positive differences in the control group compared with the other groups at a significant level (P<0.05), as shown in (appendices 9) , figure (4.19) .

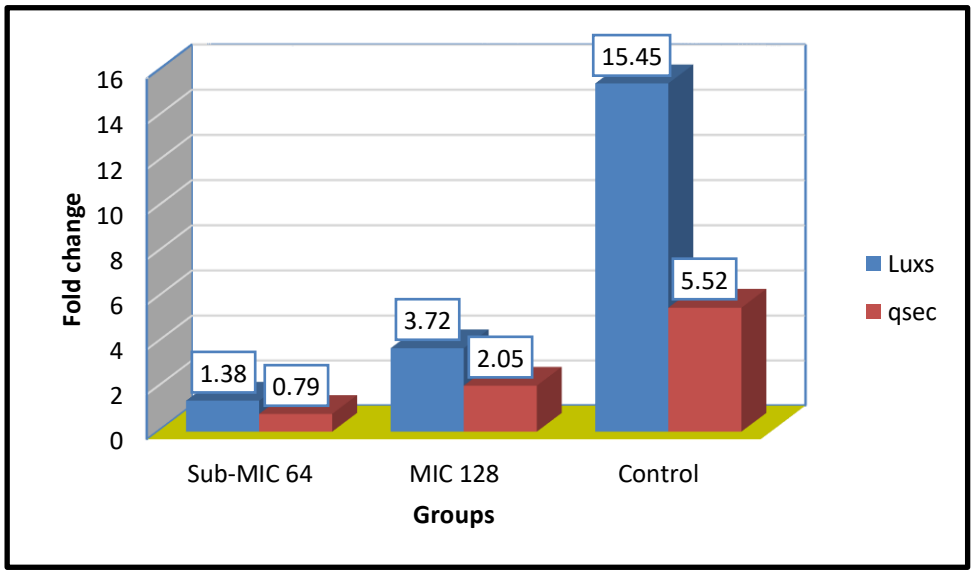

Figure (4.19) : Fold change (gene expression) for *LuxS* gene and *qseC* gene in *E.coli* .

While in *Enterococcus faecalis* the results showed that a higher value of *ESP* gene expression in *Enterococcus faecalis* was (38.13) in the control group, but a lower value of *ESP* gene expression was (1.32) in Sub-MIC 16 group. There are significant differences among the Sub-MIC 16 group, MIC 32 group, and control group in gene expression of the *ESP*

gene, the gene expression of MIC 32 group showed positive significant differences as compared with Sub–MIC 16 group at significant level (P<0.05).

The results showed that a higher value of *HLY* gene expression in *Enterococcus faecalis* was (22.18) in the control group, but a lower value of *HLY* gene expression was (2.21) in Sub-MIC 16 group. The findings demonstrated no significant differences between Sub-MIC 16 group and MIC 32 group. However, the control group showed significant positive differences in gene expression of the *HLY* gene at a significant level (P<0.05), as shown in (appendices 10) , figure (4.20) .

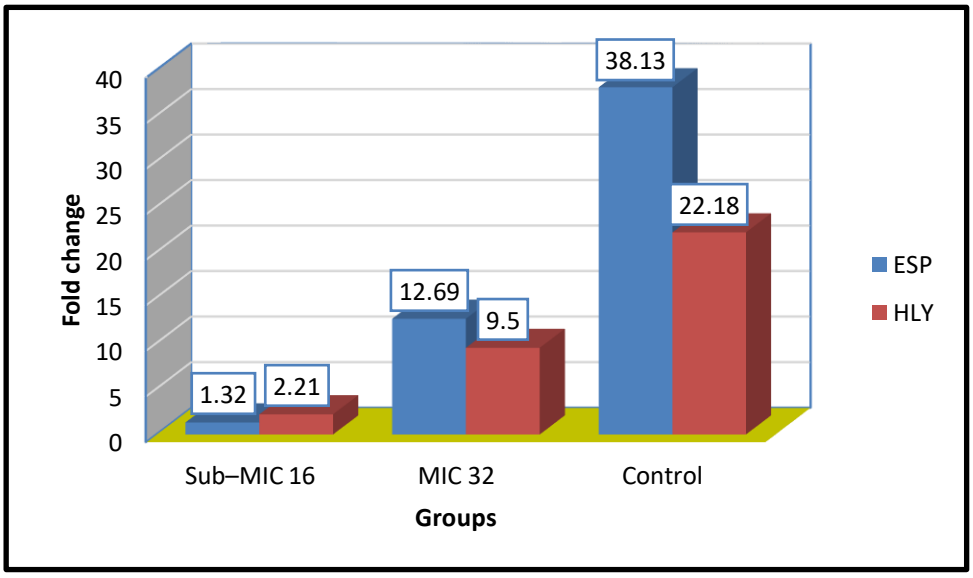

Figure (4.20): Fold change (gene expression) for *ESP* and *HLY* gene in *E. faecalis* .

The higher value of *gelE* gene expression in *Enterococcus faecalis* was (4.70) in the control group, but the lower value of *gelE* gene expression was (0.41) in the Sub-MIC 32 group. There are no significant differences between Sub-MIC 32 group and MIC 64; however, the control group showed significant positive differences as compared with the other groups gene expression of *gelE* gene at a significant level (P<0.05).

The results showed that a higher value of *fsrA* gene expression in *Enterococcus faecalis* was (14.15) in the control group, but a lower value of *fsrA* gene expression was (2.09) in Sub-MIC 32 group. The findings demonstrated that there are significant differences among the Sub-MIC 16 group, the MIC 32 group, and the control group in gene expression of *fsrA* gene at a significant level (P<0.05), as shown in (appendices 11) , figure (4.21) .

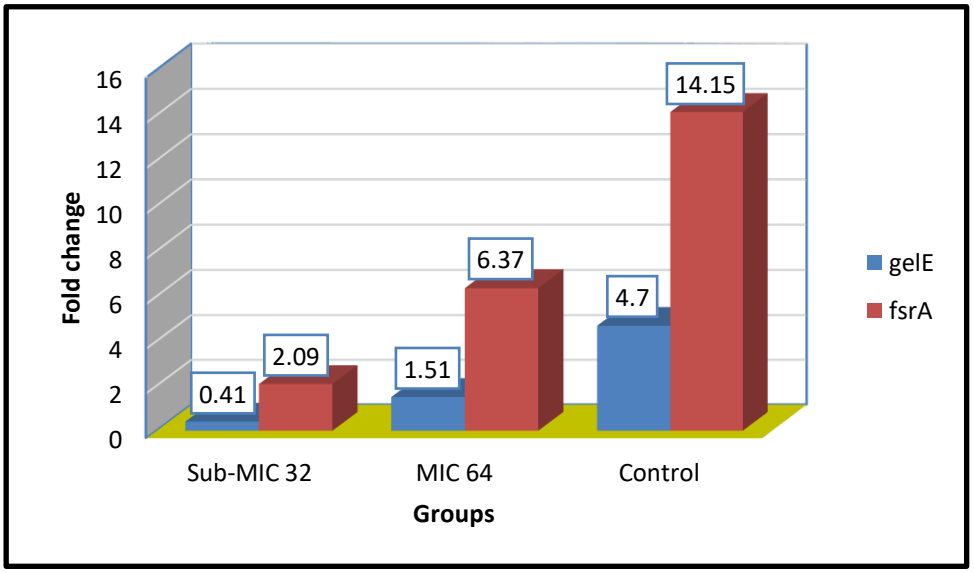

Figure (4.21): Fold change (gene expression) for *gelE* gene and *fsrA* gene in *E. faecalis* .

Studies related to this subject are almost non-existent. Therefore, our study sheds light on this aspect for the first time by studying the effect the Selenium nanoparticles on the gene expression of several genes. It is necessary to refer to many studies that deal with topics related to our topic.

Nanoparticles (NPs) have been widely studied as an alternative to antibiotic use. It is used on many microorganisms such as *Enterococcus faecalis* (Salas-Orozco *et al*., 2022). The enterococcal surface protein , *Esp*, is a high-molecular-weight surface protein of unknown function whose frequency is significantly increased among infection-derived *Enterococcus faecalis* isolates . The presence of the *esp* gene is highly

associated with the capacity of *E. faecalis* to form a biofilm on a polystyrene surface, since 93.5% of the *E. faecalis esp*-positive isolates were capable of forming a biofilm. *Esp* expression in an *E. faecalis esp*-deficient strain promoted primary attachment and biofilm formation. these results reveals that the biofilm formation is widespread among *E. faecalis*, the biofilm formation is restricted to the *E. faecalis* strains harboring *esp*, and *Esp* promotes primary attachment and biofilm formation of *E. faecalis* on abiotic surfaces (Toledo-Arana *et al*., 2001).

ESP expression in *Enterococcus faecalis* is related to the primary adherence and biofilm formation of *E. faecalis*. Twelve *E. faecalis* harboring *esp* gene strains were included, and showed MIC testing and gene expression assay showed that curcumin NPs did not show any inhibitory activity against biofilm formation. these nanoparticles contribute very little, if at all, to inhibition of the *esp* operon (Alizadeh *et al.*, 2019).

NanoZnO/Ze were tested on biofim production of *E. faecalis* and its *esp* gene expression were assessed under nanocomposite treatment . ZnO nanoparticles can effectively inhibited the biofilm formation and affected *esp* gene downregulation of *E. faecalis*. NanoZnO/Zeolite can used against the biofilm infections due to *E. faecalis* and downregulation of *ESP* gene (Partoazar *et al*., 2019).

The application of Selenium nanoparticles as antibacterials are gaining relevance in the medical field . Selenium nanoparticles showed the highest bactericidal and antibacterial properties. The antibacterial effects of selenium nanoparticles were evaluated with respect to growth, biofilm formation of *Staphylococcus aureus* strains (Verma and Maheshwari , 2017).

The strong inhibition effect of SeNPs on biofilms of MERSA isolates , the biofilm formation was intensely inhibited (more than 99%). The use of SeNPs as a tool for the treatment of bacterial infections by induction molecular changes , and increasing resistance of bacteria (Cihalova *et al*., 2015). The most widely application of Se NPs induced apoptosis is to kill cancer cells with the participation of some important signaling events, such as ROS generation, anti-apoptotic gene down-regulation, pro-apoptotic gene up-regulation and caspases activation (Cui *et al*., 2018).

Many studies found that selenium nanoparticles (SeNPs) can influence the genes expression for many genes by management of the transcription factors , and epigenetic DNA methylation . The SeNPs treatments transcriptionally upregulated the bZIP1 transcription factor by an average of 3.5 folds. the upregulation in the expression of the WRKY1 transcription factor. These findings provide that SeNPs associated molecular variations, metabolism and gene expression (parsameher *et al*., 2017 ; Ren *et al*., 2019 ; Sotoodehnia-Korani *et al*., 2020).

Selenium nanoparticles were synthesized with *Bacillus* sp. MSH-1. The ultrastructure of selenium nanoparticles was evaluated with a transmission electron microscope. The antifungal susceptibility test was performed according to the modified Clinical and Laboratory Standards Institute M27-A3 standard protocol. The expression levels of the *CDR1* and *ERG11* genes were analyzed using the quantitative real-time polymerase chain reaction (PCR) assay. The azole-resistant *C. albicans* and wild type *C. albicans* strains were inhibited by 100 and 70 µg/mL of selenium nanoparticle concentrations, respectively. The expression of *CDR1* and *ERG11* genes was significantly down-regulated in these selenium nanoparticle concentrations (Parsameher *et al*., 2017).

Dietary inorganic Se and bacterial organic Se were observed to significantly increase affect levels of gene expression of many genes such as mRNA level in GSH-Px1, GSH-Px4, DIO1, and TXNDR1, while both ADS18 and ADS2 showed high level of mRNA of DIO2 compared to sodium selenite (Dalia *et al*., 2017).

Antibacterial properties of all three nanomaterials were probed against Gram-positive *Enterococcus faecalis*. Se exhibited relatively strong antibacterial activity against both Gram-positive and possible three-pronged approach of bacterial cytotoxicity by these graphene-based materials (Niranjan *et al*., 2022).

Trans-cinnamaldehyde significantly decreased uro-epithelial cell attachment and invasion by uropathogenic *E. coli* ($p < 0.05$). Real-time quantitative polymerase chain reaction revealed that trans-cinnamaldehyde significantly decreased the expression of major genes involved in uropathogenic *E. coli* attachment and invasion of host tissue ($p < 0.05$). The down-regulating effect of trans-cinnamaldehyde on these genes potentially translated into decreased ability of uropathogenic *E. coli* to attach and invade bladder cells (Amalaradjou *et al.*, 2011).

In summary, this study highlights some possible effect of SeNPs on the gene expression of some genes such as *hly*, *FimH*, *Luxs*, *qsec* in *E.coli*, furthermore, *ESP*, *HLY*, *gelE*, and *fsrA* in *Enterococcus faecalis* . We can conclude that , use of higher dose of selenium nanoparticles leads to a decrease in the gene expression of a number of important and vital genes that affect the main functions of the microorganisms used in the study and thus reduce their pathogenicity. This subject come to support the promise of SeNPs in a wide range of medical applications.

Conclusions

and

Recommendations

Conclusions

The present study concludes that

1- The major causative agents of UTIs were *Escherichia coli* (Gram negative bacteria) followed by *Enterococcus faecalis* , *K. pneumonia* , and *Staphylococcus saprophyticus* .
2- SeNPs can be prepared using *Bacillus clausii* through biological method and the nanoparticles showed typical properties and high stability in suspension .
3- In synergistic effect of nanoparticle and antibiotic , all tested bacteria remained resistant to Ampicillin when satiated with SeNPs and only the nano effect appeared , while the synergistic effect of Doxycycline with SeNPs in all tested bacteria that sensitive to Doxycycline were decreased .
4- Selenium nanoparticles showed a high antimicrobial activity against pathogenic bacteria .
5- Antioxidant activity of selenium nanoparticle which are in acceptable range, indicating their ability of reducing free radicles
6- Selenium nanoparticles proved to have a considerable antibiofilm activity against pathogenic tested bacteria .
7- Selenium nanoparticles didn't show hemolysis .
8- Biological SeNPs had low toxicologically parameters on normal cell , so the SeNPs synthesized is safe because of its low toxicity and show anti-cancer effects against PC3 .
9- The results of Gene expression of some virulence factor revealed that SeNPs effective on genes expression by down regulation .

Recommendations

1- Synthesis of selenium nanoparticles using other microorganisms and other method and making a comparative study between them .

2- Compare between commercial selenium nanoparticles and Biological selenium nanoparticles .

3- Using the selenium nanoparticles as antifungal and antiviral , and the effects of SeNPs on some immunological parameters in lab animals and in tissue culture .

4- Further study of antimicrobial effect of SeNPs *in vivo* by using animals lab is needed

5- Detecting the roles of selenium nanoparticles in the industrial and agricultural applications as well as medical application .

6- Extensive studies about gene expression of other virulence factor of pathogenic bacteria treated with SeNPs .

References

References

Abbas, F. M. (2020). Phenotypic and molecular detection of SHV β-lactamase producing *Klebsiella pneumoniae* resistant to carbapenem from Al-Hillah Teaching Hospital environment, Babylon Province, Iraq. *EurAsian Journal of BioSciences*, 14(2), 7351-7355.

Abbas, H. S., Abou Baker, D. H., and Ahmed, E. A. (2021). Cytotoxicity and antimicrobial efficiency of selenium nanoparticles biosynthesized by *Spirulina platensis* . *Archives of Microbiology*, 203(2), 523-532.

Abbrescia, A., Palese, L. L., Papa, S., Gaballo, A., Alifano, P., and M Sardanelli, A. (2014). Antibiotic sensitivity of *Bacillus clausii* strains in commercial preparation. *Clinical Immunology, Endocrine and Metabolic Drugs* (Discontinued), 1(2), 102-110.

Abdal Dayem, A., Hossain, M. K., Lee, S. B., Kim, K., Saha, S. K., Yang, G. M., Choi, H.Y., and Cho, S. G. (2017). The role of reactive oxygen species (ROS) in the biological activities of metallic nanoparticles. *International Journal of Molecular Sciences*, 18(1), 18010120 .

Abobatta, W. F. (2018). Nanotechnology application in agriculture. *Acta Scientific Agriculture*, 2(6) , 99 - 102 .

Abood, S. H., and Ibrahim, I. A. (2017). Comparison of biofilm formation by different species of Klebsiella . *Pakistan Journal of Biotechnology*, 14(4), 531-535.

AbouElmaaty, T., Abdeldayem, S. A., Ramadan, S. M., Sayed-Ahmed, K., and Plutino, M. R. (2021). Coloration and multi-functionalization of polypropylene fabrics with selenium nanoparticles . *Polymers*, 13(15) , 13152483 .

Acar, J. F. (2000). Antibiotic synergy and antagonism. *Medical clinics of north america*, 84(6), 1391-1406.

Ahn, E. Y., Lee, Y. J., Choi, S. Y., Im, A. R., Kim, Y. S., and Park, Y. (2018). Highly stable gold nanoparticles green-synthesized by upcycling cartilage waste extract from yellow-nose skate (Dipturus chilensis) and evaluation of its cytotoxicity, haemocompatibility and antioxidant activity. *Artificial Cells, Nanomedicine, and Biotechnology*, 46(2), 1108-1119.

Al Jahdaly, B. A., Al-Radadi, N. S., Eldin, G. M., Almahri, A., Ahmed, M. K., Shoueir, K., and Janowska, I. (2021). Selenium nanoparticles synthesized using an eco-friendly method: dye decolorization from aqueous solutions, cell viability, antioxidant, and antibacterial effectiveness. *Journal of Materials Research and Technology*, 11, 85-97.

Alagesan, V., and Venugopal, S. (2019). Green synthesis of selenium nanoparticle using leaves extract of *withania somnifera* and its biological applications and photocatalytic activities . *Bionanoscience*, 9(1), 105-116.

Alam, H., Khatoon, N., Khan, M. A., Husain, S. A., Saravanan, M., and Sardar, M. (2020). Synthesis of selenium nanoparticles using probiotic bacteria *Lactobacillus acidophilus* and their enhanced antimicrobial activity against resistant bacteria. *Journal of Cluster Science*, 31(5), 1003-1011.

Alav, I., Sutton, J. M., and Rahman, K. M. (2018). Role of bacterial efflux pumps in biofilm formation. *Journal of Antimicrobial Chemotherapy*, 73(8), 2003-2020.

Ali, E. S., Sharker, S. M., Islam, M. T., Khan, I. N., Shaw, S., Rahman, M. A., Uddin, S.J., Shill, M.C., Rehman, S., Das, N., Ahmad, S., Shilpi, J.A., Tripathi, S., Mishra, S.K., and Mubarak, M. S. (2021).

Targeting cancer cells with nanotherapeutics and nanodiagnostics: Current status and future perspectives. *Seminars in Cancer Biology* , 69, 52-68 .

Aliasgharpour, M., and Rahnamaye Farzami, M. (2013). Trace elements in human nutrition: A review. *International Journal of Medical Investigation*, 2(3), 115-128.

Alizadeh, S. S., Amini, K., and Saffarian, P. (2019). Evaluating the inhibitory effect of Curcumin nanoparticles associated with expression of esp gene in *Enterococcus faecalis* biofilm. *Razi Journal of Medical Science* , 26(9) , 39-46 .

Al-Kazaz, F. F. M., Hussain, D. H., and Khalaf, S. A. (2021). The effect of copper oxide and selenium nanoparticles on vitamin d levels in women with infertility. *Plant Archives*, 21(1), 86-93.

Alkhudhayri, A.A., Wahab, R., Siddiqui, M.A., and Ahmad, J.(2020). Selenium Nanoparticles Induce Cytotoxicity and Apoptosis in Human Breast Cancer (MCF-7) and Liver (HepG2) Cell Lines. *Nanoscience and Nanotechnology Letters* , 12(3), 324-330.

Almalki, M. A., and Varghese, R. (2020). Prevalence of catheter associated biofilm producing bacteria and their antibiotic sensitivity pattern . *Journal of King Saud University-Science*, 32(2), 1427-1433.

Alvand, Z. M., Rahimi, M., and Rafati, H. (2022). Interaction of a Natural Compound Nanoemulsion with Gram Negative and Gram Positive Bacterial Membrane; A Mechanism Based study Using a Microfluidic Chip and DESI Technique. *International Journal of Pharmaceutics*, 122181.

Al-Zuhairy, A. M., and Al-Dahmoshi, H. O. (2020). Aminoglycosides and fluoroquinolones resistant genes among uropathogenic

Escherichia coli in Hilla City, Iraq. *Drug Invention Today*, 13(2) , 307 – 312 .

Amalaradjou, M. A. R., Narayanan, A., and Venkitanarayanan, K. (2011). Trans-cinnamaldehyde decreases attachment and invasion of uropathogenic *Escherichia coli* in urinary tract epithelial cells by modulating virulence gene expression. *The Journal of Urology*, 185(4), 1526-1531.

Amin, K. A., Hashem, K. S., Alshehri, F. S., Awad, S. T., and Hassan, M. S. (2017). Antioxidant and hepatoprotective efficiency of selenium nanoparticles against acetaminophen-induced hepatic damage. *Biological Trace Element Research*, 175(1), 136-145.

Anderson, H. E., Santos, I. C., Hildenbrand, Z. L., and Schug, K. A. (2019). A review of the analytical methods used for beer ingredient and finished product analysis and quality control. *Analytica Chimica Acta*, 1085, 1-20.

Angeliki, K. (2021). Toxicity of Metallic Nanoparticles in the CNS (Doctoral dissertation, National and Kapodistrian University of Athens Greece).

Anjum, S., Hashim, M., Malik, S. A., Khan, M., Lorenzo, J. M., Abbasi, B. H., and Hano, C. (2021). Recent advances in zinc oxide nanoparticles (Zno nps) for cancer diagnosis, target drug delivery, and treatment. *Cancers*, 13(18), 4570.

Archana, D., Dutta, J., and Dutta, P. K. (2013). Evaluation of chitosan nano dressing for wound healing: Characterization, in vitro and in vivo studies. *International Journal of Biological Macromolecules*, 57, 193-203.

Arunthirumeni, M., Veerammal, V., and Shivakumar, M. S. (2022). Biocontrol efficacy of mycosynthesized selenium nanoparticle

using *Trichoderma* sp. on insect pest *Spodoptera litura*. *Journal of Cluster Science*, 33(4), 1645-1653.

Ashengroph, M., and Tozandehjani, S. (2022). Optimized resting cell method for green synthesis of selenium nanoparticles from a new *Rhodotorula mucilaginosa* strain. *Process Biochemistry*, 116, 197-205.

Assafi, M. S., Ibrahim, N. M., Hussein, N. R., Taha, A. A., and Balatay, A. A. (2015). Urinary bacterial profile and antibiotic susceptibility pattern among patients with urinary tract infection in duhok city, kurdistan region, Iraq. *International Journal of Pure and Applied Sciences and Technology*, 30(2), 54 - 63 .

Aypak, C., Altunsoy, A., and Düzgün, N. (2009). Empiric antibiotic therapy in acute uncomplicated urinary tract infections and fluoroquinolone resistance: a prospective observational study. *Annals of Clinical Microbiology and Antimicrobials*, 8(1), 1-7.

Azizi, M., Ghourchian, H., Yazdian, F., Bagherifam, S., Bekhradnia, S., and Nyström, B. (2017). Anti-cancerous effect of albumin coated silver nanoparticles on MDA-MB 231 human breast cancer cell line. *Scientific reports*, *7*(1), 1-18.

Azizi, S., Ahmad, M. B., Namvar, F., and Mohamad, R. (2014). Green biosynthesis and characterization of zinc oxide nanoparticles using brown marine macroalga *Sargassum muticum* aqueous extract. *Materials Letters*, 116, 275-277.

Bader, M. S., Loeb, M., Leto, D., and Brooks, A. A. (2020). Treatment of urinary tract infections in the era of antimicrobial resistance and new antimicrobial agents. *Postgraduate Medicine*, 132(3), 234-250.

……References……

Badmus, J., Oyemomi, S. A., Yekeen, T. A., Adedosu, O. T., Adegbola, P. I., Azeez, M. A., Adebayo, E.A., and Lateef, A. (2022). Haemolytic and cytogenotoxic potential of aqueous leaf extract of *Annona muricata* and its bio-fabricated silver nanoparticles . *Caryologia , International Journal of Cytology, Cytosystematics and Cytogenetics* , 75(1) , 3-13 .

Bag, S., Ghosh, T. S., Banerjee, S., Mehta, O., Verma, J., Dayal, M., Desigamani, A., Kumar, P., Saha, B., Kedia, S., Ahuja, V., Ramamurthy, T., and Das, B. (2019). Molecular insights into antimicrobial resistance traits of commensal human gut microbiota . *Microbial ecology*, 77(2), 546-557.

Bagheri-Josheghani, S., and Bakhshi, B. (2022). Investigation of the Antibacterial and Antibiofilm Activity of Selenium Nanoparticles against *Vibrio cholerae* as a Potent Therapeutics . *Canadian Journal of Infectious Diseases and Medical Microbiology*, 2022 , 1-10 .

Baig, N., Kammakakam, I., and Falath, W. (2021). Nanomaterials: A review of synthesis methods, properties, recent progress, and challenges. *Materials Advances*, 2(6), 1821-1871.

Baker, F. J., and Silverton, R. E. (2014). Introduction to medical laboratory technology. *Butterworth-Heinemann*.

Behzadi, P. (2018). Uropathogenic Escherichia coli and fimbrial adhesins virulome. *Urinary Tract Infection: The Result of the Strength of the Pathogen, or the Weakness of the Host. Croatia: InTechOpen*, 65-83.

Behzadi, P., and Behzadi, E. (2017). Uropathogenic Escherichia coli: An ideal resource for DNA microarray probe designing. *International Conference on Bioinformatics and Biomedical Engineering* . (pp. 12-19). Springer, Cham.

Berber, S., and Çetinkaya, S. (2021). An Isolate of *Bacillus clausii* Appears to Possess Four Distinct Pectinolytic Activities. *Journal of the Institute of Science and Technology*, 11(1), 635-644.

Beris, P., and Picard, V. (2015). Non-immune hemolysis: diagnostic considerations. *In Seminars in Hematology* , 52(4) , 287-303.

Birgy, A., Madhi, F., Jung, C., Levy, C., Cointe, A., Bidet, P., Hobson, C.A., Bechet, S., Sobral, E., Vuthien, H., Ferroni, A., Aberrane, S., Cuzon, G., Beraud, L., Gajdos, V., Launay, E., Pinquier, D., Haas, H., Desmarest, M., Dommergues, M.A., Cohen, R., and Bonacorsi, S. (2020). Diversity and trends in population structure of ESBL-producing Enterobacteriaceae in febrile urinary tract infections in children in France from 2014 to 2017. *Journal of Antimicrobial Chemotherapy*, 75(1), 96-105.

Bizuayehu, H., Bitew, A., Abdeta, A., and Ebrahim, S. (2022). Catheter-associated urinary tract infections in adult intensive care units at a selected tertiary hospital, Addis Ababa, Ethiopia. *Plos One*, 17(3), e0265102.

Borah, S. N., Goswami, L., Sen, S., Sachan, D., Sarma, H., Montes, M., Peralta-Videa, J.R., Pakshirajan, K., and Narayan, M. (2021). Selenite bioreduction and biosynthesis of selenium nanoparticles by *Bacillus paramycoides* SP3 isolated from coal mine overburden leachate. *Environmental Pollution*, 285, 117519.

Bordea, M. A. (2020). The mechanisms responsible for the probiotic effects of *Bacillus* strains against rotavirus infection- tolearn . *Romanian Archives of Microbiology and Immunology*, 79(4), 304-304.

Boroumand, S., Safari, M., Shaabani, E., Shirzad, M., and Faridi-Majidi, R. (2019). Selenium nanoparticles: synthesis, characterization and

study of their cytotoxicity, antioxidant and antibacterial activity. *Materials Research Express*, 6(8), 0850d8.

Bridier, A., Sanchez-Vizuete, P., Guilbaud, M., Piard, J. C., Naitali, M., and Briandet, R. (2015). Biofilm-associated persistence of food-borne pathogens. *Food Microbiology*, 45, 167-178.

Bunu, S. J., Otele, D., Alade, T., and Dodoru, R. T. (2020). Determination of serum DNA purity among patients undergoing antiretroviral therapy using NanoDrop-1000 spectrophotometer and polymerase chain reaction. *Biomedical and Biotechnology Research Journal*, 4(3), 214 – 219 .

Calvo, J., and Martinez-Martinez, L. (2009). Antimicrobial mechanisms of action. *Enfermedades Infecciosas y Microbiologia Clinica*, 27(1), 44-52.

Caruso, S., and Poon, I. K. (2018). Apoptotic cell-derived extracellular vesicles: more than just debris. *Frontiers in immunology* , 9, 1486.

Cavalu, S., Antoniac, I. V., Fritea, L., Mates, I. M., Milea, C., Laslo, V., Vicas, S., and Mohan, A. (2018). Surface modifications of the titanium mesh for cranioplasty using selenium nanoparticles coating. *Journal of Adhesion Science and Technology*, 32(22), 2509-2522 .

Cavalu, S., Kamel, E., Laslo, V., Fritea, L., Costea, T., Antoniac, I. V., Vasile, E., Antoniac, A., Semenescu, A., Mohan, A., Saceleanu, V., and Vicas, S (2017) . Eco-friendly, Facile and Rapid Way for Synthesis of Selenium Nanoparticles. *Revista de Chimie SRL* , 68(12) , 2963 - 2966 .

Čeljuska-Tošev, E., Škerk, V., Markotić, A., Tambić-Andrašević, A., Baršić, B., Andrašević, S., Vargović, M., and Pasini, M. (2010). Struktura i djelatnost Referentnog centra Ministarstva zdravstva i

socijalne skrbi za infekcije mokraćnog sustava u razdoblju od 2005–2010 godine. *Infektološki Glasnik*, 30(2), 75-81.

Chandramohan, S., Sundar, K., and Muthukumaran, A. (2019). Reducing agents influence the shapes of selenium nanoparticles (SeNPs) and subsequently their antibacterial and antioxidant activity. *Materials Research Express*, 6(8), 0850i2.

Chaudhari, S.P., and Nikam, S.A. (2018). Biosynthesis of metallic nanopatricles .

Chawla, R., Filippini, T., Loomba, R., Cilloni, S., Dhillon, K. S., and Vinceti, M. (2020). Exposure to a high selenium environment in Punjab, India: Biomarkers and health conditions. *Science of the Total Environment*, 719, 134541.

Chen, M., Cen, H., Guo, C., Guo, X., and Chen, Z. (2020). Preparation of Cu-MOFs and its corrosion inhibition effect for carbon steel in hydrochloric acid solution. *Journal of Molecular Liquids*, 318, 114328.

Choi, Y. J., Park, J. H., Han, J. W., Kim, E., Jae-Wook, O., Lee, S. Y., ... and Gurunathan, S. (2016). Differential cytotoxic potential of silver nanoparticles in human ovarian cancer cells and ovarian cancer stem cells. *International journal of molecular sciences*, *17*(12), 2077

Chen, Y., Zou, C., Mastalerz, M., Hu, S., Gasaway, C., and Tao, X. (2015). Applications of micro-fourier transform infrared spectroscopy (FTIR) in the geological sciences—a review. *International Journal of Molecular Sciences*, 16(12), 30223-30250.

Cheng, Z., Li, M., Dey, R., and Chen, Y. (2021). Nanomaterials for cancer therapy: Current progress and perspectives. *Journal of Hematology and Oncology*, 14(1), 1-27.

Cheon, J. Y., Kim, S. J., Rhee, Y. H., Kwon, O. H., and Park, W. H. (2019). Shape-dependent antimicrobial activities of silver nanoparticles. *International Journal of Nanomedicine,* 14, 2773–2780.

Chopra, S., Harjai, K., and Chhibber, S. (2015). Potential of sequential treatment with minocycline and *S. aureus* specific phage lysin in eradication of MRSA biofilms: an in vitro study. *Applied Microbiology and Biotechnology*, 99(7), 3201-3210 .

Chudobova, D., Cihalova, K., Dostalova, S., Ruttkay-Nedecky, B., Merlos Rodrigo, M. A., Tmejova, K., Kopel, P., Nejdl, L., Kudr, J., Gumulec, J., Krizkova, S., Kynicky, J., Kizek, R., and Adam, V. (2014). Comparison of the effects of silver phosphate and selenium nanoparticles on Staphylococcus aureus growth reveals potential for selenium particles to prevent infection. FEMS Microbiology Letters, 351(2), 195-201.

Chukwudi, C. U. (2016). rRNA binding sites and the molecular mechanism of action of the tetracyclines. *Antimicrobial Agents and Chemotherapy*, 60(8), 4433-4441.

Chung, Y. C., Su, Y. P., Chen, C. C., Jia, G., Wang, H. L., Wu, J. G., and Lin, J. G. (2004). Relationship between antibacterial activity of chitosan and surface characteristics of cell wall. *Acta Pharmacologica Sinica*, 25(7), 932-936.

Cihalova, K., Chudobova, D., Michalek, P., Moulick, A., Guran, R., Kopel, P., ... and Kizek, R. (2015). *Staphylococcus aureus* and MRSA growth and biofilm formation after treatment with antibiotics and SeNPs . *International Journal of Molecular Sciences*, 16(10), 24656-24672.

CLSI (2020) . Performance standards for antimicrobial susceptibility testing. 29ed. CLSI supplement M100-S29. Wayne, PA: Clinical and laboratory standards institute .

Cojocaru, A., Sin, I., Agapescu, C., Cotarta, A., and Visan, T. (2016). Electrode Processes and SEM/EDX Analysis of Selenium films electro deposited from ionic liquids based on choline chloride. *Chalcogenide Letters*, 13(3) , 127 – 138 .

Collee, J. G., Mackie, T. J., and McCartney, J. E. (1996). Mackie and McCartney practical medical microbiology. *Harcourt Health Sciences.*

Constantinescu-Aruxandei, D., Frîncu, R. M., Capră, L., and Oancea, F. (2018). Selenium analysis and speciation in dietary supplements based on next-generation selenium ingredients. *Nutrients*, 10(10), 1466.

Costa, O. Y., Raaijmakers, J. M., and Kuramae, E. E. (2018). Microbial extracellular polymeric substances: ecological function and impact on soil aggregation. *Frontiers in microbiology*, 9, 1636.

Cremonini, E., Zonaro, E., Donini, M., Lampis, S., Boaretti, M., Dusi, S., Melotti, P., Lleo, M.M., and Vallini, G. (2016). Biogenic selenium nanoparticles: characterization, antimicrobial activity and effects on human dendritic cells and fibroblasts. *Microbial Biotechnology*, 9(6), 758-771.

Cui, D., Yan, C., Miao, J., Zhang, X., Chen, J., Sun, L., Meng, L., Liang, T., and Li, Q. (2018). Synthesis, characterization and antitumor properties of selenium nanoparticles coupling with ferulic acid. *Materials Science and Engineering*, 90, 104-112.

Dalia, A. M., Loh, T. C., Sazili, A. Q., Jahromi, M. F., and Samsudin, A. A. (2017). The effect of dietary bacterial organic selenium on growth performance, antioxidant capacity, and Selenoproteins gene

expression in broiler chickens. *BMC Veterinary Research*, 13(1), 1-11.

Daniel, W. W., and Cross, C. L. (2018). *Biostatistics: a foundation for analysis in the health sciences*. Wiley.

Das, R. K., Pachapur, V. L., Lonappan, L., Naghdi, M., Pulicharla, R., Maiti, S., Cledon, M., Dalila, L.M.A., Sarma, S.J., and Brar, S. K. (2017). Biological synthesis of metallic nanoparticles: plants, animals and microbial aspects. *Nanotechnology for Environmental Engineering* , 2(1), 1-21.

De La Cadena, E., Mojica, M. F., Castillo, N., Correa, A., Appel, T. M., García-Betancur, J. C., Pallares, C.J., and Villegas, M. V. (2020). Genomic analysis of CTX-M-group-1-producing extraintestinal pathogenic E. coli (ExPEc) from patients with urinary tract infections (UTI) from Colombia . *Antibiotics*, 9(12), 9120899 .

Deng, X., Xiong, F., Li, X., Xiang, B., Li, Z., Wu, X., Guo, C., Li, X., Li, Y., Li, G., Xiong, W., and Zeng, Z. (2018). Application of atomic force microscopy in cancer research. *Journal of Nanobiotechnology*, 16(1), 1-15.

Dhanjal, S., and Cameotra, S. S. (2010). Aerobic biogenesis of selenium nanospheres by *Bacillus cereus* isolated from coalmine soil. *Microbial Cell Factories*, 9(1), 1-11.

Dobias, J., Suvorova, E. I., and Bernier-Latmani, R. (2011). Role of proteins in controlling selenium nanoparticle size. *Nanotechnology*, 22 (19) , 195605.

Doron, S., and Snydman, D. R. (2015). Risk and safety of probiotics. *Clinical Infectious Diseases*, 60(2), 129-134.

Duntas, L. (2009). Selenium and inflammation: underlying anti-inflammatory mechanisms . *Hormone and Metabolic Research*, 41(06) , 443-447.

Dziri, R., Klibi, N., Lozano, C., Said, L. B., Bellaaj, R., Tenorio, C., Boudabous, A., Slama, K.B., and Torres, C. (2016). High prevalence of *Staphylococcus haemolyticus* and *Staphylococcus saprophyticus* in environmental samples of a Tunisian hospital. *Diagnostic Microbiology and Infectious Disease,* 85(2), 136-140.

EL-Baghdady, K. Z., Khalil, M. M., El Borhamy, M. I., and Meligi, G. (2019). Biosynthesis, characterization and cytotoxicity of selenium nanoparticles using *Bacillus tropicus* Ism 2. *Egyptian Academic Journal of Biological Sciences, G. Microbiology*, 11(1), 47-57.

El-Batal, A. I., Essam, T. M., El-Zahaby, D. A., and Amin, M. A. (2014). Synthesis of selenium nanoparticles by *Bacillus laterosporus* using gamma radiation. *British Journal of Pharmaceutical Research,* 4(11) , 1364-1386.

El-Deeb, B., Al-Talhi, A., Mostafa, N., and Abou-assy, R. (2018). Biological synthesis and structural characterization of selenium nanoparticles and assessment of their antimicrobial properties. *American Academic Scientific Research Journal for Engineering, Technology and Sciences* , 45(1), 135-170.

Eleraky, N. E., Allam, A., Hassan, S. B., and Omar, M. M. (2020). Nanomedicine fight against antibacterial resistance: an overview of the recent pharmaceutical innovations. *Pharmaceutics*, 12(2), 12020142 .

El-Ghazaly, M. A., Fadel, N., Rashed, E., El-Batal, A., and Kenawy, S. A. (2017). Anti-inflammatory effect of selenium nanoparticles on the inflammation induced in irradiated rats. *Canadian Journal of Physiology and Pharmacology* , 95(2), 101-110.

El-Ramady, H. R., Domokos-Szabolcsy, É., Abdalla, N. A., Alshaal, T. A., Shalaby, T. A., Sztrik, A., Prokisch, J., and Fári, M. (2014).

Selenium and nano-selenium in agroecosystems. *Environmental Chemistry Letters*, 12(4), 495-510.

Esmaeel, N. E., Gerges, M. A., Hosny, T. A., Ali, A. R., and Gebriel, M. G. (2020). Detection of chromosomal and plasmid-mediated quinolone resistance among *Escherichia coli* Isolated from urinary tract infection cases; Zagazig University Hospitals, Egypt. *Infection and Drug Resistance*, 13, 413 - 421.

Fan, A. M., and Vinceti, M. (2015). Selenium and its compounds. *Hamilton and Hardy's Industrial Toxicology; Wiley-Blackwell: Hoboken, NJ, USA*, 205-228.

Fang, X., Li, C. E., Zheng, L., Yang, F., and Chen, T. (2018). Dual-targeted selenium nanoparticles for synergistic photothermal therapy and chemotherapy of tumors. *Chemistry–An Asian Journal*, 13(8), 996-1004.

Fardsadegh, B., and Jafarizadeh-Malmiri, H. (2019). *Aloe vera* leaf extract mediated green synthesis of selenium nanoparticles and assessment of their in vitro antimicrobial activity against spoilage fungi and pathogenic bacteria strains. *Green Processing and Synthesis*, 8(1), 399-407.

Fardsadegh, B., Vaghari, H., Mohammad-Jafari, R., Najian, Y., and Jafarizadeh-Malmiri, H. (2019). Biosynthesis, characterization and antimicrobial activities assessment of fabricated selenium nanoparticles using *Pelargonium zonale* leaf extract. *Green Processing and Synthesis*, 8(1), 191-198.

FDA (2015) . Infant formula: the addition of minimum and maximum levels of selenium to infant formula and related labeling requirements. Final rule. *Federal Register*, 80(120), 35834-35841.

Ferreira, A. M., Bonesso, M. F., Mondelli, A. L., Camargo, C. H., and Maria de Lourdes, R. S. (2012). Oxacillin Resistance and

Antimicrobial Susceptibility Profile of *Staphylococcus saprophyticus* and Other Staphylococci Isolated from Patients with Urinary Tract Infection . *Chemotherapy*, 58(6), 482-491.

Ferro, C., Florindo, H.F., and Santos, H.A. (2021) . Selenium Nanoparticles for Biomedical Applications: From Development and Characterization to therapeutics. *Advanced Healthcare Materials* , 10(16) , 2100598.

Filipović, N., Ušjak, D., Milenković, M. T., Zheng, K., Liverani, L., Boccaccini, A. R., and Stevanović, M. M. (2021). Comparative study of the antimicrobial activity of selenium nanoparticles with different surface chemistry and structure. *Frontiers in Bioengineering and Biotechnology*, 8 , 624621.

Fils, P. E. L., Cholley, P., Gbaguidi-Haore, H., Hocquet, D., Sauget, M., and Bertrand, X. (2021). ESBL-producing *Klebsiella pneumoniae* in a University hospital: Molecular features, diffusion of epidemic clones and evaluation of cross-transmission. *Plos One*, 16(3), e0247875.

Forootanfar, H., Adeli-Sardou, M., Nikkhoo, M., Mehrabani, M., Amir-Heidari, B., Shahverdi, A. R., and Shakibaie, M. (2014). Antioxidant and cytotoxic effect of biologically synthesized selenium nanoparticles in comparison to selenium dioxide. *Journal of Trace Elements in Medicine and Biology*, 28(1), 75-79.

Foxman, B. (2010). The epidemiology of urinary tract infection. *Nature Reviews Urology*, 7(12), 653-660.

Foxman, B. (2014). Urinary tract infection syndromes: occurrence, recurrence, bacteriology, risk factors, and disease burden. *Infectious Disease Clinics*, 28(1), 1-13.

Fu, H., Yuan, J., and Gao, H. (2015). Microbial oxidative stress response: novel insights from environmental facultative anaerobic bacteria. *Archives of Biochemistry and Biophysics*, 584, 28-35.

Gajamer, V. R., Bhattacharjee, A., Paul, D., Ingti, B., Sarkar, A., Kapil, J., Singh, A.K., Pradhan, N., and Tiwari, H. K. (2020). High prevalence of carbapenemase, AmpC β-lactamase and aminoglycoside resistance genes in extended-spectrum β-lactamase-positive uropathogens from Northern India. *Journal of Global Antimicrobial Resistance* , 20, 197-203.

Gajdács, M., Ábrók, M., Lázár, A., and Burián, K. (2019). Comparative epidemiology and resistance trends of common urinary pathogens in a tertiary-care hospital: a 10-year surveillance study. *Medicina*, 55, 356.

Galić, E., Ilić, K., Hartl, S., Tetyczka, C., Kasemets, K., Kurvet, I., Milić, M., Barbir, R., Pem, B., Erceg, I., Sikirić, M.D., Pavičić, I., Roblegg, E., Kahru, A., and Vrček, I. V. (2020). Impact of surface functionalization on the toxicity and antimicrobial effects of selenium nanoparticles considering different routes of entry. *Food and Chemical Toxicology*, 144, 111621.

Gangadoo, S., Stanley, D., Hughes, R. J., Moore, R. J., and Chapman, J. (2017). The synthesis and characterisation of highly stable and reproducible selenium nanoparticles. *Inorganic and Nano-Metal Chemistry*, 47(11), 1568-1576.

Garousi, F. (2015). The toxicity of different selenium forms and compounds–Review. *Acta Agraria Debreceniensis*, (64), 33-38.

Geraghty, R. J., Capes-Davis, A., Davis, J. M., Downward, J., Freshney, R. I., Knezevic, I., Lovell-Badge, R., Masters, J.R.W., Meredith, J., Stacey, G.N., Thraves, P., and Vias, M. (2014). Guidelines for the

use of cell lines in biomedical research. *British Journal of Cancer*, 111(6), 1021-1046.

Ghimire, S., Baral, B. K., Feng, D., Sy, F. S., and Rodriguez, R. (2019). Is selenium intake associated with the presence of depressive symptoms among US adults? Findings from National Health and Nutrition Examination Survey (NHANES) 2011-2014. *Nutrition*, 62, 169-176.

Giaouris, E., Heir, E., Hébraud, M., Chorianopoulos, N., Langsrud, S., Møretrø, T., Habimana, O., Desvaux, M., Renier, S., and Nychas, G. J. (2014). Attachment and biofilm formation by foodborne bacteria in meat processing environments: causes, implications, role of bacterial interactions and control by alternative novel methods. *Meat Science*, 97(3), 298-309.

Goldstein, J. I., Newbury, D. E., Michael, J. R., Ritchie, N. W., Scott, J. H. J., and Joy, D. C. (2017). Scanning electron microscopy and X-ray microanalysis. *Springer*.

Golob, J. L., and Rao, K. (2021). Signal Versus Noise: How to Analyze the Microbiome and Make Progress on Antimicrobial Resistance. *The Journal of Infectious Diseases*, 223(3), 214-221.

Gopinath, V., Priyadarshini, S., Loke, M. F., Arunkumar, J., Marsili, E., MubarakAli, D., Velusamy, P., and Vadivelu, J. (2017). Biogenic synthesis, characterization of antibacterial silver nanoparticles and its cell cytotoxicity. *Arabian Journal of Chemistry*, 10(8), 1107-1117.

Guarino, A., Guandalini, S., and Vecchio, A. L. (2015). Probiotics for prevention and treatment of diarrhea. *Journal of Clinical Gastroenterology*, 49, 37-45.

Gunti, L., Dass, R. S., and Kalagatur, N. K. (2019). Phytofabrication of selenium nanoparticles from Emblica officinalis fruit extract and

exploring its biopotential applications: antioxidant, antimicrobial, and biocompatibility. *Frontiers in Microbiology*, 10, Article 931.

Gurung, S., Kafle, S., Dhungel, B., Adhikari, N., Shrestha, U. T., Adhikari, B., Banjara, M.R., Rijal, K.R., and Ghimire, P. (2020). Detection of OXA-48 gene in carbapenem-resistant *Escherichia coli* and *Klebsiella pneumoniae* from urine samples . *Infection and Drug Resistance*, 13, 2311 – 2321.

Hadrup, N., Loeschner, K., Skov, K., Ravn-Haren, G., Larsen, E. H., Mortensen, A., Lam, H.R., and Frandsen, H. L. (2016). Effects of 14-day oral low dose selenium nanoparticles and selenite in rat—as determined by metabolite pattern determination. *PeerJ*, 4, e2601.

Hashem, A. H., and Salem, S. S. (2022). Green and ecofriendly biosynthesis of selenium nanoparticles using *Urtica dioica* (stinging nettle) leaf extract: Antimicrobial and anticancer activity. *Biotechnology Journal*, 17(2), 2100432.

Hashem, A. H., Abdelaziz, A. M., Askar, A. A., Fouda, H. M., Khalil, A. M., Abd-Elsalam, K. A., and Khaleil, M. M. (2021). *Bacillus megaterium*-mediated synthesis of selenium nanoparticles and their antifungal activity against *Rhizoctonia solani* in Faba Bean Plants. *Journal of Fungi* , 7(3), 195.

Hassuna, N. A., Khairalla, A. S., Farahat, E. M., Hammad, A. M., and Abdel-Fattah, M. (2020). Molecular characterization of Extended-spectrum β lactamase-producing *E. coli* recovered from community-acquired urinary tract infections in Upper Egypt. *Scientific Reports*, 10(1), 1-8.

Hemalatha, T., Krithiga, G., Santhosh Kumar, B., and Sastry, T. P. (2014). Preparation and characterization of hydroxyapatite-coated selenium nanoparticles and their interaction with osteosarcoma

(SaOS-2) cells. *Acta Metallurgica Sinica* (English Letters), 27(6), 1152-1158.

Ho, C. T., Nguyen, T. H., Lam, T. T., Le, D. Q., Nguyen, C. X., Lee, J. H., and Hur, H. G. (2021). Biogenic synthesis of selenium nanoparticles by *Shewanella sp.* HN-41 using a modified bioelectrochemical system. *Electronic Journal of Biotechnology* , 54, 1-7.

Hong, X., Wen, J., Xiong, X., and Hu, Y. (2016). Shape effect on the antibacterial activity of silver nanoparticles synthesized via a microwave-assisted method . *Environmental Science and Pollution Research*, 23(5), 4489-4497.

Hosnedlova, B., Kepinska, M., Skalickova, S., Fernandez, C., Ruttkay-Nedecky, B., Peng, Q., Baron, M., Melcova, M., Opatrilova, R., Zidkova, J., Bjørklund, G., Sochor, J., and Kizek, R. (2018). Nano-selenium and its nanomedicine applications: a critical review. *International Journal of Nanomedicine*, 13, 2107 – 2128 .

Hospodarova, V., Singovszka, E., and Stevulova, N. (2018). Characterization of cellulosic fibers by FTIR spectroscopy for their further implementation to building materials. *American Journal of Analytical Chemistry*, 9(6), 303-310.

Hu, C. H., Li, Y. L., Xiong, L., Zhang, H. M., Song, J., and Xia, M. S. (2012). Comparative effects of nano elemental selenium and sodium selenite on selenium retention in broiler chickens. *Animal Feed Science and Technology*, 177(3-4), 204-210.

Huang, G., Liu, Z., He, L., Luk, K.H., Cheung, S.T., Wong, K.H., and Chen, T. (2018). Autophagy is an important action mode for functionalized selenium nanoparticles to exhibit anti-colorectal cancer activity. *Biomaterials Science*, 6(9) , 2508-2517.

Huang, T., Holden, J. A., Heath, D. E., O'Brien-Simpson, N. M., and O'Connor, A. J. (2019). Engineering highly effective antimicrobial selenium nanoparticles through control of particle size. *Nanoscale*, 11(31), 14937-14951.

Huang, X., Chen, X., Chen, Q., Yu, Q., Sun, D., and Liu, J. (2016). Investigation of functional selenium nanoparticles as potent antimicrobial agents against superbugs. *Acta Biomaterialia*, 30, 397-407.

Husen, A., and Siddiqi, K. S. (2014). Plants and microbes assisted selenium nanoparticles: characterization and application. *Journal of Nanobiotechnology*, 12(1), 1-10.

Hwang, I. S., Hwang, J. H., Choi, H., Kim, K. J., and Lee, D. G. (2012). Synergistic effects between silver nanoparticles and antibiotics and the mechanisms involved. *Journal of Medical Microbiology* , 61 (12) , 1719 – 1726 .

Ikram, M., Javed, B., and Raja, N. I. (2021). Biomedical potential of plant-based selenium nanoparticles: a comprehensive review on therapeutic and mechanistic aspects. *International Journal of Nanomedicine* , 16, 249 – 268 .

Ingale, A. G., and Chaudhari, A. N. (2013). Biogenic synthesis of nanoparticles and potential applications: an eco-friendly approach. *Journal of Nanomedicine and Nanotechnology*, 4(165), 1-7.

Ismail, Z. B. (2017). Pneumonia in dromedary camels (Camelus dromedarius): a review of clinico-pathological and etiological characteristics. *Journal of Camel Practice and Research*, 24(1), 49-54.

Jaffar, M., Pang, Y., Yuan, H., Zou, D., Liu, Y., Zhu, B., ... and Li, X. (2016). Wheat straw pretreatment with KOH for enhancing

biomethane production and ferti-lizer value in anaerobic digestion. *Chinese journal of chemical engineering*, 24(3), 404-409.

Jancel, T., and Dudas, V. (2002). Management of uncomplicated urinary tract infections. *Western Journal of Medicine*, 176(1) , 51- 55.

Jasim, B., Thomas, R., Mathew, J., and Radhakrishnan, E. K. (2017). Plant growth and diosgenin enhancement effect of silver nanoparticles in Fenugreek (*Trigonella foenum-graecum* L.). *Saudi Pharmaceutical Journal*, 25(3), 443 - 447.

Jayanthi, N., and Sudha, R. M. (2015). *Bacillus clausii*-The probiotic of choice in the treatment of diarrhoea. *Journal of Yoga and Physical Therapy*, 5(4), 1.

Jeevanandam, J., Kiew, S. F., Boakye-Ansah, S., Lau, S. Y., Barhoum, A., Danquah, M. K., and Rodrigues, J. (2022). Green approaches for the synthesis of metal and metal oxide nanoparticles using microbial and plant extracts. *Nanoscale*, 14(7), 2534-2571.

Jepson, R. G., Williams, G., and Craig, J. C. (2012). Cranberries for preventing urinary tract infections. *Cochrane Database of Systematic Reviews*, (10) .

Jia, H., Huang, S., Cheng, S., Zhang, X., Chen, X., Zhang, Y., Wang, J., and Wu, L. (2022). Novel mechanisms of selenite reduction in *Bacillus subtilis* 168: Confirmation of multiple-pathway mediated remediation based on transcriptome analysis. *Journal of Hazardous Materials*, 433, 128834.

Jiang, C., Diao, X., Wang, H., and Ma, S. (2021). Diverse and abundant antibiotic resistance genes in mangrove area and their relationship with bacterial communities-A study in Hainan Island, China. *Environmental Pollution*, 276, 116704.

Jiang, S., Ho, C. T., Lee, J. H., Van Duong, H., Han, S., and Hur, H. G. (2012). Mercury capture into biogenic amorphous selenium

nanospheres produced by mercury resistant *Shewanella putrefaciens* 200. *Chemosphere*, 87(6), 621-624.

Johansen, T. B., Bonkat, G., Cai, T., Tandogdu, Z., Wagenlehner, F., and Grabe, M. (2016). Grey zones in the field of urinary tract infections. *European Urology Focus*, 2(4), 460-462.

Johnson, L. A., and Hug, L. A. (2019). Distribution of reactive oxygen species defense mechanisms across domain bacteria. *Free Radical Biology and Medicine,* 140, 93-102.

Jolly, J., Rauf, M. A., and Ahmad, Z. (2020). Selenium nanoparticles: Small is the new big: Mini review. *Open Journal of Chemistry*, 6(1), 013-016.

Joshi, M., Bhattacharyya, A., and Ali, S. W. (2008). Characterization techniques for nanotechnology applications in textiles.

Junior, E. S., Wadt, L. D. O., Silva, K. E., Lima, R. M. B., Batista, K. D., Guedes, M. C., Carvalho, G.S., Carvalho, T.S., Reis, A.R., Lopes, G., and Guilherme, L. R. G. (2017). Natural variation of selenium in Brazil nuts and soils from the Amazon region. *Chemosphere*, 188, 650-658.

Kachuee, R., Moeini, M. M., and Souri, M. (2013). The effect of dietary organic and inorganic selenium supplementation on serum Se, Cu, Fe and Zn status during the late pregnancy in Merghoz goats and their kids. *Small Ruminant Research*, 110(1), 20-27.

Kapil, S., Kumar, T., and Sharma, V. (2020). Mechanism and challenges associated with adaptation and evolution of drug-resistant bacteria: an overview. *AsPac Journal Mol Biol Biotechnol*, 28(2), 1-18.

Karagöz, A., Acar, S., and Körkoca, H. (2015). Characterization of Klebsiella isolates by matrix-assisted laser desorption/ionization time-of-flight mass spectrometry (MALDI-TOF MS) and determination of antimicrobial resistance with VITEK 2 advanced

expert system (AES). *Turkish Journal of Medical Sciences*, 45(6), 1335-1344.

Khanna, P., Kaur, A., and Goyal, D. (2019). Algae-based metallic nanoparticles: Synthesis, characterization and applications. *Journal of Microbiological Methods*, 163, 105656.

Kheradmand, E., Rafii, F., Yazdi, M. H., Sepahi, A. A., Shahverdi, A. R., and Oveisi, M. R. (2014). The antimicrobial effects of selenium nanoparticle-enriched probiotics and their fermented broth against *Candida albicans* . *DARU Journal of Pharmaceutical Sciences*, 22(1), 1-6.

Khiralla, G. M., and El-Deeb, B. A. (2015). Antimicrobial and antibiofilm effects of selenium nanoparticles on some foodborne pathogens. *LWT- Food Science and Technology*, 63(2), 1001-1007.

Khoei, N. S., Lampis, S., Zonaro, E., Yrjälä, K., Bernardi, P., and Vallini, G. (2017). Insights into selenite reduction and biogenesis of elemental selenium nanoparticles by two environmental isolates of *Burkholderia fungorum*. *New Biotechnology*, 34, 1-11.

Khurana, A., Tekula, S., Saifi, M.A., Venkatesh, P., and Godugu, C.(2019). Therapeutic applications of selenium nanoparticles. *Biomedicine and Pharmacotherapy*, 111, 802-812.

Kiehlbauch, J. A., Hannett, G. E., Salfinger, M., Archinal, W., Monserrat, C., and Carlyn, C. (2000). Use of the National Committee for Clinical Laboratory Standards guidelines for disk diffusion susceptibility testing in New York state laboratories. *Journal of Clinical Microbiology*, 38(9), 3341-3348.

Kimura, H., Arima, T. H., Oku, T., and Sakaguchi, T. (2014). Selenium recovery and conversion by a filamentous fungus, *Aspergillus*

oryzae strain RIB40. *Asia Pacific Journal of Sustainable Agriculture, Food and Energy*, 2(2), 5-8.

Kondaparthi, P., Flora, S. J. S., and Naqvi, S. (2019). Selenium nanoparticles: An insight on its Pro-oxidant and antioxidant properties. *Front. Nanoscience Nanotechnology*, 6, 1-5.

Kora, A. J. (2018). *Bacillus cereus*, selenite-reducing bacterium from contaminated lake of an industrial area: A renewable nanofactory for the synthesis of selenium nanoparticles. *Bioresources and Bioprocessing*, 5(1), 1-12.

Krinsky, N. I., Beecher, G. R., Burk, R. F., Chan, A. C., Erdman, J. J., Jacob, R. A., ... and Traber, M. G. (2000). Dietary reference intakes for vitamin C, vitamin E, selenium, and carotenoids. *Institute of Medicine*, 19, 95-185.

Krishna, G. , Kumar, S. S., Pranitha, V., Alha, M., and Charaya, S. (2015). Biogenic synthesis of silver nanoparticles and their synergistic effect with antibiotics: a study against Salmonella sp. *International Journal of Pharmacy and Pharmaceutical Sciences*, 7(11), 84-88.

Krohn, R. M., Lemaire, M., Silva, L. F. N., Lemarié, C., Bolt, A., Mann, K. K., and Smits, J. E. (2016). High-selenium lentil diet protects against arsenic-induced atherosclerosis in a mouse model. *The Journal of Nutritional Biochemistry*, 27, 9-15.

Kumar, A., and Prasad, K. S. (2021). Role of nano-selenium in health and environment. *Journal of Biotechnology*, 325, 152-163.

Kumar, R., Shukla, S. K., Pandey, A., Srivastava, S. K., and Dikshit, A. (2015). Copper oxide nanoparticles: an antidermatophytic agent for Trichophyton spp. *Nanotechnology Reviews*, 4(5), 401-409.

Kurittu, P., Khakipoor, B., Aarnio, M., Nykäsenoja, S., Brouwer, M., Myllyniemi, A. L., Vatunen, E., and Heikinheimo, A. (2021).

Plasmid-borne and chromosomal ESBL/AmpC genes in *Escherichia coli* and *Klebsiella pneumoniae* in global food products. *Frontiers in Microbiology*, 12, 592291.

Lakshmi, S. G., Jayanthi, N., Saravanan, M., and Ratna, M. S. (2017). Safety assesment of Bacillus clausii UBBC07, a spore forming probiotic. *Toxicology Reports*, 4, 62-71.

Lenz, M., Kolvenbach, B., Gygax, B., Moes, S., and Corvini, P. F. (2011). Shedding light on selenium biomineralization: proteins associated with bionanominerals. *Applied and Environmental Microbiology* , 77(13), 4676-4680 .

Li, B., Liu, N., Li, Y., Jing, W., Fan, J., Li, D., Zhang, L., Zhang, X., Zhang, Z., and Wang, L. (2014). Reduction of selenite to red elemental selenium by *Rhodopseudomonas palustris* strain N. *Plos One*, 9(4), e95955.

Li, Y., Lin, Z., Guo, M., Xia, Y., Zhao, M., Wang, C., Xu, T., Chen, T., and Zhu, B. (2017). Inhibitory activity of selenium nanoparticles functionalized with oseltamivir on H1N1 influenza virus. *International Journal of Nanomedicine*, 12, 5733- 5743 .

Li, Y., Lin, Z., Guo, M., Zhao, M., Xia, Y., Wang, C., Xu, T., and Zhu, B. (2018). Inhibition of H1N1 influenza virus-induced apoptosis by functionalized selenium nanoparticles with amantadine through ROS-mediated AKT signaling pathways. *International Journal of Nanomedicine*, 13, 2005 –2016.

Li, Y., Lin, Z., Zhao, M., Xu, T., Wang, C., Xia, H., Wang, H., and Zhu, B. (2016). Multifunctional selenium nanoparticles as carriers of HSP70 siRNA to induce apoptosis of HepG2 cells. *International Journal of Nanomedicine*, 11, 3065 – 3076 .

Lianou, A., Nychas, G. J. E., and Koutsoumanis, K. P. (2020). Strain variability in biofilm formation: A food safety and quality perspective. *Food Research International*, 137, 109424.

Liao, G., Tang, J., Wang, D., Zuo, H., Zhang, Q., Liu, Y., and Xiong, H.(2020) . Selenium nanoparticles (SeNPs) have potent antitumor activity against prostate cancer cells through the upregulation of miR-16. *World Journal of Surgical Oncology*, 18(1) , 1-11.

Lin, Z. H., and Wang, C. C. (2005). Evidence on the size-dependent absorption spectral evolution of selenium nanoparticles. *Materials Chemistry and Physics*, 92(2-3), 591-594.

Liu, C., Fu, Y., Li, C. E., Chen, T., and Li, X. (2017) . Phycocyanin-functionalized selenium nanoparticles reverse palmitic acid-induced pancreatic β cell apoptosis by enhancing cellular uptake and blocking reactive oxygen species (ROS)-mediated mitochondria dysfunction. *Journal of Agricultural and Food Chemistry*, 65(22) , 4405-4413.

Liu, T., Bai, R., Zhou, H., Wang, R., Liu, J., Zhao, Y., and Chen, C. (2020). The effect of size and surface ligands of iron oxide nanoparticles on blood compatibility. *RSC Advances*, 10(13), 7559-7569.

Livak, K. J., and Schmittgen, T. D. (2001). Analysis of relative gene expression data using real-time quantitative PCR and the $2^{-\Delta\Delta CT}$ method. *Methods*, 25(4), 402-408.

Loy, A., Lehner, A., Lee, N., Adamczyk, J., Meier, H., Ernst, J., Schleifer, K. Wagner, M. (2002). Oligonucleotide microarray for 16S rRNA gene-based detection of all recognized lineages of sulfate-reducing prokaryotes in the environment. *Applied and Environmental Microbiology*, 68(10), 5064-5081.

Luo, H., Wang, F., Bai, Y., Chen, T., and Zheng, W. (2012). Selenium nanoparticles inhibit the growth of HeLa and MDA-MB-231 cells through induction of S phase arrest. *Colloids and Surfaces B: Biointerfaces*, 94, 304-308.

Lyu, C., Chen, J., Li, L., Zhao, Z., and Liu, X. (2022). Characteristics of Se in water-soil-plant system and threshold of soil Se in seleniferous areas in Enshi, China. *Science of The Total Environment*, 827, 154372.

MacFaddin, J. F. (2000). Biochemical tests for identification of medical bacteria, williams and wilkins. *Philadelphia, PA*, 113.

Magesh, H., Kumar, A., Alam, A., and Sekar, U. (2013). Identification of natural compounds which inhibit biofilm formation in clinical isolates of Klebsiella pneumoniae. *Indian Journal of Experimental Biology* , 51(09) , 764-772.

Mahon, C. R., Lehman, D. C., and Manuselis, G. (2018). Textbook of diagnostic microbiology-e-book. *Elsevier Health Sciences*.

Maiyo, F., and Singh, M. (2017). Selenium nanoparticles: Potential in cancer gene and drug delivery. *Nanomedicine*, 12(9), 1075-1089.

Makabenta, J. M. V., Nabawy, A., Li, C. H., Schmidt-Malan, S., Patel, R., and Rotello, V. M. (2021). Nanomaterial-based therapeutics for antibiotic-resistant bacterial infections. *Nature Reviews Microbiology*, 19(1), 23-36.

Mancuso, G., Midiri, A., Gerace, E., and Biondo, C. (2021). Bacterial antibiotic resistance: the most critical pathogens. *Pathogens* , 10 (10), 1310.

Mann, J., and Truswell, A. S. (2017) . Essentials of human nutrition. *Oxford University Press.*

Mathur T, S Singhal, S Khan.(2006) . Detection of biofilm formation among the clinical isolates of staphylococci: an evaluation of three different screening methods. *Indian journal* , l24, 0255-0857.

Maveyraud, L., and Mourey, L. (2020). Protein X-ray crystallography and drug discovery. *Molecules*, 25(5), 1030.

Medina Cruz, D., Mi, G., and Webster, T. J. (2018). Synthesis and characterization of biogenic selenium nanoparticles with antimicrobial properties made by Staphylococcus aureus, methicillin-resistant Staphylococcus aureus (MRSA), Escherichia coli, and Pseudomonas aeruginosa. *Journal of Biomedical Materials Research Part A*, 106(5), 1400-1412.

Mellinas, C., Jiménez, A., and Garrigós, M. D. C. (2019). Microwave-assisted green synthesis and antioxidant activity of selenium nanoparticles using Theobroma cacao L. bean shell extract. *Molecules*, 24(22), 24224048 .

Menon, S., KS, S. D., Agarwal, H., and Shanmugam, V. K. (2019). Efficacy of biogenic selenium nanoparticles from an extract of ginger towards evaluation on anti-microbial and anti-oxidant activities. *Colloid and Interface Science Communications*, 29, 1-8.

Mesdaghinia, A., Pourpak, Z., Naddafi, K., Nodehi, R. N., Alizadeh, Z., Rezaei, S., Mohammadi, A., and Faraji, M. (2019). An in vitro method to evaluate hemolysis of human red blood cells (RBCs) treated by airborne particulate matter (PM10). *MethodsX*, 6, 156-161.

Miglani, S., and Tani-Ishii, N. (2021). Biosynthesized selenium nanoparticles: characterization, antimicrobial, and antibiofilm activity against *Enterococcus faecalis*. *PeerJ*, 9, e11653.

Mirsoleymani, S. R., Salimi, M., Shareghi Brojeni, M., Ranjbar, M., and Mehtarpoor, M. (2014). Bacterial pathogens and antimicrobial

resistance patterns in pediatric urinary tract infections: a four-year surveillance study (2009–2012). *International Journal of Pediatrics* , 2014 , 126142 .

Mishra, P. K., Mishra, S., Bisht, S. C., Selvakumar, G., Kundu, S., Bisht, J. K., and Gupta, H. S. (2009). Isolation, molecular characterization and growth-promotion activities of a cold tolerant bacterium Pseudomonas sp. NARs9 (MTCC9002) from the Indian Himalayas. *Biological Research*, 42(3), 305-313.

Mishra, R. R., Prajapati, S., Das, J., Dangar, T. K., Das, N., and Thatoi, H. (2011). Reduction of selenite to red elemental selenium by moderately halotolerant Bacillus megaterium strains isolated from Bhitarkanika mangrove soil and characterization of reduced product. *Chemosphere*, 84(9), 1231-1237.

Mojarad-Jabali, S., Farshbaf, M., Walker, P. R., Hemmati, S., Fatahi, Y., Zakeri-Milani, P., Sarfraz, M., and Valizadeh, H. (2021). An update on actively targeted liposomes in advanced drug delivery to glioma. *International Journal of Pharmaceutics*, 602, 120645.

Motiei Pour, M., Moghbeli, M. R., Larijani, B., and Akbari Javar, H. (2022). pH-Sensitive mesoporous bisphosphonate-based TiO2 nanoparticles utilized for controlled drug delivery of dexamethasone. *Chemical Papers* , 76(1), 439-451.

Munita, J. M., and Arias, C. A. (2016). Mechanisms of antibiotic resistance. *Microbiology Spectrum*, 4(2), 4-2.

Munoz-Dávila, M. J., Roig, M., Yagüe, G., Blázquez, A., Salvador, C., and Segovia, M. (2013). Comparative evaluation of Vitek 2 identification and susceptibility testing of urinary tract pathogens directly and isolated from chromogenic media. *European Journal of Clinical Microbiology and Infectious Diseases*, 32(6), 773-780.

Murugesan, G., Nagaraj, K., Sunmathi, D., and Subramani, K. (2019). Methods involved in the synthesis of selenium nanoparticles and their different applications-a review. *European Journal of Biomedical AND Pharmaceutical Sciences*, 6(4), 189-194.

Nayak, V., Singh, K. R., Singh, A. K., and Singh, R. P. (2021). Potentialities of selenium nanoparticles in biomedical science. *New Journal of Chemistry*, 45(6), 2849-2878.

Naziri, Z., Derakhshandeh, A., Borchaloee, A. S., Poormaleknia, M., and Azimzadeh, N. (2020). Treatment failure in urinary tract infections: a warning witness for virulent multi-drug resistant ESBL-producing *Escherichia coli*. *Infection and Drug Resistance*, 13, 1839 –1850.

Ndwandwe, B. K., Malinga, S. P., Kayitesi, E., and Dlamini, B. C. (2021). Advances in green synthesis of selenium nanoparticles and their application in food packaging. *International Journal of Food Science and Technology*, 56(6), 2640-2650.

Nguyen, T. H., Vardhanabhuti, B., Lin, M., and Mustapha, A. (2017). Antibacterial properties of selenium nanoparticles and their toxicity to Caco-2 cells. *Food Control*, 77, 17-24.

Niki, E. (2010). Assessment of antioxidant capacity in vitro and in vivo. *Free Radical Biology and Medicine*, 49(4), 503-515.

Nikzamir, M., Hanifehpour, Y., Akbarzadeh, A., and Panahi, Y. (2021). Applications of dendrimers in nanomedicine and drug delivery: A review. *Journal of Inorganic and Organometallic Polymers and Materials*, 31(6) , 2246-2261.

Niranjan, R., Zafar, S., Lochab, B., and Priyadarshini, R. (2022). Synthesis and characterization of sulfur and sulfur-selenium nanoparticles loaded on reduced graphene oxide and their

antibacterial activity against gram-positive pathogens. *Nanomaterials*, 12(2), 191.

Nitzan, O., Elias, M., Chazan, B., and Saliba, W. (2015). Urinary tract infections in patients with type 2 diabetes mellitus: review of prevalence, diagnosis, and management. *Diabetes, Metabolic Syndrome and Obesity: Targets and Therapy*, 8, 129 - 136.

Oake, A., Bhatt, P., and Pathak, Y. V. (2019). Understanding surface characteristics of nanoparticles. In Surface modification of nanoparticles for targeted drug delivery (pp. 1-17). *Springer*, Cham.

Okojie, R. O., and Omorokpe, V. O. (2018). A survey on urinary tract infection associated with two most common uropathogenic bacteria. *African Journal of Clinical and Experimental Microbiology*, 19(3) , v19i3.3 .

Oliveira, B. E. C., dos Santos Ré, A. C., Aires, C. P., and Ricomini Filho, A. P. (2022). Polysaccharides in Bacterial Biofilm 27. *Polysaccharides of Microbial Origin*, 599.

Öztürk, R., and Murt, A. (2020). Epidemiology of urological infections: a global burden. *World Journal of Urology*, 38(11), 2669-2679.

Pandit, R., Awal, B., Shrestha, S. S., Joshi, G., Rijal, B. P., and Parajuli, N. P. (2020). Extended-spectrum β-lactamase (ESBL) genotypes among multidrug-resistant uropathogenic *Escherichia coli* clinical isolates from a teaching hospital of Nepal. *Interdisciplinary Perspectives on Infectious Diseases*, 2020 , 5826 .

Paparo, L., Tripodi, L., Bruno, C., Pisapia, L., Damiano, C., Pastore, L., and Berni Canani, R. (2020). Protective action of Bacillus clausii probiotic strains in an in vitro model of Rotavirus infection. *Scientific Reports*, 10(1), 1-10.

Parsameher, N., Rezaei, S., Khodavasiy, S., Salari, S., Hadizade, S., Kord, M., and Mousavi, S. A. A. (2017). Effect of biogenic selenium nanoparticles on ERG11 and CDR1 gene expression in both fluconazole-resistant and-susceptible Candida albicans isolates. *Current Medical Mycology*, 3(3), 16-20.

Partoazar, A., Talaei, N., Bahador, A., Pourhajibagher, M., Dehpour, S., Sadati, M., and Bakhtiarian, A. (2019). Antibiofilm activity of natural zeolite supported NanoZnO: inhibition of *Esp* gene expression of *Enterococcus faecalis*. *Nanomedicine,* 14(6), 675-687.

Parvej, M. S., Khan, M. I., and Hossain, M. K. (2022). Preparation of nanoparticle-based polymer composites. *In Nanoparticle-Based Polymer Composites* (pp. 55-94).

Pasquina, L. W., Santa Maria, J. P., and Walker, S. (2013). Teichoic acid biosynthesis as an antibiotic target. *Current Opinion in Microbiology*, 16(5), 531-537.

Patil, N. A., Gade, W. N., and Deobagkar, D. D. (2016). Epigenetic modulation upon exposure of lung fibroblasts to TiO2 and ZnO nanoparticles: alterations in DNA methylation. *International journal of nanomedicine*, *11*, 4509.

Patel, J. K., Patel, A., and Bhatia, D. (2021). Introduction to nanomaterials and nanotechnology. *In Emerging Technologies for Nanoparticle Manufacturing* (pp. 3-23). Springer, Cham.

Patrone, V., Molinari, P., and Morelli, L. (2016). Microbiological and molecular characterization of commercially available probiotics containing Bacillus clausii from India and Pakistan. *International Journal of Food Microbiology*, 237, 92-97.

Pearce, C. I., Coker, V. S., Charnock, J. M., Pattrick, R. A., Mosselmans, J. F. W., Law, N., Beveridge, T.J., and Lloyd, J. R. (2008).

Microbial manufacture of chalcogenide-based nanoparticles via the reduction of selenite using Veillonella atypica: an in situ EXAFS study. *Nanotechnology,* 19(15), 155603.

Pouladfar, G., Basiratnia, M., Anvarinejad, M., Abbasi, P., Amirmoezi, F., and Zare, S. (2017). The antibiotic susceptibility patterns of uropathogens among children with urinary tract infection in Shiraz. *Medicine*, 96(37), e7834.

Purohit, M. P., Verma, N. K., Kar, A. K., Singh, A., Ghosh, D., and Patnaik, S. (2017). Inhibition of thioredoxin reductase by targeted selenopolymeric nanocarriers synergizes the therapeutic efficacy of doxorubicin in MCF7 human breast cancer cells. *ACS Applied Materials and Interfaces*, 9(42), 36493-36512.

Pyrzynska, K., and Pękal, A. (2013). Application of free radical diphenylpicrylhydrazyl (DPPH) to estimate the antioxidant capacity of food samples. *Anal Methods* , 5: 4288–4295.

Pyrzynska, K., and Sentkowska, A. (2021). Biosynthesis of selenium nanoparticles using plant extracts. *Journal of Nanostructure in Chemistry*, 1-14.

Rahimi, H. R., and Doostmohammadi, M. (2019). Nanoparticle synthesis, applications, and toxicity. *In Applications of Nanobiotechnology* (pp. 1-16) . London , UK: IntechOpen .

Rahimi, M., Charmi, G., Matyjaszewski, K., Banquy, X., and Pietrasik, J. (2021). Recent developments in natural and synthetic polymeric drug delivery systems used for the treatment of osteoarthritis. *Acta Biomaterialia* , 123, 31-50.

Ralston, N. V., and Raymond, L. J. (2010). Dietary selenium's protective effects against methylmercury toxicity. *Toxicology*, 278(1), 112-123.

Ramamurthy, C. H., Sampath, K. S., Arunkumar, P., Kumar, M. S., Sujatha, V., Premkumar, K., and Thirunavukkarasu, C. (2013). Green synthesis and characterization of selenium nanoparticles and its augmented cytotoxicity with doxorubicin on cancer cells. *Bioprocess and Biosystems Engineering*, 36(8), 1131-1139 .

Ranjitha, V. R., and Ravishankar, V. R. (2018). Extracellular synthesis of selenium nanoparticles from an actinomycetes streptomyces griseoruber and evaluation of its cytotoxicity on HT-29 cell line. *Pharmaceutical Nanotechnology*, 6(1), 61-68.

Raz, R., Colodner, R., and Kunin, C. M. (2005). Who are you—Staphylococcus saprophyticus?. *Clinical Infectious Diseases*, 40(6), 896-898.

Rebelo, A., Mourão, J., Freitas, A. R., Duarte, B., Silveira, E., Sanchez-Valenzuela, A., Almeida, A., Baquero, F., Coque, T.M., Peixe, L., Antunes, P., and Novais, C. (2021). Diversity of metal and antibiotic resistance genes in Enterococcus spp. from the last century reflects multiple pollution and genetic exchange among phyla from overlapping ecosystems. *Science of The Total Environment*, 787, 147548.

Reddy, S. M., Datta, K. K. R., Sreelakshmi, C., Eswaramoorthy, M., and Reddy, B. V. (2012). Honey mediated green synthesis of Pd nanoparticles for suzuki coupling and hydrogenation of conjugated olefins. *Nanoscience and Nanotechnology Letters*, 4(4), 420-425.

Ren, S. X., Zhang, B., Lin, Y., Ma, D. S., and Yan, H. (2019). Selenium nanoparticles dispersed in phytochemical exert anti-inflammatory activity by modulating catalase, GPx1, and COX-2 gene expression in a rheumatoid arthritis rat model. Medical science monitor: *International Medical Journal of Experimental and Clinical Research*, 25, 991-1000 .

Ricciotti, E., and FitzGerald, G. A. (2011). Prostaglandins and inflammation. *Arteriosclerosis, Thrombosis, and Vascular Biology*, 31(5), 986-1000.

Ruchi, T., Sujata, B., and Anuradha, D. (2015). Comparison of phenotypic methods for the detection of biofilm production in uro-pathogens in a tertiary care hospital in India. *International Journal of Current Microbiology* , 4(9), 840-849.

Rumbaugh, K. P., and Sauer, K. (2020). Biofilm dispersion. *Nature Reviews Microbiology*, 18(10), 571-586.

Sadalage, P. S., Nimbalkar, M. S., Sharma, K. K. K., Patil, P. S., and Pawar, K. D. (2020). Sustainable approach to almond skin mediated synthesis of tunable selenium microstructures for coating cotton fabric to impart specific antibacterial activity. *Journal of Colloid and Interface Science*, 569, 346-357.

Sadeghi, M., Ebrahim-Saraie, H. S., Mojtahedi, A., Nikokar, I., and Roushan, Z. A. (2020). Genetic diversity and prevalence of aminoglycoside modifying enzymes among Escherichia coli strains isolated from inpatients with urinary tract infections. *Gene Reports*, 21, 100957.

Salas-Orozco, M. F., Niño-Martínez, N., Martínez-Castañón, G. A., Méndez, F. T., Morán, G. M. M., Bendaña-Piñeiro, A. E., Ruiz, F., and Bach, H. (2022). Proteomic analysis of an Enterococcus faecalis mutant generated against the exposure to silver nanoparticles. *Journal of Applied Microbiology*, 132(1), 244-255.

Saleh, T. A. (2021). Protocols for synthesis of nanomaterials, polymers, and green materials as adsorbents for water treatment technologies. *Environmental Technology and Innovation*, 24, 101821.

Sánchez-López, E., Gomes, D., Esteruelas, G., Bonilla, L., Lopez-Machado, A. L., Galindo, R., Cano, A., Espina, M., Ettcheto, M., Camins , A., Silva, A.M., Durazzo, A., Santini, A., Garcia, M.L., and Souto, E. B. (2020). Metal-based nanoparticles as antimicrobial agents: an overview. *Nanomaterials*, 10(2), 10020292 .

Santanu, S., Sowmiya, R., and Balakrishnaraja, R. (2015). Biosynthesis of selenium nanoparticles using citrus reticulata peel extract. *World Journal of Pharmaceutical Research*, 4(1), 1322-1330.

Sartelli, M., Weber, D. G., Ruppé, E., Bassetti, M., Wright, B. J., Ansaloni, L., ... and Siribumrungwong, B. (2016). Antimicrobials: a global alliance for optimizing their rational use in intra-abdominal infections (AGORA). *World Journal of Emergency Surgery*, 11(1), 1-32.

Satgurunathan, T., Bhavan, P. S., and Komathi, S. (2017). Green synthesis of selenium nanoparticles from sodium selenite using garlic extract and its enrichment on Artemia nauplii to feed the freshwater prawn Macrobrachium rosenbergii post-larvae . *Research Journal of Chemistry and Environment*, 21(10), 1-12.

Sattar, R., Shahzad, F., Ishaq, T., Mukhtar, R., and Naz, A. (2022). Nano-Drug Carriers: A Potential Approach towards Drug Delivery Methods. *Chemistry Select* , 7(22), e202200884.

Sattari-Maraji, A., Jabalameli, F., Node Farahani, N., Beigverdi, R., and Emaneini, M. (2019). Antimicrobial resistance pattern, virulence determinants and molecular analysis of Enterococcus faecium isolated from children infections in Iran. *BMC microbiology*, 19(1), 1-8.

Schomburg, L. (2021). Selenium Deficiency Due to Diet, Pregnancy, Severe Illness, or COVID-19—A Preventable Trigger for

Autoimmune Disease. *International Journal of Molecular Sciences*, 22(16), 22168532 .

Sentkowska, A., and Pyrzyńska, K. (2022). The Influence of Synthesis Conditions on the Antioxidant Activity of Selenium Nanoparticles. *Molecules*, 27(8), 2486.

Shah, S. T., Yehye, W. A., Saad, O., Simarani, K., Chowdhury, Z. Z., Alhadi, A. A., and Al-Ani, L. A. (2017). Surface functionalization of iron oxide nanoparticles with gallic acid as potential antioxidant and antimicrobial agents. *Nanomaterials*, 7(10), 306.

Shahbaz, M., Akram, A., Raja, N. I., Mukhtar, T., Mashwani, Z. U., Mehak, A., ... and Yousaf, T. (2022). Green synthesis and characterization of selenium nanoparticles and its application in plant disease management : A review . *Pakistan Journal of Phytopathology*, 34(1), 189-102.

Shahmoradi, S., Shariati, A., Zargar, N., Yadegari, Z., Asnaashari, M., Amini, S. M., and Darban-Sarokhalil, D. (2021). Antimicrobial effects of selenium nanoparticles in combination with photodynamic therapy against *Enterococcus faecalis* biofilm. *Photodiagnosis and Photodynamic Therapy*, 35, 102398.

Shakerimoghaddam, A., Ghaemi, E. A., and Jamalli, A. (2017). Zinc oxide nanoparticle reduced biofilm formation and antigen 43 expressions in uropathogenic *Escherichia coli*. *Iranian Journal of Basic Medical Sciences*, 20(4), 451- 456 .

Shakibaie, M., Forootanfar, H., Golkari, Y., Mohammadi-Khorsand, T., and Shakibaie, M. R. (2015). Anti-biofilm activity of biogenic selenium nanoparticles and selenium dioxide against clinical isolates of Staphylococcus aureus, Pseudomonas aeruginosa, and Proteus mirabilis. *Journal of Trace Elements in Medicine and Biology*, 29, 235-241.

Shakibaie, M., Jafari, M., Ameri, A., Rahimi, H. R., and Forootanfar, H. (2018). Biosynthesis and physicochemical characterization, and cytotoxic evaluation of selenium nanoparticles produced by streptomyces lavendulae FSHJ9 against MCF-7 cell line. *Journal of Rafsanjan University of Medical Sciences*, 17(7), 625-638.

Sharma, G., Sharma, A. R., Bhavesh, R., Park, J., Ganbold, B., Nam, J. S., and Lee, S. S. (2014). Biomolecule-mediated synthesis of selenium nanoparticles using dried Vitis vinifera (raisin) extract. *Molecules*, 19(3), 2761-2770.

Sharma, J., and Chauhan, D. S. (2014). Inhibition of Pseudomonas aeruginosa by antibiotics and probiotics combinations–In vitro study. *European Journal of Experimental Biology*, 4(6), 10-14.

Shilpi, T., Ahmed, M. N., Huq, S. A., Baul, S. K., and Khatun, M. (2013). Isolation of bacteria causing urinary tract infections and their antibiotic susceptibility profile at Anwer Khan Modern Medical College Hospital. *Anwer Khan Modern Medical College Journal*, 4(2), 23-27.

Shirley, B., and Jarochowska, E. (2022). Chemical characterisation is rough: the impact of topography and measurement parameters on energy-dispersive X-ray spectroscopy in biominerals. *Facies*, 68(2), 1-15.

Shirsat, S., Kadam, A., Naushad, M., and Mane, R. S. (2015). Selenium nanostructures: microbial synthesis and applications. *Rsc Advances*, 5(112), 92799-92811.

Shubharani, R., Mahesh, M., and Yogananda Murthy, V. (2019). Biosynthesis and characterization, antioxidant and antimicrobial activities of selenium nanoparticles from ethanol extract of Bee Propolis. *Journal of Nanomedicine and Nanotechnology*, 10:522, 1-7 .

Siddiqui, M. A., Wahab, R., Ahmad, J., Farshori, N. N., and Al-Khedhairy, A. A. (2020). Single and Multi-metal Oxide Nanoparticles Induced Cytotoxicity and ROS Generation in Human Breast Cancer (MCF-7) Cells. *Journal of Inorganic and Organometallic Polymers and Materials*, 30(10) , 4106-4116.

Silhavy, T. J., Kahne, D., and Walker, S. (2010). The bacterial cell envelope. *Cold Spring Harbor perspectives in biology*, 2(5), a000414.

Singh, N., Saha, P., Rajkumar, K., and Abraham, J. (2014). Biosynthesis of silver and selenium nanoparticles by Bacillus sp. JAPSK2 and evaluation of antimicrobial activity. *Der Pharmacia Lettre*, 6(6), 175-181.

Singh, V., Basu, A., Shivapriya, P. M., Varadwaj, P. K., Samanta, S. K., and Sahoo, A. K. (2019). Exploration of interactions of 'blood-nano interface'of carbon-based nanomaterials for biomedical applications. *Journal of Materials Research*, 34(11), 1950-1964.

Skalickova, S., Milosavljevic, V., Cihalova, K., Horky, P., Richtera, L., and Adam, V. (2017). Selenium nanoparticles as a nutritional supplement. *Nutrition*, 33, 83-90.

Slavin, Y. N., Asnis, J., Häfeli, U. O., and Bach, H. (2017). Metal nanoparticles: understanding the mechanisms behind antibacterial activity. *Journal of Nanobiotechnology*, 15(1), 1-20.

Solovyev, N., Drobyshev, E., Bjørklund, G., Dubrovskii, Y., Lysiuk, R., and Rayman, M. P. (2018). Selenium, selenoprotein P, and Alzheimer's disease: is there a link?. *Free Radical Biology and Medicine*, 127, 124-133.

Soltani, L., and Darbemamieh, M. (2021). Anti-proliferative, apoptotic potential of synthesized selenium nanoparticles against breast

cancer cell line (MCF7). *Nucleosides, Nucleotides and Nucleic acids*, 40(9), 926-941.

Sonkusre, P. (2020) . Specificity of Biogenic Selenium Nanoparticles for Prostate Cancer Therapy With Reduced Risk of Toxicity: An in vitro and in vivo Study. *Frontiers in Oncology*, 9, 1541.

Sonkusre, P., and Cameotra, S.S. (2017). Biogenic selenium nanoparticles induce ROS-mediated necroptosis in PC-3 cancer cells through TNF activation. *Journal of Nanobiotechnology*, 15(1) , 1-12.

Sonkusre, P., Nanduri, R., Gupta, P., and Cameotra, S. S. (2014). Improved extraction of intracellular biogenic selenium nanoparticles and their specificity for cancer chemoprevention. *Journal of Nanomedicine and Nanotechnology*, 5(2), 194.

Sotoodehnia-Korani, S., Iranbakhsh, A., Ebadi, M., Majd, A., and Ardebili, Z. O. (2020). Selenium nanoparticles induced variations in growth, morphology, anatomy, biochemistry, gene expression, and epigenetic DNA methylation in Capsicum annuum; an in vitro study. *Environmental Pollution*, 265, 114727.

Spiliopoulou, M., Valmas, A., Triandafillidis, D. P., Kosinas, C., Fitch, A., Karavassili, F., and Margiolaki, I. (2020). Applications of X-ray powder diffraction in protein crystallography and drug screening. *Crystals*, 10(2), 54.

Srey, S., Jahid, I. K., and Ha, S. D. (2013). Biofilm formation in food industries: a food safety concern. *Food Control*, 31(2), 572-585.

Srinivas, A. (2020). Original Research Article Anti-microbial susceptibility pattern of spores used in Bacillus clausii suspension: an in vitro study. *International Journal of Contemporary Pediatrics*, 7(5), 1.

Srivastava, N., and Mukhopadhyay, M. (2015). Green synthesis and structural characterization of selenium nanoparticles and assessment of their antimicrobial property. *Bioprocess and Biosystems Engineering*, 38(9), 1723-1730.

Suáreza, D. F., Consuegrab, J., Trajanoc, V. C., Gontijoc, S. M., Guimarãesa, P. P.G., Cortésc, M. E., Denadai, A.L., and Sinisterraa, R. D. (2014). Structural and thermodynamic characterization of doxycycline/-cyclodextrin supramolecular complex and its bacterial membrane interactions. *Colloids and Surfaces B: Biointerfaces*, 118, 194-201.

Sudha, M. R., Bhonagiri, S., and Kumar, M. A. (2013). Efficacy of Bacillus clausii strain UBBC-07 in the treatment of patients suffering from acute diarrhoea. *Beneficial Microbes*, 4(2), 211-216.

Suwanjinda, D., Eames, C., and Panbangred, W. (2007). Screening of lactic acid bacteria for bacteriocins by microbiological and PCR methods. *Biochemistry and Molecular Biology Education*, 35(5), 364-369.

Syed, A., Saraswati, S., Kundu, G. C., and Ahmad, A. (2013). Biological synthesis of silver nanoparticles using the fungus Humicola sp. and evaluation of their cytoxicity using normal and cancer cell lines. *Spectrochimica Acta Part A: Molecular and Biomolecular Spectroscopy*, 114, 144-147.

Tabibi, M., Agaei, S. S., Amoozegar, M. A., Nazari, R., and Zolfaghari, M. R. (2020). Antibacterial, antioxidant, and anticancer activities of biosynthesized selenium nanoparticles using two indigenous halophilic bacteria. *Archives of Hygiene Sciences*, 9(4), 275-286.

Tang, L., Luo, X., Wang, M., Wang, Z., Guo, J., Kong, F., and Bi, Y. (2021). Synthesis, characterization, in vitro antioxidant and hypoglycemic activities of selenium nanoparticles decorated with

polysaccharides of Gracilaria lemaneiformis. *International Journal of Biological Macromolecules*, 193, 923-932.

Toledo-Arana, A., Valle, J., Solano, C., Arrizubieta, M. J., Cucarella, C., Lamata, M., Amorena, B., Leiva, J., Penadés, J.R., and Lasa, I. (2001). The enterococcal surface protein, *Esp*, is involved in *Enterococcus faecalis* biofilm formation . *Applied and Environmental Microbiology*, 67(10), 4538-4545.

Tran, P. A., O'Brien-Simpson, N., Reynolds, E. C., Pantarat, N., Biswas, D. P., and O'Connor, A. J. (2015). Low cytotoxic trace element selenium nanoparticles and their differential antimicrobial properties against *S. aureus* and *E. coli*. *Nanotechnology*, 27(4), 045101.

Trüeb, R. M. (2020). Nutritional Disorders of the Hair and Their Management. *In Nutrition for Healthy Hair* (111-223). Springer, Cham.

Tsamesidis, I., Pouroutzidou, G. K., Lymperaki, E., Kazeli, K., Lioutas, C. B., Christodoulou, E., Perio, P., Reybier, K., Pantaleo, A., and Kontonasaki, E. (2020). Effect of ion doping in silica-based nanoparticles on the hemolytic and oxidative activity in contact with human erythrocytes. *Chemico-Biological Interactions*, 318, 108974.

Tugarova, A. V., Mamchenkova, P. V., Dyatlova, Y. A., and Kamnev, A. A. (2018). FTIR and Raman spectroscopic studies of selenium nanoparticles synthesised by the bacterium Azospirillum thiophilum. Spectrochimica Acta Part A: *Molecular and Biomolecular Spectroscopy*, 192, 458-463.

Ullah, A., Yin, X., Wang, F., Xu, B., Mirani, Z. A., Xu, B., Chan, M.W.H., Ali, A., Usman, M., Ali, N., and Naveed, M. (2021). Biosynthesis of selenium nanoparticles (via Bacillus subtilis

bsn313), and their isolation, characterization, and bioactivities. *Molecules*, 26(18), 26185559 .

Ungvári, É., Monori, I., Megyeri, A., Csiki, Z., Prokisch, J., Sztrik, A., Jávor, A., and Benkő, I. (2014). Protective effects of meat from lambs on selenium nanoparticle supplemented diet in a mouse model of polycyclic aromatic hydrocarbon-induced immunotoxicity. *Food and Chemical Toxicology*, 64, 298-306.

Upadrasta, A., Pitta, S., and Madempudi, R. S. (2016). Draft genome sequence of *Bacillus clausii* UBBC07, a spore-forming probiotic strain. *Genome Announcements*, 4(2), e00235-16.

Vachvanichsanong, P., McNeil, E. B., and Dissaneewate, P. (2021). Extended-spectrum beta-lactamase Escherichia coli and Klebsiella pneumoniae urinary tract infections. *Epidemiology and Infection*, 149 , e12, 1–7.

Van Khanh, N., and Van Cu, P. (2019). Antibacterial activity of silver nanoparticles against aeromonas spp. and Vibrio spp. isolated from aquaculture water environment in Thua Thien Hue. *Hue University Journal of Science: Agriculture and Rural Development*, 128(3B), 5-16.

Van Malderen, S. (2017). Optimization of methods based on laser ablation-ICP-mass spectrometry (LA-ICP-MS) for 2-D and 3-D elemental mapping (Doctoral dissertation, Ghent University).

Vandepitte, J., Verhaegen, J., Engbaek, K., Piot, P., Heuck, C. C., Rohner, P., and Heuck, C. C. (2003). Basic laboratory procedures in clinical bacteriology. *World Health Organization*.

Varak, K., and Priya, P. K. (2019). Synergistic Effect Of Selenium Nanoparticles (Senps) With Various Antibiotics As An Antimicrobial Activity". *Think India Journal*, 22(4), 1707-1712.

Verma, P., and Maheshwari, S. K. (2017). Minimum biofilm eradication concentration (MBEC) assay of Silver and Selenium nanoparticles against biofilm forming Staphylococcus aureus. *Journal of Medical Science And Clinical Research*, 5(4), 20213-20222.

Verma, P., and Maheshwari, S. K. (2018). Preparation of sliver and selenium nanoparticles and its characterization by dynamic light scattering and scanning electron microscopy. *Journal of Microscopy and Ultrastructure*, 6(4), 182 - 187.

Vetchinkina, E., Loshchinina, E., Kupryashina, M., Burov, A., and Nikitina, V. (2019). Shape and size diversity of gold, silver, selenium, and silica nanoparticles prepared by green synthesis using fungi and bacteria. *Industrial and Engineering Chemistry Research*, 58(37), 17207-17218.

Vincent, M. G., John, N. P., Narayanan, P. M., Vani, C., and Murugan, S. (2014). In vitro study on the efficacy of zinc oxide and titanium dioxide nanoparticles against metallo beta-lactamase and biofilm producing Pseudomonas aeruginosa. *Journal of Applied Pharmaceutical Science*, 4(7), 041-046.

Wadhwani, S. A., Gorain, M., Banerjee, P., Shedbalkar, U. U., Singh, R., Kundu, G. C., and Chopade, B. A. (2017). Green synthesis of selenium nanoparticles using Acinetobacter sp. SW30: Optimization, characterization and its anticancer activity in breast cancer cells. *International Journal of Nanomedicine*, 12, 6841–6855.

Waller, K. P., Aspán, A., Nyman, A., Persson, Y., and Andersson, U. G. (2011). CNS species and antimicrobial resistance in clinical and subclinical bovine mastitis. *Veterinary Microbiology*, 152(1-2), 112-116.

Wang, H., Wei, W., Zhang, S. Y., Shen, Y. X., Yue, L., Wang, N. P., and Xu, S. Y. (2005). Melatonin-selenium nanoparticles inhibit oxidative stress and protect against hepatic injury induced by Bacillus Calmette–Guérin/lipopolysaccharide in mice. *Journal of Pineal Research*, 39(2), 156-163.

Wang, H., Zhang, J., and Yu, H. (2007). Elemental selenium at nano size possesses lower toxicity without compromising the fundamental effect on selenoenzymes: comparison with selenomethionine in mice. *Free Radical Biology and Medicine*, 42(10), 1524-1533.

Wang, K., Taylor, K. G., and Ma, L. (2021). Advancing the application of atomic force microscopy (AFM) to the characterization and quantification of geological material properties. *International Journal of Coal Geology*, 247, 103852.

Wang, L., Hu, C., and Shao, L. (2017). The antimicrobial activity of nanoparticles: present situation and prospects for the future. *International Journal of Nanomedicine*, 12, 1227 –1249.

Wang, Y., Xue, D., Li, Y., Pan, X., Zhang, X., Kuang, B., Zhou, M., Li, X., Xiong, W., Li, G., Zeng, Z., and Yang, T. (2016). The long noncoding RNA MALAT-1 is a novel biomarker in various cancers: a meta-analysis based on the GEO database and literature. *Journal of Cancer*, 7(8), 991-1001.

WHO (2019) . Ten threats to global health .

Wisell, K. T., Kahlmeter, G., and Giske, C. G. (2008). Trimethoprim and enterococci in urinary tract infections: new perspectives on an old issue. *Journal of Antimicrobial Chemotherapy*, 62(1), 35-40.

Xia, Y., Lin, Z., Li, Y., Zhao, M., Wang, C., Guo, M., Zhang, B., and Zhu, B. (2017). Targeted delivery of siRNA using RGDfC-conjugated functionalized selenium nanoparticles for anticancer therapy. *Journal of Materials Chemistry B*, 5(33), 6941-6952.

Xiong, Y., Zhang, C., Gao, W., Ma, Y., Zhang, Q., Han, Y., Jiang, S., Zhao, Z., Wang, J., and Chen, Y. (2021). Genetic diversity and co-prevalence of ESBLs and PMQR genes among plasmid-mediated AmpC β-lactamase-producing *Klebsiella pneumoniae* isolates causing urinary tract infection. *The Journal of Antibiotics*, 74(6), 397-406.

Yang, F., Tang, Q., Zhong, X., Bai, Y., Chen, T., Zhang, Y., Li, Y., and Zheng, W. (2012). Surface decoration by Spirulina polysaccharide enhances the cellular uptake and anticancer efficacy of selenium nanoparticles. *International Journal of Nanomedicine*, 7, 835 – 844.

Yazdi, M. H., Mahdavi, M., Kheradmand, E., and Shahverdi, A. R. (2012). The preventive oral supplementation of a selenium nanoparticle-enriched probiotic increases the immune response and lifespan of 4T1 breast cancer bearing mice. *Arzneimittelforschung*, 62(11), 525-531.

Zafar, S. (2022). Review on synthesis and applications of nanomaterials. *SBK Journal of Basic Sciences and Innovative Research*, 1(2), 1-53.

Zayed, M. F., Eisa, W. H., El-Kousy, S. M., Mleha, W. K., and Kamal, N. (2019). Ficus retusa-stabilized gold and silver nanoparticles: controlled synthesis, spectroscopic characterization, and sensing properties. Spectrochimica Acta Part A: *Molecular and Biomolecular Spectroscopy*, 214, 496-512.

Zhai, X., Zhang, C., Zhao, G., Stoll, S., Ren, F., and Leng, X. (2017). Antioxidant capacities of the selenium nanoparticles stabilized by chitosan. *Journal of Nanobiotechnology*, 15(1), 1-12.

Zhang, H., Li, Z., Dai, C., Wang, P., Fan, S., Yu, B., and Qu, Y. (2021). Antibacterial properties and mechanism of selenium nanoparticles

synthesized by Providencia sp. DCX. *Environmental Research*, 194, 110630.

Zhang, H., Xia, M., and Hu, C. (2007). Effect of nano-selenium on the activities of glutathione peroxidase and type-I deiodinase in the liver of weanling pigs. *Journal of Biomedical Engineering* , 24(1), 153-156.

Zhang, H., Zhou, H., Bai, J., Li, Y., Yang, J., Ma, Q., and Qu, Y. (2019). Biosynthesis of selenium nanoparticles mediated by fungus Mariannaea sp. HJ and their characterization. Colloids and Surfaces A: *Physicochemical and Engineering Aspects*, 571, 9-16.

Zhao, S., Yu, Q., Pan, J., Zhou, Y., Cao, C., Ouyang, J. M., and Liu, J. (2017). Redox-responsive mesoporous selenium delivery of doxorubicin targets MCF-7 cells and synergistically enhances its anti-tumor activity. *Acta Biomaterialia*, 54, 294-306.

Zheng, W., Cao, C., Liu, Y., Yu, Q., Zheng, C., Sun, D., Ren, X., and Liu, J. (2015). Multifunctional polyamidoamine-modified selenium nanoparticles dual-delivering siRNA and cisplatin to A549/DDP cells for reversal multidrug resistance. *Acta Biomaterialia*, 11, 368-380.

Zhou, Y., Xu, M., Liu, Y., Bai, Y., Deng, Y., Liu, J., and Chen, L.(2016) . Green synthesis of Se/Ru alloy nanoparticles using gallic acid and evaluation of theiranti-invasive effects in HeLa cells. *Colloids and Surfaces B: Biointerfaces*, 144, 118-124.

Zhu, C., Zhang, S., Song, C., Zhang, Y., Ling, Q., Hoffmann, P. R., Li, J., Chen, T., Zheng, W., and Huang, Z. (2017). Selenium nanoparticles decorated with Ulva lactuca polysaccharide potentially attenuate colitis by inhibiting NF-κB mediated hyper inflammation. *Journal of Nanobiotechnology*, 15(1), 1-15.

Zonaro, E., Lampis, S., Turner, R. J., Qazi, S. J. S., and Vallini, G. (2015). Biogenic selenium and tellurium nanoparticles synthesized by environmental microbial isolates efficaciously inhibit bacterial planktonic cultures and biofilms. *Frontiers in Microbiology* , 6, 584.

Zou, X., Jiang, Z., Li, L., and Huang, Z. (2021). Selenium nanoparticles coated with pH responsive silk fibroin complex for fingolimod release and enhanced targeting in thyroid cancer. *Artificial Cells, Nanomedicine, and Biotechnology*, 49(1), 83-95.

Zwolak, I. (2020). The role of selenium in arsenic and cadmium toxicity: an updated review of scientific literature. *Biological Trace Element Research*, 193(1), 44-63.

Appendices

Appendix 1: Identification of E.coli by Vitek 2 compact system.

Selected Organism			99% Probability **Escherichia coli** **Bionumber:** 0405610550524610														
ID Analysis Messages																	
Biochemical Details																	
2	APPA	-	3	ADO	-	4	PyrA	-	5	lARL	-	7	dCEL	-	9	BGAL	+
10	H2S	-	11	BNAG	-	12	AGLTp	-	13	dGLU	+	14	GGT	-	15	OFF	+
17	BGLU	-	18	dMAL	+	19	dMAN	+	20	dMNE	+	21	BXYL	-	22	BAlap	-
23	ProA	-	26	LIP	-	27	PLE	-	29	TyrA	+	31	URE	-	32	dSOR	+
33	SAC	+	34	dTAG	-	35	dTRE	+	36	CIT	-	37	MNT	-	39	5KG	-
40	lLATk	+	41	AGLU	-	42	SUCT	+	43	NAGA	-	44	AGAL	+	45	PHOS	-
46	GlyA	-	47	ODC	-	48	LDC	+	53	lHISa	-	56	CMT	+	57	BGUR	+
58	O129R	+	59	GGAA	-	61	lMLTa	-	62	ELLM	-	64	lLATa	-			

Appendix 2: Identification of Enterococcus faecalis by Vitek 2 system.

Selected Organism			99% Probability **Enterococcus faecalis** **Bionumber:** 156002661773431														
ID Analysis Messages																	
Biochemical Details																	
2	AMY	+	4	PIPLC	-	5	dXYL	-	8	ADH1	+	9	BGAL	-	11	AGLU	+
13	APPA	-	14	CDEX	+	15	AspA	+	16	BGAR	-	17	AMAN	-	19	PHOS	-
20	LeuA	-	23	ProA	-	24	BGURr	-	25	AGAL	-	26	PyrA	+	27	BGUR	-
28	AlaA	-	29	TyrA	+	30	dSOR	+	31	URE	-	32	POLYB	+	37	dGAL	+
38	dRIB	+	39	lLATk	-	42	LAC	-	44	NAG	+	45	dMAL	+	46	BACI	+
47	NOVO	+	50	NC6.5	+	52	dMAN	+	53	dMNE	+	54	MBdG	+	56	PUL	-
57	dRAF	-	58	O129R	-	59	SAL	+	60	SAC	+	62	dTRE	+	63	ADH2s	-
64	OPTO	+															

Appendix 3: Identification of Klebsiella pneumoniae by Vitek 2 system.

Selected Organism			96% Probability **Klebsiella pneumoniae ssp pneumoniae** **Bionumber:** 6607734553564610 **Confidence:** Excellent identification														
SRF Organism																	
Analysis Organisms and Tests to Separate:																	
Analysis Messages:																	
Contraindicating Typical Biopattern(s) Klebsiella pneumoniae ssp pneumoniae BGUR(3),																	
Biochemical Details																	
2	APPA	-	3	ADO	+	4	PyrA	+	5	lARL	-	7	dCEL	+	9	BGAL	+
10	H2S	-	11	BNAG	-	12	AGLTp	-	13	dGLU	+	14	GGT	+	15	OFF	+
17	BGLU	+	18	dMAL	+	19	dMAN	+	20	dMNE	+	21	BXYL	+	22	BAlap	-
23	ProA	-	26	LIP	-	27	PLE	+	29	TyrA	+	31	URE	(-)	32	dSOR	+
33	SAC	+	34	dTAG	-	35	dTRE	+	36	CIT	+	37	MNT	+	39	5KG	-
40	lLATk	+	41	AGLU	-	42	SUCT	+	43	NAGA	-	44	AGAL	+	45	PHOS	+
46	GlyA	-	47	ODC	-	48	LDC	+	53	lHISa	-	56	CMT	+	57	BGUR	+
58	O129R	+	59	GGAA	-	61	lMLTa	-	62	ELLM	-	64	lLATa	-			

Appendix 4: Identification of Staphylococcus saprophyticus by Vitek 2 system.

Selected Organism				89% Probability **Bionumber:**		**Staphylococcus saprophyticus** 070002057771271											
ID Analysis Messages																	
Biochemical Details																	
2	AMY	-	4	PIPLC	-	5	dXYL	-	8	ADH1	+	9	BGAL	+	11	AGLU	+
13	APPA	-	14	CDEX	-	15	AspA	-	16	BGAR	-	17	AMAN	-	19	PHOS	-
20	LeuA	-	23	ProA	-	24	BGURr	-	25	AGAL	-	26	PyrA	+	27	BGUR	-
28	AlaA	-	29	TyrA	-	30	dSOR	-	31	URE	+	32	POLYB	-	37	dGAL	+
38	dRIB	+	39	lLATk	+	42	LAC	+	44	NAG	+	45	dMAL	+	46	BACI	+
47	NOVO	+	50	NC6.5	+	52	dMAN	+	53	dMNE	+	54	MBdG	-	56	PUL	-
57	dRAF	-	58	O129R	+	59	SAL	-	60	SAC	+	62	dTRE	+	63	ADH2s	+
64	OPTO	+															

Appendix 5: Identification of Bacillus clausii by Vitek 2 system.

Bionumber: 5373331317447671
Organism Quantity: **Selected Organism: Bacillus claussi**

Biochemical Details																	
1	BXYL	+	3	LysA	-	4	AspA	+	5	LeuA	+	7	PheA	+	8	ProA	-
9	BGAL	+	10	PyrA	+	11	AGAL	+	12	AlaA	+	13	TyrA	+	14	BNAG	-
15	APPA	(+)	18	CDEX	+	19	dGAL	-	21	GLYG	+	22	INO	+	24	MdG	(-)
25	ELLM	+	26	MdX	-	27	AMAN	-	29	MTE	+	30	GlyA	+	31	dMAN	-
32	dMNE	+	34	dMLZ	-	36	NAG	-	37	PLE	+	39	IRHA	+	41	BGLU	+
43	BMAN	(-)	44	PHC	-	45	PVATE	+	46	AGLU	(-)	47	dTAG	-	48	dTRE	+
50	INU	+	53	dGLU	+	54	dRIB	+	56	PSCNa	-	58	NaCl 6.5%	+	59	KAN	+
60	OLD	+	61	ESC	+	62	TTZ	+	63	POLYB_B	+						

Appendix 6 : XRD values of selenium nanoparticles .

	2-Theta (degree)	Theta	FWHM (degree)	Crystallite size(nm)	D(nm)
1	23.601	14.94835	0.7872	10.31472	**18.215**
2	29.8967	11.8005	0.246	33.44077	
3	44.0156	22.0078	0.7872	10.88965	

Appendix 7 : Functional groups values of FTIR .

Peak Number	X (cm-1)	Y (%T)
1	3335.96	43.40
2	2952.85	22.64
3	2922.50	16.72
4	2853.17	22.31
5	2726.72	43.02
6	1632.39	43.60
7	1516.55	43.88
8	1502.78	43.98
9	1462.11	33.05
10	1455.69	32.97
11	1376.95	37.01
12	1046.00	42.28
13	721.83	45.94
14	558.51	47.48
15	470.29	48.79

Appendix 8: Gene expression (Mean ± SE) for Hly gene and FimH gene in E.coli

Groups	*Hly* gene	*FimH* gene
Sub-MIC 32	1.51±0.98Aa	2.47±1.93Aa
MIC 64	4.11±0.98Aa	6.66±2.52Ba
Control	11.91±3.09Ba	14.31±3.73Ca

Means with different big letters in the same column and small letters in the same row are significantly different (P<0.05) .

Appendix 9 : Gene expression (Mean ± SE) for LuxS gene and qseC gene in E. coli (biofilm production and regulation)

Groups	*LuxS* gene	*qseC* gene
Sub-MIC 64	1.38±0.21Aa	0.79±0.18Aa
MIC 128	3.72±1.15Aa	2.05±0.55Aa
Control	15.45±4.43Ba	5.52±1.2Bb

Means with different big letters in the same column and small letters in the same row are significantly different (P<0.05) .

Appendix 10 : Gene expression (Mean ± SE) for ESP gene and HLY gene in E. faecalis .

Groups	*ESP* gene	*HLY* gene
Sub–MIC 16	1.32±0.15Aa	2.21±0.15Aa
MIC 32	12.69±2.52Ba	9.5±0.81Ba
Control	38.13±6.86Ca	22.18±9.03Cb

Means with different big letters in the same column and small letters in the same row are significantly different (P<0.05) .

Appendix 11 : Gene expression (Mean ± SE) of gelE and fsrA gene in E. faecalis (biofilm production and regulation)

Groups	*gelE* gene	*fsrA* gene
Sub-MIC 32	0.41±0.05Aa	2.09±0.43Aa
MIC 64	1.51±0.51Aa	6.37±1.29Bb
Control	4.70±1.33Ba	14.15±2.99Cc

Means with different big letters in the same column and small letters in the same row are significantly different (P<0.05).

الخلاصـــــــــة :

تحتل الطريقة البيولوجية لتصنيع الجسيمات النانوية مجالًا مهمًا نظرا لفائدتها الاقتصادية وكونها صديقة للبيئة عند مقارنتها بطرق التخليق الفيزيائية والكيميائية . لذلك , فان هذه الدراسة هدفت الى تصنيع جسيمات السيلينيوم النانوية (SeNPs) من خلال طريقه بايلوجية باستخدام بكتريا *Bacillus clausii* من سلاله (4G219) والتي شخصت باستخدام نظام VITEK 2 وباستخدام سلسلة مورث الحمض النووي الرايبوزي 16SrRNA . تم تحديد الخصائص الشكلية والهيكلية لجسيمات السيلينيوم النانوية بِاستخدام اِلقياس اِلطيفي اِلمرئي لِلأشعة فِوقِ البنفسجيةِ – UV visible ولن ذروة الامتصاص كانت عند الطول الموجي (260) نانومتر , المجهر الالكتروني الماسح SEM (تراوحت اقطار الجزيئات النانوية بين (37.58 - 75.16) نانومتر , حيث تبين ان الجسيمات النانوية المصنعة كانت بلورية ومستقرة الى حد ما وذات شكل قضيبي , والتحليل الطيفي للطاقة المشتتة من الاشعة السينية (EDXS) كشف ان اكثر الاشارات الحادة تعود لجزيئات السيلينيوم النانوية . في فحص XRD ، وجد أن حجم جسيمات السيلينيوم النانوية متشابه مع البيانات التي تم الحصول عليها من (AFM) مع الحجم (18.215 نانومتر ، 19. 28 نانومتر) على التوالي. اما مطياف الأشعة تحت الحمراء FTIR لجزيئات السيلينيوم النانوية فقد اظهر وجود عدد من المجاميع الوظيفية .

تم جمع مائة وخمسة وستين عينة ادرار من مرضى يعانون من أعراض سريرية ويشتبه في إصابتهم بالتهاب المسالك البولية داخل مستشفيات مختلفة في محافظة بابل للفترة من (اذار – تشرين الاول) 2021 . 115 (69.6٪) عزلة كانت موجبة الفحص ، تم تشخيص أربعة أنواع من البكتيريا الممرضة (*Escherichia coli* , *Enterococcus faecalis* , *Klebsiella pneumoniae* , *Staphyllococcus saprophyticus*) , معظمها كان مقاوم للمضادات الحيوية وبالأخص *Enterococcus faecalis* . تم فحص النشاط المضاد البكتيري لجسيمات السيلينيوم النانوية ضد الانواع الاربعه للبكتريا المرضية . تم استخدام عشرة تركيزات مختلفة من SeNPs (2 , 4 , 8 , 16 , 32 , 64 , 128 , 256 , 512 , 1024) ميكروغرام / مل . وجد ان التركيز المثبط الادنى لجزيئات السيلينيوم النانوية (MIC) هو (32 ميكروغرام / مل) والتركيز القاتل الادنى لجزيئات السيلينيوم النانوية (MBC) هو (64 ميكروغرام / مل) لكل من *Staphylococcus Saprophyticus* و *Enterococcus faecalis* ، بينما

التركيز المثبط الادنى (MIC) و التركيز القاتل الادنى (MBC) لـ *Klebsiella pneumoniae* و *Escherichia coli* فقد كان (64 ميكروغرام / مل) و (128 ميكروغرام / مل) على التوالي .

تم دراسة التأثير التآزري لـ SeNPs باستخدام ستة مضادات حيوية (Azithromycin، Ciprofloxacin، Trimethoprime / sulphamethoxazole , Doxycycline، nitrofurantoin and Ampicillin) ضد البكتيريا المرضية . انخفض التأثير التآزري لـ Doxycycline مع SeNPs في جميع البكتيريا المُختبرة الحساسة للدوكسيسايكلين ، وأصبحت العزلات التي كانت حساسة للمضاد الحيوي متوسطة المقاومة والمتوسطة المقاومة اصبحت مقاومة للمضادات الحيوية. تم تحديد النشاط المضاد للأكسدة لجزيئات السيلينيوم النانوية باستخدام (DPPH) (2,2-Diphenyl-1-picryl- hydrazyl) . حيث كان للجسيمات النانوية اعلى نشاط مضاد للأكسدة (% 39.6 , 63.1% , % 74.2) عند التراكيز (50 , 100 , 150) ميكروغرام / مل , على التوالي . لم تظهر جسيمات السيلينيوم النانوية بكل التراكيز المستخدمة أي انحلال كامل للدم الذي تم اختباره .

اما في اختبار تكوين الاغشية الحيوية الرقيقة (Biofilm) , من اصل 115 عزله , كانت 60 عزلة لها القدرة على تكوين الاغشية الحيوية . اما في اختبار ضدية تكوين الاغشية الحيوية الرقيقة (Antibiofilm) فقد تم قياس قدرة بعض انواع البكتريا على تكوين الاغشية الحيوية الرقيقة بوجود جزيئات السيلينيوم النانوية باستخدام طريقة صفيحة 96 حفرة . وجد ان التركيز المثبط الادنى (MIC) لجزيئات السيلينيوم النانوية لتكوين الاغشية الحيوية هو (128 ميكروغرام / مل) لبكتريا *Escherichia coli* and *Klebsiella pneumoniae)* و(64 ميكروغرام / مل) لبكتريا *Staphylococcus Saprophyticus* (and *Enterococcus faecalis*) , فقد وجد ان التركيز المثبط الادنى MIC لجزيئات السيلينيوم النانوية ضد تكوين الاغشية الحيوية هو ضعف التركيز المثبط الادنى MIC لجزيئات السيلينيوم النانوية في حاله البكتريا العالقه .

أظهر فحص الاستجابة السمية للخلايا لخط خلايا سرطان البروستات PC3 والخلايا الكبدية البشرية الطبيعية WRL68 عدم وجود تأثير سام لـ Se NPsعلى خلايا PC3 بتركيز 25 و 50 ميكروغرام / مل . ومع ذلك فقد اظهر الـ SeNPs بتركيز (100 , 200 , 400 ميكروغرام / مل) انخفاض في معدل بقاء خلايا PC3 مع اقصى معدل تثبيط بلغ (51.27±2.77%) لخط خلايا PC3 بتركيز (400 ميكروغرام / مل) . اما فيما يتعلق بخط خلايا (WRL68) فقد كانت حساسية الخلايا لل SeNPs اقل من تلك الموجودة في خط خلايا ال PC3 .

تم تقييم التعبير الجيني لعوامل الضراوة للجينات (*Hly*، *FimH*، *Luxs*، *qsec*) لبكتريا *E.coli* و جينات (*ESP*، *HLY*، *gelE*، *fsrA*) لبكتريا *E.faecalis* عن طريق تفاعل البلمرة المتسلسل الكمي في الوقت الحقيقي (RT- qPCR) قبل وبعد المعاملة بـالـ SeNPs , اذ كشفت النتائج أن SeNPs يؤثر على التعبير الجيني لهذه الجينات عن طريق تقليل التعبير الجيني (down regulation) .

استنتجت هذه الدراسة قدرة *Bacillus clausii* على تخليق جسيمات السيلينيوم النانوية. وقد ثبت قدرة هذه الجسيمات كمضاد بكتيري , مضاد لتكوين الغشاء الحيوي , مضادات الأكسدة , النشاط المضاد للسرطان في خط خلايا PC3 و WRL 68 واخيرا تقليل التعبير الجيني لجينات عوامل الضراوة .

جمهورية العراق
وزارة التعليم العالي والبحث العلمي
جامعة بابل
كلية العلوم
قسم علوم الحياة

التخليق الحيوي لجسيمات السيلينيوم النانوية من *Bacillus clausii* وتقيم فعاليته المضادة للبكتريا وللاغشيه الحيويه الرقيقه وفحص السمية الخلوية

اطروحة مقدمة الى
مجلس كلية العلوم / جامعة بابل
وهي جزء من متطلبات نيل درجة الدكتوراه فلسفة
في العلوم / علوم الحياة

من قبل

حوراء جواد كاظم عمران
بكالوريوس احياء مجهرية / جامعة بابل (2007)
ماجستير احياء مجهرية / جامعة بابل (2014)

بأشراف

أ.د وجدان رضا تاج الدين

2022م 1444 هـ